Investigating the Impact of Cleaning Product Formulations on Indoor Air Chemistry

Ellen Harding-Smith

Doctor of Philosophy

University of York

Environment and Geography

May 2024

Abstract

Cleaning products are a ubiquitous source of volatile organic compounds (VOCs) indoors. The chemical complexity of VOC emissions and the subsequent secondary pollutant formation complicates quantifying their role in indoor air pollution, thus hampering informed changes in consumer attitudes, product manufacturing, and regulations. This thesis addresses this uncertainty by quantifying VOC emissions from various cleaning products, examining the formation of secondary pollutants, and investigating the impacts of compositional and environmental changes on indoor air chemistry.

Analysis of 23 regular and green cleaners identified 317 VOCs, with monoterpenes being the most prevalent. Regular and green cleaners contained up to 8.6 and 25.0 mg L^{-1} monoterpenes, respectively. Simulations showed that green cleaners generally resulted in higher concentrations of formaldehyde and peroxyacetyl nitrates (PANs), though some regular cleaners produced disproportionately high secondary pollutant concentrations due to higher emissions of monoterpenes with a large k_{O3}.

Room-scale cleaning experiments measured 1.3-8.9 mg VOCs per cleaning event, with limonene dominating the secondary chemistry. Substituting limonene with monoterpenes with a higher k_{O3} increased formaldehyde and total PANs concentrations by up to 13% and 23%, respectively, while substitution with lower k_{O3} monoterpenes increased organic nitrate formation by up to 68%.

High air exchange rates and outdoor pollution levels increased secondary pollutant concentrations due to increased availability of oxidants and pollutants via infiltration. Indoor surfaces impacted indoor air chemistry through oxidant surface deposition and multi-phase chemistry. Simulations in a basic kitchen scenario showed that plastic and soft furnishings contributed most to O_3 deposition, while wood contributed most to secondary formaldehyde emissions.

Evidence from these studies suggest that altering the formulation of cleaning products and the surface area and materials of indoor surfaces can help reduce exposure to hazardous secondary pollutants. Further mechanistic and toxicological studies will be required to inform changes in product composition and building conditions for improved indoor air quality.

Contents

List of Tables

List of Figures

List of Abbreviations

ACR	Air Change Rate
AGCU	Automated Gas Calibration Unit
CLP	Classification, Labelling, and Packaging
CV	Coefficient of Variation
DIMS	Direct Injection Mass Spectrometry
DOAS	Differential Optical Absorption Spectroscopy
DOMESTIC	DOMEstic Systems and Technology InCubator
GC-FID	Gas Chromatography Flame Ionisation Detector
GC-MS	Gas Chromatography Mass Spectrometry
GC-TOF-MS	Gas Chromatography Time of Flight Mass Spectrometry
HOMEChem	House Observations of Microbial and Environmental Chemistry
ICAD	Iterative CAvity enhanced DOAS
INDCCM	INdoor Detailed Chemical Model
INCHEM-Py	INdoor CHEMical model in Python
LE	Low Emissivity
LEWF	Low Emissivity With Film
LHA	Local Hour Angle
LOD	Limit Of Detection
LUCIR	Lifting Up Communities by Intervening with Research
MCM	Master Chemical Mechanism

NIST	National Institute of Standards and Technology
NOEL	No Observed Effect Level
OA-ICOS	Off-Axis Integrated Cavity Output Spectroscopy
ODE	Ordinary Differential Equation
PAN	Peroxyacetyl Nitrate
PM	Particulate Matter
QMF	Quadrupole Mass Filter
RH	Relative Humidity
SAV	Surface Area to Volume ratio
SAR	Structure Activity Relationship
SBS	Sick Building Syndrome
SIFT-MS	Selected Ion Flow Tube Mass Spectrometry
SIM	Selected Ion Monitoring
SOA	Secondary Organic Aerosol
UGGA	Ultraportable Greenhouse Gas Analyser
VOC	Volatile Organic Compound
WACL	Wolfson Atmospheric Chemistry Laboratories
WASP	WACL Air Sampling Platform

Acknowledgments

Firstly, I would like to acknowledge the EPSRC for funding my studentship and giving me the opportunity to undertake my PhD research. I would also like to acknowledge Which? and Tincture for their provision of some of the cleaning products which have underpinned this thesis.

I would like to express my deepest appreciation to my supervisors at the University of York, Professor Nicola Carslaw and Dr Terry Dillon, for their unwavering support, insightful advice, and expertise throughout my PhD. I would also like to express my appreciation to Lisa Emberson and Sylvia Toet, my TAP and Progression meeting members, for their invaluable guidance and counsel.

I'd like to acknowledge Dr Marvin Shaw and Dr Martyn Ward at the Wolfson Atmospheric Chemistry Laboratories for their technical assistance with analytical instrumentation, as well as Dr David Shaw from the Environment and Geography Department for his help with the INCHEM-Py model.

I am incredibly grateful to have been part of such a wonderful research group throughout my PhD programme. My heartfelt thanks to Nic, Dave, Helen, Toby, Georgia, and Catherine for their camaraderie, moral support, and laughter, which made my time at the University of York truly memorable.

I would like to express my deepest gratitude to my family, especially my parents, Karen and Nicholas, for their endless love and encouragement. To my grandmother, Wendy, our weekly natters have been a welcome distraction and source of comfort. Lastly, I would like to give a special thanks to my partner, Sam, for always believing in me and reminding me of my capabilities.

Declaration

This thesis has not previously been accepted for any degree and is not being concurrently submitted in candidature for any degree other than Doctor of Philosophy of the University of York. This thesis is the result of my own investigations, except where otherwise stated. All other sources are acknowledged by explicit references.

Part of this work has been published in:

Harding-Smith, E., Shaw, D. R., Shaw, M., Dillon, T. J. and Carslaw, N. (2024), 'Does green mean clean? Volatile organic emissions from regular versus green cleaning products', Environmental Science: Processes & Impacts 26(2), 436–450, doi:10.1039/D3EM00439B

Chapter 1

Introduction

1.1 An introduction to indoor air quality

Modern issues surrounding climate change and urban air pollution have prompted extensive scientific research focussed on the outdoor environment in a bid to improve air quality and reduce our exposure to harmful pollutant concentrations. Consequently, the predominant emphasis of air quality regulations has been on the outdoor environment, for example the 2016 Paris agreement, which aimed to reduce greenhouse gas emissions and tackle climate change (Bhore, 2016). However, it is estimated that people in developed countries spend on average 90% of their time indoors, meaning that air quality indoors can be significantly more important when determining air pollutant exposure compared to outdoors (Klepeis et al., 2001). Despite this, research into indoor air quality is lagging that of outdoor air quality, with no equivalent large-scale international policies currently in place for tackling issues related to indoor air pollution.

Indoor air quality is a complex phenomenon influenced by outdoor and indoor sources of pollution, environmental conditions, housing characteristics, and behavioural factors (World Health Organization, 2010). In the last 40 years, we have seen an increase in indoor air research which aims to better understand air composition, sources, and

concentrations of pollutants, as well as the potential impacts on human health. There are numerous types of pollutants found in indoor environments, including gaseous pollutants (inorganic gases, radon, volatile organic compounds (VOCs)), biological pollutants (viruses, bacteria, mould) and particulate matter (PM). The concentration of air pollutants indoors is controlled by various physical and chemical processes, including exchange with outdoors, indoor emission sources, deposition onto indoor surfaces, and chemical transformations.

Many pollutants originating from outdoors are present in indoor environments due to ingress via ventilation systems and infiltration of the building envelope. Outdoor pollutant levels indoors depend on the building design, as well as regional air quality (Weschler and Carslaw, 2018). Increased airtightness of building envelopes in response to energy conservation measures implemented following the Arab Oil embargo of 1973 has resulted in lower air exchange rates in residential dwellings (Weschler, 2009). This reduction in ventilation rate, while improving building energy efficiencies, has resulted in more passive air exchange between indoor and outdoor environments and consequently the accumulation of air pollutants with indoor origin.

There are many sources of pollutants indoors, including building materials and furnishings, occupant activities such as cooking, cleaning, and smoking, and consumer products such as household and personal care products (Weschler and Carslaw, 2018). There is large temporal and spatial variability in pollutant emissions indoors, depending on a variety of factors including occupant behaviours and the age of materials. For example, VOC concentrations in new and renovated buildings were reported to be 1 to 2 orders of magnitude higher than in older buildings (Brown, 2002). Owing to the complex and numerous pollutant sources and limited ventilation compared to outdoors, indoor pollutant concentrations often exceed outdoor levels.

The chemical and physical processes which occur in indoor environments differ considerably from outdoor processes due to differences in the physical environment, for example larger surface area to volume ratio (SAV) and the absence of direct sunlight (Kowal et al., 2017; Manuja et al., 2019). The SAV of indoor environments is typi-

cally hundreds of times greater than outdoor environments. Consequently, partitioning and processing of pollutants on indoor surfaces is an important contributing factor to gas-phase pollutant concentrations. Ozone (O_3), a strong oxidising agent originating mainly from outdoor sources, has been measured at concentrations of 20-70% outdoor levels in part due to the deposition of O_3 onto indoor surfaces (Weschler, 2000). O_3, as well as other oxidants present indoors such as hydroxyl (OH) and nitrate (NO_3) radicals, is a major driver of indoor air chemistry. Chemical degradation of pollutants indoors give rise to secondary pollutants, many of which are more detrimental to human health than their precursors (Weschler, 2000; Nazaroff, 2021).

Clearly, indoor air quality is a multifaceted area of research, with many complex influencing factors which make it unique to outdoor air quality. Therefore, it is essential that we develop a deeper understanding of the controls of indoor air pollution to aid the development of policies and regulations for improving air quality within the built environment.

1.1.1 Why is indoor air quality important?

Increasing evidence suggests that indoor air pollution can cause or aggravate health issues, and can even cause mortality (Horvath, 1997; Medina-Ramón et al., 2005; World Health Organization, 2010). Factors which contribute to poor indoor air quality vary globally due to differences in geographical location, climate, and cultural and habitual behaviours. In developing countries, the widespread use of solid fuel burning as a source of domestic energy results in high personal exposure to air pollution. According to the WHO, this has resulted in 3.2 million premature deaths in 2020, including 237,000 deaths of children under the age of 5 (World Health Organization, 2022). In the UK and other developed nations, however, the pollutant sources and concentrations are somewhat different. From hereon, research relevant to indoor air pollution in developed countries will be the focus of this thesis.

Exposure to air pollutants, most notably through the inhalation exposure pathway, has been reported to result in a range of adverse health effects, including respiratory

diseases, triggering of asthma and allergies, acute respiratory infections, pulmonary diseases, cancer, eye and airway irritation, cognitive conditions, and increases in psychological stress (Fiedler et al., 2005; Hulin et al., 2012; Jie et al., 2011; Cincinelli and Martellini, 2017). Prolonged exposure to indoor pollutants can contribute to Sick Building Syndrome (SBS), which relates to symptoms caused by poor indoor air quality from chemical and biological contaminants, and poor ventilation (Joshi, 2008). Commonly reported symptoms include coughing, sneezing, headaches, nausea, dizziness, itching and swelling of the skin, and mucosal irritation of the throat, nose, and eyes (Norbäck, 2009). SBS was first recognised by the WHO in 1983, who estimated that up to 30% of newly built and remodelled buildings could potentially be sources of significant complaints regarding indoor air quality issues (World Health Organization, 1983).

In response to the growing amount of evidence linking indoor air pollution to adverse health effects, several guidelines have been developed for improving indoor air quality. In the UK, one of the first acknowledgements of the importance of improving indoor air quality came in 2000, with guidance for employers on how to tackle SBS in offices and workspaces (Health and Safety Executive, 2000). Other UK regulations relating to specific indoor air pollutants include bans on the use of asbestos and indoor tobacco smoking (UK Legislation, 1987, 2006). These regulations came after increasing evidence of the carcinogenic effects of PM, and in the case of tobacco smoke, VOCs, emitted from these sources (McDonald, 1985; Kim et al., 2018). Furthermore, in 2012, a regulation was established which placed limits on the VOC content in paints, varnishes and vehicle refinishing products (DEFRA, 2012).

Despite a few regulations and guidelines aimed at tackling specific pollutants and issues, there is currently no overarching legislation on indoor air quality in the UK. The WHO published indoor air quality guidelines in 2010 for selected pollutants, based on reviewing globally accumulated scientific evidence linking exposure with health outcomes (World Health Organization, 2010). However, these guidelines only cover 9 indoor air pollutants of significance, including VOCs and inorganic gases, and therefore

does not sufficiently describe the wide range of pollutants which contribute to poor indoor air quality. In 2019, the UK published a more detailed document defining indoor air quality guidelines for a broader range of VOCs based on the existing health-based guidelines proposed by other countries and organisations (Public Health England, 2019). These guidelines, summarised in Table 1.1, include both short-term and long-term limit values for 11 VOCs for which there exists scientific evidence regarding their toxicity and presence in buildings.

Table 1.1: Summary of indoor air quality guidelines for the UK, outlined by Public Health England (2019).

VOC	Short term exposure limit (μg m^{-3})	Long term exposure limit (μg m^{-3})
acetaldehyde	1420 (1 h)	280 (1 day)
α-pinene	45000 (30 min)	4500 (1 day)
benzene	No safe level of exposure can be recommended.[a]	
d-limonene	90000 (30 min)	9000 (1 day)
formaldehyde	100 (30 min)	10 (1 year)
naphthalene	-	3 (1 year)
styrene	-	850 (1 year)
tetrachloroethylene	-	40 (1 day)
toluene	15000 (8 h)	2300 (1 day average)
trichloroethylene	No safe level of exposure can be recommended.[b]	
xylenes	-	100 (1 year)

[a] Concentration of benzene with an excess lifetime cancer risk of 1:10,000, 1:100,000 and 1:1,000,000 are 17, 1.7 and 0.17 μg m^{-3}, respectively.
[b] Concentration of trichloroethylene associated with excess lifetime cancer risk of 1:10,000, 1:100,000 and 1:1,000,000 is 230, 23 and 2.3 μg m^{-3}, respectively.

There is a wealth of other air pollutants present in indoor environments, from a wide range of sources, many of which have limited measurement data and unknown health effects. Additionally, the cumulative impact of exposure to these potentially hazardous pollutants requires further investigation to gain a more holistic understanding of the health effects of poor indoor air quality.

1.1.2 Sources of indoor air pollution

An increasing number of studies are arising in the field of indoor air research aimed at identifying and apportioning the many sources of pollution indoors. This is vital for developing our understanding of the complexity of indoor air pollution, and identifying potentially hazardous pollutants which require addressing in future policies on indoor air quality. However, difficulty arises due to the large heterogeneity of chemicals found in indoor environments and the number of compounding factors influencing indoor air pollution. Often, studies report information on only a small number of pollutants over a short sampling period and in specific indoor micro-environments, making it impossible to build a holistic and quantitative view of current indoor air pollution in the UK (Lewis et al., 2022).

In the absence of indoor pollutant sources, indoor air quality is determined by outdoor air due to exchange between indoor and outdoor environments (Leung, 2015). Common indoor pollutants which are influenced by outdoor air quality include PM, CO, NO_x, O_3 and VOCs, originating from both anthropogenic and natural sources such as vehicular traffic and wildfire smoke. There are many factors which determine the importance of outdoor pollutants on indoor air quality, including building airtightness, natural and mechanical ventilation systems, geographic locations, and meteorological conditions. There is growing evidence that climate change is having adverse effects on indoor air quality due to increased outdoor pollutant concentrations, and alterations in building features and human behaviour in response to the changing climate (Nazaroff, 2013). For example, increased frequency and severity of extreme weather events such as wildfires can have profound effects on outdoor air quality, which in turn affects indoor pollutant concentrations via infiltration. A study by Shrestha et al. (2019) revealed that long-range wildfire plumes in Colorado, USA, resulted in indoor $PM_{2.5}$ concentrations up to 4.6 times outdoor concentrations, with mechanically ventilated homes exhibiting 18% higher $PM_{2.5}$ indoor/outdoor ratios compared to other homes (Shrestha et al., 2019).

With many emerging studies reporting indoor air pollutant concentrations to be greater

than outdoors, it is evident that indoor sources of air pollution can also play an important role in the pollution of indoor environments. A notable instance of this was found in a study that reported total VOC concentrations in established dwellings approximately four times higher than in outdoor air, illustrating the dominance of indoor sources (Brown, 2002).

Building materials and indoor furnishings are a passive source of pollutants indoors, resulting in higher background concentrations of some pollutants compared to outdoors. Materials such as concrete, wood, adhesives, sealants, and paint emit a range of VOCs, including hydrocarbons, phthalates, aldehydes, ketones, chlorinated compounds, and terpenes (Ruiz-Jimenez et al., 2022). Initial off-gassing of VOCs from construction materials dominate the indoor air pollution in newly built and retrofitted buildings, with VOC concentrations reported to be one to two orders of magnitude greater compared to more well-established buildings (Holøs et al., 2019; Brown, 2002). A review of longitudinal studies suggested that the off-gassing of building materials can persist for more than two years after construction (Holøs et al., 2019). While the primary VOC emissions diminish over time, secondary emissions can increase with time and be long lasting as materials continuously degrade (Brown et al., 2013). For example, formaldehyde, which is a known irritant and carcinogen, is emitted from many resins and adhesives due to the chemical degradation of urea-formaldehyde compounds in these products (World Health Organization, 2010; Salthammer et al., 2010).

Other important sources of indoor air pollutants relate to occupants and their activities. Humans themselves can influence indoor air quality, acting as a source of many pollutants (Kruza and Carslaw, 2019). Over 1000 VOC species have been identified as emissions from human breath, saliva, skin, blood, milk, urine, and faeces, highlighting the large complexity of humans as a source of indoor air pollutants (de Lacy Costello et al., 2014). VOC emissions from humans are particularly significant in highly occupied indoor environments, including offices, classrooms, and theatres. For example, a study by Tang et al. (2016) reported that human-emitted VOCs made up 57% of the VOCs measured in an occupied lecture theatre. A study by Stönner et al. (2018) iden-

tified that the most common VOCs emitted from humans were related to metabolic emissions (e.g., acetone, and methanol) and emissions from personal care products (e.g., monoterpenes, and decamethylcyclopentasilox-ane (D5)), with large variance between occupants owing to biological and behavioural differences.

VOC emissions from skin are impacted by chemical reactions which occur on the skin surface between skin-oil lipids and O_3. This phenomenon is evidenced by the impact of occupancy on indoor O_3 concentrations, in addition to the emissions of oxygenated organic compounds (Lakey et al., 2017). Wang, Ernle, Bekö, Wargocki and Williams (2022) reported VOC emissions in an occupied controlled chamber to double upon the introduction of O_3, illustrating the significance of skin surface lipid/O_3 chemistry on human VOC emissions. This chemistry can act as a source of VOC emissions for days after occupants leave due to the transfer of skin lipids onto indoor surfaces (Liu et al., 2021).

Many occupant activities, such as tobacco smoking, cooking, and the use of household products such as cleaning products, personal care products, and appliances are potentially large, transient sources of indoor air pollutants. An increasing number of studies have investigated the episodic emissions from common household activities in chamber studies and observational measurements. A key study which has contributed to our understanding of how domestic activities influence indoor air quality was carried out in 2018 in Texas, USA. The House Observations of Microbial and Environmental Chemistry (HOMEChem) study investigated the changes in concentrations of reactive trace gases, aerosol particles, and surface films in a test house during a series of sequential and layered experiments involving cooking, cleaning, variable occupancy, and window-opening (Farmer et al., 2019). Key results from this campaign showed that occupant activities such as cooking and cleaning can induce rapid changes in indoor air composition, increasing total gas-phase chemical pollutant levels by up to 4-fold (Hodshire et al., 2022). Another study of 26 residential homes in Alberta, USA, apportioned 44% of indoor VOCs to household products such as cleaning and personal care products, and 11% to combustion processes, including cooking, tobacco smoking,

and biomass burning (Bari et al., 2015).

There is large variability in the type, concentration, and frequency of indoor air pollution from occupant activities, thus making it increasingly difficult to characterise indoor environments in a representative manner. Further work must be carried out to better understand the complexity of indoor pollutant sources, and their potential impacts on occupant health.

1.2 Cleaning products

Cleaning products are chemical formulations consisting of water, solvents, preservatives, and fragrances. Specific products may also contain disinfectants, acids, bases, bleaching agents, abrasives, or enzymes to enhance their cleaning performance (Missia et al., 2012). They are formulated in a variety of forms, including aerosols, liquids, gels, pastes, and solids. Cleaning products represent a transient yet ubiquitous source of air pollutants in indoor environments through both primary emissions and secondary processes arising from reactive indoor air chemistry. Exposure to primary and secondary pollutants from cleaning products depends on the interplay of many factors, including the chemical composition of the product as well as human factors including usage frequency and duration, product amount and concentration, and mode of application. Environmental factors such as air change rate (ACR), temperature, and relative humidity (RH) are also important factors influencing the chemical fate of pollutants from indoor cleaning activities (Nazaroff and Weschler, 2004).

The use of cleaning products has been apparent throughout history, to increase hygiene, improve aesthetics, and preserve materials, with evidence of soap production from animal fats dating back to ancient civilisations (Derry, 1960). The industrial revolution marked a significant expansion in soap production and the introduction of additional cleaning agents such as ammonia (American Chemistry Council, 2023). The creation of specialised cleaning products evolved throughout the 20th century, with a surge in development and marketing occurring after World War II (Omnicom Media Group, 2017). This progression has led to an abundance of household products avail-

able today, with continuous advancements in chemistry and technology continuing to drive the innovation of cleaning products. Growing societal concern for environmental impact and drive for sustainability has led to an increase in the variety of green cleaning products available in the current market. This shift in consumer choice is expected to be a large driver of the cleaning product market, potentially prompting changes in product formulations and their resulting emissions (Mintel, 2021).

The household cleaning product industry is diverse and continually evolving, with an annual retail market value of £826 million in 2021 and a compound annual growth rate in the last 5 years of + 3% in the UK (Mintel, 2023). In 2020, a record-breaking spike in retail market value growth of + 23.3% was reported in the UK, with similar patterns observed globally, in response to the COVID-19 pandemic causing an increase in demand for disinfectant products (Mintel, 2021). The COVID-19 pandemic increased public awareness about the importance of proper cleaning and hygiene practices, resulting in increased frequency of cleaning high-touch surfaces in public buildings. These patterns illustrate the increased presence of cleaning products in our daily lives, potentially leading to higher levels of exposure to indoor air pollutants from cleaning activities.

Several surveys have been performed to assess population exposure to cleaning products, which provide important knowledge about the influence of consumer behaviour patterns on indoor air quality and the associated health risks (Weegels and Veen, 2001; Moran et al., 2012). One international survey carried out in Europe revealed that common household cleaners are used weekly in most domestic dwellings, indicating that many occupants are exposed to elevated indoor pollutant concentrations on a regular basis (Dimitroulopoulou et al., 2015). Furthermore, evidence suggests that occupational exposure to pollutants from cleaning products may be the cause of respiratory effects and asthma prevalence in cleaning staff (Coeli Mendonça et al., 2003).

The current literature surrounding the topic of indoor air pollution from cleaning has attempted to characterise the prominent primary emissions and secondary pollutants, their indoor concentrations, and the potential health risks associated with exposure. A

variety of approaches have been employed to investigate this topic, including process-scale analyses, product use surveys, chamber studies, observational measurements, and modelling studies. The subsequent sections offer a comprehensive review of the present understanding and identification of the knowledge gap, followed by contextualisation within the scope of this PhD research.

1.2.1 Primary emissions

Primary emissions from cleaning products are in part determined by the composition and concentration of volatile components in the formulation. Volatile components include VOCs and inorganic species such as hypochlorous acid (HOCl) (Singer et al., 2006; Wong et al., 2017). A considerable amount of scientific attention has been focussed on VOCs, defined as organic compounds with an initial boiling point less than or equal to 250 °C measured at a standard atmospheric pressure of 101.3 kPa. There is significant variability in VOC emissions from cleaning products, attributable to the increasing diversity of available products with precise technical specifications and properties (Wolkoff et al., 1998). In a study of the direct VOC emissions from 37 common consumer products, including cleaners, Steinemann (2015) identified 156 different compounds, of which fewer than 3% were disclosed on any product label or material safety data sheet. Additionally, 27% of the identified VOCs were listed as toxic or hazardous under US federal laws, highlighting the potential for cleaning product emissions to negatively impact indoor air quality and occupant health (Steinemann, 2015). A second study of 30 cleaning products in the USA identified a total of 735 unique VOCs, with total VOC concentrations ranging from below the limit of detection (LOD) to over 38,000 μg/g product (Temkin et al., 2023). A summary of the main chemical classes of VOCs found in cleaning products is described in Table 1.2.

Table 1.2: Typical VOCs found in cleaning products (Missia et al., 2012; Wolkoff et al., 1998).

VOC class	Examples
Alkanes	hexane, decane and tetradecane
Halogenated alkanes	1,2-dichlorpropane, methylene chloride (no longer used)
Terpenes	monoterpenes: α-pinene, limonene, and many other isomers sesquiterpenes: longifolene, and many other isomers
Aromatics	toluene, ethylbenzene, styrene
Alcohols	ethanol, 2-propanol, butanol, hexanol, 2-phenylethanol, terpene alcohols: linalool, terpineol, and many other isomers
Glycols/glycol ethers	dipropylene glycol, 2-ethoxyethanol, 2-methoxyethanol, 2-(2-ethoxyethoxy)ethanol, 2-(butoxyethoxy)ethanol, 2-(dodecyloxy)ethanol
Ethers	dioxane
Aldehydes	formaldehyde, acetaldehyde, glutaraldehyde
Ketones	acetone, butanone, 2- and 3-octanone, acetophenone
Acids	acetic acid, lactic acid

The most common classes of VOCs emitted from cleaning activities reported in the literature are terpenes and terpenoids. These are unsaturated compounds which are biologically synthesised by a large diversity of plants, and are derived from the isoprene unit (C_5H_8). Terpenes relate specifically to hydrocarbons of the formula $(C_5H_8)_n$, where $n \geq 2$, while terpenoids contain additional functional groups, usually containing oxygen. Terpenes and terpenoids consist of more than 80,000 compounds, demonstrating vast chemical and structural diversity (Christianson, 2017). The chemical structures of some common monoterpenes and monoterpenoids are shown in Figures 1.1 and 1.2, respectively.

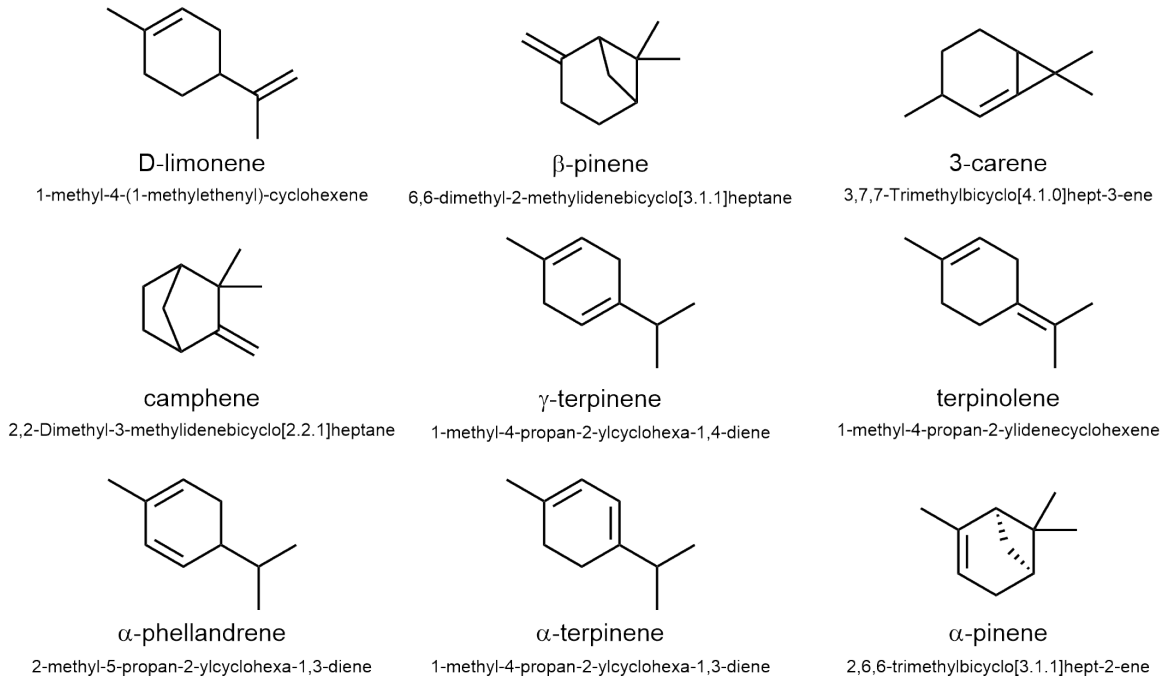

Figure 1.1: Chemical structures and corresponding IUPAC names of common monoterpene species.

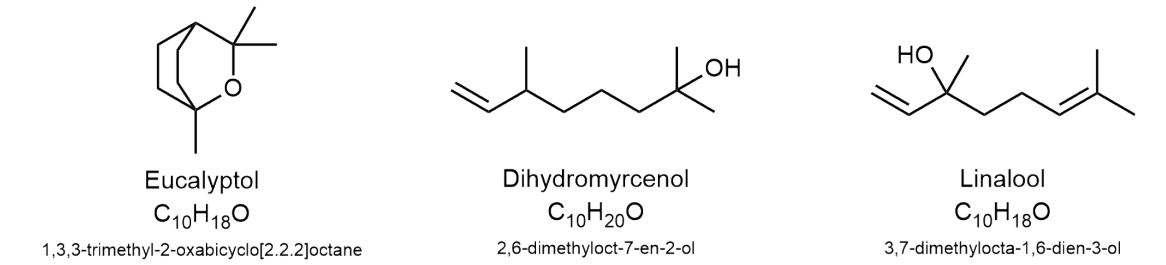

Figure 1.2: Chemical structures and corresponding IUPAC names of common monoterpenoid species.

Many different terpene and terpenoid species have been identified as components of cleaning product formulations experimentally, serving as fragrance components and active solvents. According to an extensive review performed by Milhem et al. (2020), the most common terpene species found in household products include limonene, linalool, citronellol, and β-pinene (Figure 1.3). Cleaning products typically contain individual terpenes at mass concentrations between 0.2% and 2% w/w, with a total terpene concentration of up to 5% w/w (Sarwar et al., 2004). There is large variability in the composition and concentrations of terpenes in commercially available cleaning products

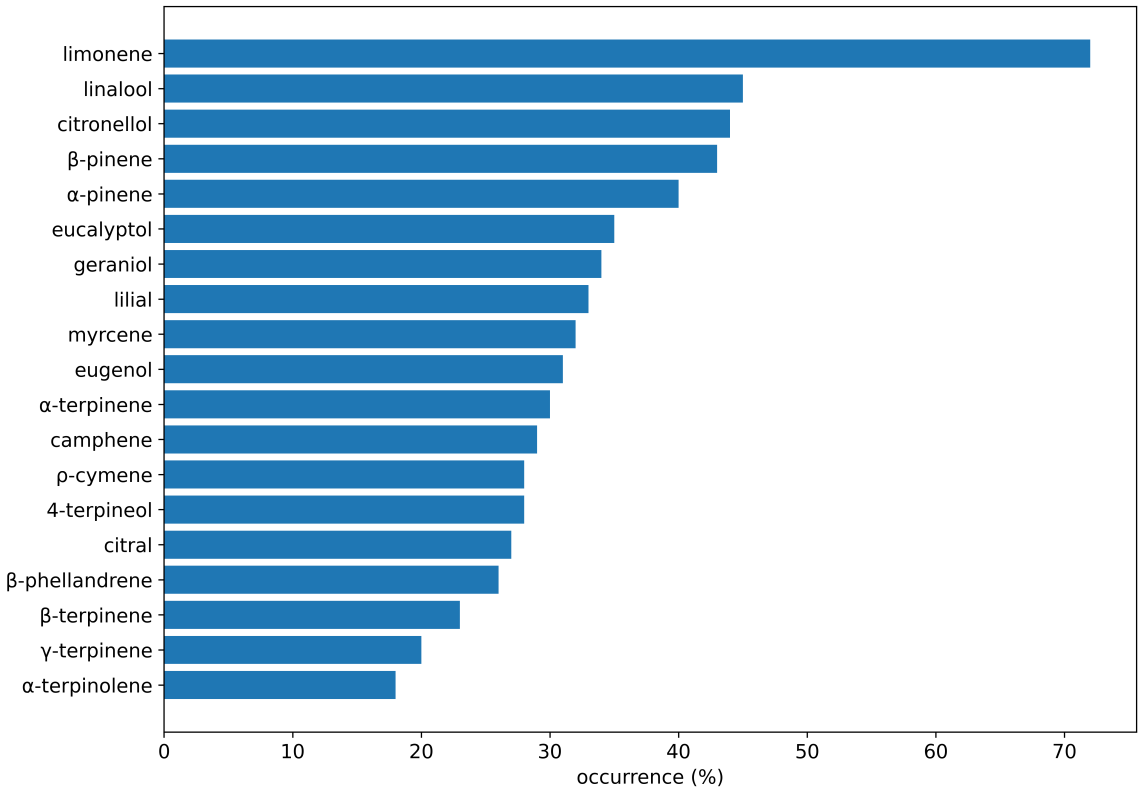

Figure 1.3: Occurrence percentages of terpenoid species identified in 450 household cleaning products, based on data reported from 14 different references published between 2001 and 2015 (according to a review by Milhem et al. (2020))

due to differences in formulation ingredients and desired fragrance profile/cleaning properties. Several studies have directly quantified the terpene content of cleaning products. Angulo Milhem et al. (2021) identified 6 to 20 different terpenoid species in 6 selected cleaning products, with total terpene concentrations ranging from 0.01% to 0.17% w/w. The dominant species identified were limonene, linalool, eucalyptol, and α-terpineol. Additionally, Singer et al. (2006) reported limonene concentrations of 14.7 and 44 mg/mL in two general purpose cleaners, corresponding to 1.47% and 4.4% w/v.

Evidence suggests that the concentration of terpenes in cleaning product solutions does not directly correlate with the concentrations emitted from product use due to differences in compound volatility and chemical affinities with other compounds in the formulations (Angulo Milhem et al., 2021). Therefore, it is essential to measure emis-

sions under realistic scenarios to better characterise the emission dynamics of VOCs associated with cleaning activities. Several studies have employed chamber studies, test house measurements and observational measurements to measure VOC emissions from cleaning under conditions which more closely reflect the high complexity of indoor environments. While chamber studies neglect the true complexity of realistic indoor environments, they are useful for investigating the impact of specific parameters under controlled conditions. For example, Harb et al. (2020) showed that temperature and relative humidity both influence the emissions of limonene from cleaning, with the highest maximum mixing ratio of 38 ppb observed at 23 °C and 50-55% RH.

Several studies have measured cleaning emissions in test houses and real-world settings, resulting in a more accurate representation of indoor environments. The most notable test house study to date is HOMEChem, which was performed in a 1,200 square-foot manufactured home (Farmer et al., 2019). The cleaning activities investigated in this study included floor mopping with a commercial bleach solution and a commercial product labelled as "all natural". Results showed that bleach cleaning resulted in double the amount of primary emissions compared to the natural product. The chemical composition of the total quantified emissions from these two cleaning events were significantly different, with the bleach cleaning event resulting in 82% chlorinated species, and the natural cleaning event resulting in 60% monoterpene species (Arata et al., 2021).

In an observational study of 25 UK houses, limonene and α-pinene were observed to be the most abundant VOCs measured, with 5-day average concentrations ranging from 18 to 14000 μg m^{-3} (Wang et al., 2017). These species showed the greatest amount of variability compared to other VOCs measured, which was attributable to variations in occupant activities between homes. The observed emission patterns showed episodic release of high concentrations of terpenes, representing the use of scented cleaning products and other household products. Calderon et al. (2022) also performed an observational study, measuring VOC concentrations in the breathing zones of women cleaning in their own homes. Results showed that cleaning activities

resulted in increased air concentration and thus exposure to a range of VOCs including chloroform, β-myrcene, and benzene derivatives depending on the type of product used. Evidence suggests that primary emissions of VOCs can persist for extended periods following the cessation of cleaning activities, resulting in prolonged exposure to potentially hazardous air pollutants (Bello et al., 2010).

Aside from the chemical composition of cleaning products, the mode of application is also an important factor which influences the primary emissions from cleaning. For example, products which are applied as a spray can lead to considerable amounts of airborne particles. One study has shown that 2.7% to 33.2% of the mass emitted from a spray bottle can contribute to airborne particle loading, of which 77% are in the relevant size range for respiratory deposition (Lovén et al., 2019). In contrast, products which are applied in diluted form can result in less VOC emissions due to some of the volatile components remaining in the solution and being disposed of down the drain as wastewater. In a chamber study carried out by Singer et al. (2006), emission factors of VOCs from a general purpose cleaner were determined under three different usage scenarios. The results illustrate the impact that different modes of application can have on primary emissions from cleaning, with dilute application resulting in lower levels of VOCs compared to the use of a full-strength cleaner (Figure 1.4).

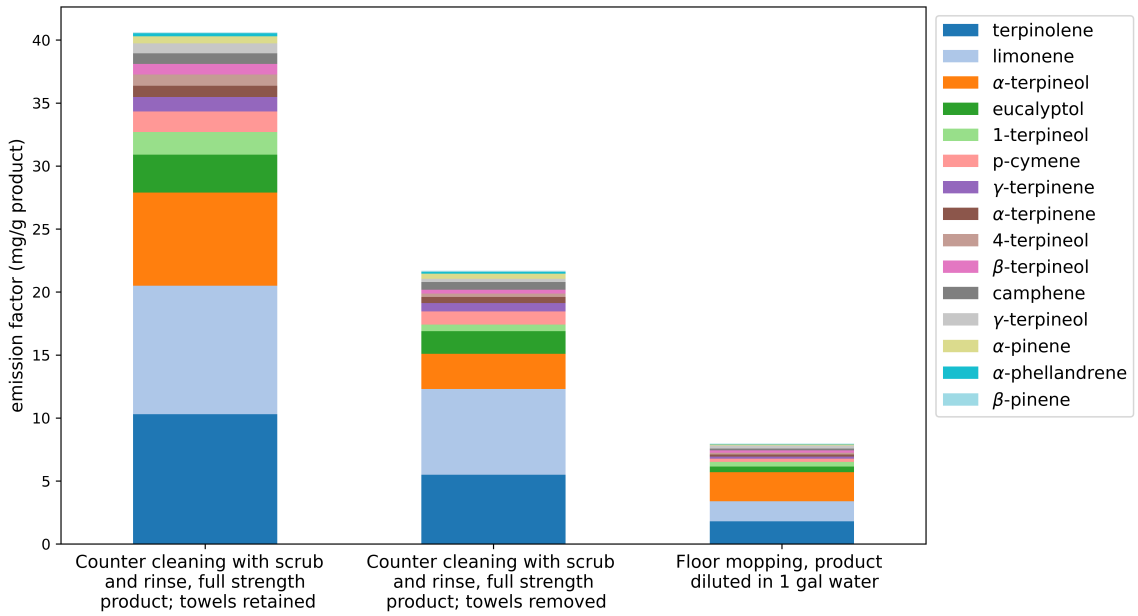

Figure 1.4: Emission factors (mg/g product) of terpenes and terpene alcohols associated with the use of a general purpose cleaner under different usage scenarios within a 50 cm^3 chamber; using full strength cleaner on counters with towels left in chamber or removed after wiping, and using diluted cleaner to mop the chamber floor (Singer et al., 2006).

1.2.2 Secondary pollutant formation through indoor air chemistry

The primary emissions arising from cleaning activities can react with oxidants present indoors such as O_3, hydroxyl (OH), and nitrate (NO_3), generating a range of secondary pollutants. In order for the gas-phase chemical processing of VOC emissions to impact the concentration of secondary pollutants indoors, the rate of reaction must be sufficient to compete with the ACR (Weschler, 2000). The rate of reactions between O_3 and unsaturated VOCs are relevant within typical ACR timescales (0.2 to 1 h^{-1}, Nazaroff (2021)), therefore ozonolysis of unsaturated species is an important source of secondary pollutants indoors.

As stated in the previous section, the use of scented cleaning products indoors can lead to the emission of high concentrations of terpenoid species, particularly monoterpenes. Terpenoids contain one or more unsaturated carbon-carbon double bonds, hence emis-

sions can be an important driver of secondary pollutant formation following cleaning. Electrophilic attack of the carbon-carbon double bond in terpenoid species generates unstable ozonides, which decompose into carbonyls and Criegee biradicals (Figure 1.5). Multiple oxidation steps initiated by O_3/terpenoid reactions result in a large range of secondary products, including reactive radical intermediates and stable products such as aldehydes, ketones, and organic acids (Weschler, 2000).

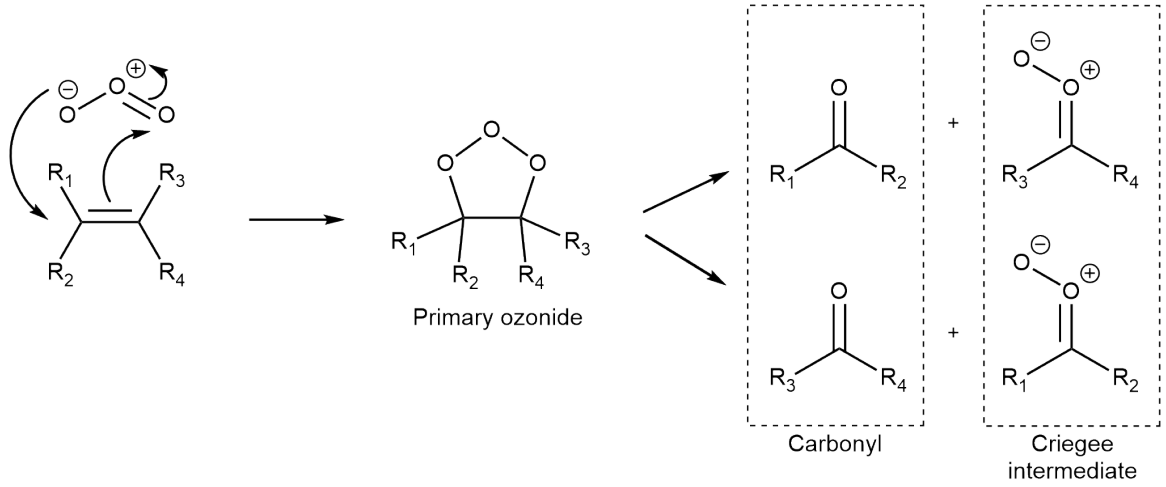

Figure 1.5: Reaction mechanism of O_3 with an unsaturated organic compound. Adapted from Weschler (2000).

Reactive intermediates generated from ozonolysis reactions include species such as the OH, hydroperoxyl (HO_2), and alkylperoxy (RO_2) radicals, which contribute to further oxidation chemistry. Reactions between VOCs and OH generate RO_2 radicals, which contribute to the regeneration of O_3 via the oxidation processes shown in Figure 1.6. Therefore, the oxidation of VOCs emitted from cleaning can drive the creation of additional oxidant and radical species, thus catalysing further oxidation reactions and increasing the oxidative capacity of the indoor environment.

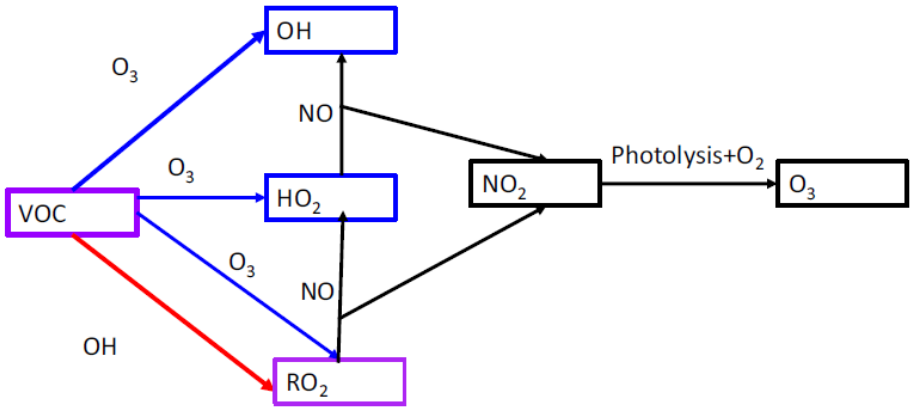

Figure 1.6: Connections between VOC oxidation chemistry, and radical and oxidant generation indoors. Taken from Carslaw and Shaw (2022).

There are many unique oxidation products which result from the oxidation of terpenes, some of which are known to have detrimental health effects. A detailed mechanistic study of limonene gas-phase oxidation pathways revealed that there are approximately 530 secondary species produced, illustrating the potentially extreme complexity of secondary chemistry which occurs following the emission of multiple reactive terpene species from cleaning activities (Carslaw, 2013). This study also identified that the composition and concentrations of secondary pollutants generated from limonene oxidation is dependent on the relative concentrations of O_3 and OH due to differences in the oxidation pathways and products of these two oxidants. Therefore, outdoor pollutant concentrations may impact indoor oxidation chemistry and subsequent secondary pollutant exposure of inhabitants due to geographical variance in outdoor O_3 concentration and the impact this has on indoor O_3 and OH concentrations.

There is growing evidence to suggest that the secondary pollutants from terpene oxidation chemistry are more hazardous to human health than the terpenes themselves. For example, Wolkoff et al. (2000) found that exposure of mice to an O_3/limonene mixture resulted in sensory irritation of the upper airways at concentrations below the no-observed-effect-levels (NOELs) of the parent compounds. Additionally, the detrimental health effects of some terpene/O_3 reaction products are well documented, such as formaldehyde, which is a sensory irritant and human carcinogen (World Health Organization, 2010). The high concentrations of terpenoid species emitted from episodic

cleaning events has the potential to drive elevated formaldehyde concentrations indoors as a result of terpene-O_3 chemistry. For example, relatively high concentrations of formaldehyde (66 μg m^{-3}) were observed in a home with limonene concentrations of approximately 800 μg m^{-3}, owing to the frequent use of cleaning products (Wang et al., 2017). Additionally, increases in indoor formaldehyde levels by the order of 10 ppb were observed by Singer et al. (2006) following various cleaning events, while simultaneous decreases in O_3 and terpenoid concentrations were observed, evidencing the occurrence of terpene/O_3 chemistry.

Many of the secondary products from VOC oxidation reactions are multi-functional and have lower vapor pressure than the parent compound. Therefore, the generation and subsequent partitioning or self-nucleation of these products can contribute to the formation of secondary organic aerosol (SOA). Several studies have provided evidence of SOA formation following the emission of terpenoid species from cleaning. A detailed chemical modelling study explored the chemical composition of SOA formed following the chemical processing of limonene emissions from a cleaning event to be 73% peroxide groups, 18% organic nitrates, ∼3% PANs and acidic material and ∼2% both carbonyl and alcoholic material (Carslaw, 2013). Youssefi and Waring (2014) simulated a cleaning event by pulse-emitting limonene into a ventilated chamber, revealing that the SOA yield directly correlated with the concentrations of limonene and O_3 introduced to the chamber. They also observed a larger SOA yield at lower ACR, demonstrating that longer residence times of reactant species promotes the formation of SOA. Furthermore, Rossignol et al. (2013) observed new particle formation of approximately 87,000 particle cm^{-3} following a cleaning event in an experimental home. Chemical characterisation of the formed particles confirmed the presence of limonene-O_3 reaction products, evidencing their origin from cleaning emissions. The production of SOA from terpene-O_3 chemistry can be significant from cleaning activities due to the potentially large transient terpene emissions. For example, Rosales et al. (2022) found that the respiratory tract dose rates of sub-10-nm SOA generated from a floor mopping event in a ventilated office were comparable to, or greater than, what one would receive from vehicle-associated aerosols outdoors in an urban environment.

A large proportion of the research regarding secondary pollutants from cleaning is focussed on gas-phase terpene-O_3 chemistry. However, the moderate vapor pressure of many terpene species, and the fact that cleaning products are often directly applied to surfaces, means that a proportion of these reactive species from cleaning are often present on indoor surfaces (Milhem et al., 2020). Surface-sorption of cleaning VOCs results in increased indoor residence times due to less removal by air exchange, thus promoting heterogeneous VOC oxidation chemistry. Evidence suggests that the probabilities of some terpene-O_3 reactions on indoor surfaces are approximately 10-100 times greater than the corresponding gas-phase reaction probabilities, highlighting the potential importance of heterogeneous chemistry on secondary pollutant formation (Springs et al., 2011). Heterogeneous chemistry may act as a significant source of secondary pollutant exposure long after cleaning activities cease, as it is not constrained by ventilation. For example, Flemmer et al. (2007) detected secondary emissions for 72 h following the introduction of surface-sorbed α-terpineol to a chamber with 100 ppb O_3 and a flow rate of 300 ml/min. Heterogeneous chemistry may also be an important contributor to SOA formation following cleaning. Waring and Siegel (2013) demonstrated that the SOA yield from limonene-O_3 surface reactions was approximately double that from equivalent gas-phase reactions in a 283 L chamber experiment, indicating stronger nucleation promotion by surface reactions.

1.2.3 Modelling

There is an increasing number of experimental studies which investigate the impact of cleaning on indoor air chemistry and the associated health risks. However, many of these studies involve laboratory and chamber studies, which are not representative of highly complex realistic environments. Several larger-scale test house studies exist, although these do not encompass the broad range of indoor environments and are costly, time-consuming, and technically challenging to execute. Experimental limitations mean that chemically significant species, such as radicals, are difficult to measure experimentally. Therefore, the development of indoor air models is a substantial requirement for better understanding the impacts of cleaning on indoor air chemistry

and to evaluate occupant exposure to primary and secondary pollutants. Modelling has the advantage of being able to provide forecasts and explore hypothetical scenarios not possible through measurements, thus providing a deeper insight into the processing of cleaning emissions indoors (Shaw et al., 2023).

One of the key models used in several studies of the impacts of cleaning on indoor air chemistry is the INdoor CHEMical model in Python (INCHEM-Py), a refactor and improvement of the INdoor Detailed Chemical Model (INDCM) (Carslaw, 2007; Shaw et al., 2023). INCHEM-Py is a zero-dimensional chemical box model which includes processes such as gas-phase and surface emissions and chemistry, physical building parameters (ventilation rate, temperature, humidity, light), surface deposition, and the effect of occupants, to predict changes in species concentrations and key reaction pathways over time.

This model was used to simulate the chemical processing of limonene emissions following the use of a cleaning product, based on experimental observations from Singer et al. (2006) of 200 ppb limonene for 30 minutes (Carslaw, 2013). The results presented in this study showed that the main gas-phase products were multi-functional carbonyl species such as limonaldehyde and 4-acetyl-1-methyl-1-cyclohexene (limonaketone), while particle-phase products were dominated by peroxide species. While the concentrations of secondary pollutants did not exceed human reference values for acute airway effects, it was noted that a realistic cleaning event would likely emit a complex mixture of reactive terpene species, which may enhance the formation of potentially hazardous secondary pollutants.

A second study by Carslaw et al. investigated the concentrations of OH and HO_2 radicals during surface cleaning with a limonene-containing cleaning product (Carslaw et al., 2017). In this study, the model reproduced measured radical concentrations indoors during a small-scale study to within 50% and often within a few %. Elevations in the concentration of secondary products from terpene oxidation, such as heptanal, limonaldehyde and limonaketone, were predicted by the model following the use of the surface cleaner.

Finally, the implications of terpene mixtures emitted from cleaning products on the indoor air chemistry was investigated by Carslaw and Shaw (2022). In this study, several simulations were performed whereby different proportions of limonene, α-pinene and β-pinene were emitted, approximating different typical mixes of terpenes found in cleaning products. The results from this study showed that pure α-pinene was the most efficient at producing particles, pure limonene for nitrated organic material, and a 50:50 mixture of β-pinene and limonene for formaldehyde. The different combinations of terpene emissions gave rise to complex secondary chemistry, revealing the need for a better understanding of the full product mixture in cleaning products, so that comprehensive assessments can be made of the likely impact of different formulations on harmful pollutant production indoors. In this study a sensitivity analysis was also performed, which revealed that higher ACR increased the average concentrations of formaldehyde and PM by $\sim$15%, while reducing that of organic nitrates by $\sim$13% for the 3-hour period following cleaning, compared to when no cleaning occurred. Furthermore, cleaning in the afternoon enhanced concentrations of secondary pollutants for all the mixtures due to higher outdoor O_3 concentrations.

These results reveal the importance of modelling studies to investigate the chemical processing of cleaning emissions in greater detail, identifying potential secondary pollutants which could have implications for occupant health. More extensive field and laboratory measurements are required to develop indoor air chemistry models further, providing measurements and experimental evidence with which to validate models and improve their accuracy in representing the complex chemical and physical processes in indoor environments. In return, indoor air models can provide a framework for interpreting experimental results and drive the direction of future experimental efforts.

1.3 Research objectives

The overarching objectives of this research were as follows:

1. To identify the volatile components within a range of cleaning product formulations, and investigate differences in VOC emissions from regular and 'green' products.
2. To conduct a series of experimental measurements to quantify the indoor air pollution arising from the use of cleaning products in semi-realistic indoor environments.
3. To perform a series of model simulations to investigate how changes in the chemical formulation, environmental conditions and indoor surfaces impact the secondary chemistry which occurs following cleaning.
4. To understand how potential changes to formulation composition, and environmental and building factors could improve indoor air quality and reduce occupant exposure to pollutants following cleaning.

1.4 Thesis outline

This thesis is structured as follows:

Chapter 2 outlines the cleaning products selected to be the focus of this study. A description of the experimental methods for the measurement of VOCs, trace gases and PM is given. A detailed description of the chemical model used to simulate indoor air chemistry is then provided.

Chapter 3 provides a detailed chemical analysis of the VOC composition of regular and green cleaning product formulations. VOC emissions from a typical cleaning activity using each product are then estimated from headspace analysis. Simulations of the cleaning activities and the resulting chemistry are evaluated to predict the secondary pollutant formation from regular and green cleaning products.

Chapter 4 presents indoor and outdoor air quality measurements from cleaning activities in a semi-realistic experimental room. VOC emissions from four cleaning activities using different products are identified. The VOC emissions are then simulated in a typical kitchen, and the resulting secondary chemistry is discussed. The impacts of individual VOC emissions and various environmental factors are investigated in model sensitivity analyses.

Chapter 5 reports measured VOC emissions from typical cooking and cleaning activities performed within a realistic indoor setting. Simulated cooking and cleaning emissions in a range of different kitchen scenarios are then used to evaluate the impacts of material-specific SAVs on background and post-activity indoor air chemistry.

Chapter 6 summarises the overall findings of this thesis and highlights potential future research areas.

Chapter 2

Methodology

2.1 Materials: Product selection

Twenty-three commercially available household cleaning products were selected for comparison (Table 2.1). Four product categories (surface cleaner, bathroom cleaner, floor cleaner and dishwashing detergent) were identified as the most frequently used household cleaners based on results from a European household survey on the use of domestic products (Dimitroulopoulou et al., 2015). Within each product category, multiple "regular" products (those which do not make a claim to be "green" in any way) and "green" products (those which make a claim such as "green", "environmentally friendly", "natural", "plant-based", "nontoxic" *etc.* in relation to the product formulation itself) were selected. The selected products included market leading brands (selected from market size data, Mintel (2023)), budget brands and upmarket brands.

Table 2.1: Product details of household cleaning products tested in this research.

ID	Class	Application mode	Regular	Green	Scented
SR1	surface cleaner	spray	✓		✓
SR2	surface cleaner	spray	✓		✓
SR3	surface cleaner	spray	✓		✓
SR4	surface cleaner	spray	✓		✓
SG1	surface cleaner	spray		✓	✓
SG2	surface cleaner	spray		✓	✓
SG3	surface cleaner	spray		✓	✓
SG4	surface cleaner	spray		✓	
BR1	bathroom cleaner	spray	✓		✓
BR2	bathroom cleaner	spray	✓		✓
BG1	bathroom cleaner	spray		✓	✓
BG2	bathroom cleaner	spray		✓	✓
BG3	bathroom cleaner	spray		✓	
FR1	floor detergent	diluted solution	✓		✓
FR2	floor detergent	diluted solution	✓		✓
FG1	floor detergent	diluted solution		✓	✓
FG2	floor detergent	diluted solution		✓	✓
FG3	floor detergent	diluted solution		✓	✓
FG4	floor detergent	diluted solution		✓	✓
DR1	dishwashing detergent	diluted solution	✓		✓
DR2	dishwashing detergent	diluted solution	✓		✓
DG1	dishwashing detergent	diluted solution		✓	
DG2	dishwashing detergent	diluted solution		✓	✓

2.2 Experimental methods

The following section describes the principles of operation and relevant operating conditions of the experimental methods used during this research. Gas Chromatography Mass Spectrometry (GC-MS) was used for the separation and characterisation of volatile compounds in the laboratory-based experiments described in Chapter 3. Selected-Ion Flow-Tube Mass Spectrometry (SIFT-MS) was used for real-time quantitative measurements of VOCs in both laboratory-based (Chapter 3) and semi-realistic room-scale experiments (Chapters 4 and 5). Additional trace gas and particle in-

strumentation was used to characterise the indoor and outdoor environments during room-scale experiments (Chapters 4 and 5). Additional measurements included $NO/NO_2/NO_x$, O_3, PM, CH_4, CO_2, H_2O, and meteorological variables.

2.2.1 GC-TOF-MS

Gas Chromatography Mass Spectrometry (GC-MS) is a powerful analytical technique which allows the separation and quantification of a wide range of volatile species in complex matrices. Separation of volatile compounds is achieved by vaporising and injecting a sample onto a chromatographic column, where compounds are separated based on their affinity for the stationary phase. Following separation, compounds are detected by mass spectrometry, whereby the molecules are ionised and subsequently separated based on their mass to charge ratio (m/z). The resulting mass spectra are used to provide information about the molecular weight and structure of the analyte, which, in addition to the retention time, can be used for compound identification.

In this work, a 7890B gas chromatograph (Agilent Technologies, USA) coupled to a 7200 Accurate-Mass Q-TOF GC/MS mass spectrometer (Agilent Technologies, USA), with a MultiPurpose Sampler MPS Dual Head autosampler (GERSTEL GmbH & Co.KG, Germany) operated in headspace mode with a pre-heating module, was used to analyse the volatile fraction of cleaning products by equilibrium headspace GC-TOF-MS.

2.2.1.1 Incubation optimisation

A range of sample incubation times and temperatures were tested to optimise sensitivity of the equilibrium headspace GC-TOF-MS analytical method for qualitative VOC characterisation. The peak areas of the top 10 chromatogram peaks obtained from analysis of SR1 at varying incubation times and temperatures are shown in Figures 2.1a and 2.1b, respectively. While increasing the incubation time and temperature across the test range generally increased the peak areas, it also increased the method duration and background noise levels, thus lowering sensitivity. Therefore, an incuba-

tion time of 5 minutes and temperature of 50 °C was selected to achieve an efficient and sensitive method for the identification of VOCs in the sample headspace.

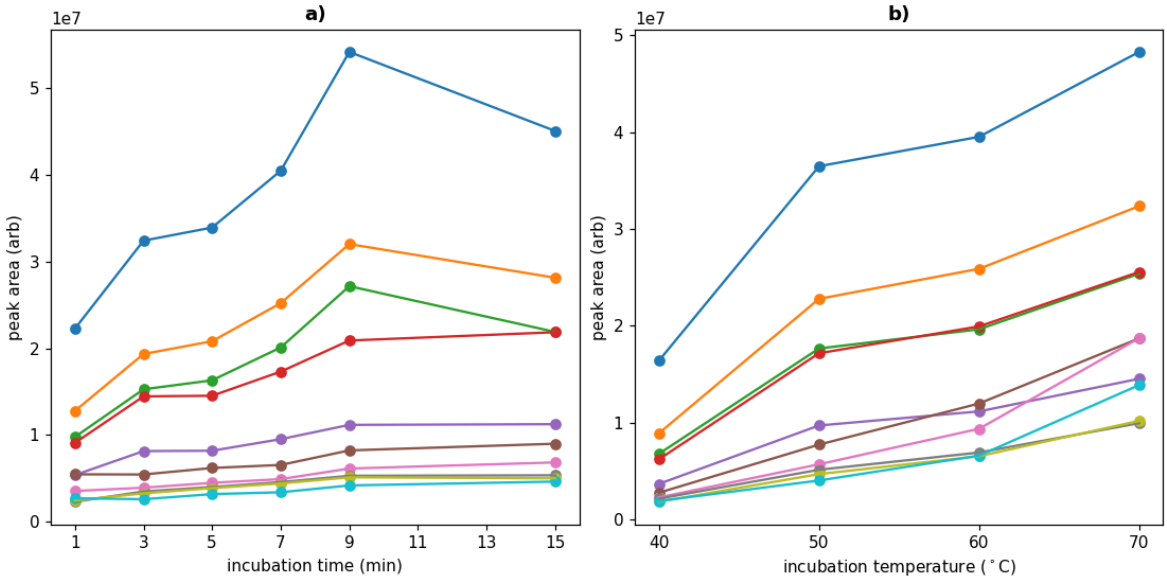

Figure 2.1: Peak areas of the top 10 peaks identified in the chromatogram of SR1 when analysed by equilibrium headspace GC-TOF-MS with varying headspace sample incubation conditions. a) incubation times varying from 1-15 minutes (incubation temperature 50 °C), b) incubation temperature varying from 40-70 °C (incubation time 5 minutes).

2.2.1.2 Operating conditions

The GC-TOF-MS was operated with a split ratio of 1:10 and an inlet temperature of 290 °C. A BPX5 column (50 m × 320 μm × 1 μm) was used for chromatographic separation, with a helium carrier gas at a flow rate of 1.5 mL/min. The duration of the method was 34 minutes, with the following oven temperature program: 40 °C (2 min), 10 °C/min to 125 °C (3 min), 10 °C/min to 300 °C (3 min). The detector temperature was 310 °C.

2.2.1.3 Monoterpene quantification

The monoterpene fraction of the cleaning products was quantified using external calibration standards to account for different sensitivities of the monoterpene compounds towards the detector. A standard solution of α-pinene, camphene, β-myrcene, α-

phellandrene, d-limonene, γ-terpinene and terpinolene in 50:50 H_2O:CH_3OH (2 μg/L) was prepared. Calibration standards were prepared and analysed in the range 125 – 1000 ng/L with the addition of internal standard. The concentrations of monoterpenes in the samples were quantified using the resultant calibration curve (Figure 2.2). For monoterpene species which were not present in the analytical standard, an average of the instrument response to all monoterpenes in the standard was assumed. For β-pinene and α-terpinene, the instrument response was assumed to be equivalent to that of their isomers, α-pinene and γ-terpinene, respectively.

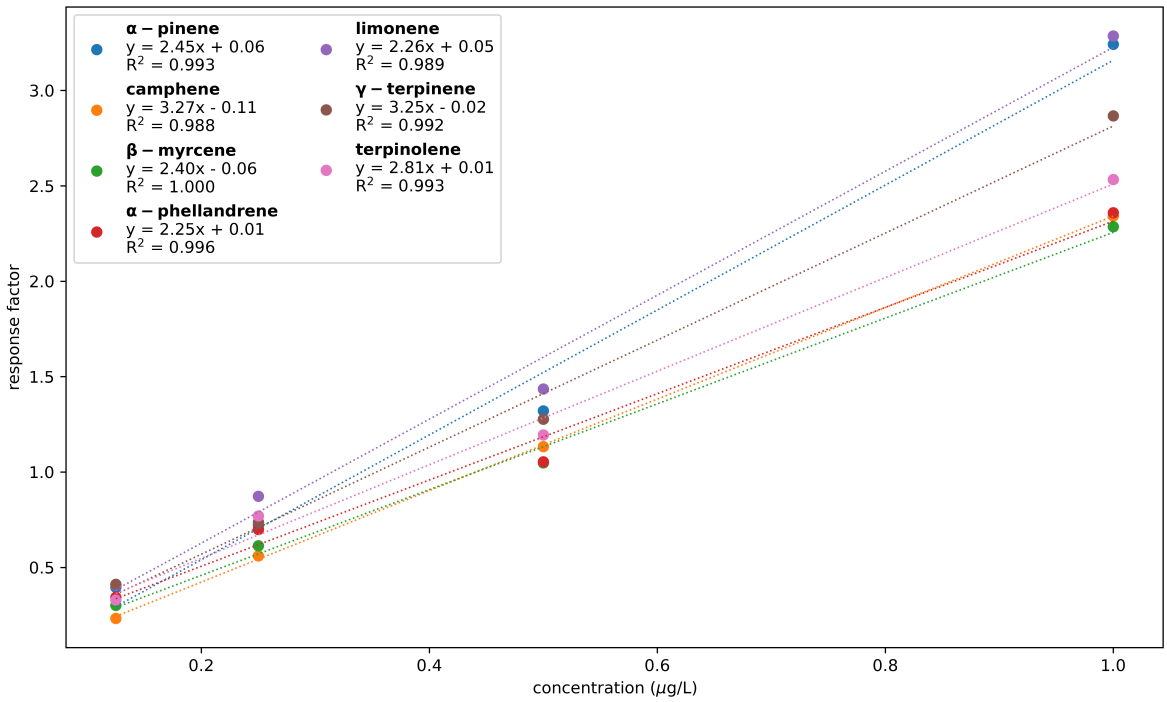

Figure 2.2: Calibration curve obtained from equilibrium headspace GC-TOF-MS of monoterpene standards in 50:50 H_2O:CH_3OH with internal standard, concentration range 0.125 - 1.00 μg/L.

2.2.2 SIFT-MS

SIFT-MS is an analytical method that was developed for accurate, real-time quantification of trace gases at detection limits of as low as parts per trillion. SIFT-MS is based on the selected ion-flow tube (SIFT) technique, which was first developed to study the fundamentals of ion-molecule reactions that occur in the terrestrial atmosphere (Smith and Adams, 1987). It was later adapted and applied to direct-injection mass

spectrometry (DI-MS) for accurate, time-resolved VOC analysis of breath (Spanel and Smith, 1996). Applications of this technique have since expanded to include real-time trace gas analysis of air and liquid headspace.

Traditional chromatographic techniques (*e.g.*, GC-MS) used to quantify trace gases in breath and air samples require cryogenic/adsorption trapping of relatively large sample volumes before chromatographic separation and subsequent detection, which typically takes tens of minutes to an hour (Phillips and Greenberg, 1992). SIFT-MS directly analyses samples with no pre-treatment, thus enabling a high time resolution of seconds. Additionally, while GC-MS techniques typically employ electron ionisation which results in extensive analyte fragmentation and loss of molecular weight information, SIFT-MS utilises soft chemical ionisation, thus resulting in high specificity (Smith and Španěl, 2005). Consequently, SIFT-MS can be used for real-time monitoring and quantification of trace gases in air and breath samples. The high time resolution of this analytical method makes it well-suited for the measurement of VOC emission profiles in fast processes.

A SIFT-MS instrument (Voice200Ultra, Syft Technologies, Christchurch, NZ) was used in this research to quantify VOCs directly emitted from cleaning products by headspace analysis and for real-time monitoring of indoor and outdoor air composition during semi-realistic cleaning experiments (Figure 2.3).

2.2.2.1 General process

Ions are generated from moist air in a microwave plasma, from which the reagent ions are selected using a quadrupole mass filter (QMF). Common reagent ions selected for positive ionisation are H_3O^+, NO^+ and O_2^+, due to their chemical inertness towards the bulk components of air (nitrogen, oxygen, argon, carbon dioxide, and water). The pure stream of reagent ions is injected into a fast-flowing inert carrier gas where excess energy is removed by collisions and the ions are carried through the flow tube. The sample gas is introduced into the carrier gas at a known flow rate at a point downstream of the ion injection point. Trace gases present in the sample gas are sub-

sequently ionised by reaction with the reagent ions in the flow tube. Owing to the multiple reagent ions used, the SIFT-MS technique is capable of ionising (and therefore detecting) a wide range of VOCs via multiple ion-molecule reaction mechanisms, summarised in Table 2.2.

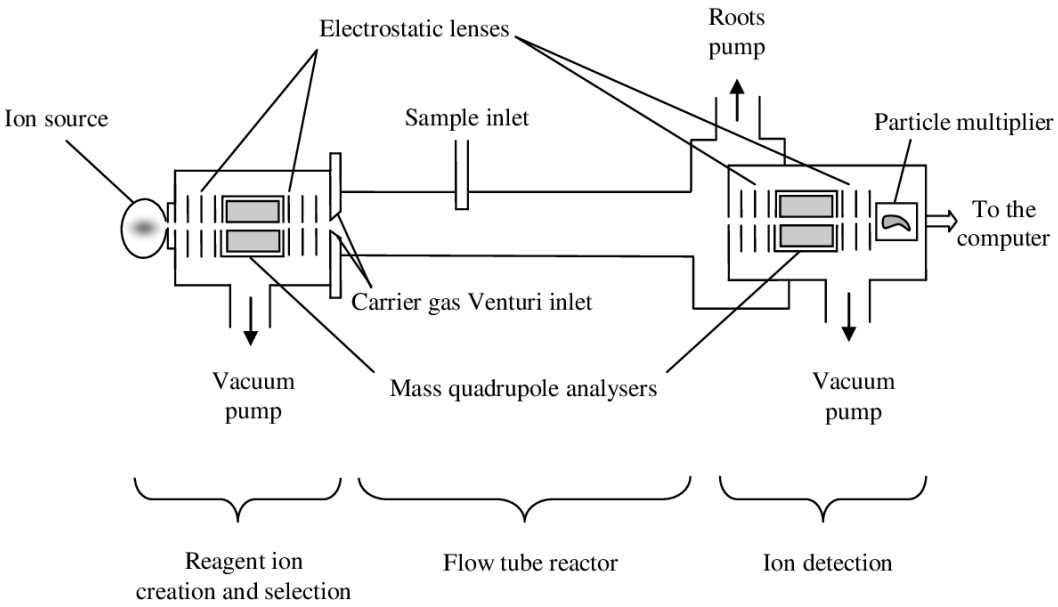

Figure 2.3: A schematic diagram of of the SIFT-MS instrument used for real-time VOC measurements (Reed, 2010).

Table 2.2: Common ion–molecule reaction mechanisms of the SIFT-MS reagent ions and the resulting product ion m/z relative to the parent molecule molecular weight.

Mechanism	Reagent ions(s)	General equation	Shift relative to parent molecule
Proton transfer	H_3O^+	$H_3O^+ + R \longrightarrow RH^+ + H_2O$	+ 1
Electron transfer	NO^+	$NO^+ + R \longrightarrow R^+ + NO$	0
	O_2^+	$O_2{}^+ + R \longrightarrow R^+ + O_2$	0
Hydride abstraction	NO^+	$NO^+ + RH \longrightarrow R^+ + HNO$	- 1
Hydroxide transfer	NO^+	$NO^+ + ROH \longrightarrow R^+ + HNO_2$	- 17
Association	NO^+	$NO^+ + R + M \longrightarrow [R \cdot NO]^+ + M$	+ 30

The characteristic product ions generated through this chemistry, as well as unreacted reagent ions, are sampled downstream from the flow tube via a pinhole orifice into

a differentially pumped QMF. Detection of the ions at each m/z is achieved using a particle multiplier detector. This information is interpreted by an on-line computer, which identifies the product ions and calculates the absolute concentration of analytes in the sample gas using the process outlined in the following section.

2.2.2.2 Compound identification and quantification

The ion-molecule reactions that occur in SIFT-MS are reproducible owing to the low energy of reagent ions, controlled through thermalisation with the carrier gas. Therefore, the product ions generated are characteristic of a particular analyte, with minimal fragmentation observed. The product ions, fragment ions, and branching ratios of ion-molecule reactions for each reagent ion are interpreted by the on-line computer to identify compounds. However, there are some cases where isobaric compounds cannot be accurately differentiated because they exhibit the same product and fragment ion m/z, and similar branching ratios.

Throughout this research, SIFT-MS was used in selected ion mode (SIM) to quantify a set of targeted compounds in real-time. In this mode, specific reagent and product ion masses are scanned by the downstream QMF, and their count rates measured repeatedly by the particle multiplier detector. The ratio of reagent and product ion count rates are used, along with the known rate coefficients of the ion-molecule reactions (taken from a large kinetic database provided by Syft Technologies) and the known dilution of the sample gas into the carrier gas, to calculate the concentration of analyte in the sample gas. The calculation, summarised in equations 2.1 and 2.2, is performed using the LabSyft Software Package (v1.6.2).

$$[M] = \frac{1}{t} \frac{\frac{I_{p1}}{D_{ep1}} + \frac{I_{p2}}{D_{ep2}} + \cdots}{f_{i1} I_{i1} k_1 + \frac{I_{i2}(\frac{k_1+k_2}{2})}{D_{ei2}} + \cdots} \tag{2.1}$$

Where $[M]$ is the number density of trace gas molecules in the flow tube, t is the reaction time, I_{p1}, I_{p2} and I_{i1}, I_{i2} are the count rates of product and reagent ions corrected for mass discrimination and dead time, respectively, k_1 is the rate coefficient

for reagent ions with M, k_2 is the rate coefficient for reactions of hydrated reagent ions with M, and D_{ep1}, D_{ep2} and D_{ei1}, D_{ei2} are the product and reagent ion differential diffusion enhancement correction factors, respectively. It is assumed that the number density of M is proportional to the sum of the signal intensities of all product ions for a given compound.

For accurate quantitation it is necessary to account for the differential diffusion of ions to the walls of the flow tube and the mass discrimination of the quadrupole mass filter, although these effects tend to cancel themselves out. The effects of differential diffusion enhance the count rate of heavier m/z ions and is corrected for in the differential diffusion enhancement correction factors (D_{ei}), while mass discrimination at the downstream QMF diminishes the count rate of heavier m/z ions and is corrected for in the count rate terms (I). These terms are also corrected for dead time, which is the minimum time between two consecutive counts after which they can be recorded as separate events.

The relative concentration of a trace gas in the sampled air (ppb) is defined as $\frac{p_a}{p_0}$, as follows:

$$\frac{p_a}{p_0} = \frac{[M]k_bT}{p\frac{(\Phi_c+\Phi_a)}{\Phi_a}} \tag{2.2}$$

Where p_a is the partial pressure of trace gas a, p_0 is atmospheric pressure, k_b is the Boltzmann constant, T is the carrier gas temperature, p is the flow tube pressure, and Φ_c and Φ_a are the flow rates of the carrier gas and sample air, respectively.

A summary of the target VOCs measured by SIFT-MS in this research are reported in Table 2.3. The target analytes, and their corresponding reagent and primary product ions used for quantification, are reported for headspace and field measurements. The full list of ion masses scanned in SIM mode is specific to each dataset and will be provided per Chapter. Because of the inability of SIFT-MS to differentiate between the product ions of monoterpenes ($C_{10}H_{16}$, m/z 136) and sesquiterpenes ($C_{15}H_{24}$, m/z 205), these species are reported as total monoterpenes and total sesquiterpenes,

respectively.

Table 2.3: A summary of the analytes measured in headspace and field experiments by SIFT-MS in selected ion monitoring (SIM) mode. The product ions used for quantification only are reported here. The full lists of ion masses scanned per study are detailed in individual chapters.

Compound	Reagent ion	Product ion	Dynamic headspace measurements	Field measurements
1,2,4-trimethyl benzene	O_2^+	$C_9H_{12}^+$	✓	
2-phenethyl acetate	O_2^+	$C_8H_8^+$		✓
	NO^+	$C_8H_8^+$	✓	
2-tert-butylcyclohexyl acetate	NO^+	$C_{10}H_{18}^+$	✓	✓
acetaldehyde	H_3O^+	$C_2H_4O \cdot H^+$	✓	✓
total sesquiterpenes	H_3O^+	$C_{15}H_{25}^+$		✓
	NO^+	$C_{15}H_{25}^+$	✓	
benzene	NO^+	$C_6H_6^+$	✓	✓
benzyl benzoate	NO^+	$C_9H_{10}O_2NO^+$	✓	✓
cinnamaldehyde	O_2^+	$C_9H_8O^+$		✓
	NO^+	$C_9H_8O^+$	✓	
citral	H_3O^+	$C_{10}H_{17}O^+$	✓	✓
dihydromyrcenol	O_2^+	$C_{10}H_{19}^+$	✓	✓
ethanol	H_3O^+	$C_2H_7O^+$	✓	✓
eucalyptol	NO^+	$C_{10}H_{18}O^+$		✓
eugenol	NO^+	$C_{10}H_{12}O_2^+$	✓	✓
formaldehyde	H_3O^+	CH_3O^+	✓	✓
lactic acid	NO^+	$CH_3CH(OH)CO^+$	✓	✓
total monoterpenes	NO^+	$C_{10}H_{16}^+$	✓	✓
m-xylene	NO^+	$C_8H_{10}^+$	✓	
methanol	H_3O^+	CH_5O^+	✓	✓

2.2.2.3 Validation, calibration and background subtraction

Owing to the stability of the ionisation process used in SIFT-MS, the product ion formation and branching ratios are determined with good accuracy. The reaction coefficients, product ion masses and branching ratios provided in the LabSyft kinetic library therefore enable good precision of quantitation for SIFT-MS. Low drifts in response (<10 %) have been reported in the literature, hence the need for regular calibrations of the instrument is regarded as low (Langford, 2023).

Regular validation should be performed using an automated process whereby the mass calibration is validated and the transmission efficiency of the downstream QMF is quantified using a certified gas standard. Using the LabSyft library with daily validation alone is reported to achieve an accuracy of ± 35% for compound quantification (Syft Technologies Training Materials, 2014; Langford et al., 2014). For all experiments performed in this research, automated SIFT-MS validation was performed regularly. However, for greater accuracy of quantitation, additional external calibrations were performed for compounds for which there were gas standards available. Compounds which were not externally calibrated were quantified based on branching ratios and reaction rate constants for reagent ions with the specific compounds (provided by the LabSyft kinetic library), and an uncertainty of ± 35% was assumed.

For each field deployment of the SIFT-MS, external calibrations were routinely performed using a custom-built automated gas calibration unit (AGCU) (Wagner et al., 2021). The AGCU was used to perform stepwise dilutions of calibrant gas, which were measured by the SIFT-MS to generate a multi-point calibration curve per compound (Figure 2.4). Two gas standards were used for SIFT-MS calibration: a 14-component gas standard (1 ppm certified National Physical Laboratory, UK) and a limonene only standard (1 ppm in N_2). The limonene standard was prepared in-house by injecting a controlled amount of liquid standard (Sigma Aldrich, 99.8 % purity) into an evacuated gas cylinder and subsequently pressurising the cylinder with research-grade N_2 (N6, BOC). The resulting limonene concentration was determined via GC-FID (calibrated using 1 ppm limonene in N_2 standard, NPL) after 7 days equilibration

at room temperature. Each gas standard was diluted in the AGCU using zero air which was provided by a heated palladium alumina-based zero air generator. The 14-component gas standard was diluted to a concentration range of 1 to 10 ppb, while the limonene gas standard was diluted to a range of 1.8 to 18 ppb. Each concentration step was measured for 3 minutes, with the first and last 30 seconds of each step being discounted to minimise the error associated with instrument equilibration between concentration steps. The resulting data was used to generate a multi-point calibration curve, from which the calibration factor was derived by linear regression analysis (Figure 2.4b).

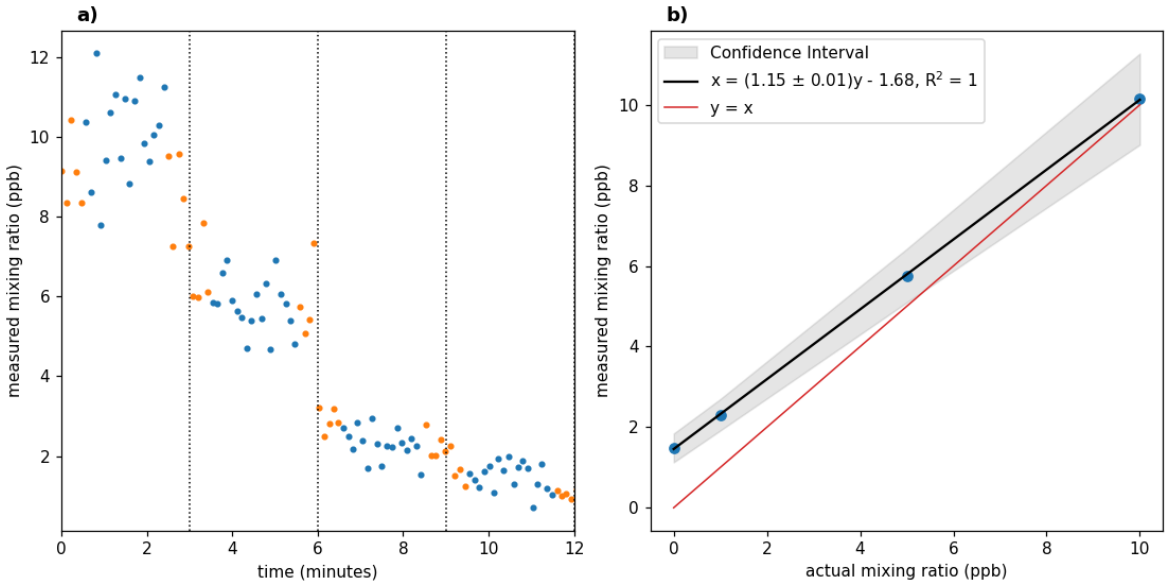

Figure 2.4: An example of SIFT-MS reference calibration for methanol using a 14-component gas standard (1 ppm certified National Physical Laboratory, UK), diluted with N_2 to 0 - 10 ppb using the AGCU. a) Mixing ratio of methanol measured during the automated step-down calibration process. The middle 2 minutes of each step (blue) were averaged to produce the multi-point calibration curve. Orange datapoints were discounted to minimise the error associated with instrument equilibration between concentration steps. b) Calibration curve produced from the automated calibration process, with linear regression analysis to determine the calibration factor (1.15) and standard error (0.01).

All data from the field measurement campaigns were calibrated using the most recently acquired calibration factors, where available. No external calibrations were performed as part of the lab-based headspace experiments. Therefore, this data was calibrated using the average of multiple calibrations performed during the period of 2020-2022 for

each compound. The error in these calibration factors were calculated as the standard deviation of the individual calibration factors. The specific calibration factors applied to SIFT-MS data will be detailed in the respective chapters.

For all measurements of indoor/outdoor air made with SIFT-MS during field measurement campaigns, the instrument background was assessed daily and subtracted from the data. The instrument background was determined as the 3-minute average VOC mixing ratios measured when sampling zero air provided by the heated palladium alumina-based zero air generator. For the headspace SIFT-MS measurements, background VOC mixing ratios were determined as the 2-minute average VOC mixing ratios measured when sampling N_2 carrier gas from the dynamic headspace apparatus prior to sample introduction. Headspace background VOC mixing ratios were calculated per sample and were subtracted from each corresponding dataset.

2.2.2.4 Operating conditions

The operating conditions of the SIFT-MS instrument used for the dynamic headspace and field measurements carried out in this research are summarised in Table 2.4.

Table 2.4: Operating conditions used for SIFT-MS measurements during the dynamic headspace measurements and field measurements carried out in this research.

Parameter	Dynamic headspace measurements	Field measurements
Flow tube temperature	120 °C	120 °C
Flow tube pressure	460 mTorr	460 mTorr
Voltage	25 V	25 V
Sample flow rate	5 sccm	100 sccm
Carrier gas flow rate	120 sccm	25 sccm
Microwave ion source current	40 mW	40 mW
Microwave ion source pressure	400 mTorr	300 mTorr

For all SIFT-MS measurements, N_2 carrier gas was used as a inexpensive and renewable alternative to helium, for which there is a global shortage. The use of N_2 as a carrier gas causes the energy of the system to be higher, resulting in the formation of adducts

such as H_3O+N_2 at 0.5 mbar and room temperature, which catalyses water clustering (Smith, 2020). To mitigate this effect, a flow tube temperature of 120 °C was used, much higher than the 27 °C temperatures of previous studies (Smith et al., 1998; Smith and Španěl, 2005).

For all SIFT-MS measurements, the total flow rate through the instrument was 125 sccm. For field measurements, the sample flow rate was 4 times the carrier gas flow rate, whereas for headspace measurements the sample flow rate was only 4% the total flow rate. The sample flow rate of the headspace measurements was set much lower than field measurements because larger VOC concentrations were achieved in the closed, small volume headspace apparatus compared to the VOC concentrations in ambient air. Therefore, it was necessary to reduce the sample flow rate and the volume of sample introduced to the headspace chamber to avoid excessive consumption of reagent ions. If more than 10% of the reagent ion signal is consumed by ion-molecule reactions with analyte molecules in the flow tube, the ratio of product ion count to reagent ion count becomes non-linear, and accurate quantification is no longer possible.

2.2.3 Additional trace gas and particle instrumentation

2.2.3.1 $NO/NO_2/NO_x$

Chemiluminescence

Concentrations of NO, NO_2 and NO_x in indoor and outdoor air were measured using a chemiluminescence NO-NO_2-NO_x analyser (Thermo Scientific, Model $42i$). This analyser uses the characteristic luminescence that is generated from Reaction 2.3 to determine the concentration of NO in a sample:

$$NO + O_3 \longrightarrow NO_2 + O_2 + h\upsilon \tag{2.3}$$

Air is drawn into the analyser and flowed through a capillary, before being split into two channels. The first channel (NO mode) is directed straight to a reaction chamber,

which is supplied with O_3 generated from dry air via a silent discharge ozonator. The second channel (NO_x mode) passes through a molybdenum NO_2-to-NO converter before being directed to the reaction chamber. The sample flow to the reaction chamber is measured by a flow sensor.

At the reaction chamber, O_3 reacts with the NO in the sample to produce excited NO_2 molecules which then decay to lower energy states, generating infrared light which is detected by a photomultiplier tube. The intensity of the luminescence generated from Reaction 2.3 is linearly proportional to the concentration of NO, thus the concentrations of NO and NO_x in the air sample is determined in the NO and NO_x modes. The concentration of NO_2 is calculated from the difference between the concentrations of NO and NO_x.

Differential absorption spectroscopy

Measurements of NO, NO_2 and NO_x in indoor and outdoor air were also made using an Airyx Iterative Cavity enhanced DOAS (ICAD) NO_x analyser. The ICAD analyser utilises iterative cavity enhanced DOAS (differential optical absorption spectroscopy) to measure the concentration of NO_2/NO_x in ambient air.

Sample air and zero air (provided by a NO_2 scrubbing system) are drawn into the ICAD NO_x analyser at a controlled flow rate via a Teflon filter to filter out aerosols, before entering the measurement cell. The measurement cell is a 40-50 cm long optical cavity with an LED light source in the spectral range between approximately 430 to 465 nm. The absorption of NO_2 in the sample gas in the UV-vis range is detected by a spectrometer, as well as the absorbance at a reference wavelength (a nearby wavelength where NO_2 does not absorb) of the zero air. The difference between sample and reference signals generates a differential signal, the strength of which is directly proportional to the concentration of NO_2 in the sample gas. Iterative analysis is performed, whereby an initial estimate of the analyte concentration is made and compared to the actual measurement, and the residuals are assessed. Multiple iterations of the analyte concentration estimate are performed until convergence is reached, thus obtaining an

accurate measurement (Horbanski et al., 2019).

Additional measurement of NO_x is achieved in a second measurement cell using the same principle. The sample gas is flowed through a NO to NO_2 converter, where gas-phase NO is titrated by O_3 (Reaction 2.3). The resulting NO_2 measurement represents the concentration of NO + NO_2 in the sample gas.

2.2.3.2 O_3

The concentration of O_3 in indoor and outdoor air was measured using a UV photometric O_3 analyser (Thermo Scientific, Model $49i$). This analyser uses O_3 absorption of UV light at wavelength 254 nm to calculate the O_3 concentration in the sample air using the Beer-Lambert Law:

$$\frac{I}{I_0} = e^{-KLC} \tag{2.4}$$

where K is the molecular absorption coefficient of O_3 at 308 cm^{-1} (at 0 °C and 1 atmosphere), L is the length of the cell (38 cm), C is the concentration of O_3 (ppm), I is the UV light intensity of the sample gas, and I_0 is the UV intensity of the reference gas.

Sample air is drawn into the analyser, before being split into two channels. One channel is flowed through an O_3 scrubber to generate the reference gas (containing no O_3). Each channel is flowed through a cell which is illuminated with a photometer lamp. The UV intensity at the opposite end of the cell is measured by a UV detector. The UV absorbance by O_3 is determined by switching the flow of reference and sample gas between the cells every 10 seconds, ignoring the light intensity for the first few seconds after switching to allow the cells to flush. The O_3 concentration in the sample gas is calculated from the Beer-Lambert equation (2.4), and as an average of the two cells.

2.2.3.3 CO_2, CH_4, H_2O

An Ultraportable Greenhouse Gas Analyzer (UGGA) (Los Gatos Research Inc., USA) was used to quantify CO_2, CH_4, and H_2O in indoor and outdoor air. The UGGA instrument uses off-axis integrated cavity output spectroscopy (OA-ICOS) to detect and quantify CO_2, CH_4, and H_2O in a gaseous matrix.

Filtered sample air is pumped through an optical cavity, into which a laser beam is directed in an off-axis configuration. Off-axis ICOS creates an effective path length of several thousand metres, thus enhancing the measured light absorption (Wagner et al., 2021). The sample absorption spectrum is measured using a photodetector, and combined with the measured gas temperature and pressure, effective path length and known line strength to determine the mixing ratios of CO_2, CH_4, and H_2O in the sample using the Beer-Lambert Law.

The UGGA instrument was operated at a 1 Hz time resolution, with a response time of 1 second. The measurement range of the UGGA was 0.01 - 100 ppm, 1 - 20000 ppm, and 500 - 70000 ppm for CH_4, CO_2, and H_2O, respectively. The instrument was calibrated using an analytical gas canister standard prior to each deployment.

2.2.3.4 PM, temperature, relative humidity

Indoor and outdoor measurements of PM_1, $PM_{2.5}$, PM_{10}, temperature and relative humidity were made using Modulair-PM air quality sensors (QuantAQ Inc., USA). For each campaign, one sensor was located on the interior of the experimental facility and another was located on the exterior, at roughly 2.4 m above ground level. Each sensor provided continuous, real-time measurements of PM concentrations, temperature and relative humidity throughout the campaigns. PM concentrations (range 0 to 2,000 $\mu g/m^3$) and particle size distributions (range 0.35 to 40.0 µm, 24 bins) are determined using multiple light scattering-based particle sensors. The sensors measured temperature in the range -40 - 85 °C (± 0.2 °C) and relative humidity in the range 0 - 100 % (± 2%).

2.3 Chemical model

Emission rates of VOCs obtained from experimental measurements throughout this thesis were applied to an indoor air chemical model to gain a deeper understanding of how primary emissions from cleaning are chemically transformed in a typical indoor environment. The advantage of using a chemical model is that it can provide information regarding species production/loss pathways and determine the formation pathways of key secondary pollutants. Additionally, chemical models can be used to provide chemical detail that is not feasible to determine experimentally through measurements (e.g., radical concentrations). However, it is important to acknowledge that while chemical models offer valuable insights, their applicability to real-world scenarios may be constrained by the simplifying assumptions they rely upon.

2.3.1 INCHEM-Py: Overview

INCHEM-Py v1.2 was used for all modelling aspects in this thesis. The Indoor CHEMical model in Python (INCHEM-Py) is an indoor air chemical model which was devised by Shaw and Carslaw (2021) and is a refactor of a previous model, the INdoor Detailed Chemical Model (INDCM) (Carslaw, 2007). INCHEM-Py is an open source 0-D box model that creates and solves a system of coupled Ordinary Differential Equations (ODEs) to predict temporal concentrations of indoor air pollutants. The Master Chemical Mechanism (MCM) is utilised in the model to provide a near-explicit chemical mechanism describing the gas phase degradation of atmospherically relevant VOCs (Jenkin et al., 1997; Saunders et al., 2003). Additional chemical schemes and mechanisms have been developed to better represent the indoor air chemistry, including additional gas-phase chemistry, surface deposition, indoor/outdoor air change, indoor photolysis processes and gas-to-particle partitioning for three common terpenes.

The general equation for the ODEs that describes the change in concentration (C) of species i through time is shown in Equation 2.5. The equation includes terms which describe the chemical processing, indoor-outdoor air exchange, deposition processes and emissions, each of which will be described in greater detail in the following sec-

tions.

$$\frac{dC_i}{dt} = \sum R_{ij} + (\lambda_r C_{i,out} - \lambda_r C_i) - \nu_{d_i} \left(\frac{A}{V}\right) C_i \pm k_t \tag{2.5}$$

Where $R_{i,j}$ is the sum of the reaction rates of species i with all other species j, λ_r is the air change rate (ACR, s^{-1}), $C_{(i,out)}$ is the outdoor concentration of species i (molecule cm^{-3}), ν_{d_i} is the deposition velocity of species i (cm s^{-1}), A/V is the surface area to volume ratio (SAV, cm^{-1}), and k_t is the emission rate (molecule cm^{-3} s^{-1}) of species i. The model assumes a well-mixed environment, hence there is no spatial complexity associated with C_i.

2.3.2 Chemical processing

Homogeneous chemical processing of air pollutants indoors is an important factor which determines the composition of indoor air and production of secondary pollutants. The chemical production and losses of gas-phase species in the model are calculated based on the MCM, modified photolysis chemistry and additional chemical reaction schemes which have been, and continue to be, developed by the user community.

2.3.2.1 The Master Chemical Mechanism

The model has been constructed based on a comprehensive chemical mechanism, the Master Chemical Mechanism (MCM) v3.3 (http://mcm.york.ac.uk). The MCM was originally developed to compile up-to-date kinetic and mechanistic data to provide a detailed mechanism which describes the tropospheric oxidation of VOCs for use in numerical models of the planetary boundary layer (Jenkin et al., 1997). However, the mechanism can also be used to describe the detailed chemistry of the indoor environment. The MCM is updated regularly, using the latest kinetic and product data where available, or structure activity relationships (SARs) in their absence (Jenkin et al., 1997). The current version of the MCM protocol (MCM v3.3) includes near-explicit degradation schemes for 143 VOCs, involving over 20,000 reactions and approximately 6,000 species.

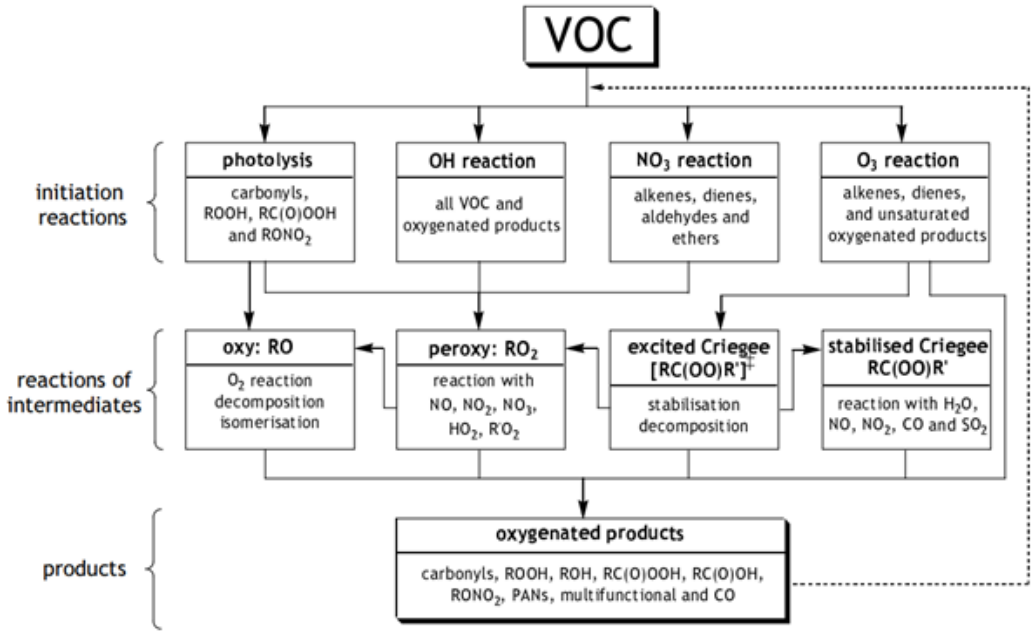

Figure 2.5: Flow chart indicating the major reactions, intermediate classes and product classes considered in the MCM protocol (Saunders et al., 2003).

The general methodology of the MCM protocol is illustrated in Figure 2.5. The degradation of VOCs is initiated by reaction with O_3, OH, or NO_3, and photolysis where applicable depending on the chemical functionality of the VOC. The products of the initiation reactions include intermediate species (oxy and peroxy radicals, Criegee intermediates), and oxygenated products. These first-generation products further degrade through gas-phase oxidation reactions until the final oxidation products of CO_2 and H_2O are generated.

Here, the initial oxidation chemistry of limonene is discussed as an example of a near-explicit chemical reaction scheme represented in the MCM. All VOCs react with OH in the presence of excess O_2 to produce peroxy radicals (RO_2), either by H-abstraction or by addition to a double bond. The limonene-OH reaction produces three peroxy radicals due to the presence of two double bonds in the structure (Eq. 2.6). In a similar fashion, VOCs can react with NO_3 radicals to form nitrooxy-substituted peroxy radicals (Eq. 2.7).

$$\begin{aligned} \text{LIMONENE} + \text{OH}\,(+\,\text{O}_2) &\longrightarrow \text{LIMAO2} \\ &\longrightarrow \text{LIMBO2} \\ &\longrightarrow \text{LIMCO2} \end{aligned} \tag{2.6}$$

$$\text{LIMONENE} + \text{NO}_3\,(+\,\text{O}_2) \longrightarrow \text{NLIMO2} \tag{2.7}$$

The peroxy radicals produced through these reactions can then react with NO, NO_2, NO_3, HO_2, or self- or cross-reactions with RO_2, to form more radicals and oxygenated species, which then react further. The main products of NO_x-RO_2 reactions are oxy radical species. Following the chemistry of the LIMBO2 peroxy radical, the NO_3-RO_2 reaction is assumed to proceed via a single channel, producing an oxy radical (RO) (Eq. 2.8). Reaction with NO can proceed via two routes producing an oxy radical or an organic nitrate ($RONO_2$). The branching ratio of these reaction pathways is determined using the SAR method (Atkinson, 1987) (Eq. 2.9). The NO_2-RO_2 reaction pathway for the limonene first-generation peroxy radicals are not considered in the mechanism for simplicity, as the peroxy nitrate product ($ROONO_3$) is relatively unstable. The RO_2-HO_2 reaction of limonene first-generation peroxy radicals is assumed to proceed exclusively via the reaction shown in Eq. 2.10, producing hydroperoxide species.

$$\text{LIMBO2} + \text{NO}_3 \longrightarrow \text{LIMBO} + \text{NO}_2 \tag{2.8}$$

$$\begin{aligned} \text{LIMBO2} + \text{NO} &\longrightarrow \text{LIBNO3} \\ &\longrightarrow \text{LIMBO} + \text{NO}_2 \end{aligned} \tag{2.9}$$

$$\text{LIMBO2} + \text{HO}_2 \longrightarrow \text{LIMBOOH} + \text{O}_2 \tag{2.10}$$

Due to the many permutations of RO_2 reactions with themselves or other peroxy radicals, it is unrealistic to represent them explicitly in the mechanism. Therefore, RO_2 self- and cross-reactions are described in the MCM by the reaction of each peroxy radical with the pool of RO_2, which is defined as the sum of the concentrations of all

RO_2, excluding HO_2. There are three product channels for primary limonene RO_2 reactions with the RO_2 pool, generating alcohols, carbonyls and oxy radical species (Eq. 2.11).

$$\begin{aligned} \text{LIMBO2} + \text{RO}_2 &\longrightarrow \text{LIMAOH} \\ &\longrightarrow \text{LIMBCO} \\ &\longrightarrow \text{LIMBO} \end{aligned} \tag{2.11}$$

The oxy radicals generated from this chemistry are assumed to further react via three routes: reaction with O_2, thermal decomposition and isomerisation by a 1,5 - H atom shift. The RO-O_2 reaction generates HO_2 which in turn can react with NO to generate OH radicals, thus further driving the oxidative gas-phase chemistry.

Unsaturated VOCs such as limonene also undergo oxidation via ozonolysis. The addition of O_3 to a double bond generates an excited ozonide, which quickly decomposes via the two available channels to form a pair of carbonyl compounds and Criegee biradicals. The general reaction is detailed in Chapter 1.2.2. For limonene, O_3 attacks the cyclic double bond in a ring-opening mechanism to produce two Criegee biradicals (Eq. 2.12).

$$\begin{aligned} \text{LIMONENE} + \text{O}_3 &\longrightarrow \text{LIMOOA} \\ &\longrightarrow \text{LIMOOB} \end{aligned} \tag{2.12}$$

The excited Criegee biradicals are either collisionally stabilised to generate stabilised Criegee biradicals or decompose to produce OH and other radicals. In the case of limonene, each Criegee biradical decomposes to generate OH via the hydroperoxide mechanism, whereby a 1,4-H atom shift occurs followed by decomposition of the resultant α, β-unsaturated hydroperoxide intermediate (Eq. 2.13).

$$\begin{aligned} \text{LIMOOA} &\longrightarrow \text{LIMALAO2} + \text{OH} \\ &\longrightarrow \text{LIMALBO2} + \text{OH} \end{aligned} \tag{2.13}$$

The degradation of VOCs summarised above results in the generation of a wide range of oxygenated products of varying complexity, which themselves further react until the final products of H_2O and CO_2 are reached.

2.3.2.2 Photolysis

There are 43 photolysis reactions currently included in the model, with reaction rates dependent on the indoor lighting conditions. Indoor lighting is driven by both artificial indoor lighting and attenuated outdoor sunlight which is passed through windows and skylights. This is represented in the model by the total indoor photolysis rate, J:

$$J = ((l\cos(\theta)^m \exp(-n\sec(\theta))\psi) + \phi \tag{2.14}$$

Where θ is the solar zenith angle, l, m and n are parameters optimised as per the discussion in Jenkin et al. (1997), ψ is the transmission factor of solar (outdoor) light, and ϕ is the indoor photolysis rate.

The outdoor photolysis rates are driven by the solar zenith angle, which is defined based on the date, time and latitude of the simulation using equations 2.15 and 2.16. The declination angle (Dec) is calculated using the number of days (d) since the 1st of January that year. This is then used, along with the latitude (Lat) and the local hour angle (LHA) to determine the solar zenith angle (θ).

$$Dec = -23.45 \times \cos\left(\frac{360}{365.25} \times (d + 10)\right) \tag{2.15}$$

$$\cos(\theta) = \sin(Lat)\sin(Dec) + \cos(Lat)\cos(Dec)\cos(LHA) \tag{2.16}$$

The attenuation of solar light present indoors is defined by the transmission factor, ψ. Values for ψ have been calculated by Wang, Shaw, Kahan, Schoemaecker and Carslaw (2022), for three different glass types based on the analysis in Blocquet et al. (2018). The three glass types represented in the model are "Glass C Sacht Self-cleaning" (Glass

C, transmission from 315 to 800 nm), "Low Emissivity" (LE, transmission from 330–800 nm), and "Low Emissivity With Film" (LEWF, transmission from 380 to 800 nm). Weighted transmission factors were calculated for each photolysing species and for each glass type based on the percentage of light transmittance through the glass at 10 nm intervals, and the absorption cross section and quantum yield of the molecule.

The indoor photolysis rate, ϕ, is driven by photolysis from artificial indoor lighting which can be set as on/off at any timepoint during the simulation. There are seven light types represented in the model (Incandescent, Halogen, LED, compact fluorescent lamps (CFL), covered or uncovered fluorescent tubes (CFT/UFT), and fluorescent tubes (FT)) covering a range of transmission spectra. Spherically integrated photon fluxes measured by Kowal et al. (2017) were used to calculate indoor photolysis rates for each light type, as described by Wang, Shaw, Kahan, Schoemaecker and Carslaw (2022).

2.3.2.3 Additional chemistry

Additional chemical reaction schemes have been developed for species which are relevant to the indoor environment but are not included in the MCM. These schemes are typically constructed by using rate coefficients for the initial oxidation steps using data from the literature, and mapping reaction products where relevant onto existing species in the MCM after a few degradation steps.

This approach has been used to develop reaction schemes for some additional terpenes (camphene, carene, γ-terpinene) and terpenoids (linalool, citral) which will be relevant for this research (Carslaw et al., 2017; Carslaw, 2007). Other species which are included as additional chemistry include long-chain aldehydes (octanal, nonanal, decanal), and chlorine (Kruza et al., 2017; Xue et al., 2015; Wong et al., 2017; Wang et al., 2020). For the purposes of this research, four additional reaction schemes for terpenoid species have been developed (dihydromyrcenol, α-terpinene, α-phellandrene, and terpinolene), described in further detail in Appendix A.

2.3.3 Exchange with outdoors

Indoor species concentrations are impacted by the influx from, and efflux to, outdoors at a rate which is determined by the air ACR. The ACR is user-defined in the model and typically ranges from 0.2 to 2 h^{-1}, depending on the airtightness of the indoor environment (Weschler, 2000).

Outdoor concentrations of 110 VOCs are set as static concentrations using representative data sourced from published literature and measurement databases. Outdoor O_3, NO, NO_2 and $PM_{2.5}$ are defined using diurnal profiles for three European locations (urban London (UK), suburban London (UK), urban Bergen (Norway)) based on measured data from 2018 in the EEA (2018) air quality database. The diurnal profiles were obtained for each species in each location by overlaying hourly average data from Q3 (July, August, September) in solar time, taking an average for each hour, and fitting the resulting datapoints to a trigonometric Fourier function. An additional diurnal profile is provided for Milan (Italy) based on a 2-week measurement period in August 2003 (Terry et al., 2014), using the same mathematical approach as for the other profiles. All other species present in the model that do not have a defined outdoor concentration are assumed to be zero.

2.3.4 Partitioning processes

Partitioning of gas-phase compounds to condensed phases such as indoor surfaces and aerosol particles is an important influencing factor on the temporal concentration profiles of indoor air pollutants. Deposition to indoor surfaces is particularly important due to the characteristic high SAV of indoor environments. In INCHEM-Py, partitioning of gas-phase species to particles and indoor surfaces are included.

2.3.4.1 Particle formation

Gas-to-particle partitioning is considered for terpene oxidation products only (limonene, α-pinene, β-pinene) (Carslaw et al., 2012). Particle formation is initiated by organic seed particles (assumed to be 30 % of outdoor particles) which originate from outdoors

and ingress at a rate determined by the ACR. Sorptive partitioning of terpene species to the particle phase is determined by thermodynamic equilibrium, where the partitioning coefficient ($m^3\ \mu g^{-1}$) is the ratio between the rate of adsorption and desorption of the species to/from the particle phase. The details of how this is calculated is included in Carslaw et al. (2012). The total number (molecule cm^{-3}) and concentration ($\mu g\ cm^{-3}$) of suspended particles generated from terpene partitioning are estimated through time based on the partitioning coefficient of each individual species.

2.3.4.2 Irreversible surface deposition

The irreversible deposition of 3371 gas-phase species onto indoor surfaces is calculated by INCHEM-Py (Shaw et al., 2023). The rate at which species partition onto indoor surfaces is calculated as the product of the species deposition velocity (cm s^{-1}) and the total SAV of a room (cm^{-1}). Specific deposition velocities are provided for 22 species, however all other species which are assumed to deposit onto indoor surfaces in the model have deposition velocities which are estimated based on their chemical functionality (Carslaw et al., 2012; Shaw et al., 2023).

2.3.4.3 Oxidant surface deposition and secondary pollutant emission

For H_2O_2 and O_3, surface-specific deposition mechanisms have been developed which consider the rates of deposition and secondary pollutant emissions from multiple indoor surface materials (Carter et al., 2023). Loss rates of O_3 and H_2O_2 to indoor surfaces and subsequent emission of aldehydes is calculated from the specific deposition velocities and SAVs of the following materials: metal, glass, wood, plastic, linoleum, paint, paper, concrete, soft furnishings, and skin. The O_3 deposition rate (F_{O_3}, s^{-1}) and secondary pollutant emission rates (E_i, molecule $cm^{-3}\ s^{-1}$) are calculated using equations 2.17 and 2.18, respectively. Analogous equations are also used for H_2O_2.

$$F_{O_3} = \nu_{d_{O_3}} \frac{A}{V} \tag{2.17}$$

$$E_i = \frac{A\nu_{d_{O_3}} Y_i C_{O_3}}{V} \tag{2.18}$$

Where $\nu_{d_{O_3}}$ is the surface deposition velocity of O_3 (cm s^{-1}), $\frac{A}{V}$ is the SAV of an indoor surface material (cm^{-1}), Y_i is the production yield of gas-phase species following deposition (dimensionless), and C_{O_3} is the bulk concentration of indoor O_3 (molecule cm^{-3}). Oxidant deposition velocities onto specific indoor surface materials and their corresponding production yields were determined from a range of experimental literature, described by Carter et al. (2023) and references therein.

2.3.5 Emissions

Indoor emissions can be included in the model as direct emissions which remain constant for the duration of the simulation, or timed emissions which are emitted at a given rate for a specified time period. Breath emissions are optionally included in the model as direct emissions of acetone, ethanol, methanol, isopropanol and isoprene. The rate of emission is dependant on the number of adults and children occupying the simulated indoor environment (Kruza and Carslaw, 2019; Weschler et al., 2007). Intermittent VOC emissions from occupant activities such as cleaning can be included in the model as timed emissions, as will be demonstrated in subsequent chapters.

2.3.6 This work: model development and initialisation

Experimentally derived VOC emission rates were applied to the model to investigate the indoor air chemistry following cleaning events. All simulations were run for a duration of 24 hours, with cleaning VOC emissions generally input as timed emissions at midday. Of the VOC species measured by SIFT-MS (and the monoterpenes identified by GC-MS), 10 species were present in the MCM and therefore were represented in the model as fully explicit degradation schemes (Table 2.5). A further 5 species were present in the model as pre-existing custom reaction schemes which had been developed based on literature rate coefficients of the first few oxidation steps, then mapped onto species present in the MCM. This same approach was used to develop

degradation schemes for a further 4 VOC species as part of this research (Appendix A).

Three species were represented in the model using proxy species. Total sesquiterpenes were assumed to be 100% β-caryophyllene, which is present in the MCM. Butyl pyruvate (MW = 144.47 g mol^{-1}) was used as a proxy species to represent 2-phenethyl acetate and 2-tert-butylcyclohexyl acetate because it has a similar molecular weight and possesses the same functionality as the two acetate species. Mass correction was applied to 2-phenethyl acetate and 2-tert-butylcyclohexyl acetate emission rates input to the model as butyl pyruvate to preserve the mass. Finally, four VOCs measured by SIFT-MS were not input into the model because there were either no published rate coefficients available, or they were not considered important drivers of the chemistry.

2.3.6.1 Average kitchen setting

Throughout this thesis, cleaning emissions were simulated in an 'average kitchen' scenario to investigate the chemical processing of cleaning VOCs in an indoor environment representative of a typical residential dwelling. The model was initialised to simulate a typical domestic kitchen in suburban London, based on the model parameterisation defined by Carter et al. (2023) and used by Davies et al. (2023). An overview of the model settings is provided in Table 2.6.

Table 2.5: Summary of VOC species measured experimentally, and how their chemical degradation schemes are represented in INCHEM-Py.

Compound	INCHEM-Py name	MCM	INCHEM-Py additional chemistry	Proxy species	Not included
1,2,4-trimethyl benzene	TM124B	✓			
2-phenethyl acetate	BOXCOCOME			✓	
2-tert-butylcyclohexyl acetate	BOXCOCOME			✓	
acetaldehyde	CH3CHO	✓			
total sesquiterpenes	BCARY			✓	
benzene	C6H6	✓			
benzyl benzoate	-				✓
cinnamaldehyde	-				✓
citral	GERANCO		✓		
dihydromyrcenol	DHMOL		✓		
ethanol	C2H5OH	✓			
eucalyptol	-				✓
eugenol	-				✓
formaldehyde	HCHO	✓			
lactic acid	CH3CHOHCO2H		✓		
total monoterpenes:					
limonene	LIMONENE	✓			
β-pinene	BPINENE	✓			
α-pinene	APINENE	✓			
carene	CAR		✓		
camphene	CAMPHENE		✓		
α-phellandrene	APHEL		✓		
α-terpinene	ATERPINENE		✓		
γ-terpinene	GTERP		✓		
terpinolene	TERPINOLENE		✓		
m-xylene	MXYL	✓			
methanol	CH3OH	✓			

Table 2.6: INCHEM-Py model parameters and settings used for the 'average kitchen' simulations.

Parameter	Setting	Notes
Particles	True	
Additional chemistry	True	carene, camphene, γ-terpinene, α-terpinene, terpinolene, α-phellandrene, dihydromyrcenol, citral, lactic acid
Temperature	293.05 K (19.9 °C)	Based on mean values from extensive monitoring of air quality in homes across the UK (Ministry of Housing, Communities & Local Government (UK Government), 2019)
RH	53.8%	
Number density of air	2.51 x 10^{19} molecule cm^{-3}	
ACR	0.5 h^{-1}	Median value from a range of residential properties in Europe, North America and central Asia (Nazaroff, 2021)
Diurnal	True	
Location	London suburban	
Date	21-06-2020	
Latitude	51.45	Latitude of the suburban London monitoring station
Artificial lighting	Incandescent	
Light on times	07:00 – 19:00	
Glass type	Low emissivity	Wavelength range 330-800 nm
SAV – Total	0.02533 cm^{-1}	
Soft furnishings	0.0008 cm^{-1}	
Painted	0.0099 cm^{-1}	
Wood	0.0067 cm^{-1}	
Metal	0.0031 cm^{-1}	
Concrete	0.0005 cm^{-1}	
Paper	0.0001 cm^{-1}	
Linoleum	0.0007 cm^{-1}	
Plastic	0.0022 cm^{-1}	
Glass	0.0006 cm^{-1}	
Skin	0.0008 cm^{-1}	
		Total room volume of 25 m^3, total surface area of 63.27 m^2 based on values calculated by Manuja et al. (2019). Surface material-specific surface areas defined by Carter et al. (2023) based on measurements from Manuja et al. (2019). Assumed 1 person in the room, skin surface area of 2 m^2.
O_3/H_2O_2 deposition	True	
Occupancy	1 adult	
Timed emissions	True	Experimentally derived cleaning VOC emissions input at approx. midday
dt	60 s	Headspace emissions (Chapter 3)
	15 s	Room-scale emissions (Chapters 4 & 5)
t_0	0 s	
Seconds to integrate	86400 s	1 day

Chapter 3

Does Green mean Clean? Volatile Organic Emissions from Regular versus Green Cleaning Products

This chapter includes material that has been previously published in Environmental Science: Processes & Impacts (Harding-Smith et al., 2024). It has been adapted and integrated into this thesis to provide a comprehensive examination of the VOC emissions from regular and green cleaners, and their impact on indoor air chemistry.

3.1 Introduction

Household cleaning products are widely used in the built environment to promote cleanliness and hygiene (Wolkoff et al., 1998). Cleaning products generally constitute complex mixtures of chemicals including water, solvents, surfactants, preservatives and fragrances. Depending on the usage purpose, other compounds can be included such as disinfectants, acids, bases, bleaching agents, abrasives, or enzymes (Missia et al., 2012). Many of the components of cleaning products are volatile, and therefore cleaning products can be a major source of VOCs in indoor environments.

The fragrance component of household cleaners is a key selling point to consumers,

promoting the perception of a clean environment through the concealing of malodours (Herz et al., 2022). Natural and synthetic fragrance ingredients used in scented products are chemically complex mixtures containing terpene and terpenoid compounds. Consequently, cleaning products have been identified as one of the largest sources of terpenes indoors (Wang et al., 2017). In a study of 25 UK homes, highly variable indoor concentrations of limonene and α-pinene were measured at much higher concentrations than outdoors (mean indoor/outdoor ratios of 8 and 6, respectively), evidencing the intermittent use of fragranced products such as household cleaners indoors (Wang et al., 2017).

Many terpenoid species are susceptible to oxidation by oxidants present indoors such as O_3, and OH and NO_3 radicals. Such chemistry results in the production of a wide range of secondary pollutants, such as organic nitrates, carbonyls (such as formaldehyde), peroxyacetyl nitrate-type species (RCO_3NO_2, henceforth PANs) and PM (Carslaw, 2013). Some secondary pollutants from terpenoid oxidation have been associated with adverse health effects (World Health Organization, 2010; Nielsen and Wolkoff, 2010; Koenig et al., 1989; Berkemeier et al., 2016; Zhang et al., 2015), although the toxicology of many secondary pollutants remains poorly characterised. Evidence suggests that occupant exposure to pollutants from cleaning products may cause adverse respiratory effects and asthma prevalence in cleaning staff (Coeli Mendonça et al., 2003). Some secondary pollutants are more detrimental to health than the parent VOC (Buchanan et al., 2008), hence it is important to study both the primary VOC emissions from cleaning and the chemical transformations that follow to improve indoor air quality and reduce occupant health risks.

The chemical composition of cleaning product formulations is often unclear from the product labels, as manufacturers are not required to disclose all formulation ingredients. This was illustrated in a study of 134 common consumer products, where fewer than 4% of the identified VOCs were listed as product ingredients (Nematollahi et al., 2019). The fragrance component of consumer products is often listed as “parfum”, or an equivalent term, with no chemical detail about the fragrance components. Under

regulation (EC) 648/2004, disclosure of specific fragrance compounds is only required if they are allergenic and at a concentration exceeding 0.01%. As such, there is large variability and uncertainty in the current knowledge of primary VOC emissions and secondary pollutants from indoor cleaning activities.

An increasing awareness surrounding the environmental and health impacts of household products has driven a recent shift in consumer choice towards "green" products, with the assumption that they are less polluting and therefore less harmful than their regular counterparts (Bearth et al., 2017). However, owing to the ambiguity surrounding the chemical composition of cleaning products, it is not possible to substantiate these consumer perceptions in relation to indoor air pollution. Additionally, there is no official designation of "green" and no standard certification to ensure that products marketed as "green" have lower concentrations of chemicals of concern (Calderon et al., 2022). Research comparing the VOC emissions from regular and green cleaners remains limited. Several studies suggest that there is no significant difference between regular and green cleaners (Steinemann, 2009, 2015; Steinemann et al., 2021; Nematollahi et al., 2019), however other studies have observed reduced air concentrations of hazardous VOCs from green cleaners (Temkin et al., 2023; Calderon et al., 2022; Harley et al., 2021). To our knowledge, there currently exists no studies investigating the secondary pollution from fragranced regular and green cleaners.

Therefore, the aim of this study was to investigate the primary VOC emissions and resultant secondary pollutant formation from 10 regular and 13 green cleaning products. The VOC composition of the cleaners was determined by headspace analysis techniques, and results were used to estimate VOC emission rates during a typical cleaning event on a realistic scale. The chemical transformations of reactive monoterpene emissions were investigated using INCHEM-Py, and the resulting key harmful secondary pollutants were identified. This is the first study to investigate the chemical processing of complex mixtures of reactive terpene emissions relevant to commercially available products, including those marketed as "green".

3.2 Methodology

3.2.1 Cleaning products

Twenty-three commercially available household cleaning products were selected for comparison, including 10 "regular" and 13 "green" cleaning products. Full details of the cleaning products tested, including their classification, application mode, and whether they were fragranced, can be found in Chapter 2, Table 2.1.

3.2.2 Experimental

3.2.2.1 Equilibrium headspace GC-TOF-MS

Equilibrium headspace GC-TOF-MS was used to qualitatively characterise the volatile fraction of the cleaning product formulations. The GC-TOF-MS principles of operation and operating conditions are described in Section 2.2.1. Floor and dishwashing detergent samples were prepared (as per manufacturer instructions) by diluting with deionised water, while surface and bathroom cleaners were analysed as the neat product formulation. 1 mL aliquots of sample were dispensed into 20 mL glass headspace sample vials. Each sample was heated to 50 °C and intermittently agitated at 250 rpm for 5 minutes in the pre-heating module to allow equilibration of the headspace. Following the equilibration period, 250 μL of gaseous headspace was injected into the GC-MS system and analysed using the method outlined in Section 2.2.1.2.

Visualisation and processing of the GC-MS data were performed using the MassHunter Workstation Software (Version 7.0 Qualitative Analysis, Agilent Technologies). The background-subtracted mass spectrum of each peak was extracted, and compounds were tentatively identified by spectral library matching using the National Institute of Standards and Technology (NIST) Mass Spectral Search Program (version 2.3, NIST) and an R match factor of > 700. Inter-comparison of peak identification results relative to retention time was performed to improve confidence in identification.

3.2.2.2 Dynamic headspace SIFT-MS

A Voice200 SIFT-MS (Syft Technologies) was used to quantify volatile components of the cleaning product formulations by dynamic headspace sampling, as described by Yeoman et al. (2020). The SIFT-MS principles of operation and operating conditions are described in Section 2.2.2. A 50 cm^3 gas-tight vessel was used as a headspace sampling chamber, which comprised of a stainless-steel screw-down lid and Viton O-ring seal and two 1/16 in. stainless steel Swagelok bulkhead connectors to provide an inlet and outlet (Yeoman et al., 2020). VOC-free N_2 diluent gas was supplied to the chamber from a Teflon bag connected to the inlet. The SIFT-MS was connected to the chamber outlet and was supplied with a 5 mL/min flow of sample gas via a mass flow controller. The sampling chamber was thermostatically controlled at 25 °C to achieve a stable ambient temperature throughout the experiment.

The SIFT-MS was operated in selected ion monitoring (SIM) mode, dynamically measuring 15 VOCs with a time resolution of 6 seconds (54 masses scanned, 0.1 second ion dwell time). The VOCs measured using each reagent ion in the SIFT-MS SIM method are shown in Table 3.1, along with the species molecular weights, product ions, rate coefficients and branching ratios. Whether or not the product ion was used for quantification is also shown in the 'included in analysis' column.

Table 3.1: The compounds measured by SIFT-MS using each reagent ion, and their corresponding product ion molecular masses (MM), chemical formulae, rate coefficients and branching ratios. Whether or not the product ion was used for quantification is also shown in the 'included in analysis' column.

Reagent ion	Compound	MM (g mol^{-1})	Product ion	Reaction rate ($\times$ 10^{-9} cm^3 $molecule^{-1}$ s^{-1})	Branching ratio (%)	Included in analysis
H_3O^+	1,2,4-trimethylbenzene	121	$C_9H_{12}.H^+$	2.40	100	
	2-phenethyl acetate	105	$C_8H_9^+$	3.50	80	
	acetaldehyde	45	$C_2H_4O.H^+$	3.70	100	✓
	total sesquiterpenes	205	$C_{15}H_{25}^+$	2.50	64	✓
	benzyl benzoate	151	$C_8H_7O_3^+$	3.70	60	
		169	$C_8H_7O_3^+.H_2O$	3.70		
	cinnamaldehyde	133	$C_9H_8OH^+$	2.00	100	
	citral	153	$C_{10}H_{17}O^+$	3.00	60	✓
		171	$C_{10}H_{17}O^+.H_2O$	3.00		
	ethanol	47	$C_2H_7O^+$	2.70	100	✓
	formaldehyde	31	CH_3O^+	3.40	100	✓
	total monoterpenes	137	$C_{10}H_{17}^+$	2.60	30	
	m-xylene	107	$C_8H_{10}.H^+$	2.30	100	
	methanol	33	CH_5O^+	2.70	100	✓
NO^+	2-phenethyl acetate	104	$C_8H_8^+$	2.90	85	✓
	2-tert-butylcyclohexyl acetate	138	$C_{10}H_{18}^+$	2.80	40	✓
	acetaldehyde	43	CH_3CO^+	0.69	80	
		61	$CH_3CO^+.H_2O$	0.69		

	total sesquiterpenes	204	$C_{15}H_{24}^+$	2.00	38	
	benzene	78	$C_6H_6^+$	1.50	55	✓
		108	$NO.C_6H_6^+$	1.50	45	
	benzyl benzoate	180	$C_9H_{10}O_2NO^+$	2.50	45	✓
	cinnamaldehyde	132	$C_9H_8O^+$	2.00	100	
	citral	151	$C_{10}H_{15}O^+$	2.50	35	
	ethanol	45	$C_2H_5O^+$	1.20	100	
		63	$C_2H_5O^+.H_2O$	1.20		
	eugenol	164	$C_{10}H_{12}O_2^+$	2.40	100	✓
	lactic acid	73	$CH_3CH(OH)CO^+$	2.50	50	✓
	total monoterpenes	88		2.20	25	
		136	$C_{10}H_{16}^+$	2.20	75	✓
	m-xylene	106	$C_8H_{10}^+$	1.90	100	✓
O_2^+	1,2,4-trimethylbenzene	120	$C_9H_{12}^+$	2.00	85	✓
	2-tert-butylcyclohexyl acetate	57	$C_4H_9^+$	4.50	45	
	benzene	78	$C_6H_6^+$	1.10	100	
	cinnamaldehyde	132	$C_9H_8O^+$	2.00	100	✓
	dihydromyrcenol	59	$C_3H_7O^+$	2.90	50	✓
		77	$C_3H_7O.H_2O^+$	2.90		
		139	$C_{10}H_{19}^+$	2.90	15	
	eugenol	164	$C_{10}H_{12}O_2^+$	1.90	100	

For each sample, background measurements of the headspace chamber were acquired for approximately 10 minutes prior to sample introduction. 1 μL of sample was then decanted onto a small open vial and placed into the sampling chamber immediately. The headspace gas was then measured for a further 60 minutes, or until VOC concentrations stabilised at background concentrations.

Background VOC concentrations, defined as the mean concentration of a 2-minute period immediately prior to sample introduction, were subtracted from the data. The LODs, calculated as 3.2 $\times$ the standard deviation of the background measurements, are shown in Table 3.2.

Table 3.2: Limits of detection (average $\pm$ standard deviation of 23 samples) of the species measured by SIFT-MS.

Species	LOD (μg m^{-3})
formaldehyde	13.35 $\pm$ 2.58
acetaldehyde	5.25 $\pm$ 1.01
methanol	10.18 $\pm$ 1.62
ethanol	20.00 $\pm$ 7.70
total monoterpenes	9.67 $\pm$ 5.72
total sesquiterpenes	22.22 $\pm$ 6.49
dihydromyrcenol	30.41 $\pm$ 9.43
eugenol	2.47 $\pm$ 0.45
citral	15.91 $\pm$ 3.39
cinnamaldehyde	7.20 $\pm$ 2.02
2-tert-butylcyclohexyl acetate	20.72 $\pm$ 9.24
2-phenethyl acetate	3.53 $\pm$ 0.76
1,2,4-trimethyl benzene	3.60 $\pm$ 0.85
benzyl benzoate	8.81 $\pm$ 2.52
benzene	5.12 $\pm$ 2.70
m-xylene	3.46 $\pm$ 0.68
lactic acid	10.36 $\pm$ 10.07

Data were calibrated for acetaldehyde, benzene, ethanol, methanol, and total monoterpenes using calibration factors determined from gas standards, as described in Section 2.2.2.3. The calibration factors applied to the data were calculated as the averages

of the calibration curve slopes from multiple instrument calibrations, and the associated uncertainties calculated as the average of the standard errors (Table 3.3). For all other species, concentrations were determined using literature compound specific rate constants provided by the LabSyft kinetic library and ion transmission data which was obtained from weekly instrument validation (see Section 2.2.2.3). The uncertainty in these uncalibrated measurements was assumed to be ± 35 %, as recommended in Syft training resources (Syft Technologies Training Materials, 2014; Langford et al., 2014). Other sources of uncertainty in the experimental method for the quantification of VOCs in cleaning product formulations were identified as: 1 μL sample volume measurement (± 5 %), and headspace sample gas flow rate (± 1 %).

Table 3.3: The calibration factors and associated uncertainties used in this study, determined from multiple instrument calibrations using gas standards.

Species	Calibration factor	Relative uncertainty (%)
acetaldehyde	0.52 ± 0.05	9
ethanol	1.02 ± 0.11	11
benzene	0.81 ± 0.04	4
total monoterpenes[a]	0.78 ± 0.06	8
methanol	1.17 ± 0.02	2

[a]Limonene used as calibration gas.

The concentration (C) of species i in the cleaning product formulation (μg μL^{-1}) was calculated from the integral of the calibrated, background subtracted SIFT-MS data using Equation 3.1.

$$C_i = \frac{\int_{t_0}^{t} C_i dt \times \nu}{V_{sample}} \tag{3.1}$$

Where $\int_{t_0}^{t} C_i dt$ is the integral of C_i with respect to time, t_0 and t are the times at which the sample was introduced to the headspace chamber and the end of the sampling period, respectively, ν is the sample flow rate (8.3×10^{-7} m^3 s^{-1}), and V_{sample} is the sample volume (1 μL).

The measured concentration profiles showed a peak shortly after sample introduction followed by a decline back to baseline concentrations in most cases, indicating that the VOC source was depleted within the duration of the sampling time. The integral of the VOC peak was therefore assumed to be equivalent to the total amount of that VOC emitted from the sample under the given conditions. VOC concentration profiles which showed no or insignificant peaks were identified by visual inspection of the data and were discounted from subsequent analysis.

The VOC concentrations were used to estimate emission rates for subsequent modelling of a typical cleaning event in a domestic kitchen environment. The following assumptions were made:

- Product volume: The volume of cleaning product used during a realistic cleaning event was assumed to be 10 mL for surface and bathroom cleaners (based on semi-realistic cleaning experiments), 107 mL for floor cleaners (based on an assumed floor surface area of 8.36 m^2 (25 m^3 room volume, UK standard 2.4 m height ceiling (Manuja et al., 2019)) and a floor solution application of 12.82 g/m^2 (Singer et al., 2006)), and 50 mL for dishwashing detergent.
- Dilution factor: Manufacturer guidance was used to calculate a dilution factor where possible. Otherwise, dishwashing detergents were assumed to have a dilution factor of 0.001 (0.1 % v/v).
- Room volume: An average kitchen volume of 25 m^3 was assumed based on a detailed study of the volume and surface areas of 9 kitchens (Manuja et al., 2019).
- Emission period: An emission period of 3 minutes was assumed, based on previous cleaning activity experiments.

Using these assumptions, VOC emission rates ($k_{Em(i)}$, molecule cm^{-3} s^{-1}) were determined using Equation 3.2:

$$k_{Em(i)} = \frac{C_i \times V_{product} \times F_{dil} \times N_A}{t \times V_{room} \times M_w} \tag{3.2}$$

Where $V_{product}$ is the volume of cleaning product used in a cleaning event (μL), F_{dil} is the dilution factor for cleaning products used as a dilute solution, t is the emission period (s), V_{room} is the volume of the room (cm^3), N_A is Avogadro's constant (6.022 $\times$ 10^{23} mol^{-1}), and M_w is the molecular weight of species i (μg mol^{-1}).

Estimating realistic-scale VOC emissions in this way has limitations. Emission rates were calculated based on the assumption that all VOCs were emitted from the cleaning product during a cleaning activity period of 3 minutes. However, there is evidence to suggest that indoor emission sources such as cleaning products can emit VOCs for a period following the activity due to reversible surface partitioning and emissions from product residues (Meininghaus et al., 1999; Nazaroff and Weschler, 2004). Complex emission dynamics including multi-phase interactions (i.e., partitioning of VOCs to organic or aqueous surface films) and the effects of different product application modes are not taken into consideration here. Finally, it is acknowledged that the VOC species targeted for this analysis do not account for all volatile components of the cleaning products, and some VOC emissions are not accounted for. However, our results do provide a comparative study between the different cleaners and importantly, between the green and regular products.

The approach used in this study to estimate VOC emission rates from product formulation compositional data was evaluated by applying it to data reported in a previous study (Singer et al., 2006). The terpene composition of a pine oil-based general-purpose cleaner reported by Singer et al. (2006) was used, along with their experimental protocol for a floor mopping experiment (experiment N), to determine individual monoterpene emission rates using Equation 3.2. The emission rates were then applied to INCHEM-Py to simulate the cleaning experiment, using the approach described in this study. The simulation resulted in a peak monoterpene concentration of 165 ppb, which was 32% of the 1-hour average total monoterpene concentration of 513 ppb reported by Singer et al. (2006). However, the theoretical maximum monoterpene concentration in the Singer et al. (2006) experiment was estimated to be 186 ppb, assuming all terpene emissions originated from the 105 mL dispensed cleaning solution

only. The discrepancy between the two values is likely to be caused by additional emissions originating from the preparation of the cleaning solution in the room and from the bulk solution during the cleaning event. Consequently, the emission rates estimated by our method could be 2-3 times too low, depending on how the cleaning is carried out.

3.2.2.3 Speciated monoterpene emission rates

The total monoterpene emission rates calculated from dynamic headspace SIFT-MS measurements were quantitatively speciated per product using equilibrium headspace GC-TOF-MS. Each sample was prepared and analysed using the same instrumentation and methodology specified in Sections 2.2.1 and 3.2.2.1, with the exceptions of: i) the sample volume (550 μL), ii) the inclusion of an internal standard (550 μL of 10 μg/L dimethylaniline solution in methanol), iii) the sample incubation temperature (35 °C), and iv) splitless injection. The sample incubation temperature was reduced to align more closely with the SIFT-MS analysis conditions and realistic room temperatures, lessening the impact of temperature on the liquid-gas partitioning of monoterpenes. The inclusion of an internal standard was used to normalize the data through the calculation of the response factor (the ratio of the peak area of each analyte to the peak area of the internal standard in the sample). This process compensated for variability in instrument response, sample preparation, and matrix effects of the different product formulations.

The quantified monoterpene fraction was used to calculate the relative abundance ratios of monoterpenes in each cleaning product, which were applied to the total monoterpene emission rates determined from SIFT-MS to calculate individual monoterpene emission rates for each cleaner.

3.2.3 Model simulations

INCHEM-Py v1.2 was used to model the indoor air chemistry following the emission of VOCs from cleaning. A full description of INCHEM-Py is provided in Section 2.3. The model was initialised to represent an average kitchen setting, described in detail in Section 2.3.6.1.

To simulate a cleaning activity, the speciated monoterpene emission rates were applied to the model per cleaner as timed emissions at midday for an assumed cleaning period of 3 minutes. All other VOC emission rates determined from SIFT-MS analysis were not included in these simulations, because the VOCs were either not available in the model, or they exhibit low reactivity and therefore were not considered important drivers of indoor air chemistry. Cleaners with no observed monoterpene emission (SG4, BR2, BG3, DG1) were discounted from all subsequent analyses.

The chemical degradation of nine monoterpene species are represented in the model as either fully explicit reaction schemes provided by the MCM (α-pinene, β-pinene, d-limonene) (Jenkin et al., 1997; Saunders et al., 2003; Atkinson and Arey, 2003), or as proxy-schemes (camphene, carene and γ-terpinene (Carslaw, 2007), α-phellandrene, α-terpinene, and terpinolene (Appendix A)). Inclusion of these nine monoterpenes accounted for >95% of the total amount of monoterpenes identified from GC-MS analysis. Other monoterpenes identified (tricyclene, cyclofenchene, allocimene, α-thujene, α-fenchene, β-myrcene, sabinene, β-ocimene, β-phellandrene) were not included in the model because either their oxidation rate coefficients were not available in the literature, and/or they were not present in significant abundance.

3.3 Results and discussion

3.3.1 Characterisation of VOCs

High resolution GC-TOF-MS was used to analyse the headspace composition of the cleaning products selected for this study. A total of 317 VOCs occurrences were observed, representing 97 VOC identities emitted from 23 cleaning products. Of the 317 VOCs emitted from the cleaners, 64 VOCs were detected just once, 34 VOCs were detected twice, and 42 VOCs were detected in three or more cleaners. The green cleaners exhibited 6% more VOC occurrences and 36% more individual VOCs compared to the regular cleaners, demonstrating the variety in VOC composition of the green product formulations. The identified VOCs included 18 monoterpenes, 23 monoterpenoids, 8 sesquiterpenes, 17 alcohols, 17 esters, 6 aldehyde/ketone species and 8 other hydrocarbons (aromatics, alkanes, alkenes). The prevalence of the main chemical classes identified from regular and green cleaners is shown in Figure 3.1.

Monoterpenes and monoterpenoids were the most commonly identified species in both regular and green cleaners, with five monoterpenes/monoterpenoids being identified in over 50% of the cleaners tested: limonene, eucalyptol, β-pinene, 3-carene and linalool. Limonene was the most prevalent VOC identified in regular and green cleaners, which is consistent with other studies of fragranced consumer products (Steinemann, 2015; Temkin et al., 2023). The detected monoterpenoid species included 8 alcohols, 8 esters, 4 ethers, 2 ketones and 1 aldehyde. The monoterpene alcohols were common in both regular and green cleaners, while monoterpene esters were twice as prevalent in the regular cleaners. The median number of monoterpenes and monoterpenoids was greater for the regular cleaners compared to the green cleaners, although the spread of monoterpenes was greater for green cleaners. This can be explained by the inclusion of 3 non-fragranced green cleaners in the analysis, which contained only 1 monoterpene, d-limonene. The monoterpenes α-thujene, β-ocimene, β-myrcene and allocimene were identified in green cleaners only, while α-fenchene was only identified in a regular cleaner ("ocean" scented). The greater variety of monoterpene compounds in green cleaners could be an indication that naturally derived fragrance ingredients (such as es-

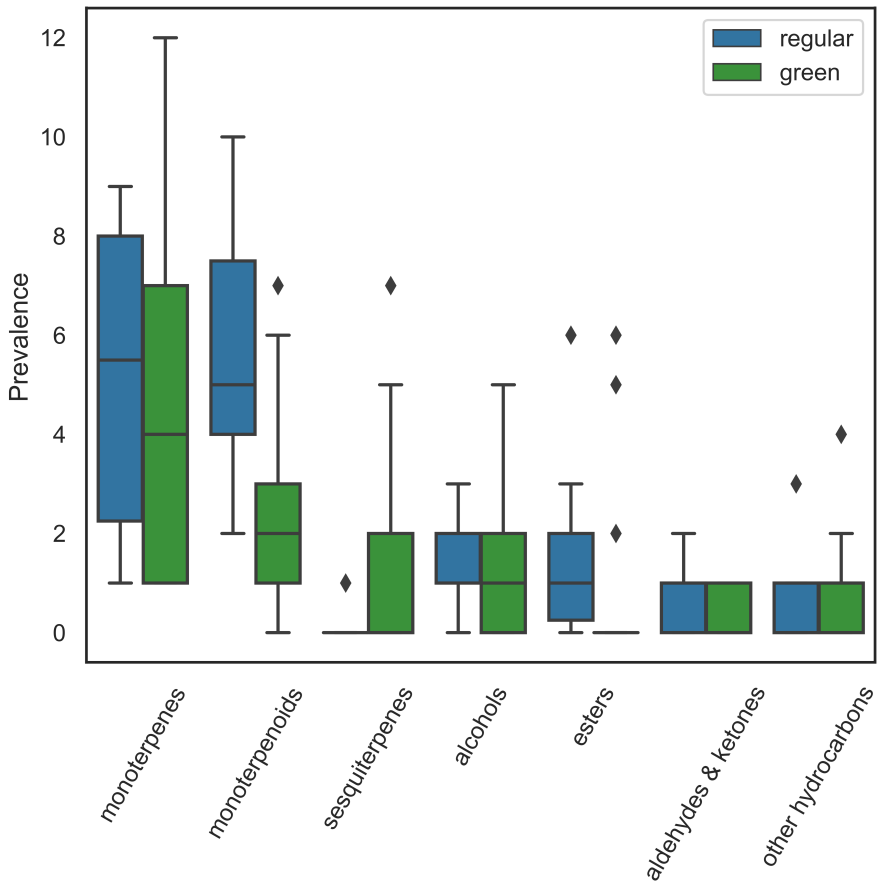

Figure 3.1: The distribution of the number of VOCs of different chemical classes detected from regular (n=10) and green (n=13) cleaners by equilibrium headspace GC-TOF-MS. Boxes show median (central mark), 25th percentile and 75th percentile (box limits) values. Whiskers extend to the data points that are within the range of the 25th percentile minus 1.5 times the IQR and the 75th percentile plus 1.5 times the IQR. Diamond-shaped markers represent outliers.

sential oils, which usually contain more than 100 different chemical substances (Lassen et al., 2008)) are more commonly used in the formulation of green cleaners.

A greater number of green cleaners contained sesquiterpenes compared to regular cleaners, while esters, aldehydes and ketones were more prevalent in the regular cleaners. A possible explanation for this difference could be that green cleaners typically use natural fragrances such as essential oils or plant extracts which consist largely of biologically synthesised terpene compounds (including monoterpenes and sesquiterpenes) and oxygenated terpene derivatives (Teixeira et al., 2013; Milhem et al., 2020).

Conversely, regular products typically incorporate synthetically derived fragrance mixtures, which will utilise synthetic aroma chemicals such as esters and other carbonyls to replicate a "natural-identical" scent (although the exact chemical composition of synthetic fragrances is often proprietary information) (Lassen et al., 2008).

3.3.2 Targeted quantification of VOCs

SIFT-MS was used with dynamic headspace sampling to directly quantify a targeted subset of VOCs in the cleaning product formulations. The compounds targeted in this analysis were selected based on the information obtained from the product ingredient lists, results from GC-MS analysis, and common VOCs reported in the literature regarding cleaning product emissions.

The headspace VOC concentrations increased immediately after the sample was introduced into the sample chamber, as the VOCs partitioned from the liquid to the gas phase. Over the duration of the 60-minute measurement period the VOC concentrations peaked and then declined as the emission source was depleted, finally returning to background concentrations. An example of the VOC concentration profiles measured from a green surface cleaner (SG2) is shown in Figure 3.2. This characteristic VOC concentration profile supported the assumption that the total amount of each VOC in the product formulation was released within the measurement period.

The mass concentrations of VOCs in the cleaning product formulations are reported in Table 3.4. The total VOC mass concentrations measured in this study ranged from 9.3 to 25441 mg/L, which is comparable to a study by Temkin et al. (2023), who reported mass concentrations ranging from 0.97 to 38035 mg/L (μg/g) from 30 regular and green cleaning products. DR1, SG1, and SG3 were the cleaners containing the largest total mass concentration of VOCs, with the measured compounds accounting for 2.5%, 2.0% and 1.3% of the total sample (w:v%). Ethanol was the greatest contributor to total VOC concentration for these cleaners, and was identified in 15 of the 23 samples, suggesting that it may be used as a common solvent in cleaning product formulations. Ethanol was explicitly listed as an ingredient in only one product (FG2),

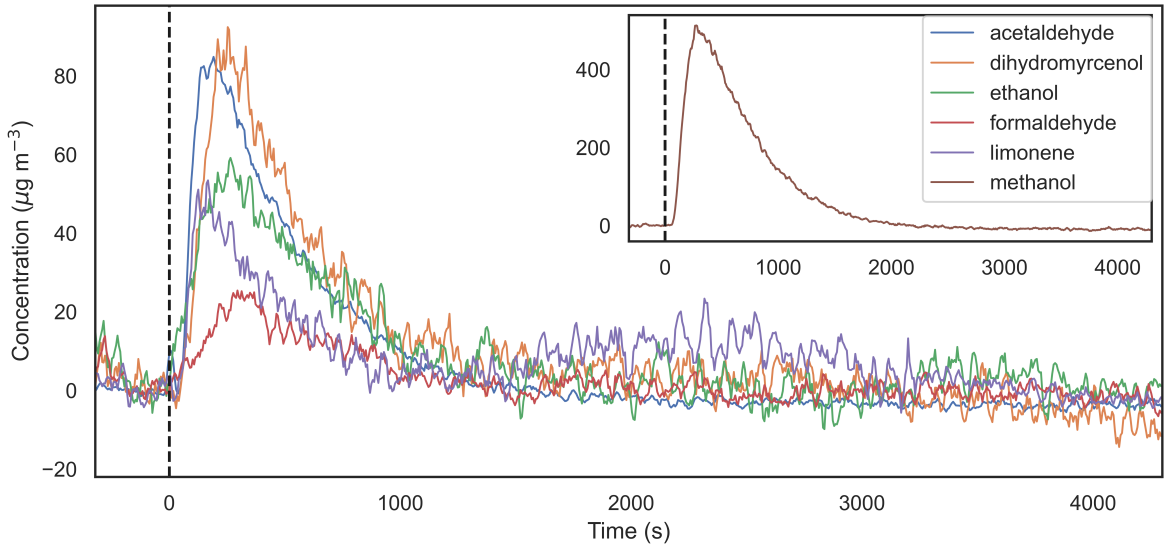

Figure 3.2: The concentration profile of VOCs measured from cleaner SG2 by SIFT-MS with dynamic headspace sampling. t_0 = time when sample was introduced to the headspace chamber (black dashed line). Inset shows the measured concentration of methanol on an enhanced y-axis scale for clarity.

although a further 8 included 'alcohol' in the ingredient list. Methanol was also identified as a component of most of the cleaning product formulations, with quantifiable measurements made from 17 of the 23 cleaners ranging from 1418 to <10 mg/L.

Table 3.4: VOC mass concentrations measured from cleaning product formulations by headspace SIFT-MS (mg/L).

sample ID	acetaldehyde	total monoterpenes	methanol	dihydromyrcenol	2-tert-butylcyclohexyl acetate	ethanol	formaldehyde	citral	lactic acid	2-phenethyl acetate	1,2,4-trimethylbenzene	total sesquiterpenes	m-xylene	cinnamaldehyde	eugenol	benzyl benzoate	benzene	total
DR1	194.7	30.7	1418.4	236.9	56.2	22439.8	255.3	54.0	728.2	-	5.9	16.4	-	4.8	-	-	-	25441.3
SG1	160.3	19.0	-	151.3	11.6	18727.2	188.1	5.1	666.0	-	-	3.5	-	-	-	-	-	19932.1
SG3	173.8	8.9	-	57.1	40.3	12047.9	199.4	14.4	270.4	14.9	10.8	-	12.3	-	0.9	-	-	12850.9
FG4	139.2	167.4	13.4	218.8	43.2	-	79.7	110.4	9206.0	6.2	6.1	41.5	1.9	86.6	-	-	-	10120.4
FG2	83.8	6.1	111.0	44.2	15.7	6198.9	71.8	14.2	164.7	1.9	1.3	21.1	-	66.9	-	9.6	-	6811.3
BG2	7.4	13.2	337.1	12.8	6.2	506.8	18.3	11.2	-	1.8	-	-	-	-	-	4.0	-	918.8
BG1	4.9	7.4	-	6.6	-	607.0	11.3	13.0	0.2	-	-	-	-	-	-	-	-	650.4
DG2	11.5	11.1	2.9	31.1	9.8	493.2	9.6	3.8	1.9	-	1.9	-	1.0	-	-	-	0.5	578.3
SR4	3.1	1.8	4.5	-	-	115.4	2.2	-	-	-	-	-	-	-	-	-	-	127.0
DR2	7.1	26.8	12.3	37.6	6.5	3.9	-	6.3	-	1.6	-	-	-	-	-	-	-	101.9
FG1	4.8	9.1	7.3	48.3	-	4.7	4.6	-	-	-	-	-	1.2	-	-	-	-	79.9
SG2	4.4	5.1	44.8	5.9	3.7	5.4	1.8	-	-	1.9	-	-	-	-	-	-	-	73.0
SR3	0.8	3.5	5.6	9.3	41.3	-	-	-	-	-	-	-	-	-	-	-	-	60.5
FR2	1.6	1.8	4.6	36.5	7.4	-	-	5.3	-	-	-	-	-	-	1.2	-	-	58.5
SR1	3.1	1.3	21.3	12.7	3.7	1.5	-	1.9	-	-	-	-	-	-	-	-	-	45.5
BR1	0.2	2.8	-	9.9	16.6	6.0	1.0	-	-	-	-	-	-	-	-	-	-	36.5
DG1	3.8	-	32.0	-	-	-	-	-	-	-	-	-	-	-	-	-	-	35.8
BR2	0.6	-	1.6	9.8	20.4	-	-	-	-	0.6	-	-	-	-	-	-	-	33.1
FR1	0.6	6.0	8.5	5.4	2.8	3.6	-	-	-	-	-	-	-	-	-	-	-	26.8
FG3	2.8	2.6	-	-	-	11.9	-	-	-	-	-	-	-	-	-	-	-	17.3
BG3	1.2	-	15.8	-	-	-	-	-	-	-	-	-	-	-	-	-	-	17.0
SR2	0.9	2.8	2.4	-	4.4	-	-	-	-	-	-	-	-	-	-	-	-	10.5
SG4	-	-	-	-	-	-	-	-	9.3	-	-	-	-	-	-	-	-	9.3

Formaldehyde and acetaldehyde were also emitted from most of the cleaning products at mass concentrations as high as 255.3 mg/L and 194.7 mg/L, respectively. These results are consistent with Temkin et al. (2023), who observed formaldehyde and acetaldehyde emissions from over 30% of a range of regular and green cleaning products in the U.S. market. Short chain aldehydes such as formaldehyde and acetaldehyde are pollutants of concern in the indoor environment due to their known or suspected toxicity, carcinogenicity and mutagenicity (World Health Organization, 2010; ECHA, 2023). These results suggest that while they were not listed ingredients for any of the formulations, some cleaning products may be primary sources of formaldehyde and acetaldehyde in the built environment.

Lactic acid was identified as a component of 7 green cleaners and 1 regular cleaner. This compound was included in the ingredient list of 5 of the green cleaners including SG1 and SG3, for which relatively large mass concentrations were measured (660.0 and 270.4 mg/L, respectively). However, the largest mass concentrations of lactic acid were measured from FG4 (9206.0 mg/L) and DR1 (728.2 mg/L), which did not state lactic acid as an ingredient. Lactic acid is used in the green cleaning industry as a descaling and antimicrobial agent, which is produced by fermentation based on natural and renewable resources, and used as an alternative to synthetic alternatives such as inorganic acids (Hwang et al., 2022).

Of the 23 cleaners studied, 20 listed fragrance components (usually non-specific e.g., 'parfum') in their ingredients, with 10 explicitly listing limonene. The results from SIFT-MS were in good agreement with this observation, as monoterpenes were measured in 19 of the fragranced cleaners. Monoterpenes were undetected in the 3 unfragranced cleaners (DG1, BG3, SG4), as well as fragranced cleaner BR2. Of the fragranced cleaners, the average mass concentration of total monoterpenes was 8.6 and 25.0 mg/L for regular and green cleaners, respectively. Although there is limited information available regarding liquid composition of cleaning products, this value is low compared to those reported in other studies. Singer et al. (2006) reported a mass concentration of 44850 mg/L (44.85 mg/mL) of monoterpenes in a pine oil-

based general-purpose cleaner , while Angulo Milhem et al. (2021) reported mass concentrations ranging from 15.0 to 992.6 mg/L (μg/g) of monoterpenes from 6 essential oil-based cleaners. However, it is worth noting that the chemical formulation of cleaning products is likely to vary widely depending on the type of cleaning agent, the manufacturer, and regional regulations and policies regarding product formulation (with the latter likely changing over time, making it particularly hard to compare between studies separated by significant time periods). Additionally, both of these past studies focussed on cleaning products which were essential oil-based (i.e., an essential oil was listed as an ingredient of the cleaner), whereas this was not a requirement for product selection in this study. Essential oils are mainly composed of terpenes and terpenoids, therefore formulations containing these ingredients are likely to have a larger concentration of monoterpenes compared to other products (Dhifi et al., 2016).

Other fragrance compounds identified in the product formulations included dihydromyrcenol ($C_{10}H_{20}O$, found in 17 cleaners), citral ($C_{10}H_{16}O$, found in 11 cleaners), sesquiterpenes ($C_{15}H_{24}$, found in 4 cleaners), cinnamaldehyde (C_9H_8O, found in 3 cleaners) and eugenol ($C_{10}H_{12}O_2$, found in 2 cleaners). It is worth nothing that monoterpene alcohols ($C_{10}H_{18}O$) were not measured by the SIFT-MS, and therefore concentrations of species such as linalool and eucalyptol, which were identified in the formulations using GC-MS, were not quantified.

Emission rates of the measured VOC species from a typical cleaning activity on a realistic scale were estimated using the approach outlined in Section 3.2.2.2. The emission rates were used to initialise an indoor air chemistry model to gain a better understanding of the chemical fate of VOC emissions following cleaning, and the potential for harmful secondary pollutant formation.

3.3.3 Monoterpene emissions and implications for indoor air chemistry

To investigate the production of secondary pollutants from terpene oxidation chemistry following cleaning, the measured monoterpene emission rates were used to drive

the indoor air chemistry model, INCHEM-Py (Shaw et al., 2023). It was anticipated that the different combinations of monoterpene emissions in the cleaning simulations would give rise to different concentrations of secondary pollutants. This was observed by Carslaw and Shaw (2022), who found that emissions of a 50:50 mix of limonene and α-pinene resulted in more efficient production of formaldehyde than the same concentration of the individual terpenes, while emissions of each monoterpene individually resulted in more efficient production of radical species and PM. Therefore, the secondary chemistry resulting from the complex terpene mixtures contained within fragranced cleaning products is likely to depend not only on the chemical reactivity of the individual species towards indoor oxidants, but also on the interplay between the chemical transformations and relative concentrations of each compound emitted from the cleaner.

The chemical reactivity of the nine monoterpenes included in the model simulations is described in Table 3.5. For each monoterpene, the rate of reaction is generally fastest with OH, followed by NO_3. The rate of reaction with O_3 is much slower, with rate coefficients of the order of 10^{-14} to 10^{-19}. However, due to the high reactivity and instability of radical species, OH and NO_3 are short lived and are present in indoor environments at much lower concentrations compared to O_3, which has a longer lifetime and originates mostly from outdoor environments (Nazaroff and Weschler, 2022). Therefore, initial oxidation of monoterpenes is generally more likely to occur via ozonolysis. The most reactive monoterpene towards O_3 is α-terpinene, while the least reactive is camphene.

Oxidation of a monoterpene can lead to net OH production or loss, depending on the balance between OH formation through ozonolysis, versus OH loss through reaction with the monoterpene. At any time, this balance depends on the ratio of the rate coefficients for reactions with OH and O_3 and the OH yield following ozonolysis for a particular monoterpene, and the OH and O_3 concentrations. Table 3.5 shows a proxy for this metric in the final column, which represents the balance between formation and loss of OH for each monoterpene using the O_3 and OH concentrations estimated

Table 3.5: Rate coefficients for the reactions of monoterpenes relevant to this study with OH, NO_3, and O_3 at 298 K, the yield of OH formed from the reactions between the monoterpenes and O_3 and the OH production/loss ratio*. The rate coefficients and OH yields of d-limonene, α-pinene and β-pinene are from the MCM (*MCM*, 2023). All other rate coefficients and OH yields are from IUPAC Atmospheric Chemical Kinetic Data Evaluation (IUPAC, 2023), using the preferred values where possible.

Monoterpene	Rate coefficient (cm^3 $molecule^{-1}$ s^{-1})			OH yield (%)	OH production/loss
	k(OH)	$k(NO_3)$	$k(O_3)$		
α-terpinene	3.5×10^{-10}	1.8×10^{-10}	1.9×10^{-14}	0.38	1.77
terpinolene	2.2×10^{-10}	9.7×10^{-11}	1.6×10^{-15}	0.70	0.44
α-phellandrene	3.2×10^{-10}	7.3×10^{-11}	2.9×10^{-15}	0.32	0.25
α-pinene	5.3×10^{-11}	6.2×10^{-12}	9.4×10^{-17}	0.80	0.12
d-limonene	1.6×10^{-10}	1.2×10^{-11}	2.1×10^{-16}	0.87	0.10
γ-terpinene	1.7×10^{-10}	2.9×10^{-11}	1.6×10^{-16}	0.81	0.07
3-carene	8.8×10^{-11} [a]	9.1×10^{-12}	4.9×10^{-17}	0.86	0.04
β-pinene	7.9×10^{-11}	2.5×10^{-12}	1.9×10^{-17}	0.35	0.01
camphene	5.3×10^{-11} [b]	6.6×10^{-13}	5.0×10^{-19}	0.18	0.00

[a] Atmos. Chem. Phys. 2021, 21, 12665– 12685, DOI: 10.5194/acp-21-12665-2021
[b] Atmospheric Environment. Part A. General Topics, (1990), 2647-2654, 24(10)
∗ The final column shows an estimate of the ratio of OH production: loss calculated as $k(O_3)[O_3] \times$ OH yield / k(OH)[OH], where $[O_3] = 1.06 \times 10^{11}$ molecule cm^{-3} and $[OH] = 1.23 \times 10^6$ molecule cm^{-3} (simulated indoor concentrations at 12:00).

by the model at midday. Under these conditions, α-terpinene will contribute most per ppb to OH production indoors, due to its large O_3 rate coefficient compared to the OH rate coefficient. Camphene is the least important for OH production per ppb due to its very low O_3 rate coefficient. Depending on the mixtures of these monoterpene species indoors, one might expect quite different oxidation chemistry and hence secondary pollutant formation indoors.

The total monoterpene emission rates applied to the model are shown in Figure 3.3a. Emission rates ranged from 5.9×10^5 to 2.0×10^8 molecule cm^{-3} s^{-1} (equivalent to 85 ppt h^{-1} and 29 ppb h^{-1}, respectively) with the top 7 emitters being green cleaners. Dishwashing detergents were the lowest emitters of monoterpenes, likely owing to the large dilution upon use of these products. The relative abundance ratios of monoterpene isomers used to speciate the total monoterpene emissions are shown in Figure 3.3b. Limonene was the most abundant monoterpene in most cleaners, with

two cleaners emitting 100% limonene. Other cleaners consisted of unique monoterpene profiles relating to the specific formulation ingredients of each product.

To illustrate the differences in reactivity towards indoor oxidants, the speciated monoterpene emission rates and relative abundance ratios for each cleaner were scaled to their corresponding O_3 and OH rate coefficients (Table 3.5) in Figure 3.3c/d and 3.3e/f, respectively. This process is illustrative given that monoterpenes react readily with O_3 and OH indoors.

The relative magnitude of the k_{O3}/k_{OH}-scaled emission rates increased or decreased in comparison to the total monoterpene emission rates per cleaning product, depending on the concentration and chemical reactivity of the different mixtures of monoterpene species emitted. SG1 had the highest monoterpene emission rate of all the cleaning products, consisting entirely of limonene, and also gave the largest value when scaled to k_{O3} and k_{OH}. Cleaning products which contained the most reactive monoterpenes α-terpinene, α-phellandrene and terpinolene typically resulted in an increase in the relative magnitude of the k_{O3}-scaled emission rate. This was particularly observed for cleaners SG2, SR4, DR1, and FR2, which were the 4 largest emitters of these compounds. Interestingly, the cleaners containing the most reactive monoterpenes were mainly regular products. Conversely, when there were greater contributions to the total monoterpene emission rate from less reactive species such as camphene, β-pinene and 3-carene, a decrease in the relative magnitude of the k_{O3}-scaled emission rate was observed. This was the case for cleaners FG4, FG3 and SR2, which were among the highest emitters of these relatively low-reactivity monoterpenes.

The total monoterpene emission rates of the regular surface cleaners SR4 and SR1 were of similar magnitude (1.87×10^7 molecule cm^{-3} s^{-1} and 1.43×10^7 molecule cm^{-3} s^{-1}, respectively), however the magnitude of the k_{O3}-scaled emission rates were considerably different for these two cleaners. The monoterpene emissions from SR1 consisted of 2% the most reactive monoterpenes and 58% of the less reactive monoterpenes, while those from SR4 consisted of 38% of reactive monoterpenes and 13% of low-reactivity monoterpenes. When scaled to the O_3 rate coefficients, the reactive

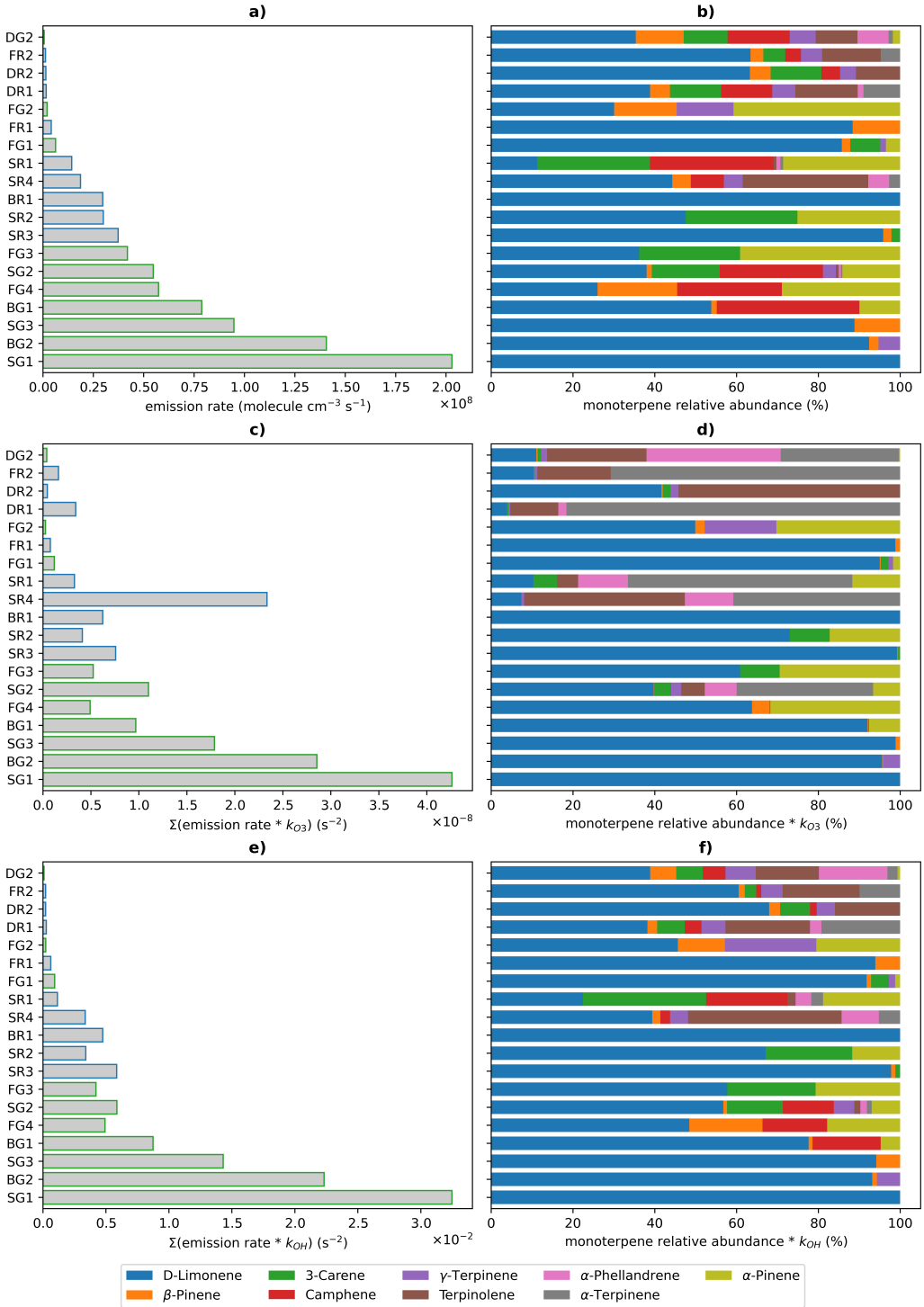

Figure 3.3: a) Estimated total monoterpene emission rates per product (green edge bars = green cleaners, blue edge bar = regular cleaners). b) The relative abundance (%) of monoterpenes used to speciate the total monoterpene emission rates. c) The sum of the monoterpene emission rates scaled to their respective O_3 rate coefficients per product. d) The relative abundance (%) of monoterpenes scaled to their respective O_3 rate coefficients. e) The sum of the monoterpene emission rates scaled to their respective OH rate coefficients per product. f) The relative abundance (%) of monoterpenes scaled to their respective OH rate coefficients.

monoterpene emissions contributed 72% and 91% for SR1 and SR4, respectively, despite these species only making up 2% of the overall monoterpene emission rate for SR1. This demonstrates that the more reactive species will dominate the chemistry and sequester the most O_3 from the indoor atmosphere, thus limiting the reactions of other monoterpenes with O_3. Therefore, reactive species such as α-terpinene, α-phellandrene and terpinolene will have a greater impact on the indoor air chemistry and resulting secondary pollutant concentrations, compared to less reactive species such as camphene, β-pinene and 3-carene.

With respect to monoterpene-OH chemistry, changes in the magnitude of k_{OH}-scaled emission rates relative to the total monoterpene emission rates were less pronounced compared to that of the k_{O3}-scaled emission rates. Table 3.5 shows that the monoterpene k_{OH} values span a smaller range compared to the k_{O3} values, meaning that there is less variability between the different monoterpene isomers with respect to their reactivity towards OH. Consequently, the k_{OH}-scaled monoterpene relative abundance in Figure 3.3f showed a similar pattern to the monoterpene relative abundance in Figure 3.3a, with limonene acting as the dominant terpene for most cleaners. These results suggest that the chemical identity of monoterpene species emitted from cleaners has a smaller impact on the resulting secondary chemistry from OH oxidation compared to O_3 chemistry.

In the simulated cleaning events, the peak total monoterpene mixing ratio following the timed emissions ranged from <0.2 to 4.8 ppb. These concentrations are low compared to a study performed by Singer et al. (2006), who reported an average concentration of 2857 μg m^{-3} (513 ppb) monoterpenes in the first 60 minutes after mopping the floors of a 50 cm^3 chamber with a pine oil-based general-purpose cleaner. By contrast, in the HOMEChem campaign, an increase in limonene concentration of roughly 3 ppb was reported when mopping the floors of an experimental house with a terpene cleaner, much closer to our observed results (Farmer et al., 2019). The results reported in the literature demonstrate the large variability in terpene emissions from cleaning, likely arising from differences in product composition, dependencies on behavioural factors

such as how the product is used/applied and how long for, and environmental factors such as ventilation conditions. These dependencies result in wide variations in experimental methodologies used to assess the VOC emissions from cleaning activities, thus limiting the ability to make meaningful comparisons of the reported results (Angulo Milhem et al., 2021).

The effect of monoterpene emissions on oxidant and radical species concentrations were investigated in greater detail to understand the chemical transformations that take place following a cleaning event. Figure 3.4 shows the relative change in concentration of various species compared to a baseline simulation for the regular and green surface cleaners only, for simplicity. Following cleaning, OH concentrations showed a rapid decrease as they reacted with the monoterpenes introduced to the system. The exception is SR4, which showed an increase in OH radicals following cleaning. Figure 3.3 shows that this product contained α-terpinene, which is very effective at producing OH (see Table 3.5). SG1 showed the biggest decrease in OH concentration, which is

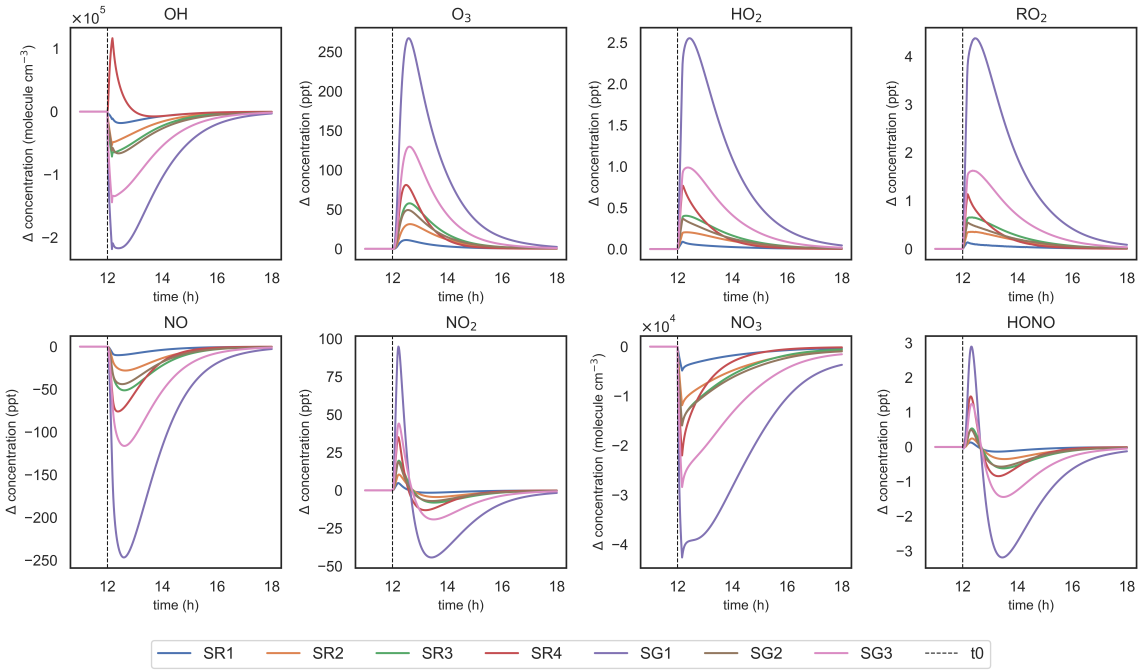

Figure 3.4: Relative change in concentration of key indoor species from 11-18 h for each surface cleaner simulation, compared to a baseline simulation (no emissions). Dashed line shows t_0 (12:00), when the cleaning activity commenced.

composed entirely of limonene. Under these conditions, limonene effectively removed the OH.

For all cleaning simulations, the concentration of O_3 increased compared to the baseline simulation despite the occurrence of monoterpene-O_3 reactions. This is due to the production of peroxy (RO_2) and hydroxy (HO_2) radicals from monoterpene oxidation chemistry which react with nitric oxide (NO) to generate nitrogen dioxide (NO_2), as evidenced by the changes in these species' concentrations shown in Figure 3.4. NO_2 undergoes photolysis to generate an oxygen atom, which then rapidly reacts with O_2 to generate O_3. Additionally, the sequestration of NO by reaction with RO_2 and HO_2 limits O_3 loss via reaction with NO, thus enhancing O_3 concentrations in the system compared to baseline. The greatest increase in O_3 concentration was observed for SG1 and SG3 which were the two largest monoterpene emitters, both consisting of over 85% limonene. SR4 caused the next largest increase in O_3, despite having the second smallest monoterpene emission of the surface cleaners. Figure 3.3b shows that this product contained highly reactive monoterpenes (30% terpinolene, 3% α-terpinene and 5% α-phellandrene) resulting in efficient HO_2 and RO_2 production, hence more efficient NO_2 production and NO removal, favouring an overall increase in O_3 concentration.

The concentrations of NO_2 and nitrous acid (HONO) both showed an initial increase following cleaning, followed by a rapid decrease to concentrations lower than the baseline simulation a few hours after cleaning. The main pathway of NO_2 production in the model is via the NO+O_3 reaction, therefore the concentration of NO_2 will depend critically on the concentrations of NO and O_3. Initially after cleaning, the NO and O_3 concentrations were sufficient for efficient production of NO_2. However, as time proceeded, NO concentrations declined due to the increasing concentrations of RO_2 and HO_2 radicals, thus NO concentration became the limiting factor for NO_2 production, causing a decline in NO_2 concentrations relative to the baseline simulation. The main production pathway for HONO in the model is via heterogeneous chemistry of NO_2 on indoor surfaces at a rate of $(2.9 \pm 1.8) \times 10^{-3}$ m min^{-1} (Wainman et al., 2001;

Kurtenbach et al., 2001), hence the concentration of HONO was strongly coupled to the concentration of NO_2 under these conditions.

The concentration of NO_3 radicals was low and decreased in all simulations owing to its high reactivity towards VOCs, particularly unsaturated compounds such as monoterpenes (Atkinson and Arey, 2003). This chemistry further contributes to the production of RO_2 and nitrooxy-substituted RO_2 radicals and organic nitrates, which are an important precursor for SOA (Carslaw et al., 2012).

The impact of the chemistry following cleaning on the production of secondary pollutants was evaluated for each cleaner. The percentage change in concentration of formaldehyde, PANs and organic nitrates are shown in Figure 3.6. These species were selected based on their known or suspected health impacts. formaldehyde is well understood to be a carcinogen (Nielsen and Wolkoff, 2010; World Health Organization, 2010) and is produced via the reaction of oxy radicals (RO) with ambient oxygen (Figure 3.5, pathway 2). There is less evidence regarding the detrimental health effects of PANs and organic nitrates, although they are both suspected of being irritants (Altshuller, 1978; Zhang et al., 2015; Koenig et al., 1989; Berkemeier et al., 2016). PANs are formed by reaction of peroxyacetyl radicals (RCO_3) with NO_2 (Figure 3.5, pathway 3), while organic nitrates are formed as minor reaction products of RO_2+NO chemistry (Figure 3.5, pathway 1).

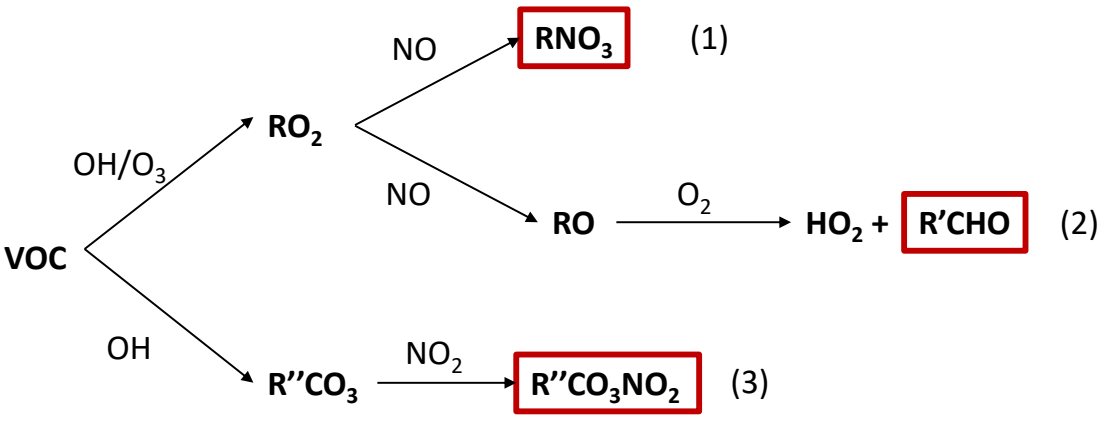

Figure 3.5: The general VOC oxidation chemistry leading to the formation of key secondary pollutants: organic nitrates (RNO_3), formaldehyde (HCHO) and PAN species (RCO_3NO_2).

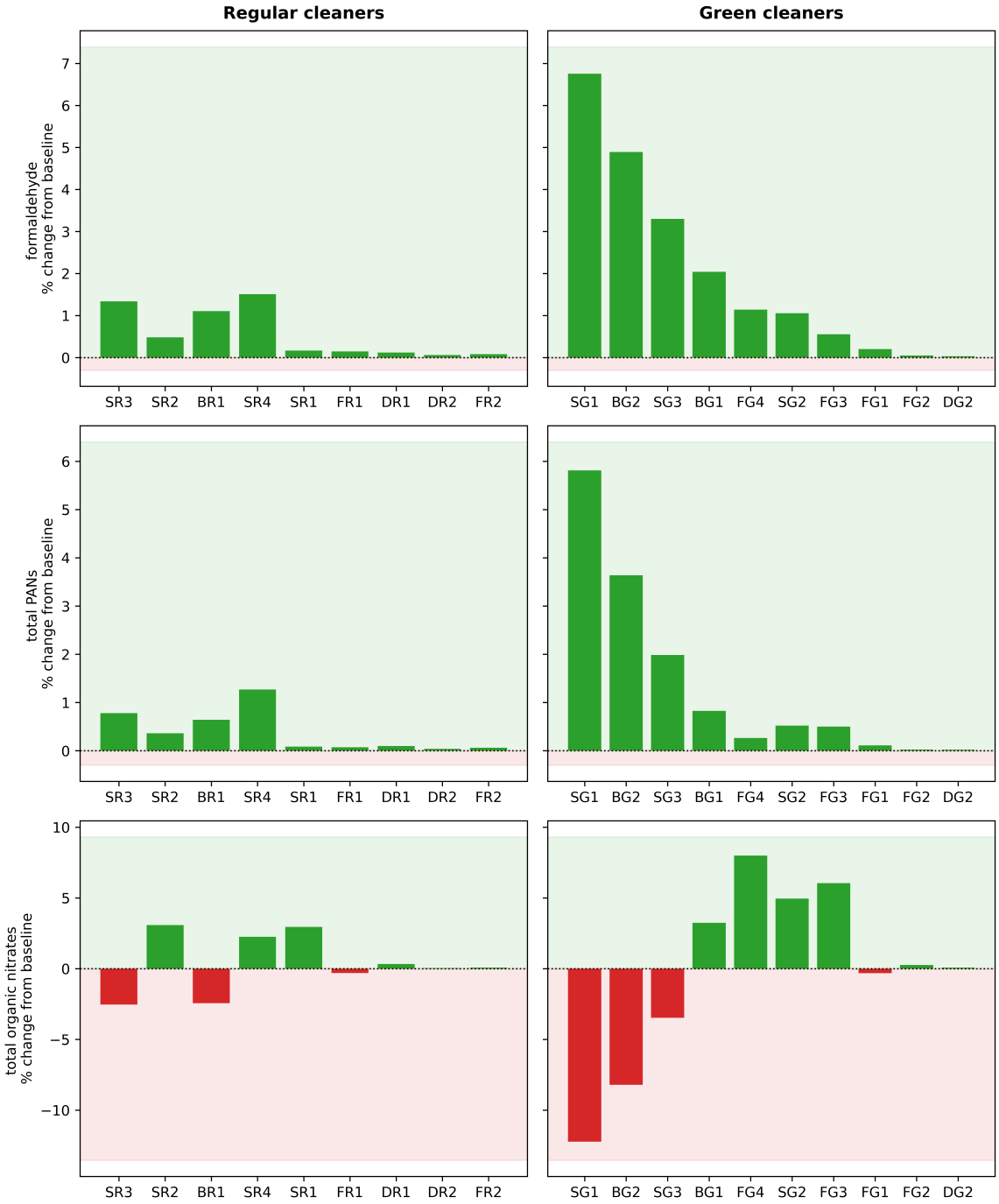

Figure 3.6: Percentage difference in 3-hour post-emission average concentrations of secondary pollutants formaldehyde, total PANs, and total organic nitrates, compared to the baseline simulation for regular (LHS) and green (RHS) cleaners.

Formaldehyde was produced in all cleaning simulations as a product of monoterpene oxidation. The extent of formaldehyde production varied from <0.1 to 6.8% relative to the baseline simulation over an average of 3 hours following cleaning. This relates to absolute formaldehyde mixing ratios of <2 ppb for all simulations, which is well below the safe exposure limits (World Health Organization, 2010). However, it is worth noting that while formaldehyde concentrations fall below the recommended exposure limit of 0.1 ppm under these conditions (Golden, 2011), larger concentrations are likely to arise from cleaning events involving multiple products and/or for longer cleaning periods. This is a particularly important consideration when evaluating occupational exposure to hazardous pollutants from cleaning, as professional cleaners will likely be exposed to higher concentrations of pollutants and for a much longer time than considered in this study.

Increases in formaldehyde concentration remained below 2% for all regular cleaners, while larger changes were observed for some green surface and bathroom cleaners (SG1, BG2, SG3, BG1). The increase in formaldehyde concentration correlated well with the magnitude of total monoterpene emissions shown in Figure 3.3a. The exception was SR4, which produced a similar increase in formaldehyde concentration as FG3 (1.5% and 1.1% increase in formaldehyde, respectively), despite SR4 having a total monoterpene emission rate of less than half that of than FG3 (1.9×10^7 molecule cm^{-3} s^{-1} and 4.2×10^7 molecule cm^{-3} s^{-1}, respectively). Again, this can be attributed to the high reactivity of the monoterpenes emitted from SR4 towards indoor oxidants, leading to efficient RO_2 formation, and subsequent formaldehyde production via reaction pathway 2 in Figure 3.5.

PAN species were produced in all cleaning simulations, owing to the oxidation of emitted monoterpenes by OH to produce RCO_3 species which further react via pathway 3 in Figure 3.5. The formation of PANs following cleaning was small for most cleaners, with only three cleaners resulting in a 3-hour average change of >1% from the baseline simulation. SG1 was the largest producer of PANs, resulting in a 3-hour average absolute mixing ratio of 25 ppt. SG1 was the largest emitter of total monoterpenes,

consisting entirely of limonene which has a relatively high OH rate coefficient (Table 3.5). The formation of PAN species was dependent on the magnitude of monoterpene emissions from the cleaning event and the reactivity of the emitted monoterpenes towards OH.

Finally, the concentration of organic nitrate compounds showed positive and negative changes in the simulations of both regular and green cleaning emissions. The formation of organic nitrates is dependent on the branching ratio of RO_2+NO reactions to form RO ($\geq 80\%$) or organic nitrate species ($\leq 20\%$) (Davies et al., 2023). Hence, the specific RO_2 species formed via initial oxidation of monoterpene species determines the yield of organic nitrate via pathway 1 in Figure 3.5. This is further evidence of how the complex mixture of different VOCs in cleaning products can influence the indoor air chemistry and the concentrations of potentially hazardous air pollutants.

3.4 Chapter summary

Mass spectrometric techniques coupled with headspace sampling have been implemented to characterise and quantify the VOCs present in a range of regular and green household cleaning products. While the composition of each product formulation was unique, it was found that both regular and green cleaners contained VOCs pertaining to the broad chemical classes of monoterpenes, monoterpenoids, sesquiterpenes, alcohols, esters, carbonyls and other hydrocarbons. Monoterpenes and monoterpenoids were the most common compounds identified in the formulations of fragranced cleaners.

Targeted quantitative analysis of each formulation showed that there was large variety in the concentrations of VOCs in the product formulations. A comparison of the compounds detected versus those disclosed by manufacturers on the product labels supported evidence of ambiguity regarding cleaning product compositional information, highlighted in previous studies (Steinemann, 2009, 2015). Alcohols (ethanol and methanol) were measured in high concentrations from some regular and green cleaners, while lactic acid was observed in predominantly green cleaners. These observations highlight potential compositional differences in the formulations of regular and green cleaners, for which there is currently very little information in the available literature.

The implications of reactive monoterpene emissions from each cleaner on the indoor air chemistry was investigated using a detailed chemical model. The results of the model simulations highlighted the significance of both the quantity and the chemical reactivity of monoterpene emissions on the concentrations of oxidants, radicals and secondary pollutants indoors. In the present study, green cleaners were generally larger sources of monoterpene emissions compared to regular cleaners, resulting in larger increases in harmful secondary pollutants such as formaldehyde and PANs. However, emissions of highly reactive monoterpenes such as α-terpinene, terpinolene and α-phellandrene were observed from more regular cleaners than green cleaners, resulting in a disproportionately large impact on the concentrations of radical species

and the production of formaldehyde.

The production of secondary pollutants from cleaning emissions reported in this study are unlikely to cause detrimental health effects to occupants. However, there is significant variability in product formulations and occupant/environmental factors that would influence the VOC emissions from cleaning and subsequent chemical processing. In this study, the cleaning activity was assumed to occur for 3 minutes with typical ventilation conditions of 0.5 h^{-1}. It is important to note that, in real-life scenarios, cleaning activities may last longer and involve the use of several different products within a short time frame. Additionally, lower ventilation rates, such as those found in modern, energy-efficient buildings, may occur. These conditions could lead to higher indoor VOC concentrations, thus increasing the potential for secondary pollutant formation. Therefore, it is necessary to investigate a broader range of products and study VOC emissions from cleaning on a more realistic scale to better understand how cleaning can contribute to indoor air pollution.

As sales of green cleaning products are increasing there exists a greater need for better regulation of these products. More transparent disclosure of cleaning product formulation ingredients is required to better inform consumers about potential exposure risks. Also, more careful consideration is required for the potential exposure to secondary pollutants resulting from chemical processing of the mixtures of reactive primary VOC emissions from cleaning. The quantity and chemical reactivity of monoterpene compounds used to provide fragrance for cleaning products should be carefully considered in the formulation development stage of product manufacture, and the potential implications on indoor air pollution assessed. These findings are also applicable to other fragranced household products, such as personal care products and laundry products.

Chapter 4

Impacts of Cleaning Product Formulation Composition and Environmental Conditions on Indoor Air Chemistry

4.1 Introduction

Cleaning activities are a large source of VOCs indoors, including terpenes, alcohols, esters, glycol ethers, hydrocarbons, and carbonyl species (Wolkoff et al., 1998). Many of these VOCs react with oxidants present indoors to form more functionalised and potentially harmful secondary pollutants. One particular class of reactive VOCs emitted from fragranced household products, including cleaners, is monoterpenes (Nazaroff and Weschler, 2004). Monoterpenes contain carbon-carbon double bonds, making them particularly susceptible to oxidation by O_3, which infiltrates indoor environments from outdoor air (Weschler, 2000; Wolkoff et al., 2008). The ozonolysis of monoterpenes generates a wealth of oxidised products, in addition to intermediate reactive radicals such as OH, which further drive VOC oxidation chemistry indoors (Carslaw, 2013). Products of VOC oxidation include formaldehyde, organic nitrated species, and PAN

species, which are known or suspected to cause adverse health effects (Davies et al., 2023).

Exposure to the primary and secondary pollutants from cleaning activities depends on both the chemical composition of the cleaning product and usage patterns, such as the frequency and duration of use, and the diffusion and application mode of the product. An increasing number of studies have aimed to characterise the VOC emissions from cleaning activities indoors. However, large variability exists between studies, in part due to the large heterogeneity of cleaning product composition and experimental factors such as loading factor, application procedure, and amount of product used (Milhem et al., 2020).

Arata et al. (2021) demonstrated the variability in product composition by observing different chemical compositions and quantities of VOC emissions from floor mopping with two cleaners. Natural cleaners predominantly emitted terpenoid compounds, while bleach cleaners emitted chlorinated compounds. Additionally, the Lifting Up Communities by Intervening with Research (LUCIR) intervention study found that conventional bleach products, disinfecting wipes, and dish soap resulted in elevated concentrations of hazardous VOCs such as chloroform, while 'natural' all-purpose cleaners resulted in increases in concentration of some fragrance compounds of concern (Calderon et al., 2022).

Singer et al. (2006) demonstrated that product use patterns may also influence the resulting VOC emissions. They found that using a neat surface cleaner resulted in higher VOC emissions compared to floor mopping with a dilute solution. Furthermore, leaving used cleaning towels in the room considerably increased the concentrations of pollutants indoors for several hours after the cleaning event, highlighting how differences in cleaning protocols can significantly affect indoor air pollution levels.

The chemical processing of reactive VOC emissions from cleaning depends on various environmental factors, including the ACR, outdoor pollutant concentrations, indoor SAV, and levels of indoor light (Weschler and Carslaw, 2018). Only a limited number of studies have evaluated the dynamic processes affecting primary and secondary

pollutant emissions from cleaning, frequently utilising controlled test environments such as emission chambers. For example, Destaillats et al. (2006) used a 198-L flow reaction chamber to demonstrate that the production of secondary pollutants from household product emissions depended primarily on O_3 concentration, as well as other parameters such as the ACR. While emission chambers offer valuable insights into the chemical processing of VOCs relevant to cleaning emissions, their limitations - such as their smaller size, short testing duration, and lack of surface interactions - often result in an oversimplification of real-world conditions (Milhem et al., 2020). This makes it challenging to fully capture the complexity and variability of indoor environments in these studies.

VOC emissions from cleaning have also been examined on a more realistic scale through observational and test house studies. Observational studies provide measurements under real-world conditions. However, due to the presence of multiple indoor pollutant sources, complex surface interactions, and the complexity of occupant behaviour, apportioning specific pollutant emissions to a particular source is challenging. Additionally, observational studies typically target a small subset of VOCs, measured using traditional passive sampling coupled with chromatographic analysis. For example, Wang et al. (2017) conducted continuous whole-air sampling over five days in 25 UK residences, obtaining quantitative measurements of 8 VOCs. This study showed greater variability in the 5-day average concentrations of monoterpenes compared to other measured VOCs, inferring differences in occupant use patterns of fragranced household and personal care products. Traditional sampling approaches do not capture the full spectrum of VOCs or account for temporal variations in indoor air quality, highlighting the importance of high time-resolution VOC measurement techniques (Liu et al., 2019).

The HOMEChem study, conducted in a test house facility at the University of Texas, performed chemically comprehensive measurements using real-time instrumentation to provide insight into temporal variations in indoor air composition during simulated cooking, cleaning and occupancy activities (Farmer et al., 2019). Test house studies

such as HOMEChem offer valuable insight into the effects of short-duration processes on indoor air quality under conditions resembling real-life settings, while allowing for better control over experimental variables. However, these studies are resource-intensive, requiring significant time, cost, and labour. Consequently, only a few studies exist, which do not fully explore the large range of available cleaning products, variations in occupant behaviour affecting emission dynamics, or environmental conditions influencing the fate of cleaning VOC emissions. Most detailed scientific studies to date have been carried out in the USA, focusing on building types characteristic of the country, such as those with mechanical ventilation, timber construction, and crawl spaces. This specificity does not accurately represent buildings in other countries, which have different climates, construction materials, and ventilation systems. These differences can significantly influence indoor air chemistry and, consequently, our understanding of indoor air quality on a global scale (Mannan and Al-Ghamdi, 2021).

While many realistic-scale studies have focussed on characterising the primary VOC emissions from indoor cleaning activities, few have quantified the gaseous secondary pollutants resulting from chemical transformations of these primary emissions. For this purpose, chemical models are a powerful tool for understanding the reactions that can occur following cleaning. For example, Carslaw and Shaw (2022) used a detailed chemical model for indoor air chemistry based on the explicit MCM to examine the secondary chemistry resulting from mixtures of limonene, α-pinene, and β-pinene cleaning emissions. This study revealed detailed changes in oxidant, radical and secondary pollutant concentrations following cleaning, with 3-hour average concentrations of formaldehyde, organic nitrate species, and PM enhanced by 1.8 ppb, 400 ppt, and 1.1 $\mu g/m^3$, respectively, from different proportions of terpene emissions.

Carslaw and Shaw (2022) acknowledged that the relationship between the chemical composition of cleaning emissions and the resulting chemistry is complex and requires further investigation to understand the chemical transformations of complex VOC mixtures from realistic cleaning emissions. This need was further explored by Harding-Smith et al. (2024), who investigated the secondary chemistry from a broader range

of terpene species at concentrations relevant to real-life cleaning formulations (see Chapter 3). This study used simplistic headspace sampling to estimate emissions from the cleaners, thus not accounting for complex emission dynamics which may be present in realistic indoor environments. Therefore, it is important to address this issue by conducting realistic-scale measurements of VOC emissions from a range of cleaners, considering their diverse compositions and application modes, to understand the impact secondary chemistry more comprehensively.

In this study, the impacts of typical household cleaning products on indoor air quality were investigated using a combination of experimental and modelling techniques. Firstly, scripted cleaning activities were performed in a semi-realistic, experimental kitchen facility using regular and green cleaning products, applied as a neat spray to kitchen surfaces and as a dilute solution for mopping the floors. During experiments, indoor and outdoor concentrations of a range of targeted VOCs, PM, NO_x, and O_3 were measured in real time using a suite of online instrumentation. Secondly, measured emission rates were applied to the INCHEM-Py model to estimate the chemical and physical processing of VOCs following cleaning activities in a typical kitchen setting. The impact of varying VOC emissions and environmental conditions on the resulting indoor air chemistry and secondary pollutant formation were assessed by performing two separate model sensitivity analyses. The aim of this study was to identify the chemical components and environmental conditions which lead to the greatest potential exposure to hazardous secondary pollutants.

4.2 Methodology

4.2.1 The DOMESTIC facility and diagnostic equipment

A 4-week experimental campaign was conducted during May 2021 at the Thornton Science Park, University of Chester, UK, with the purpose of investigating the impacts of cooking and cleaning on indoor air chemistry. The experiments were performed at the DOMEstic Systems and Technology InCubator (DOMESTIC) facility (Figure 4.1). The DOMESTIC facility comprised two 6.1 m shipping containers; one where the cooking and cleaning experiments were conducted (experimental container), and one which housed diagnostic equipment (instrument container).

The experimental container was fitted as a domestic kitchen ($\approx$ 4.3 x 2.2 x 2.3 m) with an electric cooker, extraction hood, stainless steel worktop and laminate floor, and had a single north-facing window, an external door, and an internal door to a small bathroom ($\approx$ 1.5 x 2.2 x 2.3 m). All internal and external doors were closed during cooking and cleaning experiments to minimise the effects of mixing between spaces.

The instrument container was connected to the experimental container via a duct which housed sample lines, allowing indoor air from the experimental container to be sampled by the diagnostic equipment housed in the instrument container. Additional sampling lines were directed from the experimental container to the Wolfson Atmospheric Chemistry Laboratory (WACL) Air Sampling Platform (WASP), a mobile laboratory which housed further diagnostic equipment. Indoor and outdoor air were monitored throughout the experimental campaign using an array of real-time diagnostic equipment (Table 4.1). Further details of each instrument can be found in Chapter 2, Section 2.2.

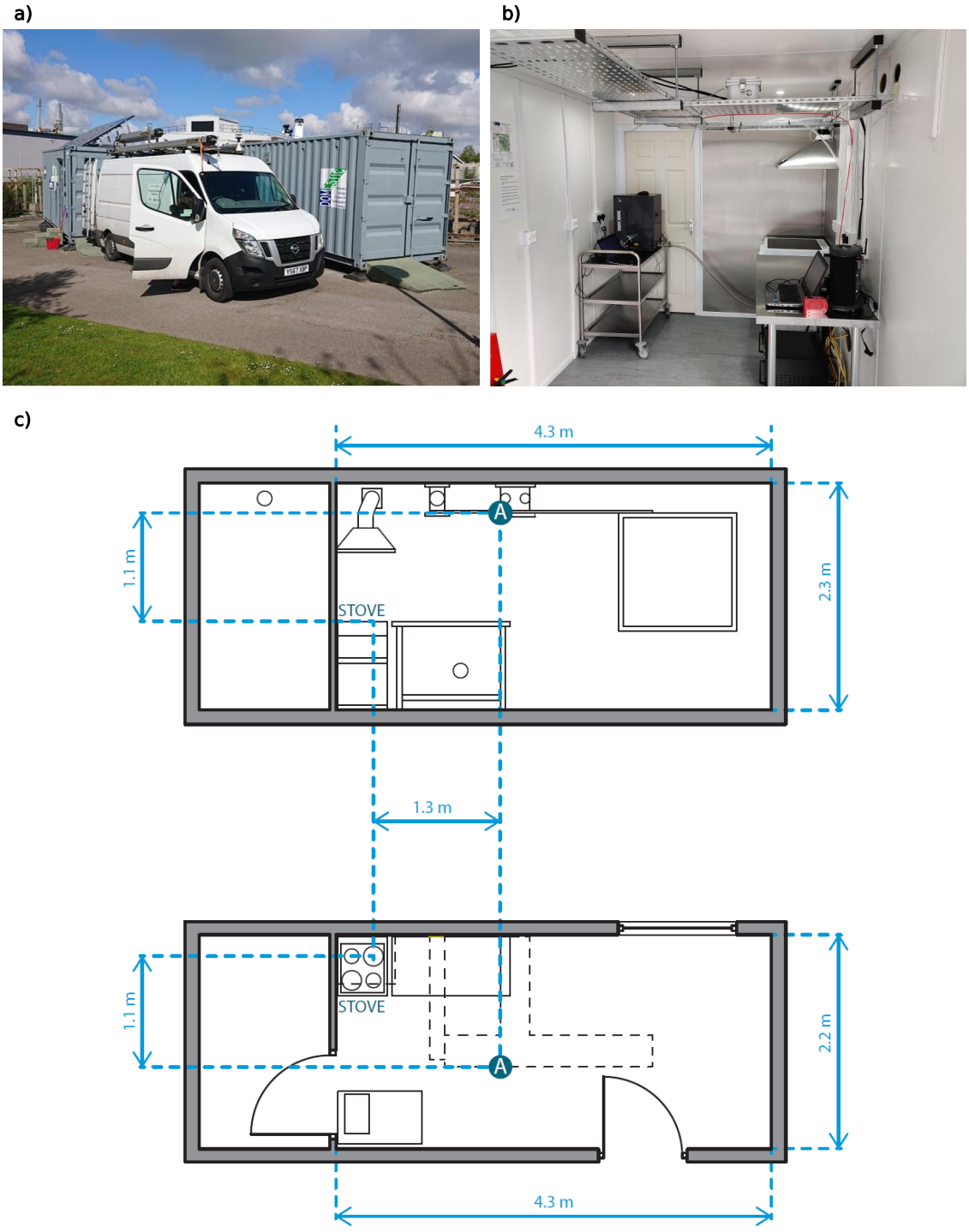

Figure 4.1: Details of the DOMESTIC facility. a) External view of the experimental and instrument containers, and the WASP. b) Internal view of the experimental container. c) Section and plan views of the experimental container detailing the facility dimensions, positioning of furnishings, and the sampling point of indoor measurements (marked 'A').

Table 4.1: Diagnostic equipment used during the DOMESTIC campaign.

Measurement	Instrument	Sampling location	Time resolution
VOCs	Voice200 ultra SIFT-MS	Indoors/Outdoors [a]	∼7 s
O_3	Thermo Scientific Model 49i O_3 analyser	Outdoors	1 min
$NO/NO_2/NO_x$	Airyx ICAD	Indoors	∼2 s
$NO/NO_2/NO_x$	Thermo Scientific Model 42i (NO-NO_2-NO_x) Analyser	Outdoors	5 min
PM/Temp/RH	Quant-AQ MODULAIR-PM	Indoors/Outdoors [b]	1 min
$CO_2/H_2O/CH_4/O_3$	Los Gatos Research UGGA	Indoors	1 s
Meteorological data	Davis Met Station Vantage Pro2	Outdoors	1 min

[a] Alternating sampling locations were controlled by integrated valve switching, typically 30 minutes indoors followed by 5 minutes outdoors.
[b] Complimentary analysers were positioned indoors and outdoors throughout campaign, achieving continuous indoor and outdoor measurements.

A Voice200 ultra SIFT-MS (Syft Technologies, Christchurch, New Zealand) was used to quantify air concentrations of targeted VOCs in the experimental container and outdoors. The SIFT-MS principles of operation and operating conditions are described in Section 2.2.2. Air was sampled to the SIFT-MS via a multi-port switching valve consisting of polytetrafluoroethylene (PTFE)-internally-coated solenoid valves (12VDC, GEMS (Wagner et al., 2021)). A sequential cycle of 30 minutes indoor, followed by 5 minutes outdoor sampling was used throughout the measurement periods.

The SIFT-MS was operated in selected ion monitoring (SIM) mode, dynamically measuring 17 VOCs and inorganic gases with a time resolution of 6.9 seconds (59 masses scanned, 0.1 second dwell time). The VOCs measured using each reagent ion in the SIFT-MS method are shown in Table 4.2, along with the species molecular weights, product ions, rate coefficients and branching ratios. Whether or not detection of a species on that particular reagent ion was used for quantification is also shown in the 'Included in Analysis' column.

Table 4.2: The compounds measured by SIFT-MS using each reagent ion, and their corresponding product ion molecular masses (MM), chemical formulae, rate coefficients and branching ratios. Whether or not the product ion was used for quantification is also shown in the 'Included in Analysis' column.

Reagent Ion	Compound	MM (g mol^{-1})	Product Ion	Reaction Rate ($\times 10^{-9}$ cm^3 $molecule^{-1}$ s^{-1})	Branching ratio (%)	Included in Analysis
H_3O^+	2-phenethyl acetate	105	$C_8H_9^+$	3.50	80	
	acetaldehyde	45	$C_2H_4O.H^+$	3.70	100	✓
	acetonitrile	42	$CH_3CN \cdot H^+$	5.10	100	✓
		60	$CH_3CN \cdot H^+ \cdot H_2O$	5.10		
	total sesquiterpenes	205	$C_{15}H_{25}^+$	2.50	64	✓
	benzyl benzoate	151	$C_8H_7O_3^+$	3.70	60	
		169	$C_8H_7O_3^+ \cdot H_2O$	3.70		
	cinnamaldehyde	133	$C_9H_8OH^+$	2.00	100	
	citral	153	$C_{10}H_{17}O^+$	3.00	60	✓
		171	$C_{10}H_{17}O^+ \cdot H_2O$	3.00		
	ethanol	47	$C_2H_7O^+$	2.70	100	✓
	formaldehyde	31	CH_3O^+	3.40	100	✓
		49	$H_2CO \cdot H^+ \cdot H_2O$	3.40	100	
		61	$(H_2CO)_2 \cdot H^+$	3.40	100	
		67	$H_2CO \cdot H^+ \cdot (H_2O)_2$	3.40	100	
		79	$(H_2CO)_2 \cdot H^+ \cdot H_2O$	3.40	100	
	total monoterpenes	137	$C_{10}H_{17}^+$	2.60	30	
	methanol	33	CH_5O^+	2.70	100	✓

	nitrous acid	48	$H_2NO_2^+$	2.70	67	
NO^+	2-phenethyl acetate	104	$C_8H_8^+$	2.90	85	
	2-tert-butylcyclohexyl acetate	138	$C_{10}H_{18}^+$	2.80	40	✓
	acetaldehyde	43	CH_3CO^+	0.69	80	
		61	$CH_3CO \cdot H_2O^+$	0.69		
	total sesquiterpenes	204	$C_{15}H_{24}^+$	2.00	38	
	benzyl benzoate	180	$C_9H_{10}O_2NO^+$	2.50	45	✓
	cinnamaldehyde	132	$C_9H_8O^+$	2.00	100	
	citral	151	$C_{10}H_{15}O^+$	2.50	35	
	ethanol	45	$C_2H_5O^+$	1.20	100	
		63	$C_2H_5O^+ \cdot H_2O$	1.20		
	eucalyptol	154	$C_{10}H_{18}O^+$	2.40	94	✓
	eugenol	164	$C_{10}H_{12}O_2^+$	2.40	100	✓
	lactic acid	120	$NO^+ \cdot C_3H_6O_3$	2.50	50	✓
	total monoterpenes	88		2.20	25	
		136	$C_{10}H_{16}^+$	2.20	75	✓
O_2^+	2-phenethyl acetate	104	$C_8H_8^+$	3.00	100	✓
	2-tert-butylcyclohexyl acetate	57	$C_4H_9^+$	4.50	45	
	cinnamaldehyde	132	$C_9H_8O^+$	2.00	100	✓
	dihydromyrcenol	59	$C_3H_7O^+$	2.90	50	✓
		77	$C_3H_7O \cdot H_2O^+$	2.90		
	eugenol	164	$C_{10}H_{12}O_2^+$	1.90	100	
	nitrogen oxide	46	NO_2^+	0.62	100	✓

Daily validation and external calibration of the SIFT-MS were performed during the experimental campaign, as described in Section 2.2.2.3. The daily calibration factors applied to the data are described in Table 4.3.

Table 4.3: Mean ± standard deviation of the SIFT-MS calibration factors obtained during the DOMESTIC campaign.

Species	Calibration factor ± standard error			
	19/05/21	20/05/21	24/05/21	26/05/21
methanol	1.97 ± 0.05	1.50 ± 0.05	1.22 ± 0.09	1.31 ± 0.36
ethanol	2.56 ± 0.09	1.68 ± 0.12	1.18 ±0.07	2.82 ±0.73
acetonitrile	1.38 ± 0.03	1.22 ± 0.03	1.16 ± 0.06	1.13 ± 0.06
total monoterpenes [a]	4.03 ± 0.08	7.26 ± 0.53	13.96 ± 1.30	5.06 ± 0.01

[a] Limonene used as calibration gas

The instrument background was also assessed daily by sampling zero air from an in-house heated palladium alumina-based zero air generator for a 3-minute period. Background VOC mixing ratios, defined as the 3-minute average of the zero air measurements, were subtracted from the data where available. The LODs were calculated as 3.2 times the standard deviation of the zero air measurements, and are shown in Table 4.4.

The instrument background concentrations of benzyl benzoate, cinnamaldehyde, eugenol, 2-phenethyl acetate and 2-tert-butylcyclohexyl acetate were only measured on one day during the campaign (26/05/2021) due to differences in SIFT-MS SIM methods used. Therefore, the LODs reported for these species are from this day only, and are assumed to be an appropriate estimation of their LODs across the whole sampling period. Citral, dihydromyrcenol and lactic acid were not included in any SIM method used to perform calibration and zero air measurements throughout the campaign. Consequently, the instrument background was not corrected for these species, and no LODs were available. Additionally, background concentrations of formaldehyde and acetaldehyde were not subtracted from the data due to issues with negative values. Therefore, all measurements of citral, dihydromyrcenol, lactic acid, formaldehyde and

acetaldehyde may include contributions from the instrument background. This was accounted for in the reported LODs of formaldehyde and acetaldehyde, which were calculated as the instrument background concentration plus the LOD calculated from zero air measurements.

Table 4.4: The limits of detection (ppb) of species measured by SIFT-MS. Values reported are the average ± standard deviation of the LODs measured for each of the four cleaning experimental days.

Species	LOD (ppb)
acetaldehyde [a]	6.9 ± 2.1
acetonitrile	0.4 ± 0.1
benzyl benzoate [b]	0.5
cinnamaldehyde [b]	0.2
ethanol	1.7 ± 0.2
eucalyptol	0.1 ± 0.0
eugenol [b]	0.4
formaldehyde [a]	4.7 ± 1.9
methanol	1.3 ± 0.2
nitrogen oxide	3.3 ± 0.3
total monoterpenes	0.2 ± 0.0
total sesquiterpenes	1.3 ± 0.3
2-phenethyl acetate [b]	0.2
2-tert-butylcyclohexyl acetate [b]	0.5

[a] LOD = mean of the zero air measurements plus 3.2 × the standard deviation of the zero air measurements.
[b] Species LODs from 2021/05/26 only reported. No zero air measurements available for other experimental days.

4.2.2 Ventilation

All air vents in the experimental chamber were closed throughout the campaign to emulate the ventilation of a typical residential dwelling (0.5 h^{-1}, Nazaroff (2021)) more closely. Natural ventilation only was used for all cleaning experiments during this campaign. The ACR of the DOMESTIC facility was estimated on 6 occasions by rapidly releasing a tracer gas into the space and measuring its decay. Acetonitrile was chosen

as the tracer gas because it is chemically inert, has a low deposition velocity, and is measurable by SIFT-MS. 0.2% acetonitrile in N_2 was released to achieve a mixing ratio of approximately 200 ppb before immediately exiting the room, and the concentration was monitored for several hours afterwards, without any further disturbance. The ACR was estimated through log-linear regression analysis of the background subtracted acetonitrile concentrations over a 2-hour period following the release (Equation 4.1). Note that the initial 10 minutes of measurements were discounted to ensure that the tracer gas was well mixed in the space.

$$\ln(C) = -\lambda t + ln(C_0) \tag{4.1}$$

Where the gradient of the regression, λ, is the ACR (h^{-1}), t is the time from release (hours), C is the elevation of acetonitrile above background concentrations (ppb) and C_0 is the elevation of acetonitrile above background at $t = 10$ mins. The result of this analysis for the 6 tracer release instances is shown in Figure 4.2a. The average ACR during the campaign was 0.77 ± 0.16 h^{-1}.

The correlation of estimated ACR with the average wind speed and direction during the tracer release measurement periods is shown in Figure 4.2b. Increased wind speeds and northerly winds resulted in higher ACR in the experimental container during the campaign. It is likely that day-to-day variability in meteorological conditions resulted in differences in the ACR between experimental days, thus affecting the residence times of species indoors. However, the ACR was not measured for each cleaning experimental day. Therefore, the average ACR (0.77 h^{-1}) was assumed across the sampling period for the purpose of calculating VOC emission rates, as discussed in Section 4.2.4.

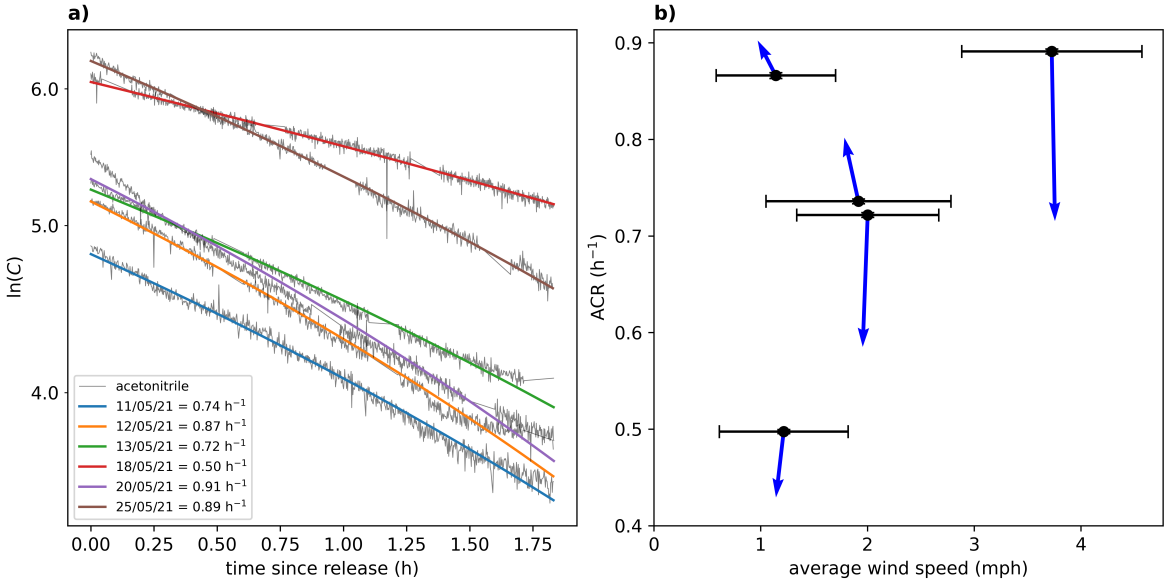

Figure 4.2: a) Log-linear regression analysis of acetonitrile tracer gas decay profiles measured by SIFT-MS on 6 days during the DOMESTIC campaign. b) Correlation of air exchange rate with the average wind speed over the 2-hour period during which the regression analysis was performed. Black error bars represent ± standard deviation for each variable. 2-hour average wind direction is represented by a blue arrow for each data point. No meteorological data were available for 20/05/2021.

4.2.3 Cleaning protocol

Four single-product cleaning experiments were performed during the DOMESTIC campaign, whereby a scripted cleaning activity was conducted at midday, followed by approximately 20 hours of monitoring the indoor air with minimal perturbation from experimentalists. Regular and green surface and floor cleaners (SR1, SG2, FR1, FG2, see Table 2.1) were selected for these experiments to explore the variability in emissions of indoor air pollutants from regular and green cleaning products with typical application modes dependent on cleaning product (surface spray/ floor mop with dilute solution).

Prior to each experiment, the external door and window were opened to ventilate the room until concentrations reached a steady-state. The door and window were then closed, and the room was left to equilibrate for a minimum of 1 hour before beginning the cleaning activity. All products were used following manufacturer instructions: surface cleaners (≈ 10 mL) were sprayed onto the stainless-steel worktop surface and

wiped with a damp cloth after 1 minute, and floor cleaners (≈ 60 mL FR1, ≈ 30 mL FG2) were diluted with 5 L of cold water and applied to the floor using a mop. Once the cleaning activity was complete, the room was vacated and all cleaning equipment was removed from the room.

4.2.4 Simulated cleaning experiments

To investigate the chemical processing of VOC emissions from the cleaning experiments, INCHEM-Py was used, as described in Section 2.3. The model was initialised to represent an average kitchen setting, described in detail in Section 2.3.6.1. Briefly, the kitchen was assumed to have a volume of 25 m^3 and a surface area of 63.27 m^3, with specific SAVs of different surface materials defined based on a detailed analysis of the indoor surfaces of 9 domestic kitchens in the USA (Manuja et al., 2019; Carter et al., 2023). Outdoor VOC and trace gas concentrations were defined based on measurements taken in a suburban London location, and ingress/egress of species was controlled by an ACR of 0.5 h^{-1}, typical of residential dwellings (Nazaroff, 2021). Indoor attenuated light was defined by the model based on an assumed latitude of 51.45 °N, date 20/06/2020, and LE glass glazed windows (transmission 330-800 nm, (Blocquet et al., 2018)). Artificial incandescent lighting was on between 07:00 and 19:00 h. There was assumed to be one adult present in the room for the duration of the simulation.

To simulate the cleaning activities, timed VOC emissions were input to the model at 13:00 h. The VOC emission rates were determined from the experimental SIFT-MS data by calculating the rate of increase in species concentration during the cleaning period, as demonstrated in Figure 4.3a for a representative emission of total monoterpenes. For species where multiple gradients were observed in the emission peak, these were calculated individually and input into the model as separate timed emissions to accurately simulate the measured VOC emissions. VOC emission rates were corrected by taking into account the ACR of the experimental container (assumed 0.77 h^{-1}), which has a dilution effect on the measured VOC concentrations. To do so, a ventila-

tion correction factor (the product of the ACR and species concentration, as a function of time) was added to the modelled VOC emission rates over the duration of the timed emissions (Figure 4.3b).

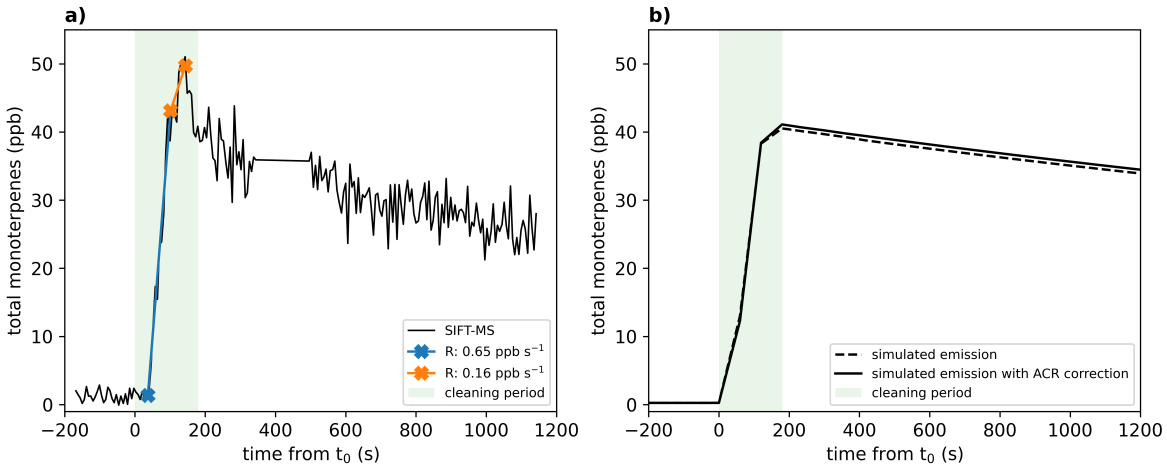

Figure 4.3: a) The total monoterpene mixing ratios measured by SIFT-MS during a cleaning experiment. Emission rates (indicated by coloured lines) are calculated from the gradient between the base and peak of an emission, and are shown in the legend in units of ppb s^{-1}. b) Simulated total monoterpene mixing ratios with (solid line) and without (dashed line) correcting the emission rates for dilution due to air exchange. This protocol was used for all other VOC emissions (not shown here). The shaded green area highlights the time period when cleaning took place.

The simulated peak VOC mixing ratios were slightly lower than those measured by SIFT-MS. This discrepancy is likely due to the way VOC emissions were input to the model, using an exponentially increasing rate over the first 5 seconds of emission. This approach was necessary to address an integrator issue that prevented the solver from managing large, sudden increases in VOC emission rates. Additionally, the simulated decay of VOC mixing ratios post-emission was generally slower compared to those observed experimentally. This observation indicates the presence of removal processes in the real environment that are not accounted for in the simulation. The underestimation of the peak VOC concentrations coupled with the overestimation of VOC concentrations for an extended period after the emission event have contrasting implications for predicting indoor air chemistry following cleaning activities. The underestimation of peak concentrations might lead to an initial underestimation of the impact of immediate VOC chemistry. However, the model maintains elevated VOC levels for longer

than observed experimentally, thereby potentially overestimating the formation of secondary pollutants following cleaning activities over several hours. Thus, refining the model to better match the experimental data is crucial for more accurate predictions of indoor air quality and secondary pollutant formation following VOC emissions.

Emissions were included in the model for the following species: ethanol, methanol, acetaldehyde, dihydromyrcenol, citral, limonene, α-pinene, β-pinene, 3-carene, camphene, γ-terpinene, terpinolene, α-phellandrene, α-terpinene, β-caryophyllene (as a model proxy for total sesquiterpenes) and butyl pyruvate (as a model proxy for the acetate species 2-tert-butylcylohexyl acetate and 2-phenethyl acetate, with appropriate mass corrections). Emission rates of individual monoterpene species were estimated using the monoterpene relative abundance ratios, calculated from headspace GC-MS analysis of the cleaning products (see Chapter 3), to speciate the total monoterpene emission rates measured by SIFT-MS.

4.2.5 Sensitivity studies

Two sensitivity studies were performed based on the measured VOC emissions from the room-scale cleaning experiments. In the first sensitivity study, the model parameters were kept constant (i.e., assuming the average kitchen setting) while individual VOC emissions were omitted/substituted to determine the influence of the individual species on the overall chemistry that occurs following the cleaning events. In the second sensitivity study, the timed VOC emissions were kept constant (i.e., assuming the same cleaning conditions, SG2) while the model parameters were modified to investigate the impact of changing the environmental conditions of the simulated indoor setting.

The different scenarios investigated, and the corresponding model parameters used in the second sensitivity study are outlined in Table 4.5. The base scenario corresponds to the VOC emissions measured from SG2 simulated using the average kitchen settings, as described in Section 2.3.6.1. The effects of increasing and decreasing the surface area of the 25 m^3 kitchen by $\pm$ 10% of the base scenario surface area while assuming one adult in the kitchen at all times (skin surface area = 2 m^3) were investigated in

the Low SAV and High SAV scenarios. The effects of varying the level of attenuated light were investigated by changing the emissivity of the glass in the LEWF and Glass C scenarios. The time of year and time of day were varied relative to the base scenario in the Winter, Morning and Evening scenarios. Finally, the effects of increasing the number of occupants, the ventilation rate, and outdoor pollutant levels were investigated in the Family, High ACR and Polluted scenarios, respectively.

Table 4.5: Simulation parameters for the environmental factor sensitivity analysis for the SG2 cleaning event. The base scenario, representing the average domestic kitchen, is highlighted in grey. For all other scenarios, the altered parameter is shown in bold.

Scenario	SAV (cm^{-1})	Glass type	Date (DD/MM)	Time (hh:mm)	Occupancy	AER (h^{-1})	Location
Base	0.0253	LE	21/06	13:00	1 adult	0.5	London suburban
Low SAV	**0.0212**	LE	21/06	13:00	1 adult	0.5	London suburban
High SAV	**0.0292**	LE	21/06	13:00	1 adult	0.5	London suburban
LEWF	0.0253	**LEWF**	21/06	13:00	1 adult	0.5	London suburban
Glass C	0.0253	**Glass C**	21/06	13:00	1 adult	0.5	London suburban
Winter	0.0253	LE	**21/12**	13:00	1 adult	0.5	London suburban
Morning	0.0253	LE	21/06	**08:00**	1 adult	0.5	London suburban
Evening	0.0253	LE	21/06	**18:00**	1 adult	0.5	London suburban
Family	0.0253	LE	21/06	13:00	**2 adults, 2 children**	0.5	London suburban
High ACR	0.0253	LE	21/06	13:00	1 adult	**2**	London suburban
Polluted	0.0253	LE	21/06	13:00	1 adult	0.5	**Milan**

4.3 Results and discussion

4.3.1 Indoor/Outdoor air composition

The trace gas and particle measurements made during background and activity periods of the four cleaning only experimental days were interpreted to understand the composition of the indoor and outdoor air during the campaign. Background measurements were defined as the periods between 00:00-09:00 and 15:00-00:00 each day to discount the periods when the indoor air was affected by high ventilation (09:00-11:30) or cleaning activities (11:30-15:00, approximately 30 minutes pre-activity and 3 hours post-activity). The normalised probability distributions of the trace gas and particle measurements taken over the four cleaning experimental days are shown in Figure 4.4 for the defined background and cleaning activity periods.

Background O_3 concentrations were widely distributed outdoors, ranging from 4 to 50 ppb, while indoor background concentrations were lower and ranged from 0 to 18 ppb. O_3 concentrations during the activity period were also greater outdoors than indoors, with generally larger concentrations compared to the background period owing to the diurnal profile of outdoor O_3 (peak concentrations are usually in the afternoon). The primary source of O_3 in indoor environments is infiltration from outdoors, therefore indoor O_3 concentrations generally track outdoor concentrations with attenuation owing to indoor loss processes such as surface deposition (Weschler et al., 1989). During the cleaning activity period, the average indoor O_3 concentration was 6 ppb, with an I/O ratio of 16%. These measurements were comparable with previous studies, which report average indoor concentrations of 6 ppb and an I/O ratio of 25% (Nazaroff and Weschler, 2022).

Outdoor concentrations of NO_x/NO_2 were consistently greater than indoor concentrations throughout the experimental days. Diurnal variability of NO_x was observed outdoors, with an average concentration of (5.4 $\pm$ 3.7) ppb during the background period, whereas indoor concentrations remained more consistent (1.6 $\pm$ 0.8 ppb). During the background period the average I/O ratio of NO_x was 0.30, which increased to 0.65

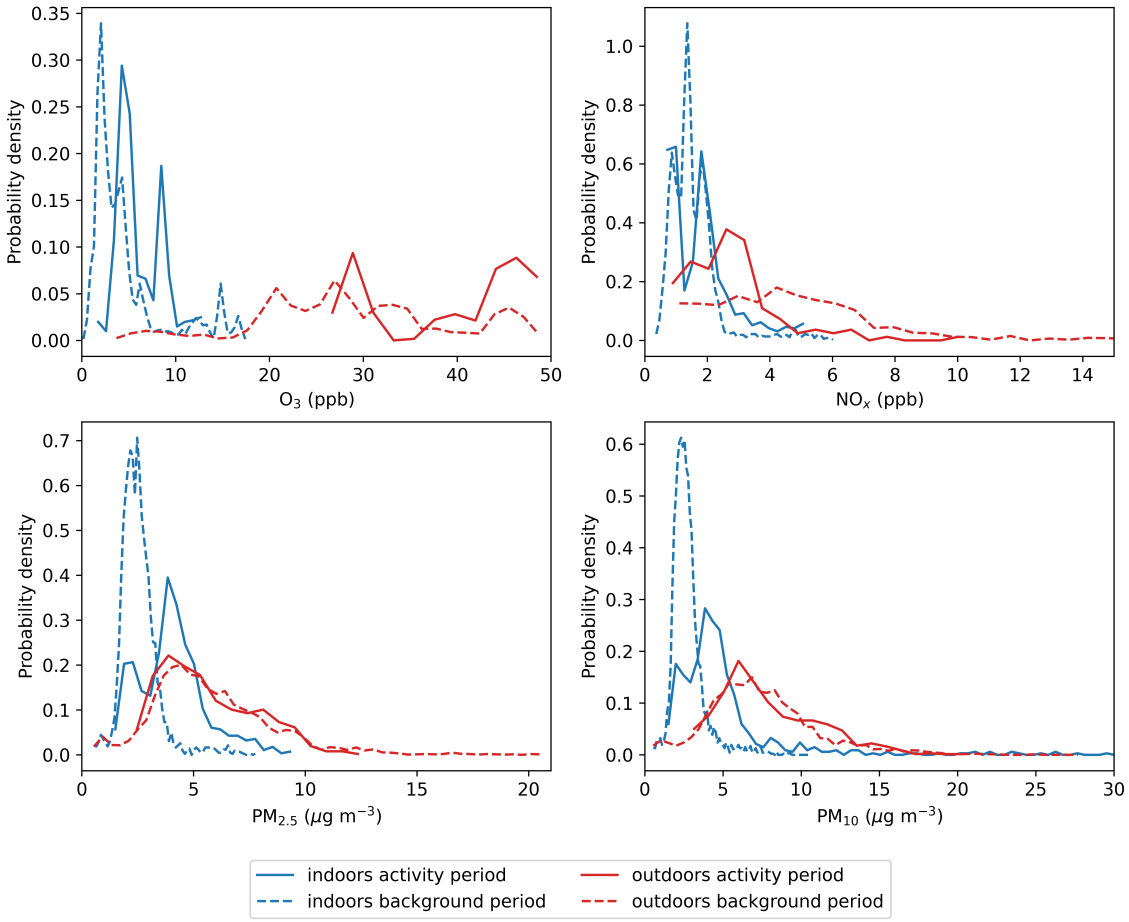

Figure 4.4: Normalized probability distributions of measured trace gas mixing ratios and particle mass concentrations for cleaning experiment days (19th, 20th, 24th, 26th May 2021) for indoor (red) and outdoor (blue) 1 min average measurements. The activity period includes data from 11:30 – 15:00 h to include roughly 30 minutes pre-activity and 3 hours post-activity. The background period includes data from 15:00 - 09:00 h. Data from 9:00 – 11:30 was not included to avoid the period when the external door was open for ventilation.

during the activity period owing to lower outdoor concentrations during the activity period caused by NO_2 photolysis. Overall, the indoor concentrations of NO_x measured during the campaign were low compared to previous studies (Farmer et al., 2019). However, it is worth noting that major indoor sources of NO_x such as gas-powered appliances were not in use during the cleaning experiments. Due to experimental constraints it was not possible to zero the NO_x analysers, resulting in some uncertainty in the results. Consequently, measured NO_2 concentrations exceed NO_x concentrations on some occasions, causing negative concentrations of NO to be reported. It is likely

that indoor and outdoor NO concentrations were below the LOD of the analysers during the campaign, and therefore are not shown in Figure 4.4.

PM concentrations were generally greater outdoors than indoors, with average outdoor concentrations of 6.0 and 7.7 μg m^{-3} $PM_{2.5}$ and PM_{10}, respectively. Outdoor PM concentrations during the background and activity period were comparable, whereas there was a clear difference between PM concentrations indoors during the background and activity periods. The average indoor PM concentration during the activity period was 63% and 96% greater than during the background period for $PM_{2.5}$ and PM_{10}, respectively. This suggests that the cleaning activities were sources of $PM_{2.5}$ and PM_{10} indoors.

While the average outdoor PM levels were below the global air quality guideline values provided by WHO, elevated concentrations of up to 21 and 28 μg m^{-3} $PM_{2.5}$ and PM_{10} were measured, respectively, exceeding the 24-hour guideline $PM_{2.5}$ concentration of 15 μg m^{-3} (World Health Organisation, 2021). Similarly, elevated concentrations of outdoor NO_x of up to 27 ppb were measured during the campaign, exceeding the 24-hour guideline NO_x concentration of 13 ppb. Periods of elevated PM and NO_x concentrations were observed randomly during the campaign, possibly because of intermittent flaring at an oil refinery less than 1 km away from the DOMESTIC facility (Figure B.1). Gas flaring is a prominent source of VOCs, CO, CO_2, SO_2, polyaromatic hydrocarbons (PAHs), NO_x and PM (Orimoogunje et al., 2010). This nearby pollution source may have impacted the measured concentrations of trace gases and PM in outdoor air and also indoor air due to infiltration.

The median indoor and outdoor VOC mixing ratios measured during the background periods of the cleaning experiment days are reported in Table 4.6. The I/O ratios of the median mixing ratios are also reported for each VOC measured during the campaign. For comparison to another measurement campaign carried out in the USA, the background indoor mixing ratios and I/O ratios reported from the HOMEChem study are included for species which were measured in both campaigns (Arata et al., 2021).

Table 4.6: Median background mixing ratios (ppb) of VOCs in indoor and outdoor air during the cleaning experiment days, and the corresponding indoor:outdoor ratios. Values calculated as the mean ± standard deviation of data between (t_0 + 3 h) – 09:00 (+ 1 day). Data reported only for species where measured indoor and outdoor mixing ratios were above the limits of detection.

Species	Indoors		Outdoors	I/O ratio	
	DOMESTIC	HOMEChem	DOMESTIC	DOMESTIC	HOMEChem
total monoterpenes	5.3	1.4	0.2	35.2	2-10
ethanol	23.4	12.6	11.1	2.1	2-10
acetaldehyde	17.0	5.2	5.5	3.1	>10
dihydromyrcenol	12.2	-	3.4	3.6	-
methanol	240.6	40.0	5.1	47.1	>10
formaldehyde	5.6	-	2.3	2.4	-

The VOCs with the largest indoor background mixing ratios were methanol, ethanol, acetaldehyde and dihydromyrcenol. The indoor background mixing ratios of ethanol and acetaldehyde were 2 – 3 times greater in this study compared to HOMEChem, while that of methanol was over 6 times greater. It is important to take into consideration the difference in room volume between DOMESTIC (single room, ≈ 22 m^3) and HOMEChem (full test-house, experimental volume 235 m^3). The much larger volume of HOMEChem means that indoor VOC emissions were more diluted, resulting in smaller background VOC mixing ratios. Additionally, the test house used in the HOMEChem study was much more established than the DOMESTIC facility, being assembled 10 years prior to the campaign. The DOMESTIC facility was assembled less than 2 years before the campaign discussed here, hence it is likely that background emissions from off-gassing of construction materials were more considerable than for HOMEChem.

Methanol, and to a lesser extent total monoterpenes, had particularly high I/O ratios during this campaign. Measurements of these species made during a background experimental day (when no indoor activities took place) showed a gradual increase in indoor mixing ratio throughout the day, following a period of high ventilation in the morning (Appendix B, Figure B.2). These observations provide evidence of background emis-

sion sources of methanol and monoterpenes. The walls of the DOMESTIC facility were lined with processed wooden boards containing wood, resins and glues, which can be large sources of VOCs including methanol (Adamová et al., 2020). Therefore, it was likely that off-gassing of the relatively new building materials was the main source of methanol emissions indoors. Indoor emission sources of monoterpenes in DOMESTIC may include off-gassing building materials (in a similar manner to methanol) or re-emission from cleaning product residue on indoor surfaces.

4.3.2 VOC emissions from cleaning

Following scripted, single-product cleaning activities with regular and green surface and floor cleaners, emissions of 4–7 VOC species were identified per experiment. The cumulative concentrations of emitted VOCs measured during each cleaning activity are shown in Figure 4.5. The corresponding VOC emission rates and their timings relative to the start of the cleaning activity (t_0) are reported in Table 4.7.

Monoterpenes and dihydromyrcenol were emitted from all four products during the cleaning experiments, while acetaldehyde, eucalyptol and 2-tert-butylcyclohexyl acetate were emitted from three of the cleaners. Total monoterpenes were the largest emission from all cleaners except for FG2, for which ethanol emissions dominated the total VOC emissions. The regular and green surface cleaners were larger sources of total monoterpenes compared to the floor cleaners. This observation is in agreement with results from headspace analysis of the product formulations described in Chapter 3, which showed that while the floor cleaners contained a greater mass concentration of monoterpenes compared to the surface cleaners (Table 3.4), the use of floor cleaners as a diluted solution resulted in these products being smaller emission sources than the spray cleaners which were applied as the neat solution (Figure 3.3). Cleaner SG2 contained a larger mass concentration of monoterpenes than SR1, resulting in larger total monoterpene emissions during cleaning.

Overall, the magnitude of the VOC emissions observed in this semi-realistic study are greater than those predicted from headspace measurements in the previous chapter,

Table 4.7: VOC emission rates and emissions per cleaning event determined from SIFT-MS measurements during each cleaning experiment. For species where two gradients were observed in the emission peak, individual emission rates are reported as emission rate 1 and emission rate 2. The time, in seconds from t_0, during which the emissions occurred is also shown for clarity.

ID	Species	VOC emissions						Total emission (mg per cleaning event)
		t_{start} (s)	t_{end} (s)	Emission rate 1 (molecule cm^{-3} s^{-1})	t_{start} (s)	t_{end} (s)	Emission rate 2 (molecule cm^{-3} s^{-1})	
SR1	acetaldehyde	-2	106	4.08×10^8	106	135	2.25×10^9	0.18
	total monoterpenes	71	97	1.21×10^{10}	97	279	6.52×10^8	2.16
	2-tert-butylcyclohexyl acetate	31	278	1.14×10^8	-	-	-	0.20
	eucalyptol	22	152	9.04×10^7	-	-	-	0.07
	dihydromyrcenol	16	224	6.71×10^8	-	-	-	0.79
	citral	9	287	7.25×10^7	-	-	-	0.11
	2-phenethyl acetate	79	257	7.47×10^6	-	-	-	0.01
SG2	acetaldehyde	5	126	3.91×10^8	-	-	-	0.08
	methanol	20	109	3.30×10^9	-	-	-	0.34
	total sesquiterpenes	-8	300	2.91×10^7	-	-	-	0.07
	total monoterpenes	37	101	1.62×10^{10}	101	143	3.92×10^9	5.95
	2-tert-butylcyclohexyl acetate	12	191	5.15×10^7	-	-	-	0.09
	eucalyptol	34	97	4.13×10^9	97	136	1.13×10^9	1.69
	dihydromyrcenol	0	109	1.07×10^9	-	-	-	0.66
FR1	total monoterpenes	5	138	1.40×10^8	138	283	7.90×10^8	0.66
	2-tert-butylcyclohexyl acetate	37	3805	9.40×10^6	-	-	-	0.35
	eucalyptol	64	298	2.64×10^7	-	-	-	0.03
	dihydromyrcenol	-6	422	1.14×10^8	-	-	-	0.27
FG2	acetaldehyde	2	291	1.20×10^8	-	-	-	0.06
	ethanol	60	144	1.27×10^{10}	144	331	5.21×10^9	3.39
	total monoterpenes	108	135	3.60×10^9	135	303	4.00×10^8	0.82
	dihydromyrcenol	4	317	2.11×10^8	-	-	-	0.37

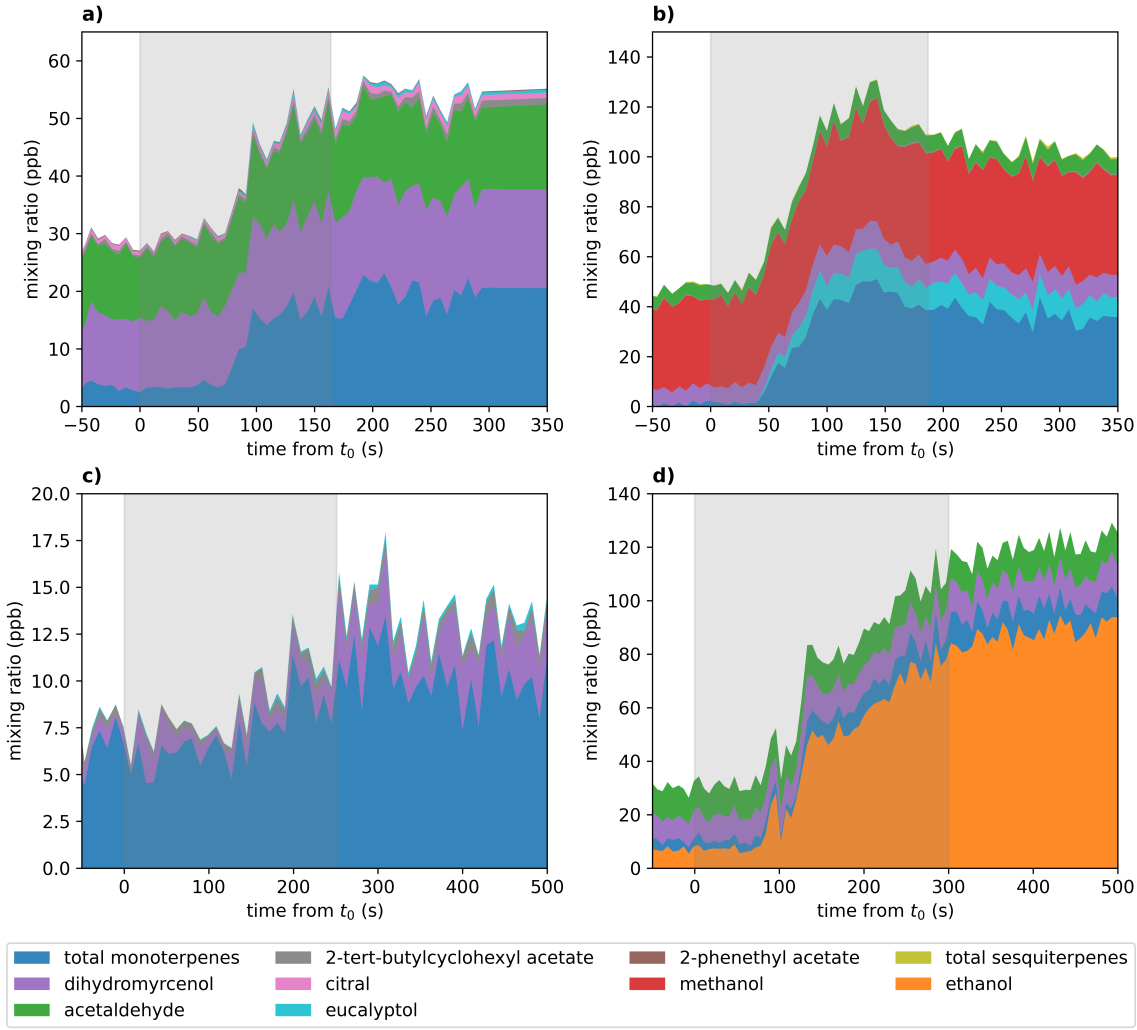

Figure 4.5: Mixing ratios of VOCs measured by SIFT-MS during the cleaning experiments a) SR1, b) SG2, c) FR1, d) FG2. The grey shaded area signifies the cleaning period, with 0 s (t_0) being the time point when cleaning commenced. Only the total mixing ratios of VOCs for which an emission peak was observed are shown.

particularly for spray cleaners. This could indicate that the emission dynamics, not taken into account in the previous chapter, have a significant impact on the VOC emissions from cleaning products. The spray application mode of the surface cleaners may result in larger VOC emissions than the dilute solution of the floor cleaners due to aerosolization of the product. This was observed by Lovén et al. (2023), who showed that the total airborne mass fraction was up to a third of the mass dispensed from spray cleaning products during typical use. Additionally, the partitioning of VOCs between the gas phase and the aqueous liquid may also affect the observed

VOC emissions, particularly from dilute cleaning solutions. The application of dilute cleaning solutions onto floors creates a thin aqueous surface film, to which water-soluble organic species (e.g., formaldehyde, acetaldehyde, ethanol) may absorb, thus impacting the gas-phase concentrations of these VOCs (Ault et al., 2020; Duncan et al., 2018). There is currently little research into the effects of aqueous surface films on the partitioning of VOCs between phases during surface cleaning activities. Partitioning of hazardous compounds such as formaldehyde will affect personal exposure to such air pollutants, and therefore warrants further investigation.

The levels of terpenoid species emissions measured in this study are comparable in magnitude to those documented in other room-scale studies investigating VOC emissions from cleaning activities. For example, a study conducted in a realistic sized chamber (40 m^3) reported maximum limonene and eucalyptol concentrations of (38.7 $\pm$ 7) ppb and (2.0 $\pm$ 0.3) ppb, respectively, from a typical cleaning event (Harb et al., 2020). In this study, the maximum concentrations of monoterpenes and eucalyptol observed from the 4 cleaning experiments were 13.9 – 51.0 ppb and 0.25 – 13.2 ppb, respectively. Furthermore, in the HOMEChem study, 12.5 mg of monoterpenes and 0.2 mg of monoterpene alcohols (i.e., eucalyptol) per mopping event were reported when the test-house floors were mopped with a natural cleaning product (Arata et al., 2021). The total monoterpene emissions per cleaning event reported in this study were 2 – 19 times lower than those reported by Arata *et al.*, while emissions of eucalyptol were greater for SG2 and lower for SR1, FR1 and FG2, than the monoterpene alcohol emissions reported from the HOMEChem study. There exists large variability in the reported VOC emissions from cleaning activities in the literature owing to differences in the composition of cleaning product formulations and experimental design. Nonetheless, the results reported in this study are somewhat comparable to other realistic-scale cleaning studies.

4.3.3 Base case cleaning simulations

The VOC emission rates calculated from the experimental data for each cleaning experiment were input to the INCHEM-Py model to simulate the cleaning activities in a typical kitchen. Total monoterpene emissions were speciated using the relative abundance ratios of monoterpene species determined from headspace GC-MS analysis of each product formulation (Chapter 3) to represent the monoterpene chemistry more accurately in the simulations. Emissions of eucalyptol were excluded from the simulations because this compound is not present in the model. Eucalyptol is inert towards ozonolysis, with a rate coefficient of $< 1.5 \times 10^{-19}$ cm^3 molecule^{-1} s^{-1} (Atkinson et al., 1990), and is therefore expected to make a negligible difference to the simulated chemistry.

Simulations of a cleaning event with each cleaning product were performed in an 'average kitchen' setting (Section 4.2.4) at 13:00 h, defined as the base case cleaning scenario. The activity-induced change in emitted VOC concentrations (the difference in concentration between the cleaning simulations and a baseline simulation with no cleaning emissions) is shown in Figure 4.6. The increase in the emitted total VOC mixing ratios was greatest from cleaning with FG2 (71.4 ppb), while FR1 resulted in the lowest increase in total VOC mixing ratio (6.4 ppb). The activity-induced change in VOC mixing ratios remained elevated for several hours following emission. The time taken for the VOC mixing ratio to drop below 5% of the maximum mixing ratio was 5.63, 4.97, 5.50, and 2.38 hours for SR1, SG2, FR1, and FG2, respectively.

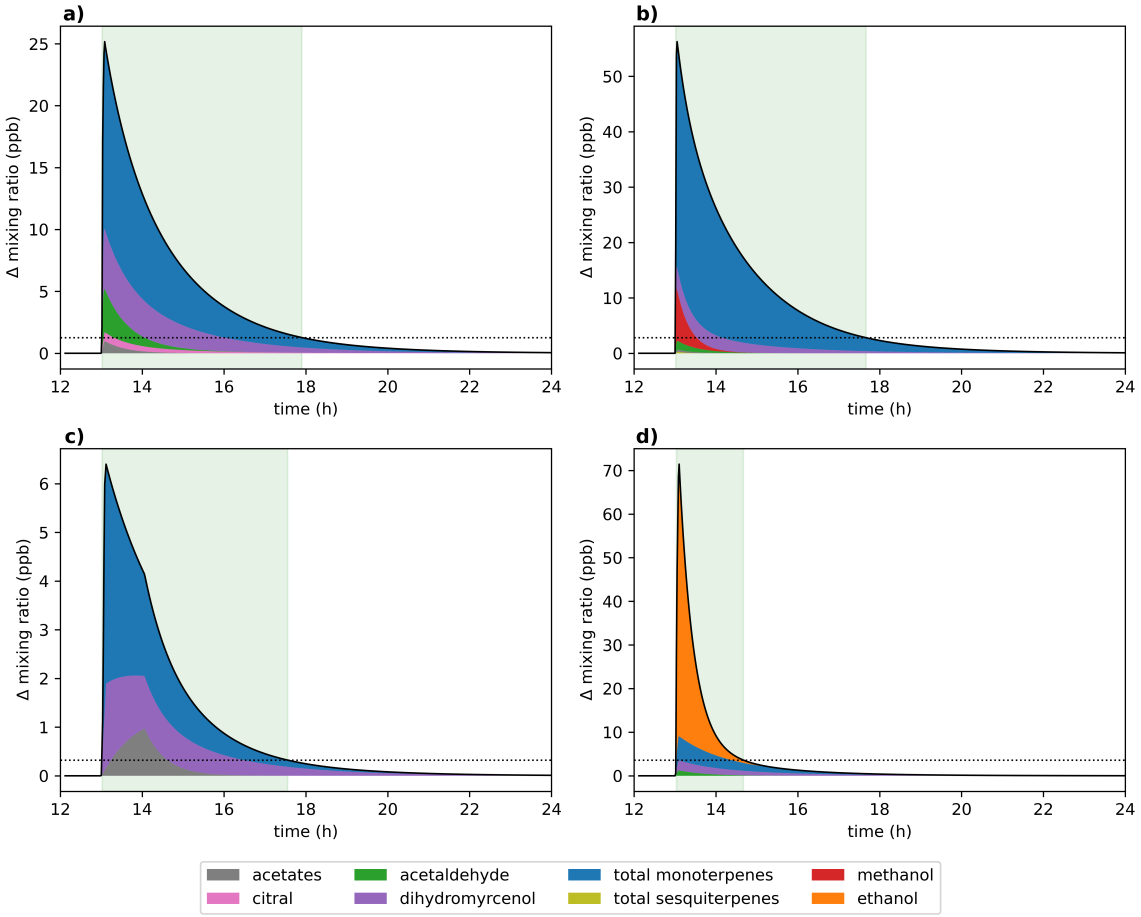

Figure 4.6: The activity-induced change in cleaning VOC concentrations for a) SR1, b) SG2, c) FR1, d) FG2, from 12 -24 hours. The cleaning event started at 13:00 h. The shaded green area represents the period when the total activity-induced change in concentration of the cleaning VOC emissions is greater than 5% (2σ, dashed horizontal line) of the maximum.

The decay rate of the emitted VOCs from FG2 was more than twice as fast as all other cleaners. The rate at which the mixing ratios of emitted VOCs decline back to background indoor concentrations was dependent on the rates of production versus the loss by indoor/outdoor exchange, surface interactions, and chemical processing. In the base case simulations, the ACR was constant (0.5 h^{-1}), hence surface processes and chemical reactivity were the main factors influencing the temporal changes in emitted VOC mixing ratios after the simulated cleaning event. Figure 4.7 shows the sum of reaction rates for the emitted VOC production/loss pathways at the peak total VOC mixing ratio (i.e., immediately after cleaning finished) for each cleaning

simulation.

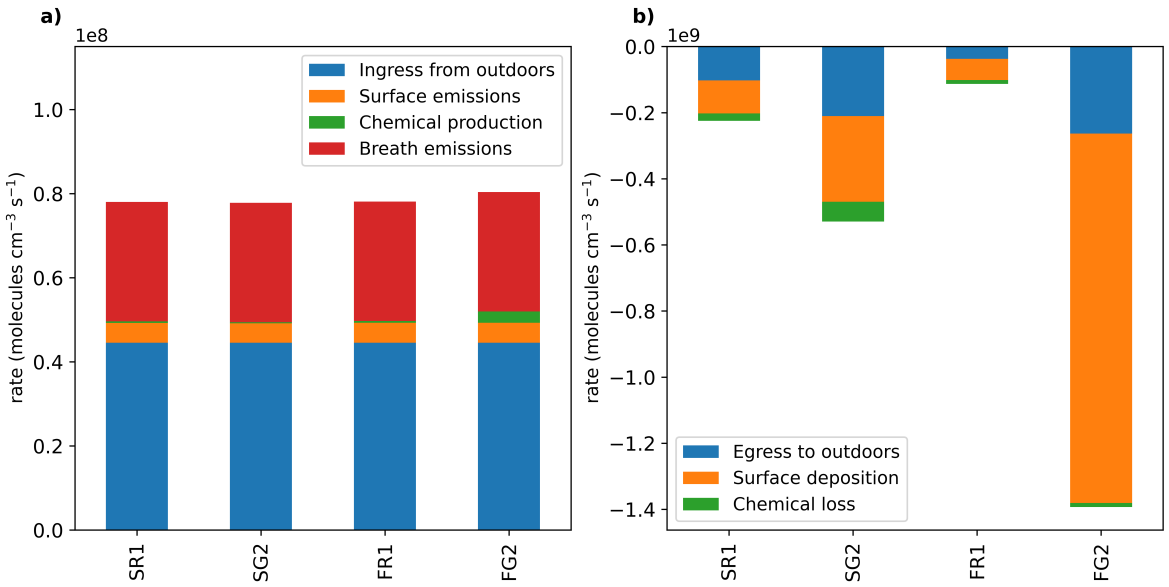

Figure 4.7: The rate of a) production and b) loss of cleaning VOC emissions at the peak total cleaning VOC concentrations per product (i.e., immediately after cleaning finished). Production/loss via different pathways: ventilation, surface processes, chemistry, breath emissions.

Following the emission period, the rate of production of the emitted VOC species was less than the rate of loss for all simulations, resulting in a decline in the VOC mixing ratios over time following the cleaning event. The main VOC production pathway in all cleaning simulations was ingress from outdoor air via air exchange. Breath emissions from single occupancy were also an important source of ethanol and methanol in all simulations. Acetaldehyde was produced in all simulations from O_3 surface chemistry. Gas-phase chemical transformations were the least important production pathway of VOCs emitted from cleaning, but contributed most to acetaldehyde production in the FG2 simulation, owing to the large emission of ethanol, which generated acetaldehyde via reaction with OH.

The rate of loss of the emitted VOC species showed greater variability between cleaning simulations compared to the rate of production. Losses due to air exchange with outdoors was proportional to the VOC concentrations, hence air exchange was a more important loss pathway for FG2 and SG2 because these products were larger emitters of VOCs in comparison to FR1 and SR1. Conversely, the rates of loss to surfaces

and through chemical processes are species-dependent and therefore are affected by the chemical properties of the emitted VOCs. Surface deposition was the most significant loss pathway for VOCs emitted from FG2, because ethanol was the largest emission from this product. Ethanol had a surface deposition rate of 2.4 h^{-1} in the base case simulations, hence it was effectively removed from the system via surface deposition. For all other simulations, monoterpenes were the largest emission. These species do not deposit on surfaces in the model; therefore, surface deposition was a less effective loss pathway. Chemical processes were a less effective loss pathway for emitted VOCs compared to air exchange and surface deposition. Losses due to chemical transformations was most significant for SG2, because this product was the largest emitter of reactive monoterpene compounds, including α-terpinene, α-phellandrene and limonene.

To investigate the chemical transformations of cleaning VOC emissions in greater detail, the concentrations of key oxidants, radical species and secondary products were examined (Figure 4.8). Activity-induced changes in concentration of each species were observed for all cleaning simulations at the time of the cleaning event, demonstrating that the emitted VOCs participate in indoor air chemistry. Perturbations in species concentrations persisted for 6 - 7 hours after the cleaning event, despite the emission events lasting $<$ 5 minutes. However, comparison between measured and simulated VOC concentrations indicated that some loss processes are not fully accounted for in the model (see Section 4.2.4). Therefore, these results are likely to overestimate the actual perturbation in species concentrations following cleaning. Overall, the activity-induced changes in concentration of oxidants, radicals and secondary pollutants were of a much smaller magnitude (10^{-3} - 10^{-1} ppb) compared to the species that were directly emitted from the cleaning activities (10^{0} - 10^{2} ppb).

A decrease in the concentration of OH radicals and concurrent increase in the concentration of HO_2 and peroxy radicals was observed following the cleaning events, evidencing the oxidation of emitted VOCs. The greatest decrease in OH concentration compared to the baseline simulation was observed for SG2, which also emitted

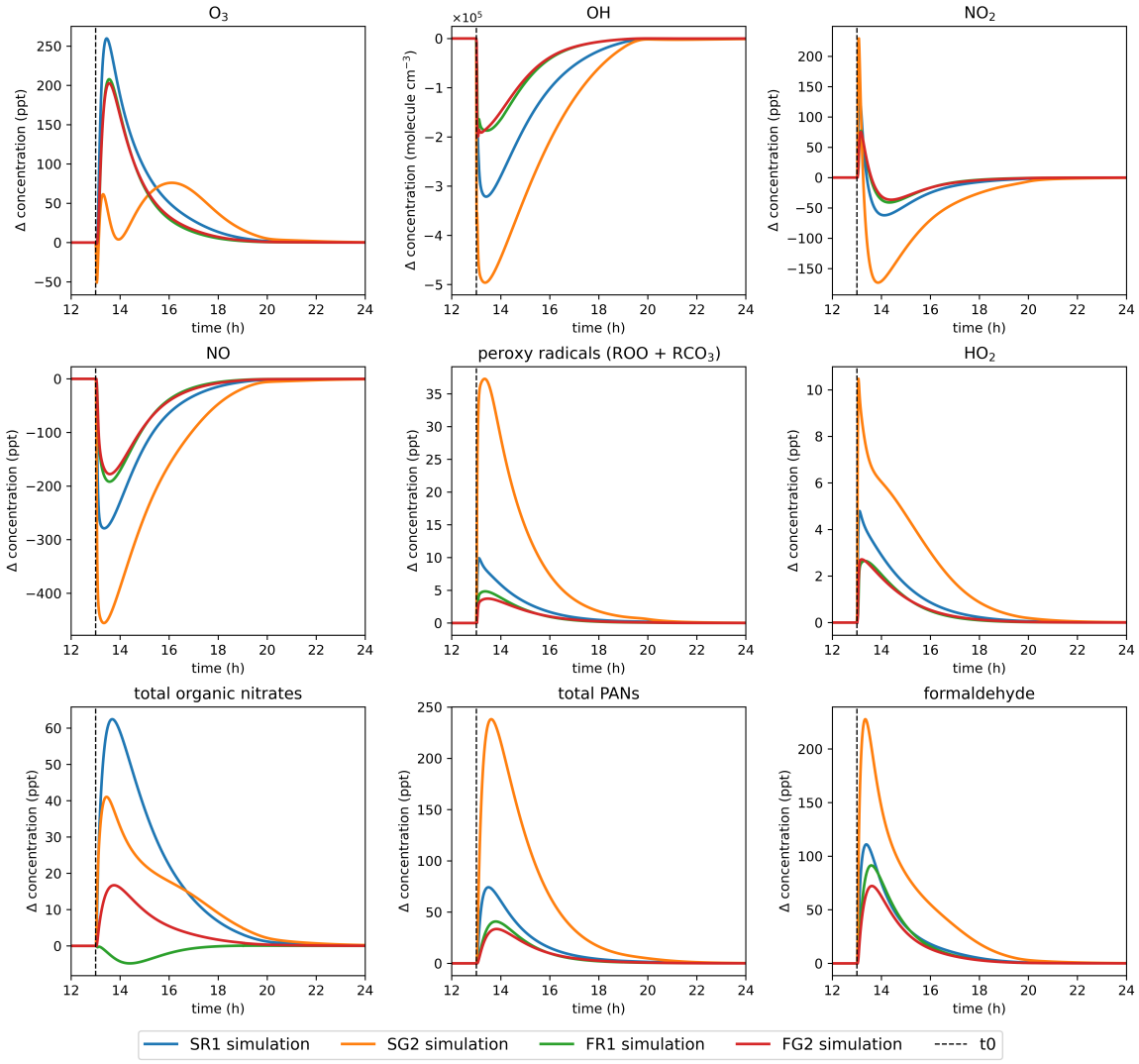

Figure 4.8: Activity-induced changes in mixing ratio or concentration of key oxidants, radical species, and secondary pollutants during the four cleaning simulations between 12:00 and 24:00 h.

the largest amount of monoterpenes (5.95 mg per clean) and total VOC (8.88 mg per clean). Despite FG2 being the second largest source of VOC emissions, a greater decrease in OH radicals was observed for SR1. This is due to the fact that while the total amount of VOC emitted from SR1 was 75% of that emitted from FG2, SR1 emitted 2.6 times more reactive monoterpenes than FR1. These results emphasise that both the quantity and the chemical reactivity of VOC emissions from cleaning can impact the resulting indoor air chemistry.

VOCs with unsaturated carbon bonds also undergo oxidation by reaction with O_3

to generate OH, HO_2 and peroxy radicals species indoors. In the simulated cleaning events the concentration of O_3 increased in concentration compared to the baseline simulation for all cleaning simulations, except SG2. This observation can be accounted for by the fact that NO concentrations decreased following cleaning due to reaction with the HO_2 and peroxy radicals generated from VOC oxidation (reactions 4.2 and 4.3). Lower concentrations of NO resulted in less removal of O_3 from the system via Reaction 4.4. Therefore, the production of peroxy radicals from VOC oxidation resulted in decreased NO concentration, thus allowing O_3 to accumulate.

$$RO_2 + NO \longrightarrow RO + NO_2 \tag{4.2a}$$

$$RO_2 + NO \longrightarrow RNO_3 \tag{4.2b}$$

$$HO_2 + NO \longrightarrow HO + NO_2 \tag{4.3}$$

$$NO + O_3 \longrightarrow NO_2 + O_2 \tag{4.4}$$

Conversely, in the SG2 simulation the activity-induced change in concentration of O_3 was negative. In this case, the removal of O_3 via ozonolysis of the emitted VOCs was greater than the increase in O_3 due to the suppression of Reaction 4.4. SG2 was the largest source of monoterpene species, which are particularly susceptible to ozonolysis due to the presence of unsaturated carbon bonds in their chemical structure. Therefore, the overall oxidative capacity of the indoor environment depends on the concentrations of VOCs emitted from cleaning activities and their relative reactivity towards OH and O_3.

To estimate the effects of VOC emissions from cleaning on the formation of hazardous secondary pollutants, the simulated mixing ratios of organic nitrates, PANs and formaldehyde were investigated. These species were focussed on because they are generated by indoor air chemistry and are known or suspected to be hazardous to human health (World Health Organization, 2010; Nielsen and Wolkoff, 2010; Zhang

et al., 2015; Vyskocil et al., 1998; Koenig et al., 1989; Berkemeier et al., 2016). Organic nitrate species are generated via Reaction 4.2b, while PANs are generated by Reaction 4.5.

$$RCO_3 + NO_2 \longrightarrow RCO_3NO_2 \tag{4.5}$$

Formaldehyde is ubiquitous in indoor and outdoor air and is generated through various OH-initiated and ozonolysis reactions. In indoor environments, the primary source of secondary formaldehyde arises from ozonolysis reactions, owing to the relatively high abundance of unsaturated species such as terpenes from indoor sources, and the low concentration of OH resulting from low levels of photolysis indoors compared to outdoors. Initial ozonolysis generates RO_2 radicals, which then react with NO via Reaction 4.2a to form RO radicals. Subsequent reaction of RO with O_2 forms aldehyde species, as represented by the general Reaction 4.6. When the RO radical is CH_3O, formaldehyde is formed as the product of Reaction 4.6.

$$RO + O_2 \longrightarrow HO_2 + R'CHO \tag{4.6}$$

In all simulations, the mixing ratio of PANs and formaldehyde increased relative to the baseline simulation. Total PANs increased by up to 208 ppt, while formaldehyde increased by up to 227 ppt shortly after the cleaning events, relative to baseline values of 430 ppt and 823 ppt, respectively. In all cleaning simulations, the oxidation of emitted VOCs by OH radicals generated peroxyacetyl radicals (RCO_3, a subset of organic peroxy radicals), which subsequently reacted with NO_2 to generate PANs (Reaction 4.5). Similarly, VOC oxidation by O_3/OH/NO_3 generated peroxy radicals which further reacted with NO to generate alkoxy radicals (RO). The formation of RO via this reaction pathway resulted in increased formaldehyde formation relative to the baseline simulation via Reaction 4.6. SG2 was the most efficient at producing PANs and formaldehyde because this cleaning product was the largest emitter of reactive VOCs, resulting in more peroxy radicals from VOC oxidation, which further reacted

to produce these secondary products. All other cleaning products resulted in similar mixing ratios of peroxy radical species, hence similar increases in formaldehyde and total PANs concentrations were observed.

The activity-induced change in mixing ratio of organic nitrates showed a different trend compared to other secondary pollutants, increasing in all simulations except for FR1. The production of organic nitrates is primarily dependent on the propensity of peroxy radicals formed by oxidation of VOCs to react with NO via Reaction 4.2a or 4.2b. In the SR1, SG2 and FG2 cleaning simulations, the peroxy radical species produced from oxidation of emitted VOCs resulted in more efficient $RO_2 + NO$ chemistry compared to the baseline simulation, thus causing an increase in total organic nitrate mixing ratio. SR1 showed a greater increase in organic nitrate compared to SG2, despite SG2 emitting 2.5 $\times$ more total measured VOC and 2.8 $\times$ more monoterpenes compared to SR1. Conversely, FR1 resulted in a decrease in total organic nitrate mixing ratio relative to the baseline simulation. FR1 had the lowest emission of monoterpenes, consisting of limonene and β-pinene only. Limonene, β-pinene and α-pinene are present in the simulations at background mixing ratios of 47, 34 and 90 ppt, respectively, due to ingress from outdoors. Following the FR1 cleaning event, the concentrations of limonene and β-pinene were elevated relative to that of α-pinene. Consequently, the efficiency of organic nitrate formation from the oxidation of α-pinene decreased relative to the baseline simulation. The increase in organic nitrate formation from the oxidation of emitted VOCs was insufficient to outweigh the reduction in organic nitrates formed from α-pinene oxidation, thus resulting in an overall decrease in the activity-induced change in organic nitrate concentration. These results indicate that the chemical composition of the VOC emissions from cleaning products has a clear impact on the potential for organic nitrate production indoors. This is discussed further in the following section.

4.3.4 Sensitivity to formulation composition

To investigate the impact of each VOC emission on the indoor air chemistry, a series of sensitivity tests were conducted whereby individual VOC emissions were removed from the simulated cleaning events. For simplicity, results from the sensitivity tests of SG2 only are discussed here, as the indoor air chemistry was most perturbed following use of this product in the simulations. Figure 4.9 shows the change in relevant oxidants, radical species, and secondary pollutant concentrations relative to the base case simulation (when all cleaning VOC emissions are included), when each monoterpene emission is omitted from the simulation of SG2 cleaning. The largest changes in species concentrations compared to the base case simulation were observed for limonene, and to a lesser extent the other monoterpenes, indicating that the monoterpene emissions dominated the indoor air chemistry following the cleaning event with SG2. Removing the other emitted VOCs (sesquiterpenes, dihydromyrcenol, acetates, acetaldehyde, methanol) had a negligible effect on the chemistry and therefore, the results are not shown in Figure 4.9 for simplicity. Full results from the sensitivity study for each cleaning product is summarised in Appendix B, Figures B.3-B.6.

The results from this sensitivity analysis for all four cleaning products revealed that monoterpene emissions had the greatest impact on the concentrations of oxidants, radicals and secondary pollutants (see Appendix B). This suggests that monoterpenes were the most significant VOC emission from both regular and green fragranced cleaning products, in terms of impact on the indoor air chemistry. Other VOC chemical classes emitted from the cleaning products investigated in this study were typically emitted at much lower concentrations (e.g., sesquiterpenes) and/or were less reactive (e.g., alcohols and acetates) compared to the monoterpenes. For example, while 3.39 mg of ethanol was emitted from the cleaning experiment with FG2 compared to 0.82 mg total monoterpenes (Table 4.7), the observed decrease in O_3 and increase in OH was $<$ -0.1% and 0.7%, and -1.2% and 15.3% compared to the base case simulation when these species were removed from the simulation, respectively.

Removal of individual monoterpene emissions from the SG2 cleaning simulation gener-

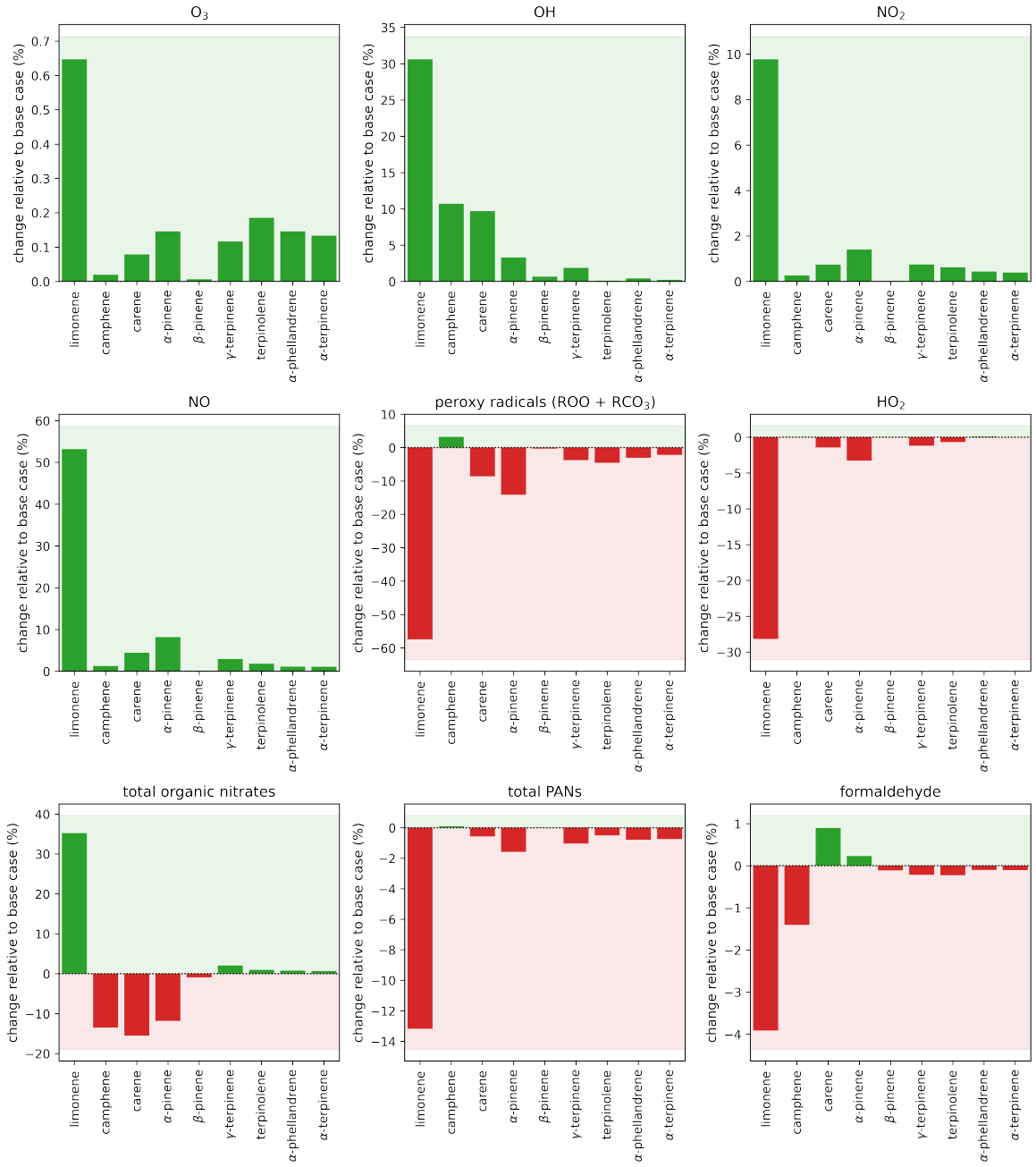

Figure 4.9: Percentage change in average concentrations of oxidants, radicals and secondary species following cleaning with SG2 when individual monoterpene emissions were omitted compared to the base case simulation. The omitted VOC is denoted by the x-axis label. Positive changes compared to the base case simulation are shown in green, while negative changes are shown in red. Average species concentrations are calculated from t_0 to 5.5 h after t_0.

ally resulted in increases in O_3 (< 1%) OH (< 31%), NO (< 52%), and NO_2 (< 10%) and decreases in HO_2 (< 29%) and peroxy radicals (< 58%) compared to the base case simulation. Removal of the monoterpene emissions decreased the overall concentration of reactive VOCs following cleaning, causing less VOC oxidation chemistry to occur. This resulted in an increase in the concentration of oxidants O_3 and OH, and a concurrent decrease in the production of HO_2/peroxy radical species. The reduced production of HO_2 and peroxy radicals caused an increase in NO and NO_2 due to the suppression of Reactions 4.2, 4.3 and 4.5.

In all cases, the average mixing ratio of total PANs decreased by up to 13.2% relative to the base case simulation when the monoterpene emissions were removed due to the suppression of Reaction 4.5, indicating that all monoterpene emissions from SG2 contributed to PAN formation. However, the omission of some monoterpene emissions resulted in an increase in average organic nitrate and formaldehyde concentrations relative to the base case simulation, suggesting that different mixtures of VOC emissions can result in more/less efficient production of harmful secondary pollutants.

Overall, the secondary chemistry resulting from the cleaning event was largely dominated by limonene, constituting the largest portion (35%) of monoterpene emissions from SG2. To delve deeper into the effects of various monoterpene emissions on indoor air chemistry, additional simulations were conducted. In these simulations, limonene emissions from SG2 were replaced with other monoterpene species while keeping all other VOC emissions (and hence the total VOC concentration) constant. The results, depicted in Figure 4.10, offer insights into the potential implications of substituting limonene with alternative fragrance compounds in the product formulation on indoor air chemistry.

When the limonene emission was assumed to be different monoterpenes, the resulting change in average O_3 and OH concentrations relative to the base scenario ranged from -11.6 – 0.9% and -0.7 – 27.5%, respectively. This is because different monoterpenes react with oxidants at varying rates and yield varying amounts of OH from ozonolysis reactions. The relative change in O_3 concentration was positive when limonene was

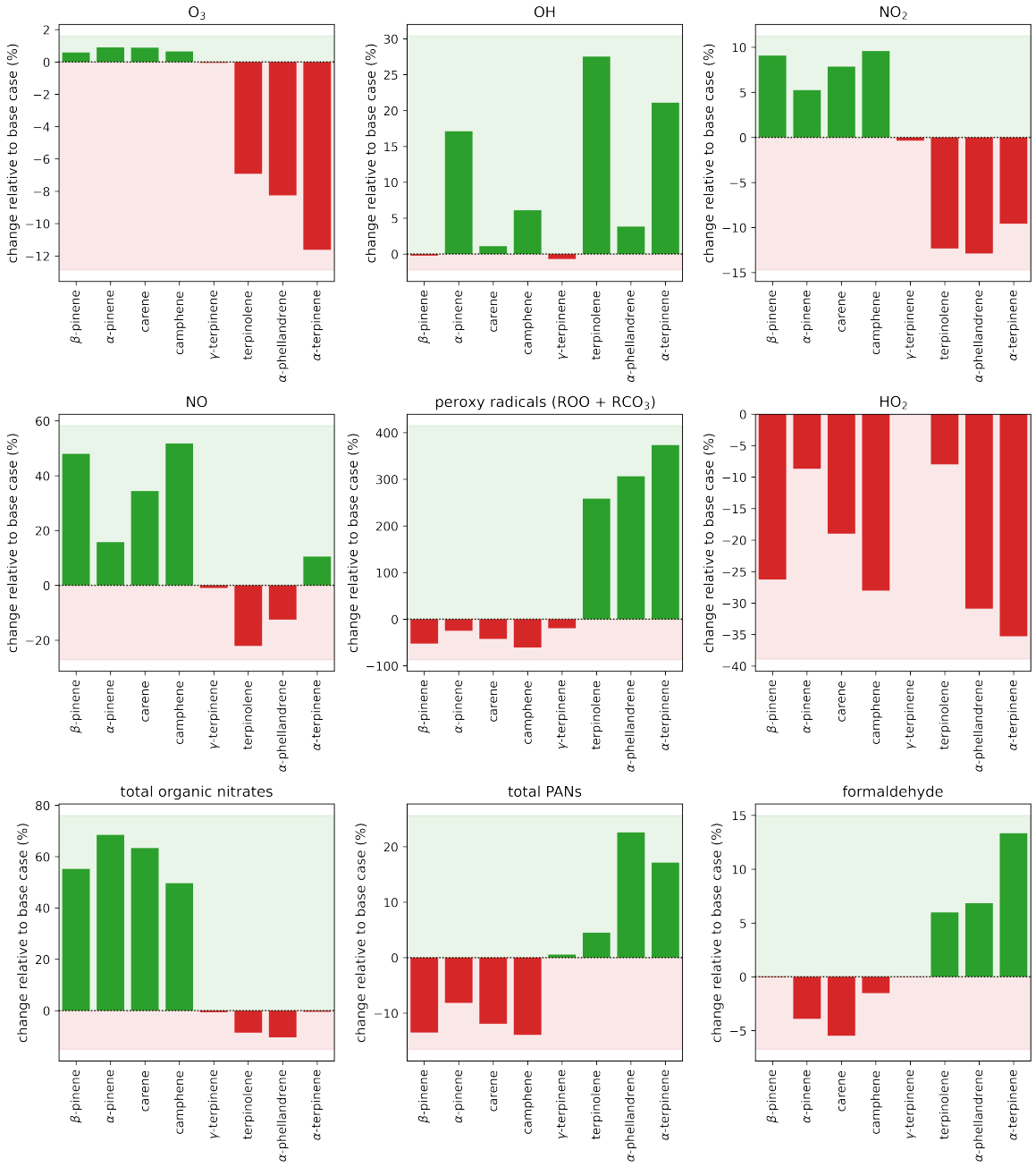

Figure 4.10: Percentage change in average concentrations of oxidants, radicals and secondary species following cleaning with SG2 when the limonene emission was substituted with a different monoterpene species compared to the base case simulation. The substituted monoterpene is denoted by the x-axis label. Positive changes compared to the base case simulation are shown in green, while negative changes are shown in red. Average species concentrations are calculated from t_0 to 5.5 h after t_0.

substituted with a monoterpene with a lower k_{O3} compared to limonene, and vice versa. The change in NO_2 concentration showed a positive correlation with the relative change in O_3, suggesting that O_3 was limiting NO_2 formation via Reaction 4.4.

In all cases, when the limonene emission was substituted with an alternative monoterpene emission, the average concentration of HO_2 radicals was less than in the base scenario, illustrating that limonene is the most effective monoterpene at producing HO_2. However, this was not the case for RO_2 radicals, which showed considerable increases of up to 373% when the limonene emission was substituted with terpinolene, α-phellandrene and α-terpinene. This is because these species react more readily with OH and O_3 than limonene, resulting in efficient peroxy radical formation from oxidation of the emitted monoterpenes. Similarly, compared to the base scenario, the average concentration was elevated by up to 120 ppt (13% increase) for formaldehyde and 121 ppt (23% increase) for PANs, while the average concentration of organic nitrates was reduced by up to 10% when the limonene emission was assumed to be a more reactive species. α-terpinene was the most effective at producing formaldehyde, whereas α-phellandrene was the most effective at producing PANs.

The relative changes in oxidant, radical and secondary species observed when the major monoterpene emission was assumed to be γ-terpinene were small compared to all other scenarios, suggesting that the secondary chemistry was similar to limonene. The rate coefficients of γ-terpinene oxidation by O_3 and OH are of the same magnitude as for limonene. Additionally, the chemical degradation scheme of γ-terpinene is represented in the model as a proxy scheme based on the MCM limonene scheme (Appendix A, *MCM* (2023)). Therefore, substitution of the limonene emission with the same amount of γ-terpinene results in similar secondary chemistry following cleaning.

Substitution of the limonene emission with α/β-pinene, camphene and carene resulted in average peroxy radical concentrations of up to 61% less than the base scenario, resulting in reduced formation of PANs and formaldehyde. The reduction in formaldehyde formation was more pronounced when α-pinene and carene were assumed to be the major monoterpene emission compared to β-pinene and camphene, with β-pinene

showing almost no difference relative to the base case. Unlike the other monoterpenes discussed here, β-pinene and camphene possess a terminal C=C bond. The primary ozonide that is generated from the addition of O_3 to the unsaturated bond decomposes via two possible channels to produce a pair of Criegee intermediate and carbonyl species. For β-pinene and camphene, the favoured channel (60%) for decomposition of the primary ozonide produces formaldehyde plus a Criegee intermediate, thus, formaldehyde is a direct product of ozonolysis for these monoterpenes. Therefore, despite their lower reactivity compared to limonene, β-pinene and camphene were still relatively effective at producing formaldehyde.

Conversely, an increase in the average concentration of total organic nitrates was observed when the limonene emission of SG2 was substituted with less reactive monoterpenes. The most significant increase in organic nitrate formation was observed when the major monoterpene emission was assumed to be α-pinene, resulting in an increase of 43 ppt (68% increase) relative to the base scenario. The formation of organic nitrate from VOC oxidation chemistry depends on i) the yield of peroxy radicals from reaction with OH (and to a lesser extent, O_3), ii) the branching ratio of RO_2 + NO reactions (Reaction 4.2a : 4.2b), and iii) the yield of nitrated peroxy radicals, and their subsequent reaction with RO_2/HO_2 (Berkemeier et al., 2016; Jenkin et al., 1997; Saunders et al., 2003). While these species produced less peroxy radicals compared to the base scenario, they were more effective at producing organic nitrates compared to all other monoterpenes. Based on the representation of monoterpene chemistry in INCHEM-Py, a greater proportion of the RO_2 radicals produced from the initial oxidation step of these species reacted with NO via Reaction 4.2b compared to limonene (and the more reactive monoterpenes which are represented in the model based on the MCM scheme of limonene, see Appendix A). These results show that replacement of limonene with less chemically reactive monoterpenes may cause considerable increases in the formation of organic nitrates.

Similar results have been observed in previous studies which have simulated the chemical processing of cooking and cleaning VOC emissions. Davies et al. (2023) found

that when assuming all monoterpene emissions from cooking a chicken stir-fry were limonene, the concentrations of formaldehyde and PANs increased, and organic nitrates decreased compared to the base case simulation when limonene, camphene and α-pinene were emitted. Conversely, when all emissions were assumed to be α-pinene, an increase in the total organic nitrates and PANs, but decrease in formaldehyde was observed. Further, Carslaw and Shaw (2022) reported that limonene was almost twice as effective at producing formaldehyde compared to α-pinene when all emissions from a cleaning event were assumed to be the single monoterpene. However, when assuming a 50:50 mix of limonene and α-pinene the resulting increase in formaldehyde concentration was greater still due to the complex interplay of different oxidation mechanisms. This demonstrates that the production of harmful secondary pollutants from complex emission sources such as cleaning activities depends not only on the amount of VOCs emitted and their reactivity, but also on how the degradation pathways of each species impact one another in the complex chemical system of the indoor environment. Further work should be carried out to understand this behaviour and thus identify combinations of VOCs that can be used to provide fragrance to cleaning product formulations, while also minimising the detrimental impact of their emissions on the indoor air quality.

4.3.5 Sensitivity to environmental factors

The secondary chemistry that results from cleaning is not only affected by the chemical composition of the VOC emissions, but also the ambient conditions of the indoor environment. Therefore, a sensitivity study was performed whereby various model parameters were modified to simulate a range of different indoor environments (Figure 4.11). Results were compared to see how these changes impact the chemical processing of VOC emissions from a typical cleaning event. SG2 was used as the representative example of a cleaning event in this analysis. The model parameters modified in this study are detailed in Table 4.5, and include the indoor SAV, attenuated light levels, occupancy, ventilation rate, and outdoor pollution conditions.

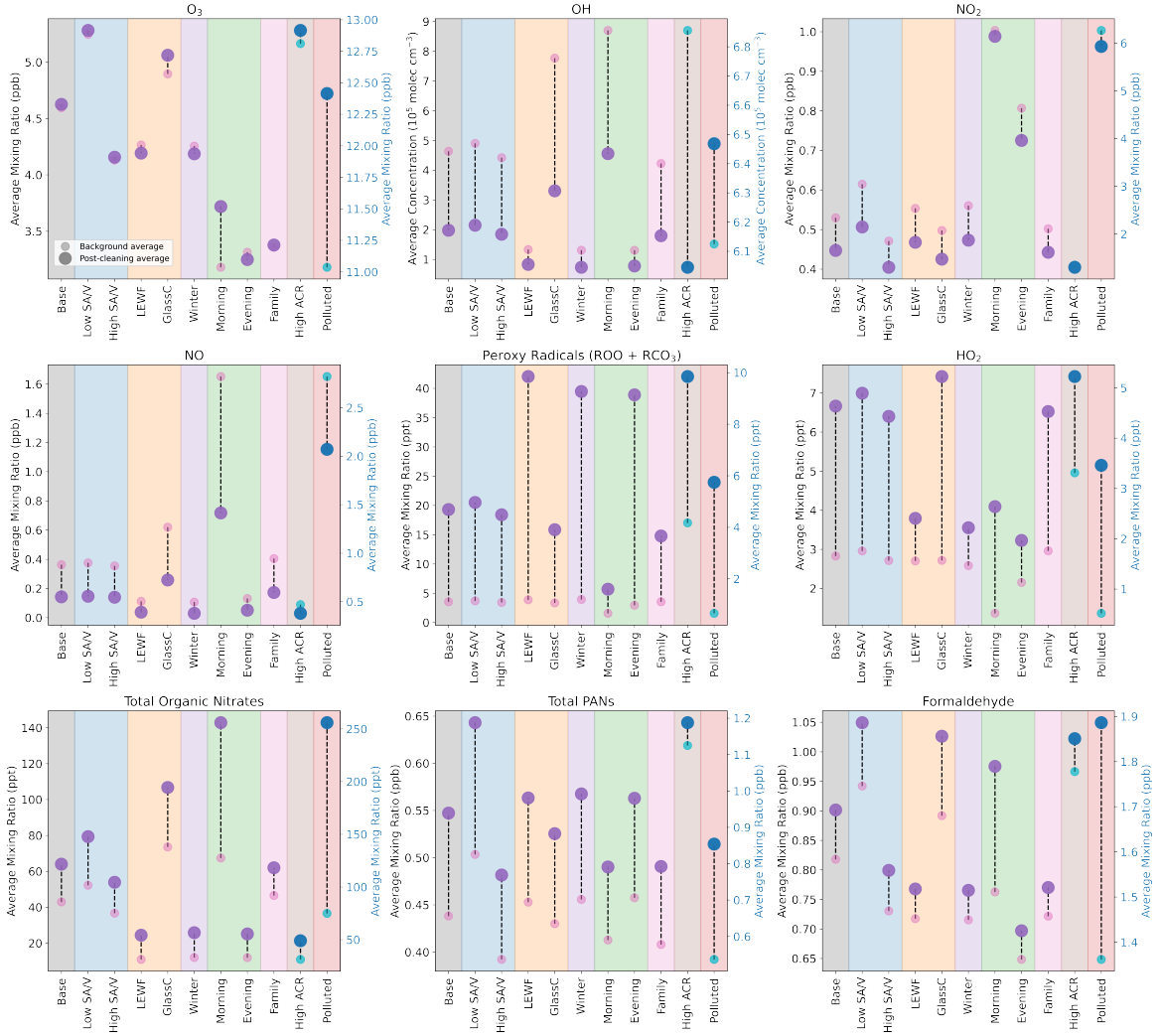

Figure 4.11: Change in average mixing ratios or concentrations of secondary species following cleaning with SG2 under different conditions. Small pink/blue circles give the average background levels without any cleaning, and the large purple/ dark blue circles show the average concentration/ mixing ratio following the cleaning activity. Different coloured shaded areas correspond to simulations when different ambient conditions are varied: grey = average kitchen base case, blue = indoor SAV, orange = glass type, purple = time of year, green = time of day, pink = occupancy level, brown = ACR, red = outdoor pollution levels. The high ACR and polluted scenario (blue/dark blue) correspond to the right-hand y-axis (blue), while all other scenarios (pink/purple) correspond to the left-hand y-axis. Averages are calculated from t_0 to 5.5 h after t_0.

4.3.5.1 Surface area to volume ratio

To investigate the effects of different SAV ratios on the indoor air chemistry, the material-specific surface areas defined in the base scenario were increased (high SAV) and decreased (low SAV) by 10%, except for skin which remained at 2 m^2 in each scenario to emulate a single adult occupancy. Generally, the background average concentration of species in the low SAV scenario was greater than the base scenario, and lower in the high SAV scenario due to increased surface deposition in the high SAV scenario. This was particularly pronounced for O_3, which increased by 650 ppt (+14%) in the low SAV scenario and decreased by 465 ppt (-10%) in the high SAV scenario. The relative proportion of different surface materials was kept constant between scenarios (except for skin), hence the main cause for this change was due to an increased total surface area in the high SAV scenario. Note, changing the relative proportions of the different surface materials while keeping the SAV constant would also impact the rates of O_3 and H_2O_2 surface deposition due to differences in the surface deposition velocities of these species onto different surface materials in the model (this is explored further in Chapter 5). Increased O_3 deposition in the high SAV scenario reduced the efficiency of gas-phase VOC oxidation chemistry. However, increasing the SAV also promotes heterogeneous chemistry, which results in the production of potentially harmful secondary pollutants such as aldehydes (Kruza et al., 2017).

The difference in oxidant and radical species concentrations between the background and post-clean periods was of a similar magnitude in the low SAV and high SAV scenarios compared to the base scenario. This indicates that the chemical processing of cleaning VOC emissions was marginally affected when the SAV changed. Monoterpene emissions dominated the indoor air chemistry following the cleaning activity. These species do not deposit onto surfaces in the model, hence increasing the SAV did not deplete the concentration of reactive VOCs available to be oxidised. The increase in secondary pollutant concentrations post-clean were slightly greater in the low SAV scenario (and lower in the high SAV scenario) because there was more O_3 present to react with the VOCs emitted from the cleaning activity. The average increases

in formaldehyde concentrations were 65 ppt, 79 ppt, and 102 ppt in the high SAV, base, and low SAV scenarios, respectively, reflecting the differences in O_3 concentration observed.

4.3.5.2 Photolysis

The levels of attenuated indoor lighting, and therefore the extent of indoor photolytic chemistry, is impacted by the composition of glass used in windows, the time of day and the time of year. The effects of these factors on the indoor air chemistry following cleaning were investigated in the glass C, LEWF, morning, evening, and winter scenarios.

In the base scenario, the glass was assumed to be LE, which allows the transmission of light in the range 330-800 nm and is likely to be representative of many modern windows (Wang, Shaw, Kahan, Schoemaecker and Carslaw, 2022). When the glass type was assumed to be LEWF (allows transmission of wavelengths 380-800 nm), average background concentrations of O_3, OH and NO decreased compared to the base scenario. In the LEWF scenario, the rate of photolysis of NO_2 to generate $NO + O$ was reduced, thus limiting indoor O_3 formation via $O + O_2$ chemistry. Additionally, the rate of HONO photolysis was reduced in this scenario compared to the base scenario, resulting in lower OH concentrations. Despite the lower background concentrations of oxidants in the LEWF scenario, the increase in average peroxy radical concentrations following cleaning was approximately double that of the base scenario. Following the initial oxidation of VOCs emitted from the cleaning event, the peroxy radicals produced were removed from the system via reaction with NO (Reaction 4.2). Lower NO concentrations in the LEWF scenario reduced the efficiency of these reactions, thus resulting in lower background and post-activity average concentrations of organic nitrates and formaldehyde.

When the glass was assumed to have higher emissivity (Glass C, allows transmission wavelengths 315-800 nm), the opposite trend was observed due to higher rates of photolysis indoors. In this scenario, the background levels of oxidants were greater com-

pared to the base and LEWF scenarios, causing more efficient oxidation of VOCs emitted from the cleaning activity. Despite the larger concentrations of oxidants present, the overall increase in average peroxy radical concentration between the background and post-clean periods was smaller than that observed in the base and LEWF scenarios because the higher background concentration of NO resulted in more efficient NO + RO_2 chemistry. The background concentrations of organic nitrates and formaldehyde were 31 ppt and 74 ppt higher in the Glass C scenario compared to the base scenario, respectively. Additionally, larger increases in concentrations of these species were observed following cleaning compared to the base and LEWF scenarios, illustrating more efficient secondary pollutant production from the chemical processing of cleaning VOC emissions when higher emissivity glass was used.

Simulating the cleaning event at different times of day and during different seasons also impacted the indoor photolysis chemistry. In the base scenario, the cleaning event was simulated at 13:00 during the summer, when light levels in the room were high. In the Winter scenario, the cleaning event was simulated during December when light levels were lower at 13:00 due to a larger solar zenith angle. Overall, the average background and post-clean concentrations of key oxidants and secondary pollutants in the Winter scenario were analogous to those observed in the LEWF scenario, indicating that a similar decrease in the rate of photolysis reactions occurred in each simulation.

In the morning and evening scenarios the simulated light levels were less than those in the base scenario due to higher solar zenith angles. In the evening scenario, this resulted in an expected decrease in average background O_3, OH and NO concentrations and a concurrent increase in NO_2 concentrations due to lower rates of photolysis. The elevated background NO_2 concentration was exacerbated by higher outdoor NO_2 concentrations resulting from rush hour traffic, which ingress indoors due to air exchange. Lower concentrations of organic nitrates and formaldehyde were observed in the evening scenario due to reduced oxidant concentrations compared to the base scenario. However, in the morning scenario, while the average background concentration of O_3 was low, matching the diurnal profile observed outdoors, the concentration of

OH and NO were elevated compared to the concentration in the base scenario. In the morning hours, a surge in OH concentration was observed indoors due to the build-up of species such as HONO which were rapidly photolysed once the sun rises, generating OH. Additionally, the elevated indoor NO_2 concentrations resulting from morning rush-hour traffic were photolysed to generate NO. High OH and NO concentrations in the morning resulted in efficient VOC oxidation following cleaning. A smaller increase in the average concentration of peroxy radical species was observed in the morning scenario compared to the base scenario because there was more NO available to participate in RO_2 + NO chemistry. Consequently, the increase in organic nitrate and formaldehyde concentrations in the morning were 3.4 and 2.5 times the increase seen in the base scenario.

4.3.5.3 Occupancy

In the family scenario there is assumed to be two adults and two children in the room, compared to one adult in the base scenario. The increased occupancy in the family scenario resulted in an increase in skin surface area (6 m^2) compared to the base scenario (2 m^2), in addition to greater breath emissions (ethanol, methanol, isopropanol, isoprene and acetone). The average background concentrations of key oxidants and radical species in the family scenario were similar to those observed in the base scenario, with the exception of O_3 which was 1.2 ppb lower in the family scenario. Deposition of O_3 onto indoor surfaces was greater in the family scenario due to the increased surface area of skin, which is the surface material with the highest O_3 deposition velocity represented in the model. The lower availability of O_3 in the family scenario resulted in less efficient oxidation of VOCs, thus slightly lower concentrations of peroxy radicals were observed. Despite the increase in concentration of isoprene from breath emissions, which generates formaldehyde as a product of ozonolysis, the average background concentration of formaldehyde was 96 ppt lower in the family scenario compared to the base scenario. This illustrates that O_3 was the limiting factor for formaldehyde production from ozonolysis of VOCs during the background and post-clean periods. The overall increase in formaldehyde between the background and post-

clean period for the family scenario was 58% of that observed in the base scenario. The lower O_3 concentrations in the family scenario also resulted in reduced concentrations of PANs, although little difference in organic nitrate was observed.

4.3.5.4 Indoor/outdoor exchange and outdoor conditions

In the base scenario, the ACR was assumed to be 0.5 h^{-1}, corresponding to a residence time of 2 hours for inert species. To investigate the impact of increasing the ventilation of the room, the ACR was increased to 2 h^{-1} in the high ACR scenario, corresponding to a residence time of 0.5 hour for inert species. Increasing the ACR resulted in indoor species concentrations converging towards outdoor concentrations, which were defined based on measurements made in a London Suburban location. Consequently, average background concentrations of key species O_3, NO and NO_2 increased compared to the base scenario in addition to other species which were present outdoors, not shown in Figure 4.11. While not directly affected by outdoor concentrations, the background concentrations of short-lived species such as OH also increased compared to the base scenario due to enhanced VOC/O_3 chemistry, thus increasing the overall oxidative capacity of the indoor environment.

The increased ACR in the high ACR scenario resulted in more rapid dilution of VOCs emitted from cleaning activities due to exchange with outdoors. Therefore, the residence time of reactive VOCs indoors was reduced, limiting their availability for oxidation and the resulting production of secondary pollutants indoors. This effect resulted in a lower reduction in NO and increase in peroxy and hydroxyl radicals between the background and post-activity periods for the high ACR scenario compared to the base scenario. The average background and post-activity concentration of organic nitrates in the high ACR scenario was similar to the base scenario because although there were higher oxidant concentrations, the oxidation products were not able to accumulate and contribute to organic nitrate formation before being ventilated outdoors. However, the concentrations of formaldehyde and total PANs were 2.2 and 2.6 times the concentrations observed in the base scenario, respectively. In the London Suburban data used to parameterise outdoor species concentrations, formaldehyde and PANs were defined as

2.4 and 2.2 ppb, respectively, which is higher than the background concentrations observed in the base scenario. Therefore, the overall effect of increasing the ACR on these species was to increase their indoor concentrations due to ingress from outdoors.

To investigate the effects of changing the outdoor pollution levels on the indoor air chemistry following cleaning, the diurnal concentration profiles of key pollutants O_3, NO and NO_2 were set based on data from Milan during a particularly polluted period in August 2003 (Terry et al., 2014), shown in Figure B.7. Consequently, the average indoor background concentrations of these species indoors were over 2.4, 7.8 and 11.8 times greater in the polluted scenario compared to the base scenario, respectively. Greater concentrations of O_3 in the polluted scenario resulted in increased indoor concentrations of OH compared to the base scenario due to more efficient VOC/O_3 chemistry. Despite the higher levels of oxidants and therefore higher rates of VOC oxidation chemistry, the concentration of peroxy radicals were lower in the polluted scenario compared to the base scenario, with a smaller increase in concentration post-clean observed. This is because the peroxy radical species produced from VOC oxidation chemistry are readily removed by reaction with NO (Reaction 4.2), which is much more abundant in the polluted scenario due to higher outdoor concentrations. Consequently, the concentrations of secondary pollutants in the polluted scenario were much greater than the base scenario. The largest increases in total organic nitrates (220%), total PANs (51%) and formaldehyde (34%) between the background and post-clean period were observed in this scenario compared to all other scenarios. Therefore, these results show that the outdoor pollution levels are likely to be the most important factor determining the production of secondary pollutants from indoor air chemistry following cleaning.

4.4 Chapter summary

This study has demonstrated that cleaning is a source of air pollutants indoors, including PM and VOCs. Experimental measurements showed that both regular and green cleaning products result in the direct emission of a range of VOCs, including monoterpenes, monoterpenoids, sesquiterpenes, alcohols, aldehydes and esters. Modelling of the measured cleaning emissions showed that monoterpenes had the strongest influence on the concentrations of hazardous secondary pollutants following the cleaning event. Other VOC emissions were less important drivers of the indoor air chemistry due to their lower reactivity and/or smaller emission rates compared to monoterpenes.

Monoterpenes are ubiquitous in cleaning products and other fragranced household and personal care products, hence their emissions indoors are highly likely to influence occupant exposure to potentially hazardous pollutants such as formaldehyde, organic nitrates and PANs that are efficiently produced as secondary products from monoterpene oxidation. The extent to which these secondary pollutants are produced depends on the abundance and chemical reactivity of the monoterpenes emitted from cleaning. Therefore, it is expected that occupant exposure could be minimised by careful consideration of the quantities and chemical identities of the monoterpene species used to provide fragrance to cleaning products. For example, the substitution of more reactive monoterpenes such as limonene and terpinolene for less reactive species such as carene, could reduce concentrations of formaldehyde and PANs following cleaning, although organic nitrate species would be generated more efficiently. To make informed decisions on product formulation changes that could improve indoor air quality, more comprehensive toxicological information on these secondary pollutants is needed. Reducing the total concentration of monoterpenes emitted from cleaning would be most effective at minimising exposure to secondary pollutants following cleaning. Therefore, non-fragranced products may be a better option than green or regular fragranced cleaners for minimising the effects of cleaning on indoor air pollution.

Modelling of different environmental conditions highlighted the importance of outdoor oxidant species concentrations on the resulting indoor air chemistry. With higher out-

door pollution levels, and therefore increased oxidant concentrations, the oxidative capacity of the indoor environment is increased due to ingress of outdoor oxidants. Therefore, it is expected that the ongoing challenge of air pollution, particularly in major cities, may intensify the potential exposure to harmful secondary pollutants indoors following cleaning. Additionally, the merits of increased building air tightness for improved energy efficiency should be carefully considered with relation to the residence times of indoor pollutants from occupant activities such as cleaning, and the ingress of oxidants and other air pollutants from outdoors. Indeed, while it may be beneficial to increase ventilation following cleaning to dilute indoor emissions, it may result in increased secondary chemistry and/or ingress of hazardous pollutants from outdoors depending on the outdoor conditions. The impact of indoor cleaning emissions on outdoor air quality should also be considered, as there is increasing evidence showing that indoor emission sources are impacting outdoor air quality (McDonald et al., 2018).

Going forwards, it would be beneficial to study the impacts of a wider range of cleaning products and activities on indoor air quality to better encapsulate the range of cleaning products and occupant behaviours that influence indoor air pollution from cleaning. Additionally, more detailed measurements under a variety of different environmental conditions would be beneficial to validate the results from model sensitivity studies. More detailed and realistic experimental studies would highlight discrepancies between experimental and model results, thus enabling better parameterisation of the model for improved representation of indoor air chemistry and processes.

Chapter 5

The Impact of Surfaces on Indoor Air Chemistry Following Cooking and Cleaning Activities

The cooking VOC emission rates and a contribution to the statistical analysis reported in Section 5.3.2.1 of this chapter were provided by Dr Helen Davies.

5.1 Introduction

Many emission sources contribute to indoor air pollution, including building materials and furnishings, combustion sources such as stoves, candles and log burners, and occupant activities such as cooking and cleaning (Liu et al., 2019; Wang, Xiong and Wei, 2022; Destaillats et al., 2008; Davies et al., 2023; Nazaroff and Weschler, 2004). The numerous and highly variable indoor emission sources often result in pollution levels greater indoors compared to outdoors (Brown, 2002). Together with the considerable proportion of time spent in built environments, indoor air quality is a significant factor in determining occupant exposure to air pollutants (Klepeis et al., 2001).

A growing number of studies have emerged, aiming to characterise the impacts of occupant activities on indoor air pollution (Vardoulakis et al., 2020; Audignon-Durand

et al., 2023). Cooking and cleaning are frequent occupant activities which serve as potentially large, intermittent sources of indoor air pollution in domestic and commercial environments (Liu et al., 2019; Ditto et al., 2023). Cooking activities emit a diverse range of indoor air pollutants, including VOCs, PM, and inorganic gases such as oxides of carbon and nitrogen (Farmer et al., 2019). The composition and quantity of emissions is highly dependent on the ingredients, type of oil used, cooking method (e.g., boiling, frying, etc.), and temperature (Abdullahi et al., 2013). For example, Klein et al. identified through a series of controlled chamber experiments that vegetables were a dominant source of alcohol and sulphur-containing VOCs, oils emitted predominantly aldehyde species, and herbs and pepper emitted large amounts of terpenes and terpenoids (Klein et al., 2019, 2016).

Cleaning activities also result in large emissions of VOCs and PM indoors. Likewise, the composition and quantity of emissions from cleaning is highly dependent on a range of factors, including the chemical composition of the product formulation, and the application mode (spraying, diluting, wiping, mopping *etc.*) (Singer et al., 2006). Fragranced household cleaners have been identified as a significant source of terpene species indoors, while chlorine-based bleach products emit hazardous chlorinated VOCs (Arata et al., 2021).

Many VOCs emitted from cooking and cleaning activities readily react with oxidants present indoors (O_3, OH, NO_3) to generate secondary pollutants, some of which are more hazardous than the parent compound (Nørgaard et al., 2014). In particular, monoterpenes, which are emitted both from cooking and cleaning activities, are susceptible to rapid ozonolysis due to the presence of unsaturated C=C bonds in their chemical structure. Some products of this chemistry, for example formaldehyde, organic nitrates, and PAN species, are known or suspected to have adverse health effects (World Health Organization, 2010; Nielsen and Wolkoff, 2010; Koenig et al., 1989; Berkemeier et al., 2016; Zhang et al., 2015). Therefore, it is important to characterise the fate of VOC emissions from occupant activities to determine the potential implications on occupant health.

The chemical fate of VOCs indoors differs from outdoors. The SAV is notably greater in built environments compared to outdoors spaces (Ault et al., 2020). Consequently, the relative importance of surface emissions, multi-phase reactions, and surface deposition for determining the composition and concentrations of gas-phase species is greater for the indoor environment compared to the outdoor planetary boundary layer (Abbatt and Wang, 2020). Deposition of VOCs onto indoor surfaces may have a significant influence on the peak concentration and temporal profiles of pollutants during transient emission events. Indeed, Singer et al. (2007) demonstrated for a range of compounds that surface deposition may compete with, or exceed, ventilation as the most important removal process following an emission event, depending on the intrinsic vapour pressure of the depositing compound.

Indoor surfaces influence the concentration of potentially hazardous secondary pollutants indoors (*e.g.* formaldehyde and longer chain aldehydes (Cheng et al., 2015)) by facilitating VOC oxidation chemistry. Sorption of VOCs and oxidants onto indoor surfaces removes the constraint of ventilation on residence time, thus increasing the potential for chemical transformations to occur via multi-phase interactions (Abbatt and Wang, 2020). Interactions of O_3 with surface-sorbed VOCs result in the production of oxidised products, which are often volatile enough to be emitted from indoor surfaces, thus affecting indoor air quality (Nicolas et al., 2007).

In realistic indoor settings, the ongoing deposition of VOCs onto indoor surfaces results in the creation of organic films. These films serve as a reservoir for reactive contaminants, which further influence indoor air quality via the emission of secondary pollutants (Lim and Abbatt, 2020). In kitchen environments, where VOCs such as cooking oils and terpenes from cleaning deposit on indoor surfaces, surfaces are likely to have high film coverage. Deming and Ziemann (2020) reported surface films containing up to 65% alkenes from painted walls and glass windows following cooking, cleaning, and occupancy experiments. In a study of four homes, Wang and Morrison (2006) showed that kitchen countertops exhibited consistently high secondary emission rates following exposure to O_3 between new and old homes. In contrast to carpets,

which age over time, the reactive surface films on kitchen countertops are continually replenished by occupant activities, thus suggesting that kitchen surfaces may be a dominant source of secondary pollutants (Wang and Morrison, 2006).

The deposition and subsequent multi-phase chemistry that occurs on indoor surfaces is dependent on the surface material. For instance, Won et al. (2001) demonstrated through a series of chamber experiments that carpet was the most significant sink for non-polar VOCs, while gypsum board was a significant sink for highly polar VOCs. There are an increasing number of studies which investigate the uptake of pollutants onto indoor surfaces and the products of multi-phase surface interactions. Of particular interest is O_3, on account of its ubiquitous presence indoors via infiltration from outdoors, and its importance in the oxidative processing of VOCs (Abbatt and Wang, 2020; Pei et al., 2022). The literature on O_3-surface interactions was reviewed and summarised by Carter et al. (2023), in addition to that of a less-studied oxidant, H_2O_2. The reported deposition velocities and secondary pollutant production yields were used to represent oxidant deposition and heterogeneous chemistry in the INCHEM-Py model (Shaw et al., 2023).

Domestic kitchens vary widely in their designs, with consequent impacts on surface-mediated indoor air chemistry. The physical characteristics of the room, including the total SAV and surface materials, impact the processing of VOCs which are emitted from activities frequently carried out in kitchens, such as cooking and cleaning. The room volume determines the dilution of pollutants emitted into the room, while the surface area and surface materials control the extent of surface deposition and heterogeneous chemistry. Weschler (2009) highlighted the evolving changes in indoor surfaces over time, for example the replacement of natural products with synthetic products for building materials and furnishings. This shift in the composition and complexity of indoor surfaces is likely to impact indoor air quality as a result of differing emissions, deposition, and multi-phase chemistry.

To our knowledge, the impacts of variations in realistic kitchen SAVs and surface materials on the resulting chemical fate of VOC emissions from typical occupant ac-

tivities such as cooking and cleaning have not been evaluated in detail. This study first characterises the VOC emissions from typical cooking and cleaning activities in a semi-realistic indoor environment, using real-time mass spectrometry for high time-resolved measurements. The INCHEM-Py model is then utilised to simulate the measured VOC emissions, and investigate the impacts of varying kitchen designs with respect to material-specific surface areas and total SAV. This study aims to identify building design factors relating to the SAV and material composition of indoor surfaces which impact the indoor air quality and indoor air chemistry following high emission events.

5.2 Methodology

5.2.1 The Test Pod facility and diagnostic equipment

A 4-week experimental campaign was conducted during February/March 2022 at the Department of Architecture & Built Environment, University of Nottingham, UK. The purpose of this campaign was to investigate the impact of cooking and cleaning on indoor air chemistry under semi-realistic conditions. The experiments were performed at the Test Pod facility, which is comprised of two buildings: one meeting current UK Building Regulations Part L (HM Government, 2010), and the other meeting the Passivhaus Standard (Moreno-Rangel, 2020). All experiments were performed in the Part L (test) pod to ensure that the building ventilation was representative of typical houses in the UK. The test pod had a volume of 22.2 m^3 (dimensions 3.53 m $\times$ 2.62 m $\times$ 2.40 m), with a single external door and a north-east facing window which was partially covered with an MDF board (Figure 5.1). The room consisted of linoleum tile flooring, painted plasterboard walls and ceiling, and minimal furnishings (total surface area 53.6 m^2).

An array of diagnostic equipment was used to monitor the indoor and outdoor air continuously throughout the campaign. Indoor air was sampled from the centre of the room at 2 m above the floor (blue circle, Figure 5.1). The sample lines were insulated

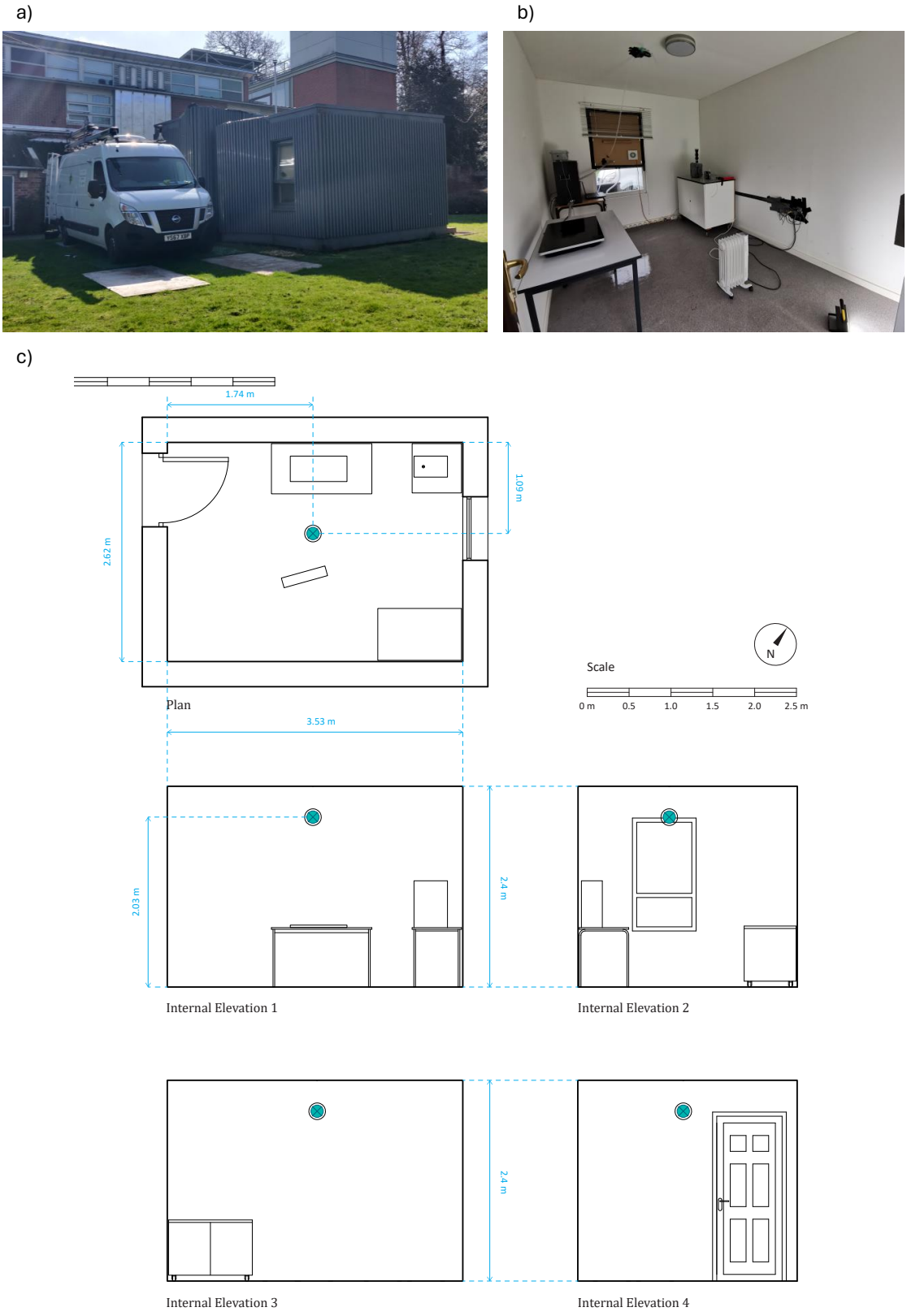

Figure 5.1: a) External view of Part L (test) pod and WASP, b) Internal view of test pod, c) Floor plan and internal elevations of test pod. Sampling location denoted by blue circle.

and connected to diagnostic equipment housed in the neighbouring Passivhaus Pod and in the WASP mobile laboratory, which was positioned adjacent to the test pod. Outdoor air was sampled from directly outside the facility at a similar height. A full description of the diagnostic equipment used during this campaign for real-time measurements of indoor and outdoor air is given in Table 5.1. Further details about each instrument can be found in Chapter 2, Section 2.2.

Table 5.1: Diagnostic equipment used during the Nottingham Pod campaign.

Measurement	Instrument	Sampling location	Time resolution
VOC	SIFT-MS	Indoors/outdoors	<10 s
O_3	Thermo Scientific Model 49i O_3 analyser	Indoors/Outdoors	1 s
$NO_x/NO_2/NO$	Thermo Scientific Model 42i (NO-NO_2-NO_x) Analyser	Indoors/Outdoors	1 s
PM/temperature/RH	Quant-AQ MODULAIR-PM	Indoors/Outdoors	1 min
$CO_2/H_2O/CH_4$	Los Gatos Research UGGA	Indoors	1 s
Meteorological data	Davis Met Station Vantage Pro2	Outdoors	1 s

A Voice200 ultra SIFT-MS (Syft Technologies, Christchurch, New Zealand) was used to quantify air concentrations of targeted VOCs in the test pod and outdoors, using the same experimental setup described in Chapter 4. The SIFT-MS principles of operation and operating conditions are described in Section 2.2.2. The specific ions measured by SIFT-MS during the cooking and cleaning experiments are shown in Table 5.2, along with the species molecular weights, product ions, rate coefficients and branching ratios. Whether or not the product ion was used for quantification is also shown in the 'included in analysis' column. Overall, 40 and 18 VOCs were measured by the SIFT-MS during cooking and cleaning experiments, respectively, with a time resolution of less than 10 seconds.

Table 5.2: The compounds measured by SIFT-MS during cooking, cleaning, or both experiments using each reagent ion, and their corresponding product ion molecular masses (MM), chemical formulae, rate coefficients and branching ratios. Whether or not the product ion was used for quantification is also shown in the 'included in analysis' column.

Reagent ion	Compound	MM (g mol^{-1})	Product ion	Reaction rate ($\times 10^{-9}$ cm^3 molecule^{-1} s^{-1})	Branching ratio (%)	Clean	Cook	Both	Included in analysis
H_3O^+	2,4-decadienal	153	$C_{10}H_{17}O^+$	4.9	100		✓		
		171	$C_{10}H_{17}O^+ \cdot H_2O$				✓		
	2-phenethyl acetate	105	$C_8H_9{}^+$	3.5	80	✓			✓
	acetaldehyde	45	$C_2H_4O \cdot H^+$	3.7	100			✓	✓
	acetonitrile	42	$CH_3CN \cdot H^+$	5.1	100			✓	✓
		60	$CH_3CN \cdot H^+ \cdot H_2O$					✓	
	acrylamide	72	$C_2H_3NH_2CO \cdot H^+$	2.1	100		✓		✓
	benzoic acid	123	$C_7H_6O_2 \cdot H^+$	3.0	100		✓		✓
	benzyl benzoate	151	$C_8H_7O_3{}^+$	3.7	60	✓			
		169	$C_8H_7O_3{}^+ \cdot H_2O$			✓			
	cinnamaldehyde	133	$C_9H_8OH^+$	2.0	100	✓			
	citral	153	$C_{10}H_{17}O^+$	3.0	60	✓			✓
		171	$C_{10}H_{17}O^+ \cdot H_2O$			✓			
	decane	161	$H_3O^+ \cdot C_{10}H_{22}$	1.6	100		✓		✓
	ethanol	47	$C_2H_7O^+$	2.7	100			✓	✓
	formaldehyde	31	CH_3O^+	3.4	100			✓	✓
	heptanal	115	$C_7H_{15}O^+$	3.7	80		✓		✓
	hexanal	101	$C_6H_{13}O^+$	3.7	95		✓		✓

		119	$C_6H_{13}O^+ \cdot H_2O$				✓		
	maltol	127	$C_6H_6O_3 \cdot H^+$	4.0	100		✓		
		145	$C_6H_6O_3 \cdot H_3O^+$				✓		
	methanol	33	CH_5O^+	2.7	100			✓	✓
	methyl cinnamate	163	$C_{10}H_{10}O_2 \cdot H^+$	3.4	100		✓		✓
		181	$C_{10}H_{10}O_2 \cdot H^+ \cdot H_2O$				✓		
	n-methylpyrrole	82	$C_5H_7N \cdot H^+$	3.0	100		✓		✓
	nonanal	143	$C_9H_{19}O^+$	2.5	86		✓		✓
	octanal	129	$C_8H_{17}O^+$	3.8	85		✓		✓
	pinonaldehyde	107		2.0	33	✓			✓
	propanal	59	$C_3H_7O^+$	3.6	100		✓		✓
	total monoterpenes	137	$C_{10}H_{17}{}^+$	2.6	30			✓	
		155	$C_{10}H_{17} \cdot H_2O^+$				✓		
	total sesquiterpenes	205	$C_{15}H_{25}{}^+$	2.5	64			✓	✓
NO^+	1,2,4-trimethylbenzene	120	$C_9H_{12}{}^+$	1.9	100		✓		✓
	1-propanol	59	$C_3H_7O^+$	0.6	100		✓		✓
		77	$C_3H_7O \cdot H_2O^+$				✓		
	2,4-decadienal	151	$C_{10}H_{15}O^+$	4.2	80		✓		✓
	2-heptenal	111	$C_7H_{11}O^+$	3.9	85		✓		✓
	2-phenethyl acetate	104	$C_8H_8{}^+$	2.9	85	✓			
	2-tert-butylcyclohexyl acetate	138	$C_{10}H_{18}{}^+$	2.8	40	✓			✓
	acetaldehyde	43	CH_3CO^+	0.7	80	✓			
		61	$CH_3CO^+ \cdot H_2O$			✓			
	acetic acid	90	$NO^+ \cdot CH_3COOH$	0.9	100			✓	✓

acetone	88	$NO^+ \cdot C_3H_6O$	1.0	100		✓		✓
acrolein	55	$C_3H_3O^+$	1.6	60		✓		✓
	86	$C_3H_4O \cdot NO^+$		40		✓		
benzene	78	$C_6H_6{}^+$	1.5	55		✓		✓
benzoic acid	105	$C_7H_5O^+$	3.0	60		✓		
benzyl benzoate	180	$C_9H_{10}O_2NO^+$	2.5	45	✓			✓
cinnamaldehyde	132	$C_9H_8O^+$	2.0	100			✓	
cinnamyl acetate	176	$C_{11}H_{12}O_2{}^+$	3.0	100		✓		✓
citral	151	$C_{10}H_{15}O^+$	2.5	35	✓			
diallyl disulfide	146	$(C_3H_5)_2S_2{}^+$	2.4	100		✓		✓
dimethyl disulfide	94	$(CH_3)_2S_2{}^+$	2.4	100		✓		✓
ethanol	45	$C_2H_5O^+$	1.2	100	✓			
	63	$C_2H_5O^+ \cdot H_2O$			✓			
eucalyptol	154	$C_{10}H_{18}O^+$	2.4	94			✓	✓
eugenol	164	$C_{10}H_{12}O_2{}^+$	2.4	100			✓	✓
furan	68	$C_4H_4O^+$	1.7	100		✓		✓
hexanal	99	$C_6H_{11}O^+$	2.5	100		✓		
lactic acid	120	$NO^+ \cdot CH_3CH(OH)COOH$	2.5	50	✓			✓
maltol	126	$C_6H_6O_3{}^+$	2.5	100		✓		✓
methyl cinnamate	162	$C_{10}H_{10}O_2{}^+$	1.4	100		✓		
	163	$C_{10}H_{10}O_2 \cdot H^+$				✓		
toluene	92	$C_7H_8{}^+$	2.2	100		✓		✓
total monoterpenes	88		2.2	25	✓			
	136	$C_{10}H_{16}{}^+$	2.2	75			✓	✓
total sesquiterpenes	204	$C_{15}H_{24}{}^+$	2.0	38			✓	

	undecane	155	$C_{11}H_{23}^+$	3.8	84		✓		
	xylenes + ethylbenzene	106	$C_8H_{10}^+$	2.0	100		✓		✓
O_2^+	2-phenethyl acetate	104	$C_8H_8^+$	3.0	100	✓			
	2-tert-butylcyclohexyl acetate	57	$C_4H_9^+$	4.5	45	✓			
	cinnamaldehyde	132	$C_9H_8O^+$	2.0	100			✓	✓
	cinnamyl acetate	134	$C_9H_{10}O_2^+$	1.5	100		✓		
	dihydromyrcenol	59	$C_3H_7O^+$	2.9	50	✓			✓
		77	$C_3H_7O \cdot H_2O^+$			✓			
	dimethyl sulfide	47	CH_3S^+	2.2	25		✓		
		62	$(CH_3)_2S^+$		60		✓		✓
	dimethyl trisulfide	111	$CH_3S_3^+$	2.2	15		✓		✓
	eugenol	164	$C_{10}H_{12}O_2^+$	1.9	100			✓	
	furan	68	$C_4H_4O^+$	1.6	100		✓		
	maltol	126	$C_6H_6O_3^+$	2.5	100		✓		
	nonane	99	$C_7H_{15}^+$	2.1	10		✓		✓
	octane	85	$C_6H_{13}^+$	1.6	50		✓		✓
	undecane	156	$C_{11}H_{24}^+$	3.2	31		✓		✓

The SIFT-MS was validated daily, and external calibration was performed six times during the experimental campaign (see Section 2.2.2.3 for details). The calibration factors applied to the data are summarised in Table 5.3.

Table 5.3: Mean ± standard deviation of the SIFT-MS calibration factors obtained during the Nottingham Pod campaign.

Species	Average calibration factor ± standard deviation
acetaldehyde	1.84 ± 0.01
acetone	0.72 ± 0.01
acetonitrile	2.94 ± 0.03
ethanol	0.94 ± 0.01
furan	0.84 ± 0.00
limonene	1.28 ± 0.02
methanol	0.85 ± 0.01
toluene	1.15 ± 0.01

[a] Limonene used as calibration gas

The instrument background was assessed by sampling zero air from an in-house heated palladium alumina-based zero air generator for a 3-minute period. Background VOC mixing ratios, defined as the 3-minute average of the zero air measurements, were subtracted from the data where available. The LODs were calculated as 3.2 times the standard deviation of the zero air measurements, and are shown in Table 5.4.

The background concentrations of dihydromyrcenol and citral were not measured during the first two instrument calibrations of the campaign due to differences in the SIFT-MS selected ion monitoring (SIM) methods used. Therefore, the average background concentrations measured during the final four instrument calibrations for these species were assumed to be an appropriate estimation of the background concentrations at the start of the campaign and were subtracted from the data. The LODs for dihydromyrcenol and citral reported in Table 5.4 are an average of the final four instrument calibrations only. Lactic acid was not included in any SIM method used to perform zero air measurements throughout the campaign. Consequently, the instru-

ment background was not corrected for this species, and no LOD was available.

Table 5.4: Mean limit of detection for targeted VOCs measured by SIFT-MS during the Nottingham Pod campaign.

Species	Average LOD
1,2,4-trimethylbenzene	0.16 ± 0.1
1-propanol	0.76 ± 0.1
2,4-decadienal	0.07 ± 0.0
2-heptenal	0.14 ± 0.0
2-phenethyl acetate	0.20 ± 0.1
2-tert-butylcyclohexyl acetate	0.25 ± 0.1
acetaldehyde	1.41 ± 0.4
acetic acid	0.61 ± 0.1
acetone	0.80 ± 0.1
acetonitrile	0.70 ± 0.2
acrolein	0.37 ± 0.1
acrylamide	0.18 ± 0.0
benzene	0.23 ± 0.0
benzoic acid	0.13 ± 0.0
benzyl benzoate	0.44 ± 0.1
cinnamaldehyde	0.12 ± 0.0
cinnamyl acetate	0.26 ± 0.1
citral	0.18 ± 0.1
decane	0.28 ± 0.1
diallyl disulfide	0.11 ± 0.0
dihydromyrcenol	1.70 ± 0.6
dimethyl disulfide	0.20 ± 0.0
dimethyl sulfide	0.46 ± 0.1
ethanol	5.88 ± 0.7
eucalyptol	0.12 ± 0.0
eugenol	0.14 ± 0.0
formaldehyde	1.52 ± 0.3
furan	1.04 ± 0.2
heptanal	0.22 ± 0.1
hexanal	0.39 ± 0.0
maltol	0.11 ± 0.0
methanol	8.22 ± 1.4

Table 5.4: Mean limit of detection for targeted VOCs measured by SIFT-MS during the Nottingham Pod campaign (continued).

Species	Average LOD
methyl cinnamate	0.20 ± 0.0
n-methylpyrrole	0.07 ± 0.0
nonanal	0.31 ± 0.1
nonane	4.98 ± 0.9
octanal	0.22 ± 0.1
octane	1.20 ± 0.3
pinonaldehyde	0.34 ± 0.1
propanal	1.85 ± 0.3
toluene	0.52 ± 0.1
total monoterpenes	0.51 ± 0.2
total sesquiterpenes	1.50 ± 0.7
undecane	0.40 ± 0.2
xylenes + ethylbenzene	0.15 ± 0.0

5.2.2 Experimental design

The experimental campaign involved three, day-long experiment types (background, cooking, cleaning). The purpose of the background days was to characterise the unoccupied test pod, including background gas and particle concentrations relating to the building and furnishing materials, stationary furnishings, and indoor/outdoor exchange. Background days involved minimal perturbation to the room, with experimentalists only briefly present periodically to take passive air samples and perform ACR assessments. Background days were assigned to one day before and after the cooking/cleaning experiments to assess the impact of recent occupant activities on background room emissions.

Each experiment was conducted on separate days to minimise complexity and to determine the indoor air pollution over approximately 20 hours following occupant activities. Prior to each experiment, the test pod was well ventilated for 1 hour by opening the external door. The room was left unperturbed for a minimum of 2 hours following the high ventilation period to allow indoor conditions to equilibrate before a scripted

cooking or cleaning activity was performed at approximately 13:00 h. Each experiment was repeated several times throughout the campaign to assess reproducibility (see Section 5.2.3).

The scripted cooking activity involved the preparation of a chicken stir-fry, based on a published recipe. Full details regarding the cooking protocol used can be found in Davies et al. (2023). The scripted cleaning activity involved the use of a market-leading lemon-scented surface spray cleaner (SR1, Table 2.1). The cleaner was applied to a tabletop (2 m^2) and wiped using a damp cloth after 1 minute. After each activity, all cooking/cleaning apparatus were removed from the room to ensure that all measured perturbations in indoor air quality derived only from the activity. The tabletop was rinsed with water between cleaning experiments to remove product residue and minimise carryover of cleaning emissions between experiments.

Throughout the campaign, the indoor temperature was manually controlled at 17 $\pm$ 1 °C using a plug-in oil heater in the centre of the room. The measured relative humidity was 47 $\pm$ 4 %. Natural ventilation only was used throughout all experiments to emulate the ventilation of a typical UK dwelling. The ACR of the test pod was measured using methane tracer gas releases on 6 days. The concentration decay was monitored by UGGA, and log-linear regression analysis of the background-subtracted data over two hours following the release resulted in an average ACR of 0.33 $\pm$ 0.06 h^{-1} (Figure 5.2).

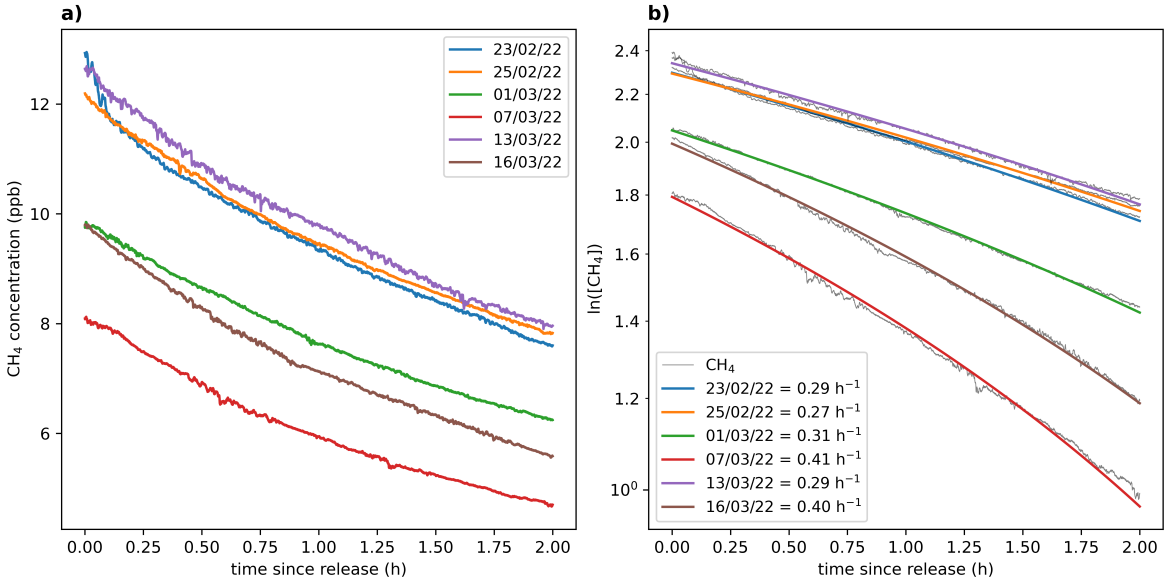

Figure 5.2: a) Concentration of methane over 2 hours following tracer release on 6 days during the campaign. b) Log-linear regression of the methane concentration decay, and the corresponding ACR for each day.

5.2.3 Experimental reproducibility

Cooking and cleaning experiments were conducted in triplicate over three consecutive days to assess reproducibility and improve reliability in results. This was made possible because each activity was scripted, meaning that the timings of emissions remained consistent between repeats. In general, the timings of VOC emission peaks measured by SIFT-MS were reproducible between replicate experiments. Whilst the relative change in VOC concentration during the emission periods were similar between repeat experiments, there was variation in the absolute concentrations of some VOCs measured during background and emission periods. The mixing ratios of total monoterpenes measured during each repeat of the cooking and cleaning experiments is shown in Figure 5.3a and 5.3b, respectively. For each measured VOC, the data from the three repeats were averaged to determine species concentration from average cooking and cleaning activities, shown as the black lines in Figure 5.3. The average cooking and cleaning data were used for all further analyses.

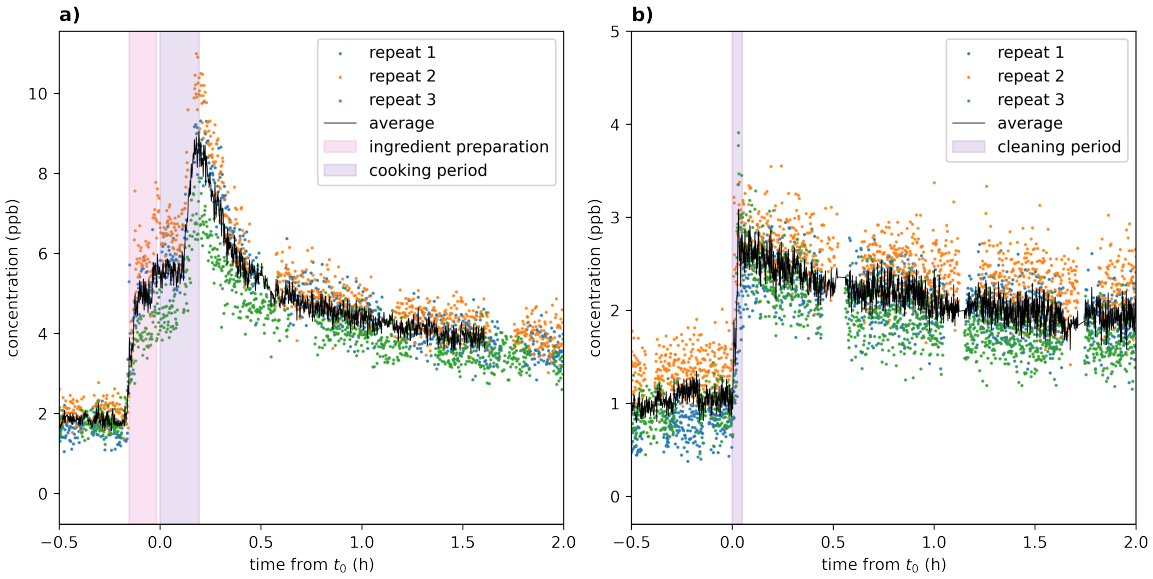

Figure 5.3: Total monoterpene mixing ratio measured by SIFT-MS during three repeat a) cooking and b) cleaning experiments. The average of the three repeats is shown as the black line.

5.2.4 Model simulations

To investigate the chemical processing of VOC emissions from the average cooking and cleaning experiments, INCHEM-Py was used, as described in Section 2.3. The model was initialised to represent an average kitchen setting, described in detail in Section 2.3.6.1. In brief, a kitchen of volume 25 m^3 and total surface area 63.27 m^2 was assumed, based on data reported by Manuja et al. (2019). The SAVs of each material considered in the model were as follows: soft furnishings = 0.081 m^{-1}; paint = 0.992 m^{-1}; wood = 0.665 m^{-1}; metal = 0.311 m^{-1}; concrete = 0.048 m^{-1}; paper = 0.008 m^{-1}; plastic = 0.220 m^{-1}; linoleum = 0.070 m^{-1}; glass = 0.058 m^{-1}; and skin = 0.080 m^{-1}. It was assumed that one person was present in the room (with a skin surface area of 2 m^2), and that the average SAV of plastic reported by Manuja et al. (2019) (0.290 m^{-1}) included 0.070 m^{-1} of linoleum (Kruza et al., 2017).

The outdoor concentrations of 110 VOCs were defined as static concentrations using representative data sourced from published literature and measurement databases, while trace gases (O_3, NO, and NO_2) were defined using diurnally varying concentrations based on measurements taken in a suburban London location. The indoor

background VOC concentrations were determined by the ingress and egress of species, which was controlled by an ACR typical of residential dwellings (0.5 h^{-1}, Nazaroff (2021)). Background emissions of acetone, ethanol, methanol, isopropanol, and isoprene were also present at emission rates corresponding to the breath emissions of one adult (Kruza and Carslaw, 2019; Weschler et al., 2007).

The indoor light levels in the average kitchen were determined based on an assumed latitude of 51.45 °N, date 20/06/2020, and LE glass glazed windows (transmission 330-800 nm, Blocquet et al. (2018)). It was also assumed that artificial incandescent lighting was on between 07:00 and 19:00, although having these lights on makes negligible difference to the results.

The VOC emissions from average cooking and cleaning activities were simulated at 12:00 and 13:00 h, respectively. Emission rates were calculated from the averaged SIFT-MS data of the three repeats for each cooking and cleaning experiment by calculating the rate of increase in species concentrations during the cooking/cleaning activity. These emission rates were then applied to the model as timed emissions, with a correction factor to account for differences in room volume between the test pod and simulated kitchen. Emissions from the cleaning experiment included acetaldehyde, methanol, ethanol, monoterpenes (limonene, carene, camphene, terpinolene, α-phellandrene, α-terpinene, α-pinene), butyl pyruvate, and dihydromyrcenol. Emissions from the cooking experiment included acetaldehyde, methanol, ethanol, acrolein, monoterpenes (limonene, α-pinene, camphene), hexanal, heptanal, octanal, nonanal, n-octane, n-nonane, 1,2,4-trimethyl benzene and dimethyl sulphide. The total monoterpene emissions from the cleaning experiment were speciated using results obtained in Chapter 3 for product SR1, while those from the cooking experiment were speciated using data from Davies et al. (2023). Model emissions of butyl pyruvate were used as a proxy for measured emissions of 2-tert-butylcyclohexyl acetate, with mass correction .Overall, the VOC emissions from the cooking activity lasted 23 minutes (including 10 minutes of ingredient preparation and 13 minutes of cooking), while those from the cleaning activity lasted 5 minutes.

5.2.4.1 Investigating the effects of kitchen design factors

Two modelling studies were performed to investigate the impact of variations in domestic kitchen SAVs and material-specific surface areas on the indoor air chemistry following a cooking and cleaning activity. The first study was performed in a theoretical kitchen, in which the materials of different components of the kitchen were randomly varied, while the second study utilised surface measurements made in real-life domestic kitchens to initialise the model (Manuja et al., 2019). In each study, the average cooking and cleaning activities were simulated at 12:00 and 13:00 h, respectively. All model parameters remained constant with the exception of the material-specific SAVs, which were varied to emulate different kitchen designs.

For the first study, simulations were performed using a 'basic kitchen' scenario. The nominal volume (height × length × width) of the basic kitchen was 29 m^3, based on the average volume reported by Manuja et al. (2019). The room volume minus contents was 23.84 m^3 and the total surface area was 72.06 m^2, resulting in a total SAV of 3.02 m^{-1}. The basic kitchen consisted of an L-shaped layout, with lower and upper kitchen cabinets spanning two of the walls. There was an internal and external door, one window, and basic kitchen amenities (sink, tap, refrigerator, oven, extractor fan, bin). The individual components of the basic kitchen, their respective surface areas, and the surface materials considered for each component are shown in Table 5.5. For the purpose of this study, tile and stone materials were classified as concrete in the model.

Table 5.5: Components of the basic kitchen scenario, their corresponding surface areas (m^2), and the likely materials of each component.

Component	Surface area (m^2)	Soft fabric	Paint	Wood	Metal	Concrete	Linoleum	Plastic	Glass	Human
Walls	15.74		✓							
External door	1.51			✓				✓	✓	
Internal door	1.51			✓						
Window	0.76								✓	
Floor	8.32	✓		✓		✓	✓			
Ceiling	12.10		✓							
Cupboards and kickboards	11.68		✓	✓				✓		
backsplash	3.21		✓			✓				
Worktop	2.62			✓		✓		✓		
Sink	0.59				✓	✓				
Tap	0.12				✓					
Oven	1.82				✓					
Oven doors	0.52								✓	
Extractor fan	1.62				✓					
Refrigerator	7.27				✓					
Bin	0.68				✓					
Occupant	2.00									✓

Based on the likely surface materials of each component defined in Table 5.5, 20 permutations of the basic kitchen were defined by randomly selecting the material of each component using the Python random.choice() method. The sum of each material SAV used to initialise the model for the 20 basic kitchen simulations is shown in Figure 5.4. In all simulations the SAV of human skin remained constant, corresponding to the presence of one adult occupant. All other SAVs varied depending on the defined material of specific kitchen components, resulting in 20 unique combinations of material SAVs.

The second modelling study involved simulating the cooking and cleaning activities using SAVs based on 1 cm resolution measurements of kitchens in nine residences in Blacksburg, Virginia, that were built between 1941 and 2003 (Manuja et al., 2019). The purpose of this study was to initialise the model using room volumes, surface areas,

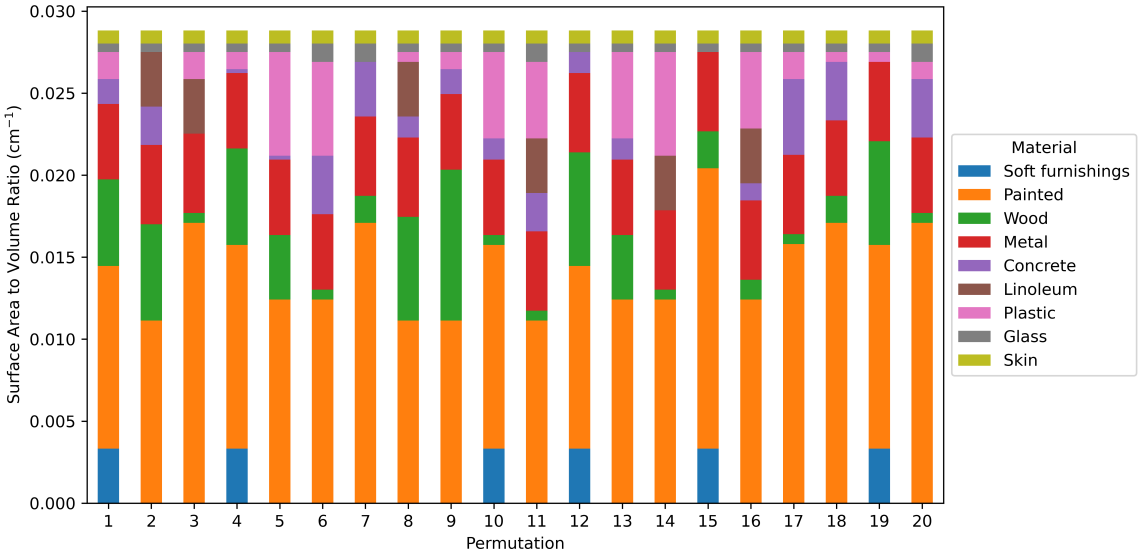

Figure 5.4: The material-specific SAVs (cm^{-1}) used to initialise the model for the 20 permutations of the basic kitchen scenario.

and surface materials which represented real domestic kitchens. The room volume ranged from 6 to 46 m^3 and the total surface area ranged from 38 to 96 m^2, resulting in total SAVs ranging from 1.61 to 7.14 m^{-1}. For the purposes of these simulations, kitchens 1-9 were defined based on descending order of the ratio of surface area to volume with contents (S*/V*, as defined in Manuja et al. (2019)). Generally, kitchens with a larger room volume resulted in a smaller SAV, however, this was also influenced by the number of contents in the room. The surface area of materials categorised by Manuja et al. (2019) as 'other' were not accounted for in our simulations. Therefore, the total surface area of 5 kitchens was underestimated by 0.6 – 32% in this study. Materials categorised as 'cardboard' and 'paper' were summed and classified as paper in the model. The surface area of plastic in each kitchen was assumed to be 75% plastic and 25% linoleum. A summary of the material-specific SAVs considered in the model for each of the nine kitchens is shown in Figure 5.5.

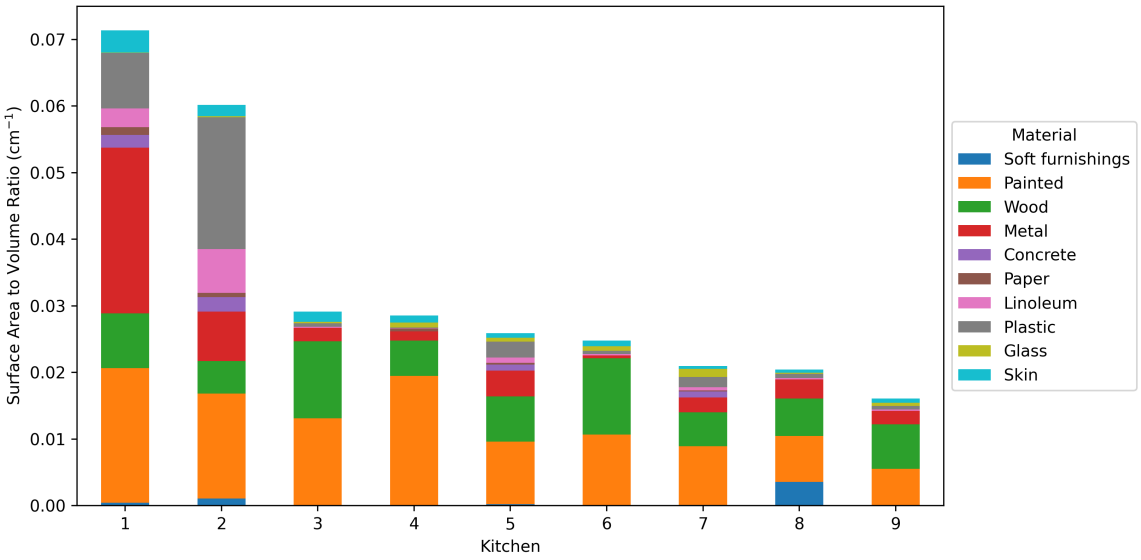

Figure 5.5: The material-specific SAVs (cm^{-1}) used to initialise the model for the real-life kitchen modelling study.

5.2.4.2 Coefficient of Variation

To compare variation in the concentrations of various species across the basic kitchen permutations, coefficients of variation (CV) were calculated. For each kitchen, background (BG) and activity (Act) simulations were carried out, and mean concentrations for each species, i, in each kitchen (k_n, where n is the kitchen number 1-20) were obtained across the period of 12:00 (t_0) to 17:30 ($\mu_{i,BG,k_n}/\mu_{i,Act,k_n}$, molecule cm^{-3} s^{-1}). For background coefficients of variation ($CV_{i,BG}$), the overall mean ($M_{i,BG}$) and standard deviation ($\sigma_{i,BG}$) of $\mu_{i,BG,k_{1-20}}$ were obtained, and CV calculated as follows:

$$CV_{i,BG} = \frac{\sigma_{i,BG}}{|M_{i,BG}|} \tag{5.1}$$

To compare the change in concentrations of species i as a result of activities across different kitchens, the average change in concentration for each species in each kitchen ($\mu_{i,\Delta C_i,k_n}$, molecule cm^{-3} s^{-1}) were calculated as $\mu_{i,Act,k_n} - \mu_{i,BG,k_n}$. The coefficient of variation for activity-induced concentration change ($CV_{i,\Delta C_i}$) was then calculated by obtaining the overall mean ($M_{i,\Delta C_i}$) and standard deviation ($\sigma_{i,\Delta C_i}$) of $\mu_{i,\Delta C_i,k_{1-20}}$ and

using the following equation:

$$CV_{i,\Delta C_i} = \frac{\sigma_{i,\Delta C_i}}{|M_{i,\Delta C_i}|} \tag{5.2}$$

5.3 Results and discussion

5.3.1 Typical cooking and cleaning VOC emissions

The average VOC emissions measured during the experimental cooking and cleaning activities are shown in Figure 5.6. The cooking activity emitted a larger concentration of VOCs compared to the cleaning activity, with a total maximum increase in emitted VOCs of 434 ppb, compared to the 15 ppb increase observed from the cleaning emissions. For both activities, the largest VOC emission was of methanol, which constituted 69% and 53% of the total VOC emissions for cooking and cleaning, respectively.

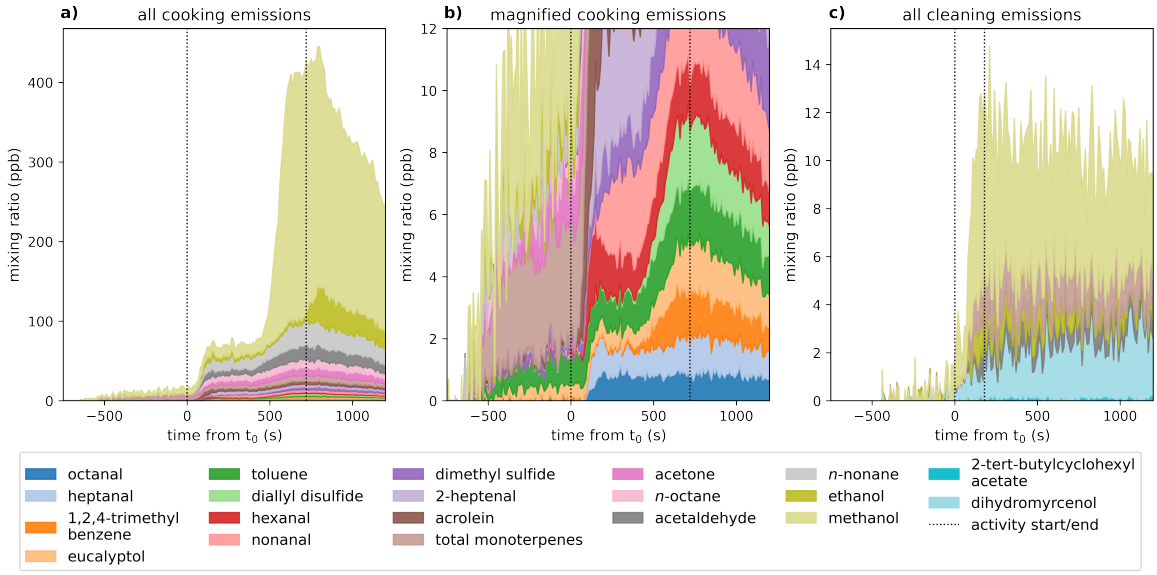

Figure 5.6: Mixing ratios of VOCs measured by SIFT-MS during the average a) cooking, b) cooking, focusing on species with lower mixing ratios, and c) cleaning experiment. The vertical dashed lines signify the start and end of the cooking/cleaning activity, with 0 s (t_0) being the time point when the activity commenced. Only the total mixing ratios of VOCs for which an emission peak was observed are shown, with the different colours indicating the contribution from each individual species. For each species, the background concentration (average of t_0-840 and t_0-760 s) has been subtracted for clarity.

Other VOC emissions measured from both activities included ethanol, acetaldehyde and monoterpenes. In all cases, cooking was a larger source of these VOCs compared to cleaning. However, cleaning was a relatively larger source of monoterpene emissions. The maximum concentration of monoterpenes during the cooking activity amounted to 7 ppb (1.6% of total maximum VOC), whereas cleaning emitted 2 ppb monoterpenes (13% of total maximum VOC). Monoterpenes are potentially important for indoor air chemistry because they are chemically reactive towards oxidants present indoors, thus have the potential to generate harmful secondary pollutants. These results indicate that while cleaning is a smaller source of VOC emissions compared to cooking, a larger proportion of the emitted species are chemically reactive species which may contribute to secondary pollutant formation.

Cooking emitted a range of species not observed from cleaning, including acrolein, trimethylbenzene, dimethyl sulphide, and a range of long chain aldehydes and alkanes. Different species peaked at different times during the activity, corresponding to the different stages in the cooking process. For example, an increase in monoterpenes of 4 ppb was observed several minutes prior to the start of the cooking period, corresponding with the preparation of spices in the room, followed by a second increase to a total of 7 ppb resulting from adding the spices to the pan at 360 s. These results clearly indicate that one or more of the spices (garlic, ginger, chilli) were a source of monoterpene emissions, which is in agreement with previous studies (Klein et al., 2016). A similar pattern was observed for eucalyptol and dimethyl disulfide to a lesser extent, the latter of which is a constituent of garlic (Abe et al., 2019).

Other notable emissions were observed during the oil heating stages (0 s, 300 s) and the addition of chicken, vegetables, and sauce to the pan (60 s, 380 s, and 660 s, respectively). The heating of oil resulted in emissions of a range of alkane and aldehyde species, the most notable being acetaldehyde (+ 18 ppb), nonane (+ 31 ppb), and propanal (+ 16 ppb). Alkane and aldehyde emissions from cooking oils have been well characterised in previous studies, highlighting the potential health risks of these emissions (Zhang et al., 2019). Alcohol emissions, particularly methanol and ethanol,

were attributed to the addition of various cooking ingredients to the pan. These emissions formed the largest contribution to the total VOC emissions during the cooking process, with an increase of approximately 300 ppb of methanol observed following the addition of vegetables, and an increase of approximately 7 ppb and 43 ppb of ethanol observed following the addition of chicken and sauce, respectively.

These observations are largely consistent with a previous study reported by Davies et al. (2023), which is based on the same scripted cooking experiment. The magnitude of emissions observed in this study were less than those reported by Davies et al. (2023), particularly for methanol, which reached a maximum mixing ratio of approximately 5 times more. However, it was concluded that there were large background emissions of methanol in the experimental facility used by Davies et al. (2023), likely from the relatively new building materials. This highlights the potentially large impact of various experimental factors, which could contribute to the observed differences between these studies. Other factors which are likely to have impacted the results include variations in ingredient sourcing and freshness, differences in cooking temperatures, and human variability in the cooking process. However, the timings of VOC emissions observed during the cooking activity showed good agreement with those reported by Davies et al. (2023), illustrating repeatability in the types of VOCs emitted during various aspects of the cooking processes.

In addition to alcohols, acetaldehyde, monoterpenes, and eucalyptol, VOC emissions unique to the cleaning activity included dihydromyrcenol and 2-tert-butylcyclohexyl acetate. In contrast to the cooking activity, the cleaning protocol was not a multi-step process, thus all VOC emissions were observed simultaneously. Overall, the emitted VOC species measured from the cleaning activity were consistent with the VOC composition of the same cleaning product (SR1) reported in Chapter 3, Table 3.4, evidencing the relationship between cleaning product formulation composition and the observed VOC emissions resulting from product use. The relative contribution of alcohols and acetaldehyde to the maximum total VOC mixing ratio observed in this study were consistent with the relative mass concentrations reported in Chapter 3. However,

we observed a larger relative emission of monoterpenes and lower relative emissions of dihydromyrcenol and 2-tert-butylcyclohexyl acetate in this study compared to that reported in Chapter 3. Furthermore, citral was reported to constitute 4.2% of the product formulation by mass, however emissions of this species were not observed in this study.

These differences in the relative proportions of VOC measured from headspace analysis of the cleaning product and from a realistic usage scenario may be due to degradation of the chemical formulation over time, as this study was performed on the same product approximately 2 years after the initial VOC compositional analysis reported in Chapter 3. Alternatively, the observed difference may indicate that different compounds demonstrate complex emission dynamics, resulting in a non-linear relationship between the cleaning product chemical composition and the emissions resulting from use. Angulo Milhem et al. (2021) reported that the liquid-to-gas transfer of terpenes from essential oil-based cleaners is driven by molecular properties such as volatility and interactions with the bulk solution, thus supporting this idea.

Using the experimental data, emission rates for each of the VOCs emitted during the average cooking and cleaning activity were calculated. These emission rates were applied to the INCHEM-Py model to simulate the emission events and investigate the secondary chemical processing of VOC emissions further. For the purposes of this study, it was assumed that the cooking activity occurred at midday and the cleaning activity commenced one hour later, representing a real-life scenario, in which cooking is followed by cleaning.

The activity-induced change in species concentrations were determined by subtracting the background simulation (no timed emissions) from the activity simulation (including timed emissions). The activity-induced change in emitted VOC mixing ratio is shown in Figure 5.7a. The y-axis is magnified in Figure 5.7b, focussing on VOCs emitted at lower concentrations. The maximum increase in total emitted VOC concentrations was approximately 300 ppb, with methanol and ethanol emissions from the cooking event at 12:00 h contributing the most to the overall increase relative to the baseline simulation.

Elevated VOC concentrations persisted for several hours following the cooking and cleaning activities. The straight-chain alkanes, nonane and octane, persisted for over 5 hours following cooking, whereas alcohol species quickly decayed in concentration following the emission event due to differences in species loss pathways.

The activity-induced change in concentration of three key classes of secondary pollutant are also shown in Figures 5.7c, d, and e. Formaldehyde, organic nitrates and PAN species are products of the VOC oxidation chemistry that occurs following the

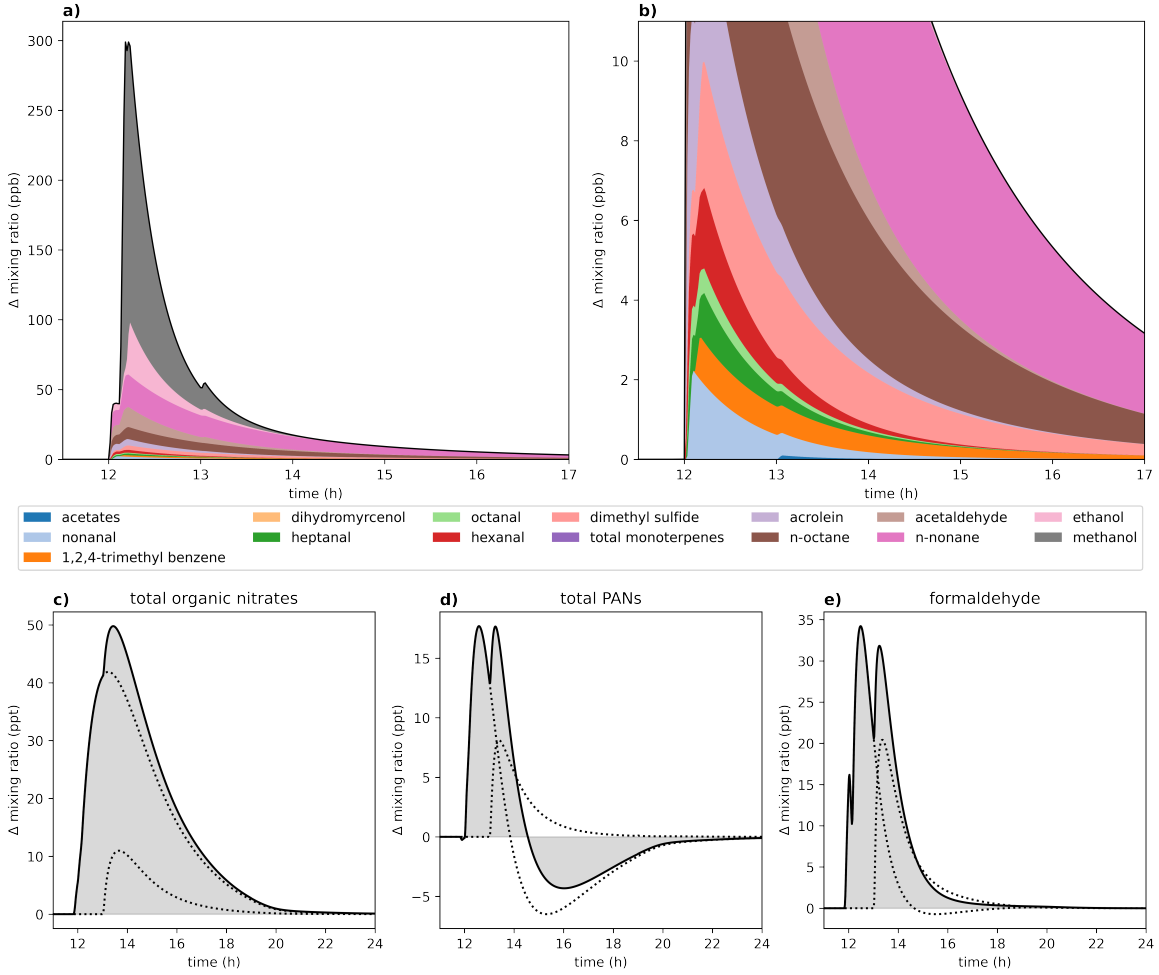

Figure 5.7: Activity-induced change in concentration of a) emitted VOCs, b) emitted VOCs, focussing on lower mixing ratios, and secondary pollutants c) total organic nitrates, d) total PANs, and e) formaldehyde, when cooking and cleaning are simulated in a typical kitchen setting at 12:00 and 13:00, respectively. The change in secondary pollutant concentrations when just cooking (at 12:00 h) and just cleaning (at 13:00 h) occurs is shown as dotted lines.

cooking and cleaning activities, and are known or suspected to have adverse health effects. Figure 5.7 shows that the concentrations of these secondary pollutants increased relative to the baseline simulation by 18 to 50 ppt, orders of magnitude smaller than the increase in primary VOC concentrations.

Both emission events contributed to the formation of secondary pollutants, thus consecutive activities had a compound effect on the total pollutant concentrations. The increase in organic nitrates compared to the baseline simulation persisted for longer compared to the other secondary products, resulting in the cleaning event elevating the maximum concentration above that achieved following cooking. Formaldehyde and PAN species were both shorter lived, hence the consecutive emission events prolonged the elevated concentrations of these species, but the cleaning event did not elevate the maximum concentration above that which was achieved from prior cooking. The dashed lines illustrate that the concentration of PAN species would have dropped by about 6 ppt a few hours following cooking. However, the additional VOC emissions from subsequent cleaning resulted in a second increase in total PANs, thus reducing the overall decline in PAN species concentrations observed.

These results illustrate that the occurrence of several occupant activities in sequence, as would be expected in a realistic scenario, can result in prolonged and exacerbated secondary pollutant concentrations resulting from the chemical processing of VOC emissions from these activities. While the concentrations observed here are below what would be expected to cause adverse health effects in occupants, it highlights the importance of considering the potential concentrations of secondary pollutants which could be achieved in occupational settings, where high emission occupant activities such as cooking and cleaning occur regularly throughout the day.

5.3.2 Impact of kitchen designs on indoor air chemistry

5.3.2.1 The basic kitchen scenario

In order to investigate the impact of variations in indoor surface materials on the indoor air chemistry, the average cooking and cleaning emissions were simulated in 20

permutations of the basic kitchen setting, as defined in Section 5.2.4.1.

For each kitchen, a background (excluding cooking and cleaning emissions) and activity (including cooking and cleaning emissions) simulation were performed. The resulting concentrations of key oxidants, radical species, and secondary pollutants in the background (dashed lines) and activity (solid lines) simulations are shown in Figure 5.8. The concentrations of secondary products formed following O_3 and H_2O_2 deposition onto different surface materials were summed for each kitchen simulation, shown as 'total surface emitted species' in Figure 5.8. These species include C_2-C_{10} straight chain aldehydes, as well as a number of other carbonyl and acid species, as outlined in Carter et al. (2023). Several of these species were also measured as primary emissions from the cooking and cleaning activities. Therefore, background concentrations only are shown in figure 5.8 to highlight the effects of indoor surface materials on their concentrations.

Figure 5.8 shows that there are two processes affecting species concentrations: i) the kitchen surface material composition, which impacts the background concentrations even in the absence of occupant activities, and ii) the VOC emissions from cooking and cleaning, which may or may not also be influenced by the surface material composition. These processes will be explored further in the following sections.

Material-dependent background concentration variation

To compare the influence of indoor surface material composition on the background concentration of oxidants, intermediates, and secondary pollutants of interest, the variation in concentrations was compared for each species across the 20 basic kitchen permutations by calculating the coefficient of variation ($CV_{i,BG}$, see Section 5.2.4.2). The $CV_{i,BG}$ values are presented in Figure 5.9 for a range of oxidants, intermediate species, and secondary pollutants from gas-phase and multi-phase chemistry. O_3, formaldehyde, and a number of surface-emitted secondary aldehydes showed $CV_{i,BG} > 0.2$ (*i.e.* standard deviation more than 20% of mean), indicating a considerable degree of variability. Therefore, the dependence of these species on indoor surface materials

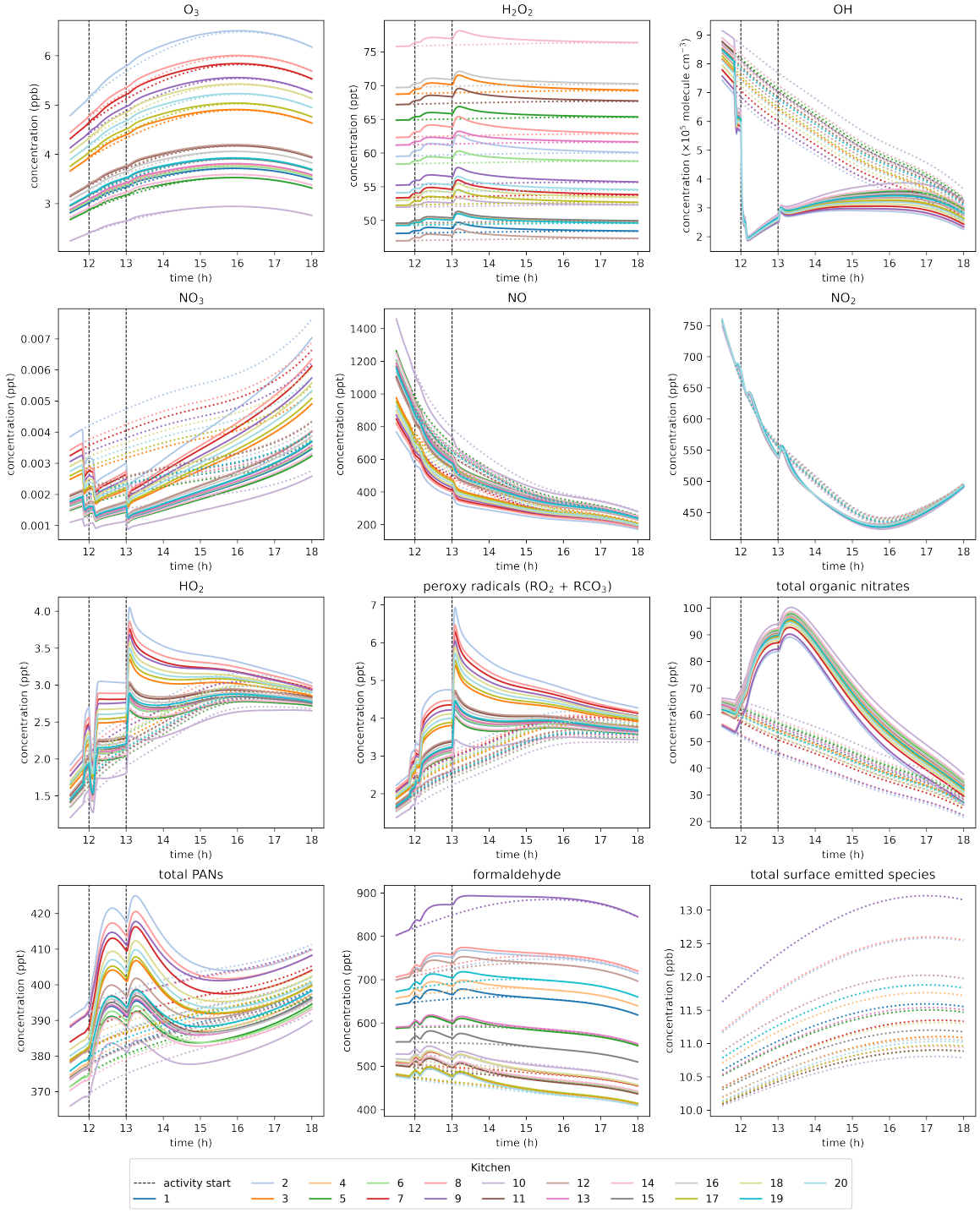

Figure 5.8: Concentrations of oxidants, intermediate species, and secondary pollutants in background (dashed lines) and activity (solid lines) simulations, in each of the 20 basic kitchen permutations. Vertical black dashed lines indicate the start of the cooking and cleaning activity at 12:00 and 13:00 h, respectively. Background only concentrations of the total surface emitted species is shown for clarity.

were investigated further. Of particular interest are O_3 and formaldehyde, as they are both potentially hazardous at sufficient concentrations, and O_3 is also fundamental in initiating VOC oxidation and subsequent formation of secondary products.

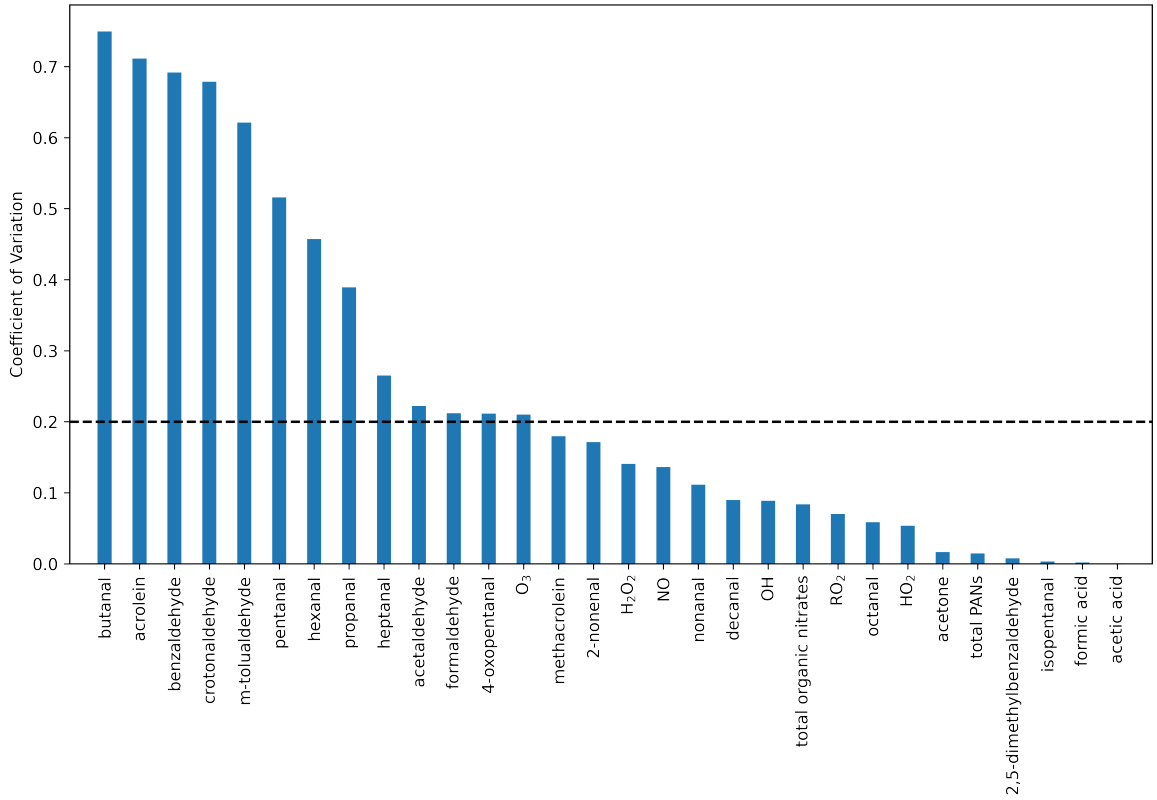

Figure 5.9: Coefficients of variation for the average background concentrations of a number of species, across the 20 different kitchen permutations. The black dashed line denotes a $CV_{i,BG}$ of 0.2, where the standard deviation is 20% of the mean. Above this value, species were considered to show a considerable degree of variability across the different kitchen permutations.

The influence of indoor surfaces on gas-phase pollutant concentrations is two-fold. Firstly, species may deposit onto indoor surfaces, thus removing them from the system. In INCHEM-Py, surface-specific deposition velocities of O_3 and H_2O_2 only are considered, while the deposition of other species is represented by constant deposition velocities, independent of surface material (Carter et al., 2023; Shaw et al., 2023). Secondly, the emission of pollutants from indoor surfaces resulting from O_3 and H_2O_2 surface interactions contributes to the gas-phase concentrations of secondary pollutants such as formaldehyde and larger straight-chain aldehydes (Carter et al., 2023).

Therefore, gas-phase species concentrations may be affected by the removal of key oxidants, thus limiting gas-phase oxidation chemistry, or by the production of secondary pollutants from multi-phase chemical transformations. As shown in Figure 5.8, the simulated concentrations of various oxidants, radical intermediate species, and secondary pollutants were affected by variations in surface materials between permutations. Therefore, indoor surfaces influence all stages of indoor air chemistry.

In the background simulations, (78 ± 3)% of O_3 deposited onto indoor surfaces. This result is comparable to previous studies, which observed 85% deposited in a simulated apartment with an ACR of 0.76 h^{-1}, and 91% in a simulated kitchen with an ACR of 0.5 h^{-1} (Kruza et al., 2017; Carter et al., 2023). The dependence of O_3 concentration on indoor surface materials ($CV_{i,BG} \approx 0.21$) resulted from variations in O_3 deposition rates and O_3 formation from the chemical processing of surface-emitted secondary aldehydes. O_3 is a major determinant of indoor air chemistry due to its ubiquitous presence indoors at chemically relevant concentrations and its reactivity towards unsaturated VOCs. Therefore, the variation in O_3 observed between simulations had consequent effects on the concentrations of intermediate and secondary products, such as formaldehyde.

To investigate the surface-dependence of O_3 and formaldehyde, linear regression analysis was performed to determine the degree of correlation between their average background concentrations and the SAV of each material in the basic kitchen scenario.

A strong negative correlation was observed between the background concentration of O_3 and plastic SAV. For example, the lowest O_3 concentrations were observed from kitchens 5, 6, and 14, which had the highest proportion of plastic surfaces. This suggests that plastic surfaces are a major determinant of indoor O_3 concentration, as evidenced by the high O_3 deposition velocity onto plastic compared to other surface materials (0.12 cm s^{-1}). Soft furnishings were present in some of the basic kitchen permutations due to the inclusion of carpeted flooring. Soft furnishings are also efficient at removing O_3 from the system, with a deposition velocity of 0.15 cm s^{-1}. The observed correlation between background O_3 and the sum of plastic and soft furnishing

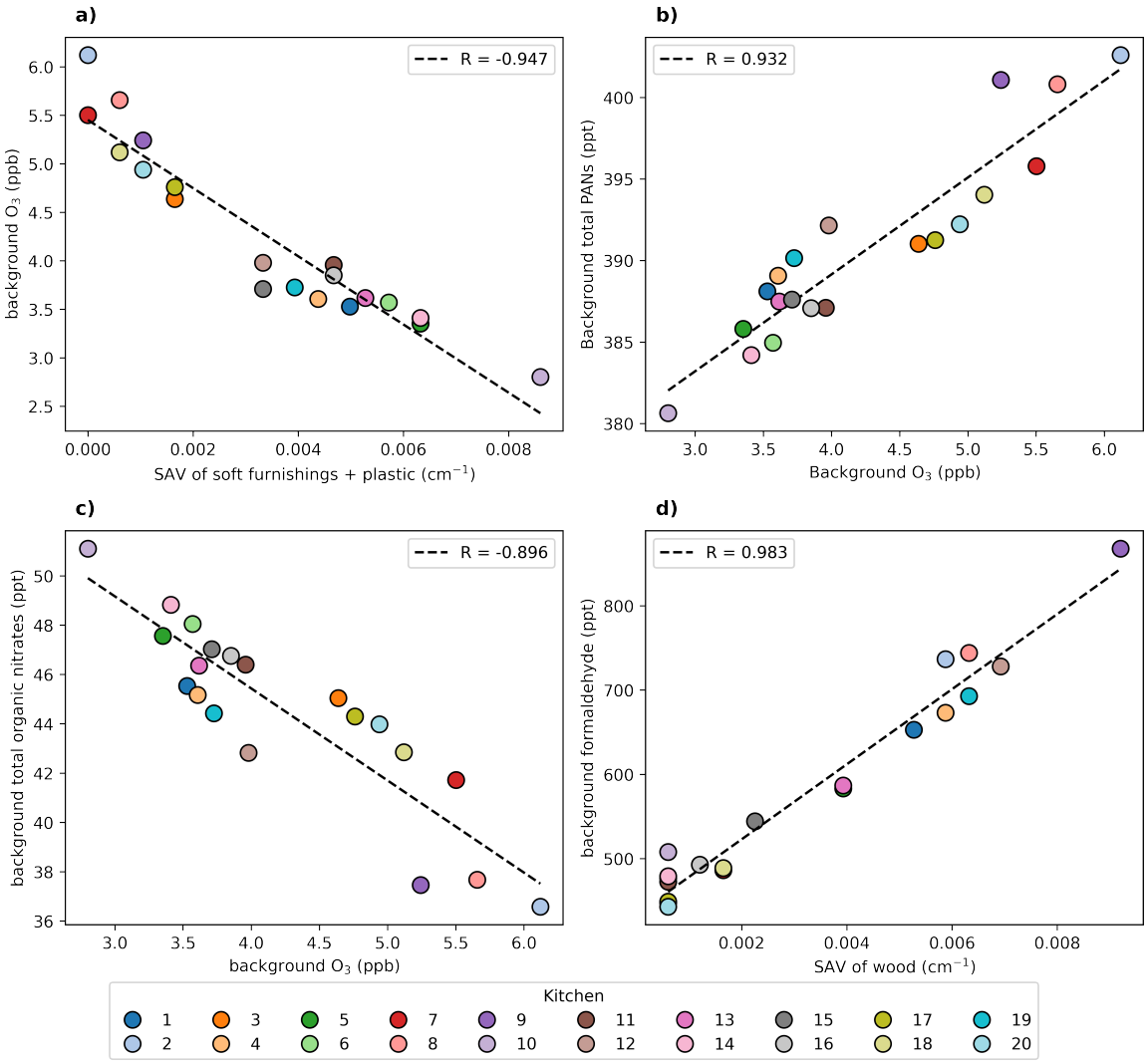

Figure 5.10: Relationship between background concentrations of a) O_3 and soft furnishings + plastic SAV, b) total PANs and O_3, c) total organic nitrates and O_3, d) formaldehyde and wood SAV. Linear regression analysis was performed to estimate the linear relationship between variables, with the lines of best fit represented by dashed lines. The Pearson correlation coefficient (R) for each plot is displayed in the legend. All the correlations presented are statistically significant ($p < 0.05$).

SAVs showed a strong negative correlation (R = -0.947), illustrating the influence of these surface materials on O_3 deposition (Figure 5.10a). Kitchen 10 had the highest combined proportion of plastic surfaces and soft furnishings, resulting in the lowest observed background O_3 concentration of approximately 2.8 ppb.

The observed variation in background O_3 concentration was expected to affect the concentration of key secondary pollutants from gas-phase VOC oxidation chemistry.

Figure 5.10b and 5.10c shows the correlation of background O_3 with total PANs and organic nitrates, respectively. A strong positive correlation was observed between O_3 and total PANs background concentrations (R = 0.932), while a negative correlation was observed between O_3 and total organic nitrates (R = -0.896). This is because at greater O_3 concentrations, the generation of RO_2 and RCO_3 radicals via VOC oxidation is more efficient. Subsequent reaction of RCO_3 with NO_2 generates PANs, thus higher O_3 concentrations increase the yield of PANs. Conversely, increasing background O_3 removes NO from the system via the reaction $O_3 + NO \rightarrow NO_2 + O_2$ more efficiently, thus limiting the availability of NO to react with RO_2 radicals to generate organic nitrates. At low background O_3 concentrations, NO accumulates, thus allowing more efficient conversion of RO_2 radicals to organic nitrate species.

Formaldehyde is also a secondary pollutant of concern due to its irritant and carcinogenic properties. Formaldehyde is an important product of both gas-phase and multi-phase chemistry. This species showed a strong correlation with wood SAV (R = 0.983, Figure 5.10d), and to a lesser extent, a negative correlation with paint SAV (not shown). The average background concentration of formaldehyde varied from 443 to 868 ppt, with the highest concentration observed from kitchen 9 which had the highest proportion of wood surfaces of all the kitchen permutations. Wood has an O_3 deposition velocity of approximately 10 times lower than soft furnishings, however, the formaldehyde production yield from wood is the highest of all surface materials (over 21 times greater than soft furnishings). Therefore, wood surfaces may have a strong influence on formaldehyde concentrations. An inverse correlation between formaldehyde and painted surfaces was observed because this surface material does not emit formaldehyde as a secondary product of multi-phase chemistry, whereas the other materials which it replaced in the kitchen permutations (wood, plastic, concrete) all produce secondary formaldehyde to some extent. These results indicate that keeping the total SAV of a room consistent, but changing the surface material composition can strongly impact the background formaldehyde concentration.

Similarly to formaldehyde, of the surface-emitted secondary carbonyls with $CV_{i,BG} >$

0.2, all species except for heptanal were strongly positively correlated with wood surfaces due to the high production yields of these species from wood compared to all other surface materials. Soft furnishings also showed a positive correlation with the simulated concentration of hexanal. The production yield of hexanal from soft furnishings is approximately 0.2 times that of wood, however, due to the high O_3 deposition velocity of soft furnishings compared to wood, the resulting impact of these surface materials on the emission of secondary hexanal was of a similar magnitude. Moderate correlations of heptanal with soft furnishings and plastic surfaces were observed, as these were the only surface materials which emitted heptanal as a product of multi-phase chemistry. An inverse correlation was observed between the concentrations of surface-emitted secondary products and the SAV of materials which did not emit them due to the substitution of emitting surfaces with non-emitting surfaces in the permutations, as discussed above for the relationship between painted surfaces and formaldehyde. Painted surfaces generally showed a negative correlation with most surface-emitted secondary carbonyls as this material only emitted C_8-C_{10} straight chain aldehydes, and at low yields compared to other materials.

In contrast to the other surface-emitted secondary products, 4-oxopentanal was only emitted from skin, which remained at a constant SAV between the different kitchens, corresponding to a single occupant. Therefore, the observed variation in this species concentration was due to changes in gas-phase oxidant concentration and/or changes in the rate of production from gas-phase chemistry induced by the variation in surface material SAVs. A perfect correlation was observed between the background concentrations of 4-oxopentanal and O_3. Thus, the availability of O_3 to deposit onto the skin surface was the only influencing factor, and differences in gas-phase chemistry had minimal effect of 4-oxopentanal formation between simulations.

These results suggest that room material composition has a complex effect on indoor air chemistry. For example, reducing the indoor concentration of O_3 by increasing the SAV of plastic surfaces and soft furnishings may be beneficial for minimising the production of PANs, but comes at the cost of increasing the concentrations of organic nitrates

and some surface-emitted secondary carbonyl species. Therefore, more comprehensive toxicological information will be essential to drive our understanding of the relative importance of these air pollutants on occupant health. This information would allow more informed decisions to be made on which material choices are most beneficial for improved indoor air quality.

Effects of materials on secondary pollutants from cooking and cleaning

The combination of surface materials not only affected the background species concentrations, but they also influenced the chemical processing of VOC emissions from cooking and cleaning activities. The activity-induced change in concentration of OH, HO_2, RO_2, formaldehyde, total PANs, and total organic nitrates for each basic kitchen permutation is shown in Figure 5.11. To quantify the effect of room surface composition on activity-induced chemistry, $CV_{i,\Delta C_i}$ values were calculated and are shown in Figure 5.11.

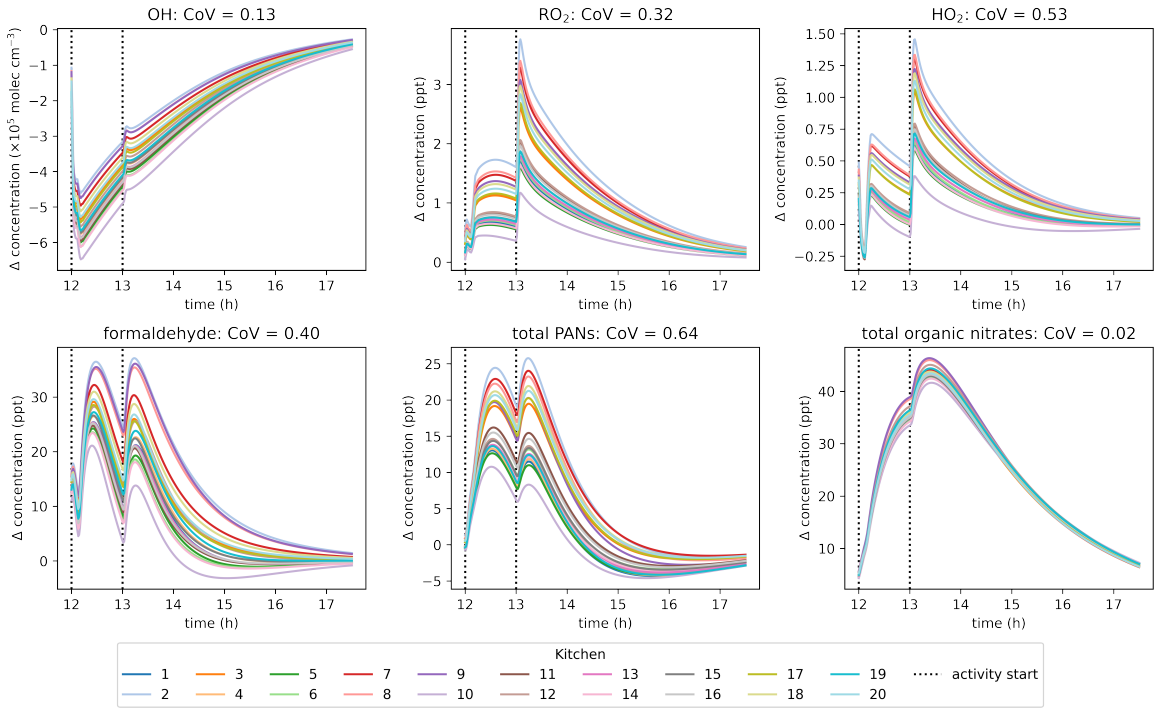

Figure 5.11: Activity-induced change in concentrations of OH, HO_2, RO_2, and secondary pollutants formaldehyde, total PANs and total organic nitrates from 12:00-17:30 h for each basic kitchen permutation. The $CV_{i,\Delta C_i}$ value for each species are shown in the headings.

The activity-induced change in OH concentration was not strongly impacted by variation in surface materials ($CV_{i,\Delta C_i} = 0.13$). Most of the observed change in OH concentration was due to reaction with the VOCs emitted from cooking and cleaning, which remained constant for all simulations. Conversely, HO_2 and RO_2 were generated as products of oxidation reactions initiated by both OH and O_3. Therefore, the difference in background O_3 discussed earlier due to variations in O_3 surface deposition between the different kitchens impacted the overall efficiency at which the emitted VOCs were oxidised to generate HO_2 and RO_2, resulting in high $CV_{i,\Delta C_i}$ of 0.32 and 0.53, respectively.

Of the secondary pollutants, high $CV_{i,\Delta C_i}$ values were observed for formaldehyde and total PANs of 0.40 and 0.64, respectively. This indicates that the activity-induced formation of these secondary pollutants were strongly influenced by variations in material-specific SAVs between simulations. However, total organic nitrates showed very little variation between simulations ($CV_{i,\Delta C_i} = 0.02$), suggesting that these species were not significantly influenced by variations in the kitchen surface materials.

The effects of surface materials on the formation of secondary pollutants following cooking and cleaning are both direct (emissions of secondary pollutants from multi-phase chemistry) and indirect (removal of oxidants by surface deposition, which would otherwise contribute to secondary pollutant formation via gas-phase indoor air chemistry). The influence of key indoor oxidants (O_3 and OH) on the observed variation in activity-induced change in secondary pollutant concentrations was investigated further in Figure 5.12. Here, linear regression analysis was performed between simulated oxidant concentration and activity-induced change in formaldehyde/PAN concentration. This analysis was not performed for organic nitrates, as the activity-induced change in this pollutant showed little variation in between simulations.

The variability in activity-induced changes in formaldehyde concentration was observed due to the influence of indoor surfaces on both the direct emissions from multi-phase chemistry and the concentrations of oxidant species contributing to the formation and destruction of formaldehyde via gas-phase reactions. Linear regression

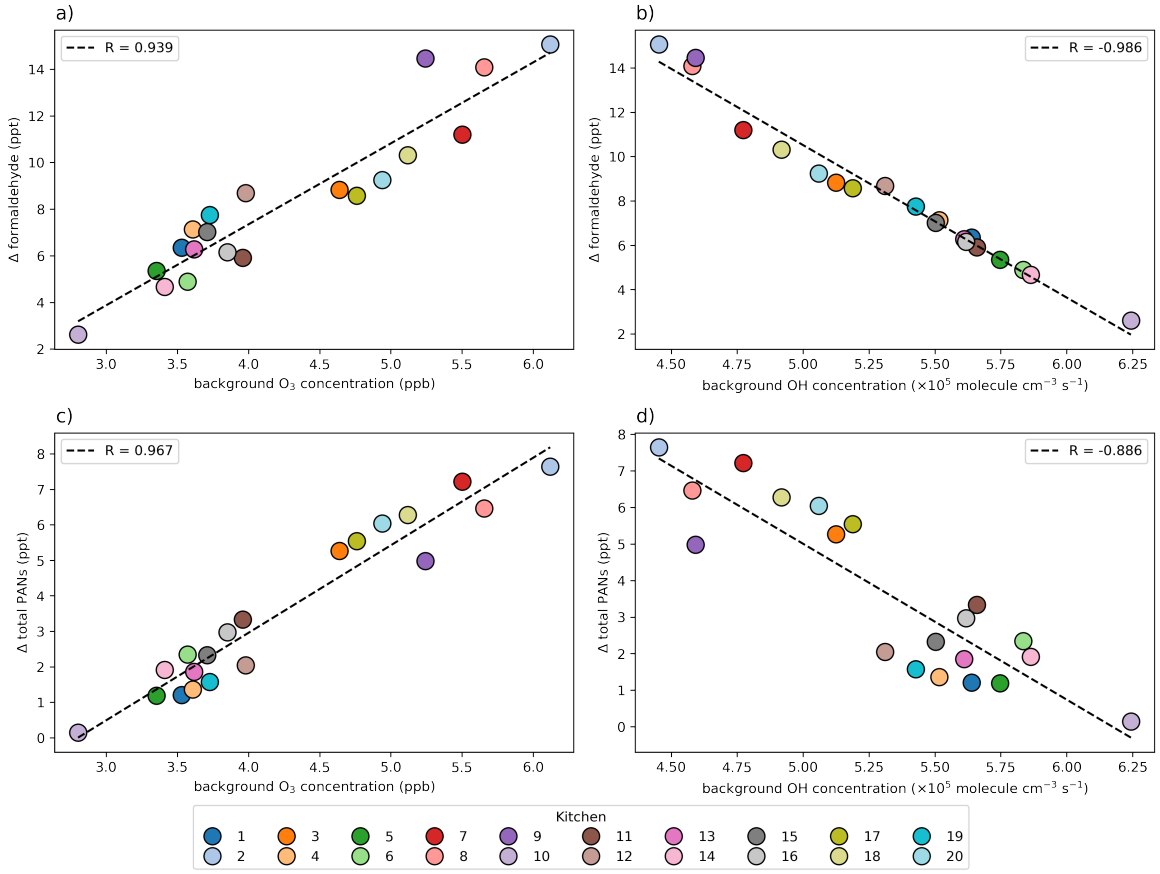

Figure 5.12: Correlation of activity-induced changes in secondary formaldehyde (a, b) and total PANs (c, d) with background O_3 (a, c) and OH (b, d) concentrations in the basic kitchen permutation simulations. Linear regression analysis was performed to estimate the linear relationship between variables, with the lines of best fit represented by dashed lines. The Pearson correlation coefficient (R) for each plot is displayed in the legend. All the correlations presented are statistically significant ($p < 0.05$).

analysis indicated a positive correlation between activity-induced changes in formaldehyde concentration and O_3 concentration (R = 0.939, Figure 5.12a), and a negative correlation with OH concentration (R = -0.986, Figure 5.12b).

As Figure 5.12 shows, indoor oxidant concentrations were a strong mediator of secondary pollutant formation following cooking and cleaning activities. Therefore, it follows that the surface materials which influenced secondary pollutant formation the most were also those that had the greatest influence on indoor O_3 concentrations (*i.e.* plastic and soft furnishings). Elevated O_3 concentrations led to more efficient ozonolysis of unsaturated VOC emissions from cooking and cleaning activities, thereby result-

ing in the production of formaldehyde as a secondary product of gas-phase chemistry. Formaldehyde is not effectively destroyed by O_3 due to its lack of C=C bonds, thus elevated O_3 concentrations yielded higher concentrations of formaldehyde (although these are small in an absolute sense). During the cooking and cleaning activities, O_3 concentrations increased slightly as a result of VOC oxidation, resulting in more O_3 deposition onto surfaces. Therefore, additional formaldehyde was produced during activities as a result of multi-phase chemistry, particularly on wooden surfaces, as well as from gas-phase oxidation of VOC emissions.

While OH also contributed to formaldehyde production via VOC oxidation pathways (similar to O_3), the destruction of formaldehyde via OH oxidation resulted in an overall negative correlation between OH concentration and the activity-induced change in formaldehyde concentration. Oxidation of formaldehyde generates HO_2 radicals which subsequently react with NO to regenerate OH radicals, thus further enhancing the observed negative correlation.

Considering both the direct and indirect effects of surface materials on formaldehyde concentration, decreasing the SAV of plastic and soft furnishings (thereby decreasing O_3 deposition) and increasing the SAV of wood (thus increasing formaldehyde emissions from multi-phase chemistry) generally increased formaldehyde formation. For example, kitchens 2, 8 and 9 had low plastic surface areas, no soft furnishings and high wood surface areas, and these were the kitchens where the most formaldehyde ($\approx$ 35 ppt) was formed following activities. However, compared to the background simulations where the average formaldehyde concentration varied by $\approx$ 3 ppb as a result of room surface composition, the difference in activity-induced formaldehyde concentration was only $\approx$ 20 ppt (over 100$\times$ smaller). Overall, this suggests that room material composition is more important to consider in the context of ambient background pollution indoors, rather than for influencing secondary chemistry of sporadic activities like cooking and cleaning.

The positive correlation observed between the background O_3 concentration and activity-induced change in total PANs was less pronounced than that with formaldehyde. For

example, while a 1 ppb increase in background O_3 resulted in a 3.2 ppt increase in formaldehyde, the same increase only enhanced the total concentration of PANs by 2.3 ppt. This is likely because while formaldehyde is generated through both gas-phase and multi-phase chemistry, PAN species are predominantly formed via gas-phase reactions and are not efficiently produced as secondary products of multi-phase chemistry. The relationship between total PANs and OH was the same as for formaldehyde, resulting in a negative correlation.

PANs and organic nitrates are both secondary products of VOC oxidation. However, while total PANs showed variation between the basic kitchen simulations as a result of surface material differences, organic nitrates showed very little variability. This is likely because PANs are formed from RCO_3 radicals, which are primarily a product of aldehyde oxidation, while organic nitrates form from RO_2 radicals, which are more general products of VOC oxidation chemistry. Following O_3 surface deposition, different surface materials yield a number of secondary products, many of which are aldehydes. For example, following O_3 deposition onto plastic, the species with the highest production yields were nonanal, decanal, acetone, formaldehyde, and acetaldehyde. Therefore, while plastic surfaces removed O_3 from the system which may otherwise facilitate gas-phase VOC oxidation chemistry, this process also enhanced surface emissions of aldehydes which can oxidise to RCO_3 radicals, and subsequently form PANs. However, aldehydes do not contribute to the formation of organic nitrates, therefore, aldehyde emissions from multi-phase chemistry did not have a large effect on their formation.

5.3.2.2 Case study: real kitchen SAVs

In addition to the type of surface materials, indoor air chemistry is influenced by the total room volume and surface area. Real-life kitchen environments vary widely in their design, including the size, shape, and material composition, thus resulting in large variability in the total and material-specific SAVs. Therefore, a series of simulations were performed whereby INCHEM-Py was initialised using material-specific SAVs from 9 residential kitchens measured by Manuja et al. (2019), encapsulating

the variability in realistic kitchen environments (Figure 5.5). For these simulations, kitchens 1-9 were ordered based on descending SAV. It was anticipated that, if the total room SAV was the dominant factor influencing species concentration, then decreasing SAV would increase species concentrations due to less surface deposition. As all other model parameters were constant, any deviation from this trend was likely to be a result of variations in the material-specific SAVs of the kitchens.

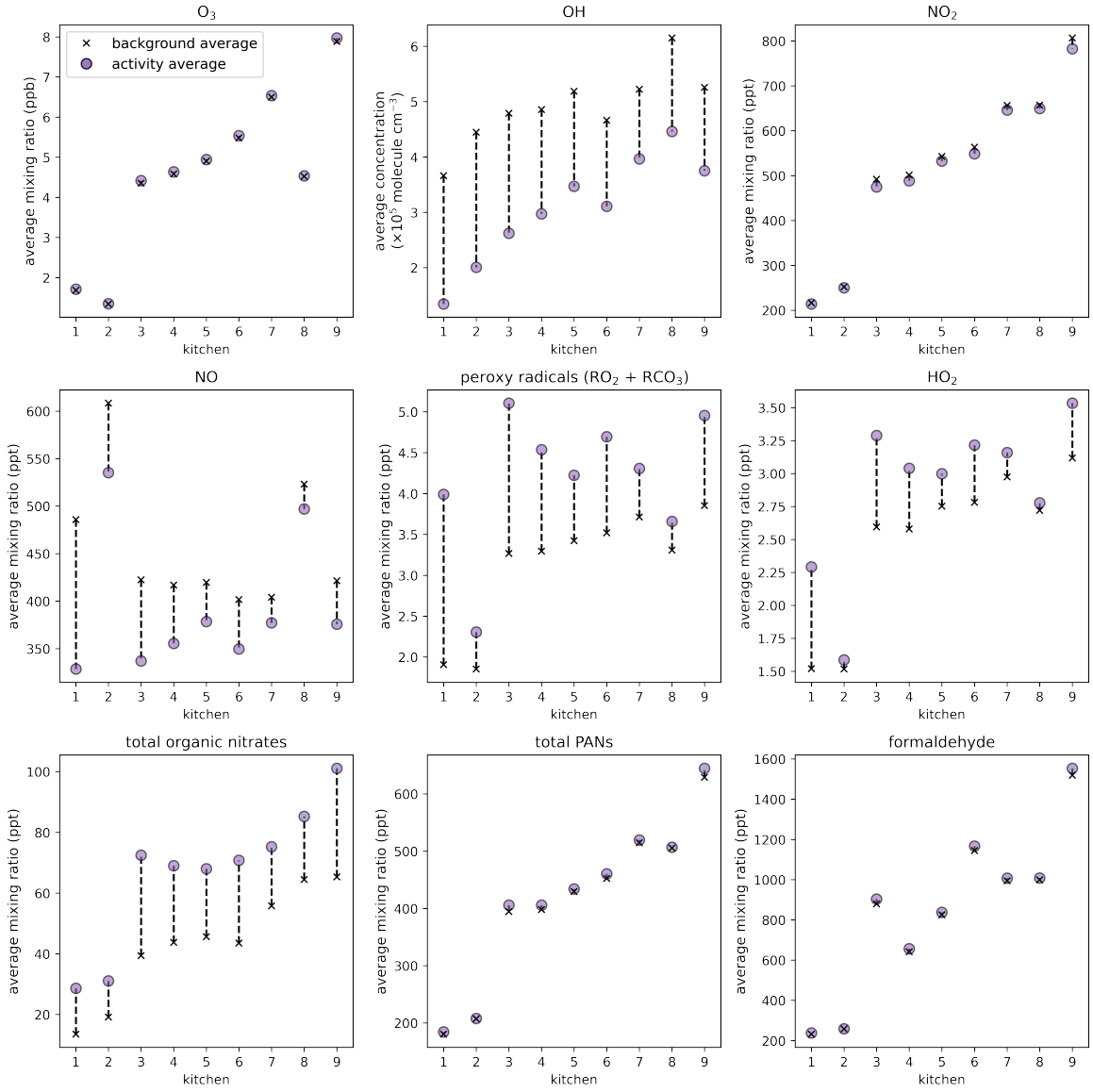

Figure 5.13: Change in average mixing ratios or concentrations of oxidants, intermediate species, and secondary pollutants between baseline and activity simulations when cooking and cleaning are simulated in the 9 kitchens described in Manuja et al. (2019), in order of decreasing total SAV. Averages calculated from t_0 to 5.5h after t_0.

Figure 5.13 shows the average concentrations of key oxidants, intermediate species, and secondary pollutants in the background and activity simulations of the 9 realistic kitchen scenarios. These results show that as the SAV decreased, the average concentration of oxidants, intermediates, and secondary pollutants generally increased. The average O_3 mixing ratio in the 9 kitchens ranged from 1.34 ppb to 7.88 ppb, with (91 $\pm$ 2)% O_3 deposited onto indoor surfaces. The relationship between kitchen SAV and average O_3 mixing ratio was not linear, illustrating the influence of surface materials on oxidant deposition. For example, kitchens 7 and 8 had similar total SAVs of 2.10 and 2.04 m^{-1}, respectively, however, the average background O_3 concentration in kitchen 8 was 2.0 ppb lower than in kitchen 7. Kitchen 8 had the largest SAV of soft furnishings (0.00355 cm^{-1}, surface area = 15.6 m^2), which has a relatively high O_3 deposition velocity. Furthermore, the average background O_3 concentration in kitchen 2 was lower than that of kitchen 1, despite kitchen 1 having a larger total SAV. Over 30% of kitchen 2 SAV was comprised of plastic, which is another surface material which has a high O_3 deposition velocity. Therefore, the presence of soft furnishings and plastic indoor surfaces has a clear impact on background O_3 concentrations as a result of increased removal by surface deposition.

The average background and activity OH concentrations showed less variability between kitchens compared to O_3, as OH is short lived, and is not directly influenced by surface deposition in the model. Kitchens 6 and 9 showed slightly lower OH concentrations than expected based on their SAVs. Kitchen 9 had a lower room volume than kitchens 7 and 8, but a lower overall SAV. The background and activity concentrations of VOCs and radical intermediates were higher in kitchen 9 owing to the lower room volume, resulting in greater consumption of OH radicals by more efficient OH chemistry. This effect also caused the lower OH concentration in kitchen 6 compared to kitchen 5 with a higher total SAV.

The background concentrations of intermediate species and secondary pollutants followed a similar trend to O_3, illustrating the significance of O_3 in driving indoor air chemistry. Higher O_3 concentrations resulted in more efficient removal of NO and

production of NO_2, as a result of the NO + O_3 → NO_2 + O_2 reaction. Additionally, higher O_3 concentrations resulted in more efficient VOC oxidation chemistry, resulting in the formation of RO_2 and HO_2 radical intermediates. Kitchens 2 and 8 showed high background NO concentrations due to the removal of O_3 by surface deposition. Therefore, the peroxy radicals and HO_2 formed from the oxidation of cooking and cleaning VOC emissions reacted more readily with NO, resulting in a relatively small increase in average peroxy radical and HO_2 concentrations between the background and activity simulations of kitchens 2 and 8.

The production of secondary pollutants following cooking and cleaning was dependent on i) the dilution of VOC emissions into the room volume, ii) the availability of indoor oxidants for gas-phase VOC oxidation, and iii) secondary emissions from indoor surfaces following multi-phase chemistry. As demonstrated in the previous section, indoor surfaces do not have a strong influence on the production of organic nitrates following VOC emission events. Figure 5.13 shows that the average background concentration of organic nitrates ranged from 14 to 65 ppt, as a result of differences in background NO and RO_2 concentrations. The increase in concentration observed between the background and post-activity simulations ranged from 11 to 34 ppt, and followed a similar trend to OH radicals. This suggests that the dilution of VOCs due to room volume were the major influencing factor on organic nitrate concentration.

The background and activity concentrations of PANs showed higher variability between kitchens compared to organic nitrates, following a similar pattern to O_3. The formation of PANs was strongly dependent on the concentration of O_3 available for gas-phase VOC oxidation chemistry, thus the influence of material-specific SAVs on O_3 deposition also impacted the concentration of PANs. The concentrations of total PANs in kitchens 2 and 8 were greater than expected given the relatively low O_3 concentration in these kitchens relative to kitchens 1 and 7 with similar SAVs, respectively. This is because with increased O_3 deposition, there was also an increase in aldehyde emissions from multi-phase ozonolysis reactions. Elevated aldehyde concentrations in kitchens 2 and 8 from increased O_3 surface interactions contributed to

the formation of PANs through the production of RCO_3 radicals from surface-derived aldehyde oxidation.

Finally, the average background concentration of formaldehyde varied from 232 to 1515 ppt between kitchens. The total SAV had a significant influence on formaldehyde concentrations. Formaldehyde deposition velocity is approximately three times higher compared to total PANs and organic nitrates. Therefore, variations in total SAV had a more pronounced effect on formaldehyde concentrations. Generally, as the total SAV decreased, average formaldehyde concentrations tended to increase due to reduced surface deposition. There was greater variability in formaldehyde concentration observed between kitchens compared to PANs. This was a result of wood surfaces being a strong source of formaldehyde emissions from multi-phase chemistry. For example, kitchens 3 and 6 had the largest wood SAVs of 0.0116 and 0.0115 cm^{-1}, respectively, and showed higher average formaldehyde concentrations compared to kitchens 4 and 5, which had comparable total SAVs but lower wood SAVs of 0.0053 and 0.0068 cm^{-1}, respectively.

The largest increase in secondary pollutants between the background and activity simulations, and highest absolute concentrations, was observed for kitchen 9, owing to its high O_3 concentration. These results suggest that the effects of kitchen SAVs on the gas-phase concentration of O_3 are most important in determining the production of secondary pollutants following cooking and cleaning activities indoors. Therefore, larger room volume, smaller surface area, and less soft furnishings and plastic surfaces may contribute to higher secondary pollutant concentrations. However, it is also important to consider the primary emissions from these surface materials to get a more holistic view of how surfaces may impact indoor air pollution. For example, while increasing the surface area of plastic in a room may effectively remove O_3 by deposition, and subsequently thwart gas-phase oxidation chemistry, it may also introduce hazardous pollutants as direct emissions from the surface material. Beel et al. (2023) identified plastics as a potentially large source of hazardous VOC emissions, including styrene, toluene, and phenol. Primary VOC emissions from surface materials have not

been considered in this study. It will be important to improve our understanding of the primary and secondary emissions from indoor surfaces, as well as their differential health impacts, to gain insight into how building designs may impact indoor air quality and the resulting impacts on occupant health. This comprehensive understanding is crucial for informing decisions about building design and management practices aimed at promoting healthier indoor environments.

5.4 Chapter summary

This study has highlighted cooking and cleaning activities as potentially large sources of VOC emissions, which have the ability to produce hazardous secondary pollutants as products of indoor air chemistry. Indoor surfaces were shown to impact the gas-phase concentration of oxidants indoors, with consequent effects on the chemical processing of VOC emissions from cooking and cleaning. Plastic surfaces and soft furnishings were the most efficient at removing O_3 by surface deposition, resulting in secondary emissions of aldehyde species. Furthermore, indoor surfaces contributed to the production of hazardous secondary pollutants via multi-phase oxidant interactions. Wood was most efficient at producing formaldehyde as a secondary pollutant from multi-phase ozonolysis reactions. Simulations performed under a range of realistic kitchen SAVs highlighted that higher secondary pollutant concentrations were achieved at lower total SAVs, however, the specific combinations of surface materials also impacted results.

These results illustrate the influence of kitchen surface materials, in addition to the total SAV of the room, on the secondary production of formaldehyde and other potentially hazardous secondary pollutants following cooking and cleaning activities. Therefore, when aiming to enhance indoor air quality and minimise occupant exposure to hazardous pollutants, considerations should be given to room volume, total surface area of contents, and the specific materials used. However, it is worth noting that ventilation remains one of the most effective methods for improving indoor air quality following high-emission occupant activities such as cooking and cleaning. Changing

trends in building designs, such as the adoption of open-plan living arrangements likely resulting in increased room volume and the incorporation of more wood and soft furnishings, are expected to influence the chemical processing of VOC emissions from typical occupant activities within these spaces.

Further research aimed at elucidating the kinetics of VOC and oxidant interactions across a broader range of indoor surface materials would be highly advantageous. Furthermore, it will be important to explore how external factors such as temperature and RH affect heterogeneous chemical reactions, given their variability from room to room and across different climates. It will also be important to consider the contributions of primary VOC emissions from surface materials towards indoor air chemistry, as building materials have been identified as a significant source of VOCs which vary with material age. Developments in our understanding of these aspects of surface effects on indoor air chemistry would facilitate future model developments, thereby enabling more comprehensive modelling investigations.

Chapter 6

Conclusions

6.1 Research gap overview

In developed countries, people spend much of their time indoors, thus highlighting the importance of maintaining good indoor air quality for occupant health and well-being. Among the myriad of factors influencing indoor air quality, the use of cleaning products stands out as a ubiquitous practice aimed at improving cleanliness and hygiene. However, these product formulations often contain a wide range of VOCs, thus posing a potential risk to indoor air quality. Many of these volatile components, added for their fragrance and solvent properties, are susceptible to oxidation, leading to the formation of potentially hazardous secondary products. Consequently, cleaning products have the potential to contribute to poor indoor air quality and cause adverse health effects among occupants.

In recent years, increasing attention has been directed towards understanding the complex interplay between cleaning products and indoor air chemistry. Studies have elucidated the complex chemical reactions occurring between common volatile components and indoor oxidants, shedding light on the impacts of cleaning activities on indoor air quality. Furthermore, investigations have revealed the potential for cleaning products to act as significant sources of VOC emissions, leading to the generation of

secondary pollutants through various chemical pathways.

Despite these advancements, considerable gaps persist in our understanding of the effects of cleaning products on indoor air chemistry. Factors such as the types of cleaning products used, application methods, indoor ventilation rates, and environmental conditions all contribute to the dynamic nature of indoor air chemistry. Furthermore, the interactions between VOCs and indoor surfaces remain a focal point of research, as surface-mediated processes play a crucial role in determining the fate and transformation of VOCs emitted from occupant activities, such as cleaning.

This thesis seeks to address these knowledge gaps by providing a comprehensive investigation into the impacts of cleaning products on indoor air chemistry. Through a combination of experimental measurements, chemical modelling, and data analysis, this thesis aims to elucidate the mechanisms governing the formation of indoor air pollutants resulting from cleaning activities. By examining the influence of various cleaning product formulations, surface materials, and environmental conditions, this thesis provides insights that can inform strategies for mitigating indoor air pollution and safeguarding human health.

6.2 Summary of findings

In Chapter 2 a range of commercially available cleaning products were selected to be the focus of this study. The products were selected based on their categorisation into the four most frequently used product types in domestic households, based on an extensive European survey (Dimitroulopoulou et al., 2015). Among these products, a range of both regular and green cleaners were selected. The purpose of this was to elucidate differences in the VOC emissions and secondary pollutants between products, as green cleaners are perceived to be safer for our health and the environment, despite a lack of regulation surrounding the marketing of products as “green”.

Chapter 3 described a comprehensive analysis of the volatile components of each product using two complimentary headspace analysis techniques. This approach was de-

signed as an efficient screening of the VOCs directly emitted from cleaning product formulations. Dynamic headspace SIFT-MS provided real-time, quantitative analysis of a targeted subset of VOCs, from which the total mass concentrations of VOCs were deduced. Results from this analysis showed that the total measured volatile fraction in the cleaning products ranged from 2.5% to less than 0.1% w/v. Further, non-targeted analysis by equilibrium headspace GC-TOF-MS detected a total of 317 VOCs from the 23 cleaning products, many of which were not listed as product ingredients.

This chapter combined the results from real-time SIFT-MS and high-resolution GC-TOF-MS to speciate the total monoterpene fraction of each product. The results were used to estimate monoterpene emission rates, which were applied to INCHEM-Py to simulate the secondary chemistry. The results revealed that green cleaners generally emitted more monoterpenes than regular cleaners, resulting in larger increases in harmful secondary pollutant concentrations following use, such as formaldehyde (up to 7%) and PAN species (up to 6%). However, emissions of the most reactive monoterpenes (α-terpinene, terpinolene and α-phellandrene), were observed more frequently from regular cleaners, resulting in a disproportionately large impact on the concentrations of radical species and secondary pollutants that were formed after cleaning had occurred. This chapter concluded that both the quantity and chemical reactivity of monoterpene compounds used to provide fragrance for cleaning products are important determinants of secondary pollutant exposure.

The speciation of monoterpene emissions from each cleaner formed the basis of Chapters 4 and 5, which described semi-realistic room scale measurements of VOC emissions from scripted cleaning activities, and subsequent modelling of results. Chapter 4 explored the VOC emissions from 4 representative surface and floor cleaners, including a regular and green product of each class. Real-time measurements revealed that cleaning activities were a source of VOC emissions, with monoterpene emissions dominating the total emitted VOCs from most cleaners (0.66 – 5.95 mg per cleaning event). Model simulations showed that monoterpene emissions produced greater perturbation on indoor air chemistry compared to other emitted VOCs, due to their

relatively high emission rates and reactivity towards oxidants. Monoterpene emissions resulted in elevations in PANs and formaldehyde concentrations of up to 208 and 227 ppt, respectively, in an average kitchen setting.

When considering the composition of monoterpene emissions from cleaning products, model sensitivity studies showed that substitution of the most common terpene, limonene, with isomers that are more reactive towards O_3 (*i.e.* terpinolene, α-terpinene, α-phellandrene), resulted in increases in the concentrations of secondary pollutants formaldehyde and PANs by up to 13% and 23%, respectively. Conversely, when substituted with less reactive monoterpenes (*i.e.* carene, camphene, α/β-pinene), the concentrations of formaldehyde and PANs decreased, although organic nitrates increased by up to 68%. These results demonstrate that while substitution of fragrance ingredients in cleaning product formulations may reduce occupant exposure to certain hazardous secondary pollutants, it may inadvertently lead to increased exposure to others. Further research will be required to improve our knowledge of the differential health effects of indoor air pollutants, thus providing insight into how such changes may impact occupant health.

Chapter 4 also explored the impacts of various environmental factors on indoor air chemistry following cleaning. These results revealed that higher indoor SAV and higher occupancy levels enhanced O_3 deposition, thus reducing the overall oxidative capacity of the indoor environment. Conversely, higher ACR and more polluted outdoor air significantly impacts the availability of indoor oxidants to chemically process cleaning VOC emissions, generating hazardous secondary pollutants. These results emphasise the importance of outdoor pollution levels on indoor pollutant concentrations. Therefore, regulating both indoor and outdoor pollution sources is essential for effectively enhancing indoor air quality.

Finally, Chapter 5 presented VOC measurements from scripted cooking and cleaning experiments performed in an experimental room built to current UK building standards. This study provided measurements in a more realistic indoor setting compared to those obtained in Chapter 4, with lower background VOC emissions from building

materials and lower outdoor pollution levels. This study focussed on a single cooking and cleaning activity, allowing the repeatability of such semi-realistic indoor air experiments to be evaluated. Results showed reasonable agreement between repeats, despite natural variability in environmental conditions.

Modelling of the cooking and cleaning VOC emissions in a basic kitchen scenario, where the surface materials of individual kitchen components were randomly varied, allowed the influence of surfaces on indoor air chemistry to be evaluated. Results from this study showed that soft furnishings and plastic surfaces were most effective at removing O_3 from the indoor environment by surface deposition, thus limiting gas-phase oxidation of VOC emissions from cooking and cleaning activities. However, multi-phase ozonolysis of VOCs resulted in emissions of a range of aldehyde species, thus contributing to the gas-phase concentration of potentially hazardous pollutants. Furthermore, elevated aldehyde concentrations contributed to the formation of PAN species through oxidation chemistry. Wood surfaces were identified as the most efficient producers of formaldehyde following oxidant deposition onto this material.

Subsequent model simulations using real-world kitchen SAVs revealed that a lower SAV resulted in higher pollutant concentrations following cooking and cleaning activities, although the specific combinations of surface materials influenced results. This observation will be important when designing kitchens for better indoor air quality, as the room volume, amount of contents, and material composition of surfaces will impact the chemical processing of VOC emissions from frequent, highly polluting, occupant activities in these spaces.

6.3 Future perspectives

The growing awareness among consumers regarding the environmental and health implications of household products has led to an increased demand for green cleaners. However, as this research and others have shown, green cleaners contribute equally, if not more, to indoor air pollution compared to conventional cleaners. Furthermore, there is limited transparency regarding the ingredients used in household cleaning

products, leading to ambiguity about their potential impacts on indoor air quality and human exposure to air pollutants. In the EU, cleaning products are controlled under regulations such as the Classification, Labeling, and Packaging (CLP) Regulation, which provide a framework for classifying and labelling hazardous chemicals. However, these regulations may not adequately address indoor air quality concerns due to a lack of information surrounding the environmental and health effects of pollutants from cleaning. Clearly, there is a need for regulations that prioritise inhalation exposure to both primary and secondary pollutants, particularly from fragrance ingredients, which are prevalent in many cleaning products.

While some eco-labels exist to provide consumers with assurance of adherence to environmental, safety and performance standards, these certifications are often optional, and greenwashing remains a common issue. Furthermore, there is currently no green cleaning certification that addresses the specific issue of indoor air pollution from cleaning activities. To address these challenges, further research is essential. Studying the impacts of cleaning products in real-life scenarios will be crucial for developing a foundational understanding necessary for the creation of effective green cleaning certifications. Additionally, more precise evaluation of the health effects associated with primary and secondary indoor air pollutants from cleaning activities will be vital for informing consumers of potential health risks and guiding them towards safer product choices.

This thesis highlights the potential differences in VOC emissions from products with different formulations and application modes. To thoroughly assess occupant exposure to VOC pollutants during domestic cleaning activities using the diverse range of products available on the market, it will be essential to test a wider variety of products. While numerous studies have examined VOC emissions from different cleaning products in various experimental setups, the lack of consistency in experimental approaches hinders meaningful comparisons between studies. Hence, establishing standardised experimental methodologies for measuring the VOC emissions from cleaning activities would be highly beneficial. This would allow a wide range of cleaning products to be

studied under comparable conditions, such as bleach, non-bleach, and corrosive products (e.g. drain cleaner). These results could be used, along with detailed product use information, to build up a better picture of occupant exposure to indoor air pollution and the potential health implications. Further, these results could aid the development of emissions inventories, allowing more accurate depiction of VOC emissions and aiding the development of air quality regulation in the UK.

This research has identified possible modifications which could be made to cleaning product formulation composition and indoor surfaces to minimise the production of hazardous secondary pollutants through the implementation of a detailed chemical model. Collaboration with the fragrance industry would be required to develop fragranced household products which retain cleaning efficacy and pleasant odour, while also reducing their impact on indoor air pollution. Further experimental investigations could be carried out to refine models such as INCHEM-Py, thus improving their ability to represent the complexities of indoor air chemistry. For instance, kinetic and mechanistic studies to explicitly define the reaction pathways of pertinent compounds, particularly unsaturated fragrance compounds commonly found indoors following household cleaning and personal care product use, would be highly beneficial. Validating model outcomes through experimental studies is crucial for enhancing result reliability, especially concerning the complex interactions of terpene mixes in indoor air chemistry. Furthermore, experimental data on the deposition, multi-phase chemistry, and emission of species from a broader range of indoor surfaces will be critical for improving surface representation in indoor chemical models.

There is currently a lack of awareness concerning indoor air quality issues, as research and evidence-based policies trail behind those addressing outdoor air quality. It is evident that more research effort is necessary to develop our understanding of the sources and fate of indoor air pollutants, their potential health risks, and strategies to mitigate indoor air pollution. Future advancements in building design should prioritise not only reducing initial emissions from building materials but also considering their long-term effects on indoor air chemistry via multi-phase interactions. This is particularly im-

portant to consider in environments such as kitchens, where high emission events such as cooking and cleaning occur frequently, thereby increasing the presence of VOCs that can transform into hazardous secondary pollutants through oxidation. Given the evolving climate and the possibility of global pandemics, understanding how shifts in occupant behaviour and environmental conditions might influence indoor air quality is imperative. For instance, in the possible event of future pandemics akin to COVID-19, it would be beneficial to explore the implications of increased disinfectant usage and lockdown measures on indoor air pollutant exposure. Moreover, with climate change altering outdoor air quality, assessing its impact on indoor air quality through factors such as air infiltration, modifications in building structures and human behaviour, and variations in indoor temperature and humidity becomes vital. All these elements have the potential to influence indoor air chemistry, resulting in heightened exposure to hazardous air pollutants.

Appendix A

INCHEM-Py Custom Reaction Schemes

The custom reaction schemes developed for this PhD are summarised in Tables A.1 (dihydromyrcenol), A.2 (α-phellandrene), A.3 (α-terpinolene), and A.4 (terpinolene). Each custom scheme has been developed as per Section 2.3.2.3, using oxidation kinetics data available in the literature to define the initial oxidation steps, and then mapping reaction products onto existing species in the MCM.

For a full explanation of the custom reaction schemes, see the files located within the model directory INCHEM-Py/shemes, available from:
https://github.com/DrDaveShaw/INCHEM-Py.git.

Table A.1: Custom gas-phase oxidation reaction scheme for dihydromyrcenol used in INCHEM-Py.

Reaction	Reaction rate coefficient (cm^3 $molecule^{-1}$ s^{-1})
DHMOL + OH $\longrightarrow$ DHMOLO2	$0.12 \times 3.8 \times 10^{-12}$
DHMOLO2 + NO $\longrightarrow$ DHMOLO + NO_2	KRO2NO $\times$ 0.772
DHMOLO2 + NO $\longrightarrow$ DHMOLNO3	KRO2NO $\times$ 0.228
DHMOLO2 + NO_3 $\longrightarrow$ DHMOLO + NO_2	KRO2NO3
DHMOLO2 + HO_2 $\longrightarrow$ DHMOLOOH	KRO2HO2 $\times$ 0.914
DHMOLO2 $\longrightarrow$ DHMOLO	$9.20 \times 10^{-14} \times RO_2 \times 0.7$
DHMOLO2 $\longrightarrow$ DHMOLOH	$9.20 \times 10^{-14} \times RO_2 \times 0.3$
DHMOLOOH + OH $\longrightarrow$ DHMOLO2	7.36×10^{-11}
DHMOLOOH $\longrightarrow$ DHMOLO + OH	J41
DHMOLNO3 + OH $\longrightarrow$ C6DICARB + NO_2	6.20×10^{-11}
DHMOLO $\longrightarrow$ C6DICARB + TBUTOLO2	KDEC
DHMOLOH + OH $\longrightarrow$ CDDICARB + HO_2	7.02×10^{-11}
DHMOL + OH $\longrightarrow$ C813O2	$0.71 \times 3.8 \times 10^{-12}$
DHMOL + O_3 $\longrightarrow$ CH3CCH3OOA + C6DICARB	$2 \times 10^{-18} \times 0.8$
DHMOL + O_3 $\longrightarrow$ LINALOOB	$2 \times 10^{-18} \times 0.2$
DHMOL + NO_3 $\longrightarrow$ DHMOLO2	2.3×10^{-14}

Table A.2: Custom gas-phase oxidation reaction scheme for α-phellandrene used in INCHEM-Py.

Reaction	Reaction rate coefficient (cm^3 $molecule^{-1}$ s^{-1})
$APHEL + O_3 \longrightarrow APHELOOA$	$2.9 \times 10^{-15} \times 0.73$
$APHEL + O_3 \longrightarrow APHELOOB$	$2.9 \times 10^{-15} \times 0.27$
$APHELOOA \longrightarrow LIMALAO2 + LIMALBO2$	$KDEC \times 0.5$
$APHELOOA \longrightarrow OH$	$KDEC \times 0.44$
$APHELOOA \longrightarrow$	$KDEC \times 0.06$
$APHELOOB \longrightarrow C92302 + CO$	$KDEC \times 0.5$
$APHELOOB \longrightarrow LIMBOO$	$KDEC \times 0.5$
$APHEL + OH \longrightarrow APHELAO2$	$3.2 \times 10^{-10} \times 0.73$
$APHEL + OH \longrightarrow APHELBO2$	$3.2 \times 10^{-10} \times 0.27$
$APHELAO2 + HO_2 \longrightarrow LIMAOOH$	$KRO2HO2 \times 0.914$
$APHELAO2 + NO \longrightarrow LIMANO3$	$KRO2NO \times 0.228$
$APHELAO2 + NO \longrightarrow LIMAO + NO_2$	$KRO2NO \times 0.772$
$APHELAO2 + NO_3 \longrightarrow LIMAO + NO_2$	KRO2NO3
$APHELAO2 \longrightarrow LIMAO$	$9.20 \times 10^{-14} \times RO_2 \times 0.7$
$APHELAO2 \longrightarrow LIMAOH$	$9.20 \times 10^{-14} \times RO_2 \times 0.3$
$APHELBO2 + HO_2 \longrightarrow PHIC3OOH$	$KRO2HO2 \times 0.890$
$APHELBO2 + NO \longrightarrow PHIC3NO3$	$KRO2NO \times 0.118$
$APHELBO2 + NO \longrightarrow PHIC3O + NO_2$	$KRO2NO \times 0.882$
$APHELBO2 + NO_3 \longrightarrow PHIC3O + NO_2$	KRO2NO3
$APHELBO2 \longrightarrow PHIC3O$	$6.70 \times 10^{-15} \times RO_2 \times 0.7$
$APHELBO2 \longrightarrow PHIC3OH$	$6.70 \times 10^{-15} \times RO_2 \times 0.3$
$APHEL + NO_3 \longrightarrow NAPHELO2$	7.3×10^{-11}
$NAPHELO2 + HO_2 \longrightarrow NLIMOOH$	$KRO2HO2 \times 0.914$
$NAPHELO2 + NO \longrightarrow NLIMO + NO_2$	KRO2NO
$NAPHELO2 + NO_3 \longrightarrow NLIMO + NO_2$	KRO2NO3
$NAPHELO2 \longrightarrow LIMBNO3$	$9.20 \times 10^{-14} \times RO_2 \times 0.3$
$NAPHELO2 \longrightarrow NLIMO$	$9.20 \times 10^{-14} \times RO_2 \times 0.7$

Table A.3: Custom gas-phase oxidation reaction scheme for α-terpinene used in INCHEM-Py.

Reaction	Reaction rate coefficient (cm^3 $molecule^{-1}$ s^{-1})
ATERPINENE + O_3 $\longrightarrow$ ATERPOOA	$1.9 \times 10^{-14} \times 0.73$
ATERPINENE + O_3 $\longrightarrow$ ATERPOOB	$1.9 \times 10^{-14} \times 0.27$
ATERPOOA $\longrightarrow$ LIMALAO2 + LIMALBO2	KDEC $\times$ 0.5
ATERPOOA $\longrightarrow$ OH	KDEC $\times$ 0.4
ATERPOOA $\longrightarrow$	KDEC $\times$ 0.1
ATERPOOB $\longrightarrow$ C92302 + CO	KDEC $\times$ 0.5
ATERPOOB $\longrightarrow$ LIMBOO	KDEC $\times$ 0.5
ATERPINENE + OH $\longrightarrow$ ATERPAO2	$3.5 \times 10^{-10} \times 0.7$
ATERPINENE + OH $\longrightarrow$ ATERPBO2	$3.5 \times 10^{-10} \times 0.3$
ATERPAO2 + HO_2 $\longrightarrow$ LIMAOOH	KRO2HO2 $\times$ 0.914
ATERPAO2 + NO $\longrightarrow$ LIMANO3	KRO2NO $\times$ 0.228
ATERPAO2 + NO $\longrightarrow$ LIMAO + NO_2	KRO2NO $\times$ 0.772
ATERPAO2 + NO_3 $\longrightarrow$ LIMAO + NO_2	KRO2NO3
ATERPAO2 $\longrightarrow$ LIMAO	$9.20 \times 10^{-14} \times RO_2 \times 0.7$
ATERPAO2 $\longrightarrow$ LIMAOH	$9.20 \times 10^{-14} \times RO_2 \times 0.3$
ATERPBO2 + HO_2 $\longrightarrow$ PHIC3OOH	KRO2HO2 $\times$ 0.890
ATERPBO2 + NO $\longrightarrow$ PHIC3NO3	KRO2NO $\times$ 0.118
ATERPBO2 + NO $\longrightarrow$ PHIC3O + NO_2	KRO2NO $\times$ 0.882
ATERPBO2 + NO_3 $\longrightarrow$ PHIC3O + NO_2	KRO2NO3
ATERPBO2 $\longrightarrow$ PHIC3O	$6.70 \times 10^{-15} \times RO_2 \times 0.7$
ATERPBO2 $\longrightarrow$ PHIC3OH	$6.70 \times 10^{-15} \times RO_2 \times 0.3$
ATERPINENE + NO_3 $\longrightarrow$ NATERPO2	1.8×10^{-10}
NATERPO2 + HO_2 $\longrightarrow$ NLIMOOH	KRO2HO2 $\times$ 0.914
NATERPO2 + NO $\longrightarrow$ NLIMO + NO_2	KRO2NO
NATERPO2 + NO_3 $\longrightarrow$ NLIMO + NO_2	KRO2NO3
NATERPO2 $\longrightarrow$ LIMBNO3	$9.20 \times 10^{-14} \times RO_2 \times 0.3$
NATERPO2 $\longrightarrow$ NLIMO	$9.20 \times 10^{-14} \times RO_2 \times 0.7$

Table A.4: Custom gas-phase oxidation reaction scheme for terpinolene used in INCHEM-Py.

Reaction	Reaction rate coefficient (cm^3 $molecule^{-1}$ s^{-1})
TERPINOLENE + O_3 $\longrightarrow$ CH3CCH3OOC + CYHEXONE	$1.6 \times 10^{-15} \times 0.5$
TERPINOLENE + O_3 $\longrightarrow$ PHCHOOA + CH_3COCH_3	$1.6 \times 10^{-15} \times 0.5$
TERPINOLENE + OH $\longrightarrow$ TERPINOLENEAO2	2.2×10^{-10}
TERPINOLENEAO2 + HO_2 $\longrightarrow$ LIMAOOH	KRO2HO2 $\times$ 0.914
TERPINOLENEAO2 + NO $\longrightarrow$ LIMANO3	KRO2NO $\times$ 0.228
TERPINOLENEAO2 + NO $\longrightarrow$ LIMAO + NO_2	KRO2NO $\times$ 0.772
TERPINOLENEAO2 + NO_3 $\longrightarrow$ LIMAO + NO_2	KRO2NO3
TERPINOLENEAO2 $\longrightarrow$ LIMAO	$9.20 \times 10^{-14} \times RO_2 \times 0.7$
ATERPAO2 $\longrightarrow$ LIMAOH	$9.20 \times 10^{-14} \times RO_2 \times 0.3$
TERPINOLENE + NO_3 $\longrightarrow$ NTERPINOLENEO2	9.7×10^{-11}
NTERPINOLENEO2 + HO_2 $\longrightarrow$ NLIMOOH	KRO2HO2 $\times$ 0.914
NTERPINOLENEO2 + NO $\longrightarrow$ NLIMO + NO_2	KRO2NO
NTERPINOLENEO2 + NO_3 $\longrightarrow$ NLIMO + NO_2	KRO2NO3
NTERPINOLENEO2 $\longrightarrow$ LIMBNO3	$9.20 \times 10^{-14} \times RO_2 \times 0.3$
NTERPINOLENEO2 $\longrightarrow$ NLIMO	$9.20 \times 10^{-14} \times RO_2 \times 0.7$

Appendix B

Supplementary Information for Chapter 4

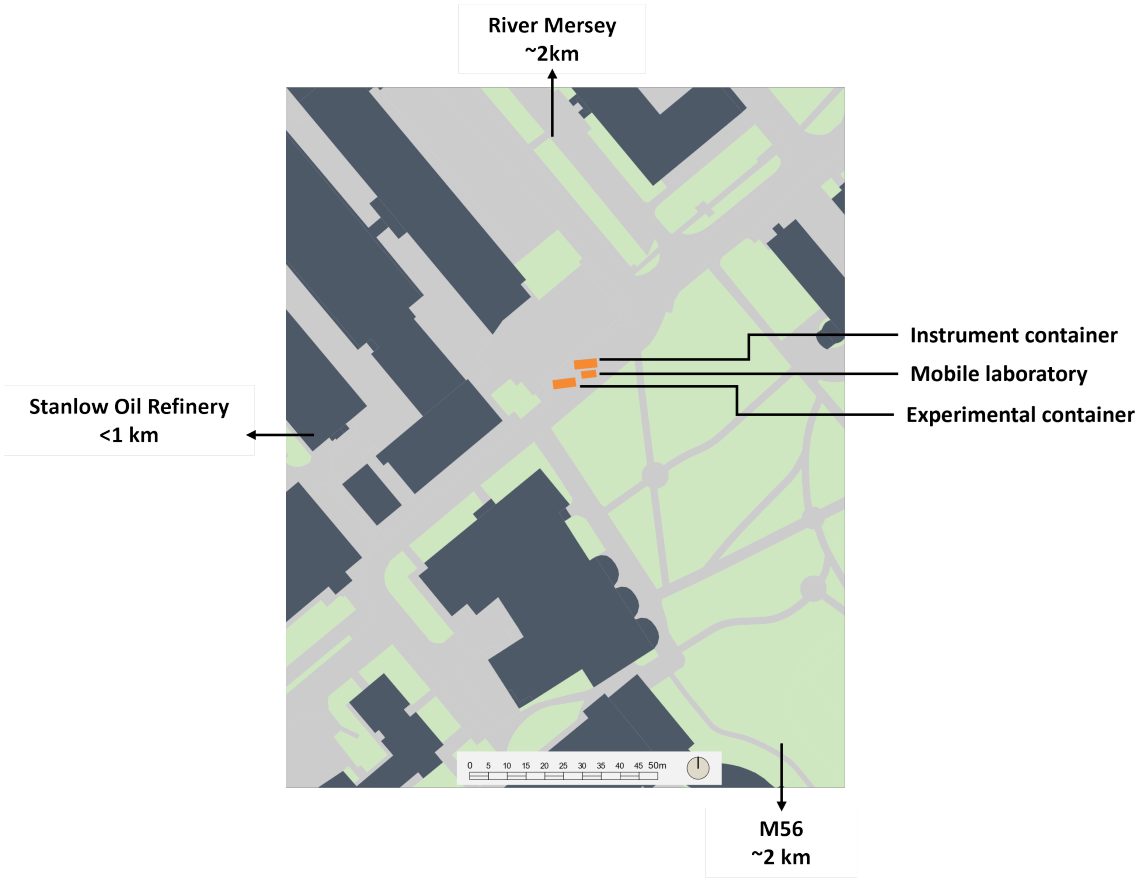

Figure B.1: Schematic of the location of the DOMESTIC facility with respect to local landmarks and potential sources of air pollution.

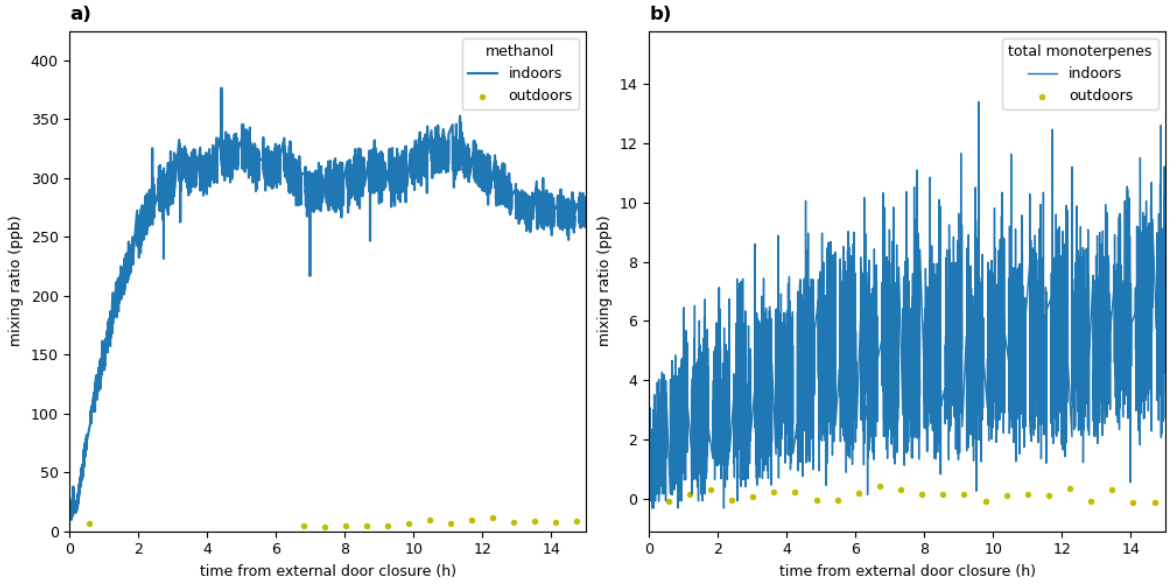

Figure B.2: Indoor (blue line) and outdoor (yellow point) mixing ratios of a) methanol, and b) total monoterpenes measured by SIFT-MS during a background experimental day, when no activities occurred indoors.

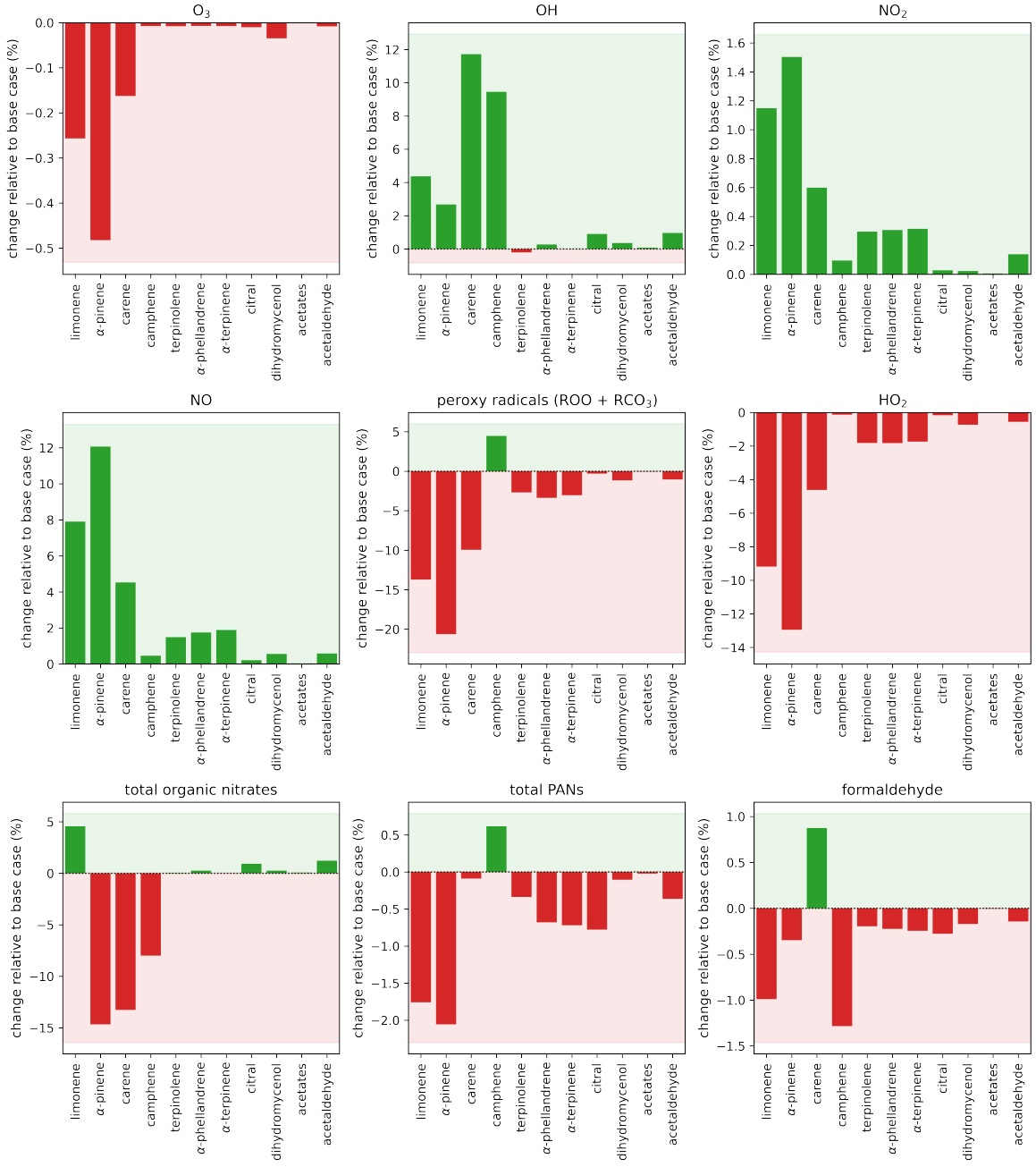

Figure B.3: Percentage change in average concentrations of oxidants, radicals and secondary species following cleaning with SR1 when individual VOC emissions are omitted compared to the base case simulation. The omitted VOC emission is given as the x-axis bar labels. Positive changes compared to the base case simulation (including all VOC emissions) is shown in green, while negative changes are shown in red. Average species concentrations are calculated from t_0 to 5.5 h after t_0.

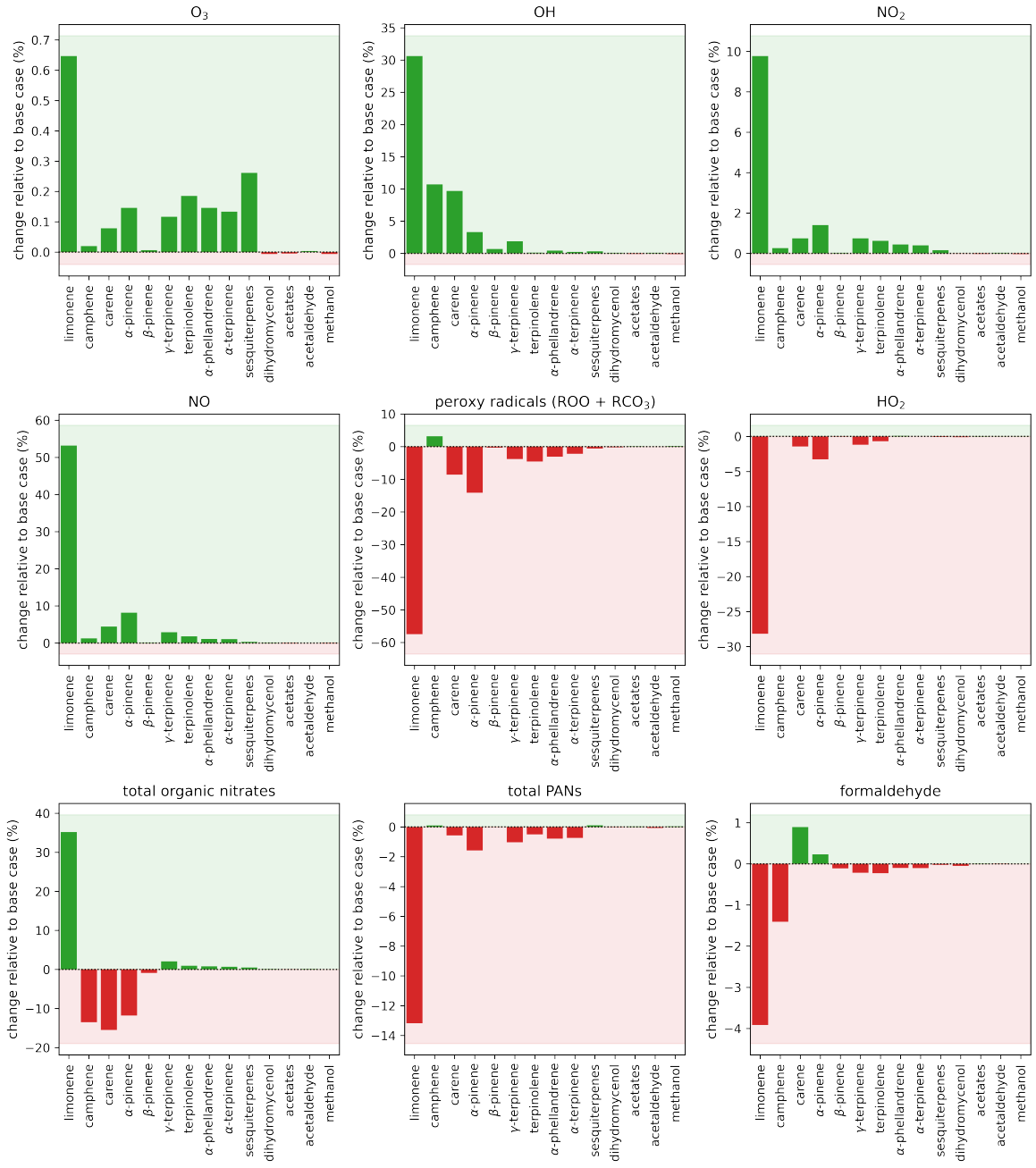

Figure B.4: Percentage change in average concentrations of oxidants, radicals and secondary species following cleaning with SG2 when individual VOC emissions are omitted compared to the base case simulation. The omitted VOC emission is given as the x-axis bar labels. Positive changes compared to the base case simulation (including all VOC emissions) is shown in green, while negative changes are shown in red. Average species concentrations are calculated from t_0 to 5.5 h after t_0.

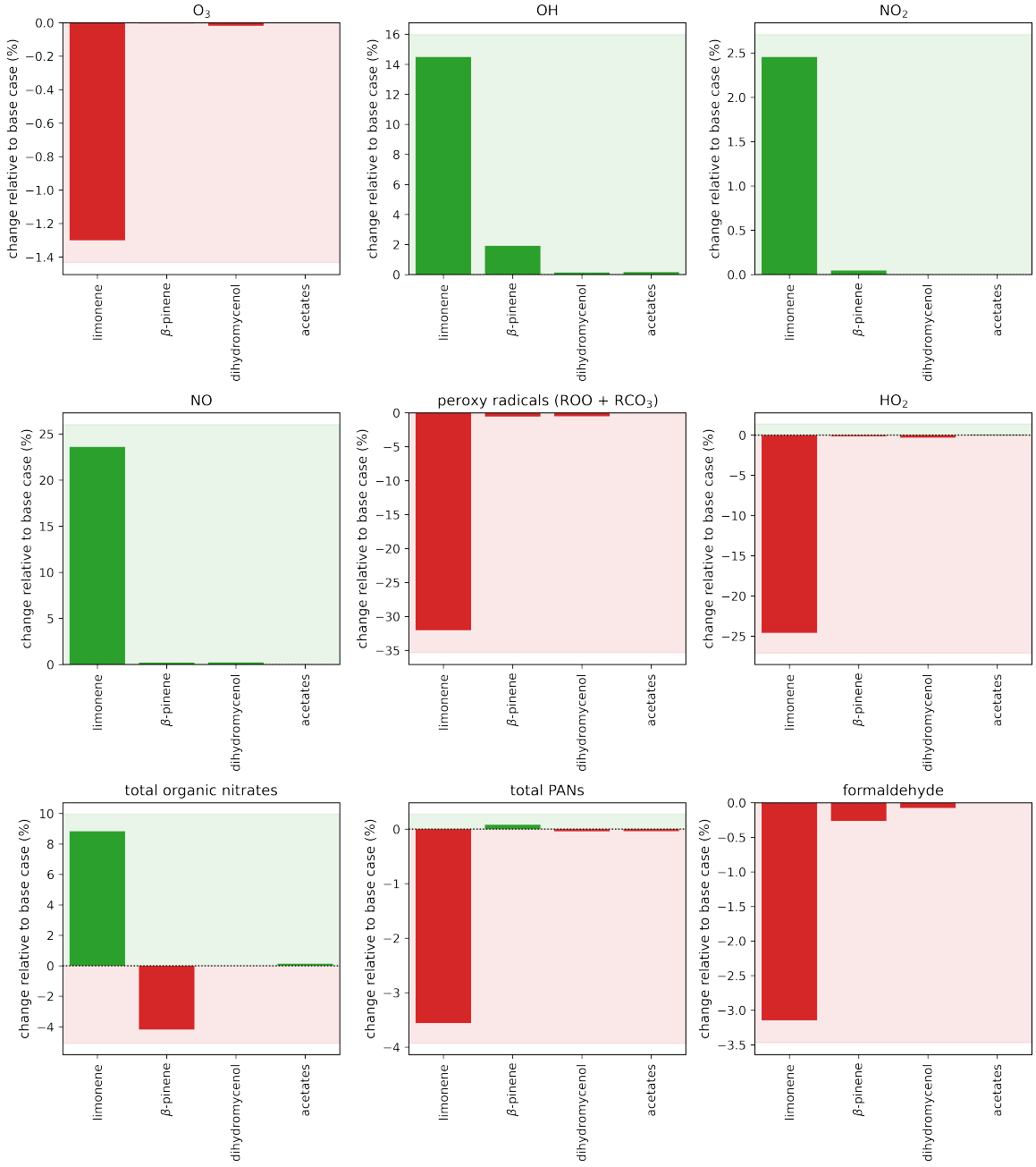

Figure B.5: Percentage change in average concentrations of oxidants, radicals and secondary species following cleaning with FR1 when individual VOC emissions are omitted compared to the base case simulation. The omitted VOC emission is given as the x-axis bar labels. Positive changes compared to the base case simulation (including all VOC emissions) is shown in green, while negative changes are shown in red. Average species concentrations are calculated from t_0 to 5.5 h after t_0.

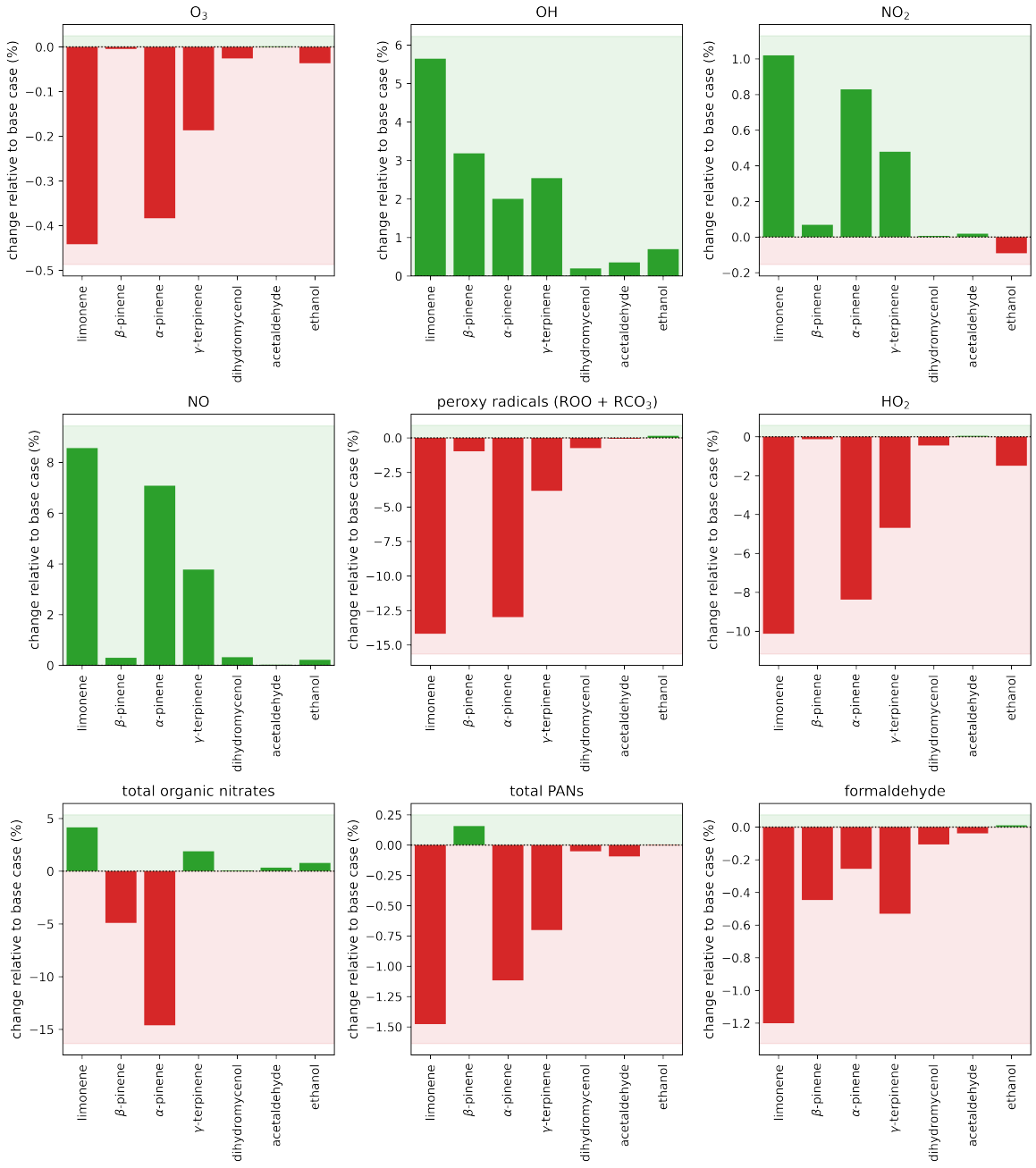

Figure B.6: Percentage change in average concentrations of oxidants, radicals and secondary species following cleaning with FG2 when individual VOC emissions are omitted compared to the base case simulation. The omitted VOC emission is given as the x-axis bar labels. Positive changes compared to the base case simulation (including all VOC emissions) is shown in green, while negative changes are shown in red. Average species concentrations are calculated from t_0 to 5.5 h after t_0.

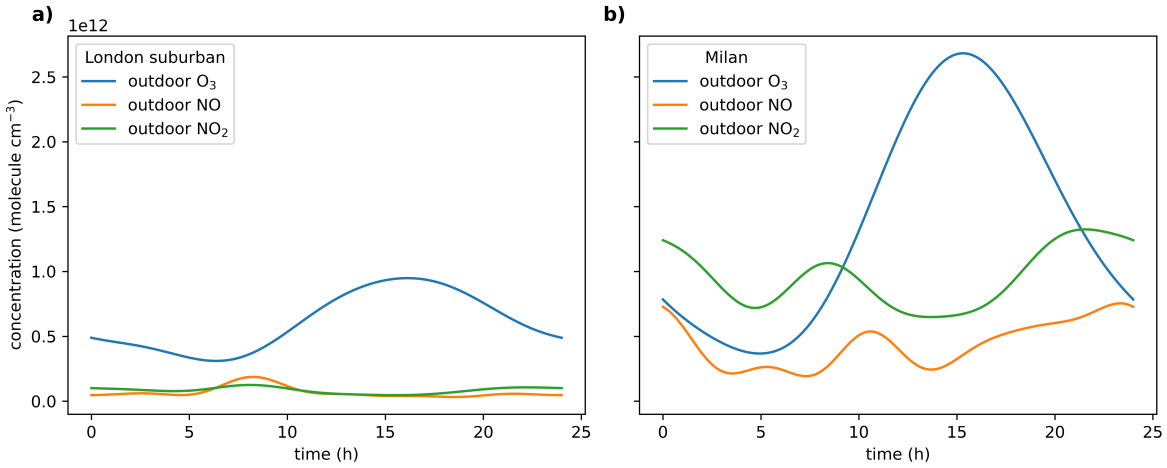

Figure B.7: Outdoor average concentration fits for a) GB0586A, suburban London, Q3 2018, and b) a two week period in Milan in August 2003 (Terry et al., 2014).

List of References

Abbatt, J. P. and Wang, C. (2020), 'The atmospheric chemistry of indoor environments', *Environmental Science: Processes & Impacts* **22**, 25–48.

Abdullahi, K. L., Delgado-Saborit, J. M. and Harrison, R. M. (2013), 'Emissions and indoor concentrations of particulate matter and its specific chemical components from cooking: A review', *Atmospheric Environment* **71**, 260–294.

Abe, K., Hori, Y. and Myoda, T. (2019), 'Volatile compounds of fresh and processed garlic (review)', *Experimental and Therapeutic Medicine* **19**, 1585–1593.

Adamová, T., Hradecký, J. and Pánek, M. (2020), 'Volatile organic compounds (VOCs) from wood and wood-based panels: Methods for evaluation, potential health risks, and mitigation', *Polymers* **12**(10), 1–21.

Altshuller, A. P. (1978), 'Assessment of the contribution of chemical species to the eye irritation potential of photochemical smog', *Journal of the Air Pollution Control Association* **28**(6), 594–598.

American Chemistry Council (2023), 'Ammonia'. Accessed: 2024-04.
URL: *https://www.chemicalsafetyfacts.org/chemicals/ammonia/*

Angulo Milhem, S., Verriele, M., Nicolas, M. and Thevenet, F. (2021), 'Indoor use of essential oil-based cleaning products: Emission rate and indoor air quality impact assessment based on a realistic application methodology', *Atmospheric Environment* **246**.

Arata, C., Misztal, P. K., Tian, Y., Lunderberg, D. M., Kristensen, K., Novoselac, A., Vance, M. E., Farmer, D. K., Nazaroff, W. W. and Goldstein, A. H. (2021), 'Volatile organic compound emissions during HOMEChem', *Indoor Air* **31**(6), 2099–2117.

Atkinson, R. (1987), 'A structure-activity relationship for the estimation of rate constants for the gas-phase reactions of oh radicals with organic compounds', *International Journal of Chemical Kinetics* **19**, 799–828.

Atkinson, R. and Arey, J. (2003), 'Gas-phase tropospheric chemistry of biogenic volatile organic compounds: A review', *Atmospheric Environment* **37**(2), 197–219.

Atkinson, R., Aschmann, S. M. and Arey, J. (1990), 'Rate constants for the gas-phase reactions of OH and NO3 radicals and O3 with sabinene and camphene at 296±2 K', *Atmospheric Environment. Part A. General Topics* **24**(10), 2647–2654.

Audignon-Durand, S., Ramalho, O., Mandin, C., Roudil, A., Bihan, O. L., Delva, F. and Lacourt, A. (2023), 'Indoor exposure to ultrafine particles related to domestic activities: A systematic review and meta-analysis', *Science of The Total Environment* **904**, 166947.

Ault, A. P., Grassian, V. H., Carslaw, N., Collins, D. B., Destaillats, H., Donaldson, D. J., Farmer, D. K., Jimenez, J. L., McNeill, V. F., Morrison, G. C., O'Brien, R. E., Shiraiwa, M., Vance, M. E., Wells, J. R. and Xiong, W. (2020), 'Indoor Surface Chemistry: Developing a Molecular Picture of Reactions on Indoor Interfaces', *Chem* **6**(12), 3203–3218.

Bari, M. A., Kindzierski, W. B., Wheeler, A. J., Héroux, M.-È. and Wallace, L. A. (2015), 'Source apportionment of indoor and outdoor volatile organic compounds at homes in Edmonton, Canada', *Building and Environment* **90**, 114–124.

Bearth, A., Miesler, L. and Siegrist, M. (2017), 'Consumers' Risk Perception of Household Cleaning and Washing Products', *Risk Analysis* **37**(4), 647–660.

Beel, G., Langford, B., Carslaw, N., Shaw, D. and Cowan, N. (2023), 'Temperature driven variations in voc emissions from plastic products and their fate indoors:

A chamber experiment and modelling study', *Science of The Total Environment* **881**, 163497.

Bello, A., Quinn, M. M., Perry, M. J. and Milton, D. K. (2010), 'Quantitative assessment of airborne exposures generated during common cleaning tasks: a pilot study', *Environmental Health* **9**(1), 76.

Berkemeier, T., Ammann, M., Mentel, T. F., Pöschl, U. and Shiraiwa, M. (2016), 'Organic Nitrate Contribution to New Particle Formation and Growth in Secondary Organic Aerosols from α-Pinene Ozonolysis', *Environmental Science and Technology* **50**(12), 6334–6342.

Bhore, S. J. (2016), 'Paris agreement on climate change: A booster to enable sustainable global development and beyond', *International Journal of Environmental Research and Public Health* **13**(11).

Blocquet, M., Guo, F., Mendez, M., Ward, M., Coudert, S., Batut, S., Hecquet, C., Blond, N., Fittschen, C. and Schoemaecker, C. (2018), 'Impact of the spectral and spatial properties of natural light on indoor gas-phase chemistry: Experimental and modeling study', *Indoor Air* **28**(3), 426–440.

Brown, S. K. (2002), 'Volatile organic pollutants in new and established buildings in melbourne, australia', *Indoor Air* **12**(1), 55–63.

Brown, V. M., Crump, D. R. and Harrison, P. T. C. (2013), 'Assessing and controlling risks from the emission of organic chemicals from construction products into indoor environments', *Environmental Science: Processes & Impacts* **15**(12), 2164–2177.

Buchanan, I. S. H., Mendell, M. J., Mirer, A. G. and Apte, M. G. (2008), 'Air filter materials, outdoor ozone and building-related symptoms in the BASE study', *Indoor Air* **18**(2), 144–155.

Calderon, L., Maddalena, R., Russell, M., Chen, S., Nolan, J. E., Bradman, A. and Harley, K. G. (2022), 'Air concentrations of volatile organic compounds associated

with conventional and "green" cleaning products in real-world and laboratory settings', *Indoor Air* **32**(11), e13162.

Carslaw, N. (2007), 'A new detailed chemical model for indoor air pollution', *Atmospheric Environment* **41**(6), 1164–1179.

Carslaw, N. (2013), 'A mechanistic study of limonene oxidation products and pathways following cleaning activities', *Atmospheric Environment* **80**, 507–513.

Carslaw, N., Fletcher, L., Heard, D., Ingham, T. and Walker, H. (2017), 'Significant OH production under surface cleaning and air cleaning conditions: Impact on indoor air quality', *Indoor Air* **27**(6), 1091–1100.

Carslaw, N., Mota, T., Jenkin, M. E., Barley, M. H. and McFiggans, G. (2012), 'A Significant role for nitrate and peroxide groups on indoor secondary organic aerosol', *Environmental Science and Technology* **46**(17), 9290–9298.

Carslaw, N. and Shaw, D. (2022), 'Modification of cleaning product formulations could improve indoor air quality', *Indoor Air* **32**(3), e13021.

Carter, T. J., Poppendieck, D. G., Shaw, D. and Carslaw, N. (2023), 'A Modelling Study of Indoor Air Chemistry: The Surface Interactions of Ozone and Hydrogen Peroxide', *Atmospheric Environment* **297**, 119598.

Cheng, Y.-H., Lin, C.-C. and Hsu, S.-C. (2015), 'Comparison of conventional and green building materials in respect of voc emissions and ozone impact on secondary carbonyl emissions', *Building and Environment* **87**, 274–282.

Christianson, D. W. (2017), 'Structural and Chemical Biology of Terpenoid Cyclases', *Chemical Reviews* **117**(17), 11570–11648.

Cincinelli, A. and Martellini, T. (2017), 'Indoor Air Quality and Health', *International Journal of Environmental Research and Public Health* **14**(11).

Coeli Mendonça, E. M., Algranti, E., De Freitas, J. B. P., Rosa, E. A., Dos Santos Freire, J. A., Santos, U. d. P., Pinto, J. and Bussacos, M. A. (2003), 'Occupa-

tional asthma in the City of São Paulo, 1995-2000, with special reference to gender analysis', *American Journal of Industrial Medicine* **43**(6), 611–617.

Davies, H. L., O'Leary, C., Dillon, T., Shaw, D. R., Shaw, M., Mehra, A., Phillips, G. and Carslaw, N. (2023), 'A measurement and modelling investigation of the indoor air chemistry following cooking activities', *Environmental Science: Processes & Impacts* **25**(9), 1532–1548.

de Lacy Costello, B., Amann, A., Al-Kateb, H., Flynn, C., Filipiak, W., Khalid, T., Osborne, D. and Ratcliffe, N. M. (2014), 'A review of the volatiles from the healthy human body', *Journal of Breath Research* **8**(1), 014001.

DEFRA (2012), 'The volatile organic compounds in paints, varnishes and vehicle refinishing products regulations'. Accessed: 2024-05.
URL: *https://www.legislation.gov.uk/uksi/2012/1715/made*

Deming, B. L. and Ziemann, P. J. (2020), 'Quantification of alkenes on indoor surfaces and implications for chemical sources and sinks', *Indoor Air* **30**, 914–924.

Derry, T. I. W. T. K. (1960), *A Short History of Technology: From the Earliest Times to A. D. 1900*, Courier Corporation.

Destaillats, H., Lunden, M. M., Singer, B. C., Coleman, B. K., Hodgson, A. T., Weschler, C. J. and Nazaroff, W. W. (2006), 'Indoor secondary pollutants from household product emissions in the presence of ozone: A bench-scale chamber study', *Environmental Science and Technology* **40**(14), 4421–4428.

Destaillats, H., Maddalena, R. L., Singer, B. C., Hodgson, A. T. and McKone, T. E. (2008), 'Indoor pollutants emitted by office equipment: A review of reported data and information needs', *Atmospheric Environment* **42**(7), 1371–1388.

Dhifi, W., Bellili, S., Jazi, S., Bahloul, N. and Mnif, W. (2016), 'Essential Oils' Chemical Characterization and Investigation of Some Biological Activities: A Critical Review', *Medicines* **3**(4), 25.

Dimitroulopoulou, C., Lucica, E., Johnson, A., Ashmore, M. R., Sakellaris, I., Stranger, M. and Goelen, E. (2015), 'EPHECT I : European household survey on domestic use of consumer products and development of worst-case scenarios for daily use', *Science of the Toal Environment* **536**, 880–889.

Ditto, J. C., Crilley, L. R., Lao, M., VandenBoer, T. C., Abbatt, J. P. D. and Chan, A. W. H. (2023), 'Indoor and outdoor air quality impacts of cooking and cleaning emissions from a commercial kitchen', *Environmental Science: Processes & Impacts* **25**, 964–979.

Duncan, S. M., Sexton, K. G. and Turpin, B. J. (2018), 'Oxygenated VOCs, aqueous chemistry, and potential impacts on residential indoor air composition', *Indoor Air* **28**(1), 198–212.

ECHA (2023), 'Substance infocard: Acetaldehyde'. Accessed: 2024-05.
URL: *https://echa.europa.eu/substance-information/-/substanceinfo/100.000.761*

EEA (2018), 'European Air Quality Portal'.
URL: *https://eeadmz1-cws-wp-air02.azurewebsites.net/*

Farmer, D. K., Vance, M. E., Abbatt, J. P. D., Abeleira, A., Alves, M. R., Arata, C., Boedicker, E., Bourne, S., Cardoso-Saldaña, F., Corsi, R., DeCarlo, P. F., Goldstein, A. H., Grassian, V. H., Hildebrandt Ruiz, L., Jimenez, J. L., Kahan, T. F., Katz, E. F., Mattila, J. M., Nazaroff, W. W., Novoselac, A., O'Brien, R. E., Or, V. W., Patel, S., Sankhyan, S., Stevens, P. S., Tian, Y., Wade, M., Wang, C., Zhou, S. and Zhou, Y. (2019), 'Overview of HOMEChem: House Observations of Microbial and Environmental Chemistry', *Environmental Science: Processes & Impacts* **21**(8), 1280–1300.

Fiedler, N., Laumbach, R., Kelly-McNeil, K., Lioy, P., Fan, Z. H., Zhang, J., Ottenweller, J., Ohman-Strickland, P. and Kipen, H. (2005), 'Health effects of a mixture of indoor air volatile organics, their ozone oxidation products, and stress', *Environmental Health Perspectives* **113**(11), 1542–1548.

Flemmer, M. M., Ham, J. E. and Wells, J. R. (2007), 'Field and laboratory emission cell automation and control system for investigating surface chemistry reactions', *Review of Scientific Instruments* **78**(1), 014101.

Golden, R. (2011), 'Identifying an indoor air exposure limit for formaldehyde considering both irritation and cancer hazards', *Critical Reviews in Toxicology* **41**(8), 672–721.

Harb, P., Locoge, N. and Thevenet, F. (2020), 'Treatment of household product emissions in indoor air: Real scale assessment of the removal processes', *Chemical Engineering Journal* **380**, 122525.

Harding-Smith, E., Shaw, D. R., Shaw, M., Dillon, T. J. and Carslaw, N. (2024), 'Does green mean clean? Volatile organic emissions from regular versus green cleaning products', *Environmental Science: Processes & Impacts* **26**(2), 436–450.

Harley, K. G., Calderon, L., Nolan, J. E., Maddalena, R., Russell, M., Roman, K., Mayo-Burgos, S., Cabrera, J., Morga, N. and Bradman, A. (2021), 'Changes in latina women's exposure to cleaning chemicals associated with switching from conventional to "green" household cleaning products: The lucir intervention study', *Environmental Health Perspectives* **129**(9), 97001.

Health and Safety Executive (2000), 'How to deal with sick building syndrome: Guidance for employers, building owners and building managers'.

Herz, R. S., Larsson, M., Trujillo, R., Casola, M. C., Ahmed, F. K., Lipe, S. and Brashear, M. E. (2022), 'A three-factor benefits framework for understanding consumer preference for scented household products: psychological interactions and implications for future development', *Cognitive Research: Principles and Implications* **7**(1), 28.

HM Government (2010), 'The building regulations 2010'. Accessed: 2024-04.
URL: *https://www.legislation.gov.uk/uksi/2010/2214/contents*

Hodshire, A. L., Carter, E., Mattila, J. M., Ilacqua, V., Zambrana, J., Abbatt, J. P. D., Abeleira, A., Arata, C., DeCarlo, P. F., Goldstein, A. H., Ruiz, L. H., Vance, M. E., Wang, C. and Farmer, D. K. (2022), 'Detailed Investigation of the Contribution of Gas-Phase Air Contaminants to Exposure Risk during Indoor Activities', *Environmental Science & Technology* **56**(17), 12148–12157.

Holøs, S. B., Yang, A., Lind, M., Thunshelle, K., Schild, P. and Mysen, M. (2019), 'VOC emission rates in newly built and renovated buildings, and the influence of ventilation – a review and meta-analysis', *International Journal of Ventilation* **18**(3), 153–166.

Horbanski, M., Pöhler, D., Lampel, J. and Platt, U. (2019), 'The ICAD (iterative cavity-enhanced DOAS) method', *Atmospheric Measurement Techniques* **12**(6), 3365–3381.

Horvath, E. P. (1997), 'Building-related illness and sick building syndrome: from the specific to the vague', *Cleveland Clinic journal of medicine* **64**(6), 303–309.

Hulin, M., Simoni, M., Viegi, G. and Annesi-Maesano, I. (2012), 'Respiratory health and indoor air pollutants based on quantitative exposure assessments', *European Respiratory Journal* **40**(4), 1033.

Hwang, J. H., Lee, S., Lee, H. G., Choi, D. and Lim, K. M. (2022), 'Evaluation of Skin Irritation of Acids Commonly Used in Cleaners in 3D-Reconstructed Human Epidermis Model, KeraSkinTM', *Toxics* **10**, 558.

IUPAC (2023), 'IUPAC Task Group on Atmospheric Kinetic Data Evaluation'.
URL: *https://iupac.aeris-data.fr/*

Jenkin, M. E., Saunders, S. M. and Pilling, M. J. (1997), 'The tropospheric degradation of volatile organic compounds: A protocol for mechanism development', *Atmospheric Environment* **31**(1), 81–104.

Jie, Y., Ismail, N. H., jie, X. and Isa, Z. M. (2011), 'Do indoor environments influence

asthma and asthma-related symptoms among adults in homes? A review of the literature', *Journal of the Formosan Medical Association* **110**(9), 555–563.

Joshi, S. M. (2008), 'The sick building syndrome', *Indian Journal of Occupational and Environmental Medicine* **12**(2), 61–64.

Kim, A. S., Ko, H. J., Kwon, J. H. and Lee, J. M. (2018), 'Exposure to secondhand smoke and risk of cancer in never smokers: A meta-analysis of epidemiologic studies', *International Journal of Environmental Research and Public Health* **15**(9).

Klein, F., Baltensperger, U., Prévôt, A. S. H. and Haddad, I. E. (2019), 'Quantification of the impact of cooking processes on indoor concentrations of volatile organic species and primary and secondary organic aerosols', *Indoor Air* **29**, 926–942.

Klein, F., Farren, N. J., Bozzetti, C., Daellenbach, K. R., Kilic, D., Kumar, N. K., Pieber, S. M., Slowik, J. G., Tuthill, R. N., Hamilton, J. F., Baltensperger, U., Prévôt, A. S. and Haddad, I. E. (2016), 'Indoor terpene emissions from cooking with herbs and pepper and their secondary organic aerosol production potential', *Scientific Reports* **6**.

Klepeis, N. E., Nelson, W. C., Ott, W. R., Robinson, J. P., Tsang, A. M., Switzer, P., Behar, J. V., Hern, S. C. and Engelmann, W. H. (2001), 'The national human activity pattern survey (nhaps): a resource for assessing exposure to environmental pollutants', *Journal of Exposure Analysis and Environmental Epidemiology* **11**(3), 231–252.

Koenig, J. Q., Covert, D. S. and Pierson, W. E. (1989), 'Effects of Inhalation of Acidic Compounds on Pulmonary Function in Allergic Adolescent Subjects', *Entmronmental Health Perspectives* **79**, 173–178.

Kowal, S. F., Allen, S. R. and Kahan, T. F. (2017), 'Wavelength-resolved photon fluxes of indoor light sources: Implications for hox production', *Environmental Science and Technology* **51**(18), 10423–10430.

Kruza, M. and Carslaw, N. (2019), 'How do breath and skin emissions impact indoor air chemistry?', *Indoor Air* **29**(3), 369–379.

Kruza, M., Lewis, A. C., Morrison, G. C. and Carslaw, N. (2017), 'Impact of surface ozone interactions on indoor air chemistry: A modeling study', *Indoor Air* **27**(5), 1001–1011.

Kurtenbach, R., Becker, K. H., Gomes, J. A. G., Kleffmann, J., Lörzer, J. C., Spittler, M., Wiesen, P., Ackermann, R., Geyer, A. and Platt, U. (2001), 'Investigations of emissions and heterogeneous formation of HONO in a road traffic tunnel', *Atmospheric Environment* **35**(20), 3385–3394.

Lakey, P. S. J., Wisthaler, A., Berkemeier, T., Mikoviny, T., Pöschl, U. and Shiraiwa, M. (2017), 'Chemical kinetics of multiphase reactions between ozone and human skin lipids: Implications for indoor air quality and health effects', *Indoor Air* **27**(4), 816–828.

Langford, V. S. (2023), 'SIFT-MS: Quantifying the Volatiles You Smell... and the Toxics You Don't', *Chemosensors* **11**(2), 111.

Langford, V. S., Graves, I. and McEwan, M. J. (2014), 'Rapid monitoring of volatile organic compounds: a comparison between gas chromatography/mass spectrometry and selected ion flow tube mass spectrometry', *Rapid Communications in Mass Spectrometry* **28**(1), 10–18.

Lassen, C., Havelund, S., Mikkelsen, S., Bondgaard, I. and Silberschmidt, M. (2008), 'Survey and health assessment of chemical substances in essential oils and fragrance oils'.

Leung, D. Y. (2015), 'Outdoor-indoor air pollution in urban environment: Challenges and opportunity', *Frontiers in Environmental Science* **2**.

Lewis, A. C., Allan, J., Carslaw, D., Carruthers, D., Fuller, G., Harrison, R., Heal, M., Nemitz, E., Reeves, C., Carslaw, N., Dengel, A., Dimitroulopoulou, S., Gupta,

R., Fisher, M., Fowler, D., Loh, M., Moller, S., Maggs, R., Murrells, T., Quincey, P. and Willis, P. (2022), 'Indoor Air Quality'.

Lim, C. Y. and Abbatt, J. P. (2020), 'Chemical composition, spatial homogeneity, and growth of indoor surface films', *Environmental Science and Technology* **54**, 14372–14379.

Liu, Y., Misztal, P. K., Arata, C., Weschler, C. J., Nazaroff, W. W. and Goldstein, A. H. (2021), 'Observing ozone chemistry in an occupied residence', *Proceedings of the National Academy of Sciences* **118**(6), e2018140118.

Liu, Y., Misztal, P. K., Xiong, J., Tian, Y., Arata, C., Weber, R. J., Nazaroff, W. W. and Goldstein, A. H. (2019), 'Characterizing sources and emissions of volatile organic compounds in a northern California residence using space- and time-resolved measurements', *Indoor Air* **29**(4), 630–644.

Lovén, K., Gudmundsson, A., Assarsson, E., Kåredal, M., Wierzbicka, A., Dahlqvist, C., Nordander, C., Xu, Y. and Isaxon, C. (2023), 'Effects of cleaning spray use on eyes, airways, and ergonomic load', *BMC Public Health* **23**(1).

Lovén, K., Isaxon, C., Wierzbicka, A. and Gudmundsson, A. (2019), 'Characterization of airborne particles from cleaning sprays and their corresponding respiratory deposition fractions', *Journal of Occupational and Environmental Hygiene* **16**(9), 656–667.

Mannan, M. and Al-Ghamdi, S. G. (2021), 'Indoor air quality in buildings: A comprehensive review on the factors influencing air pollution in residential and commercial structure', *International Journal of Environmental Research and Public Health* **18**(6), 3276.

Manuja, A., Ritchie, J., Buch, K., Wu, Y., Eichler, C. M. A., Little, J. C. and Marr, L. C. (2019), 'Total surface area in indoor environments', *Environmental Science: Processes & Impacts* **21**(8), 1384–1392.

McDonald, B. C., de Gouw, J. A., Gilman, J. B., Jathar, S. H., Akherati, A., Cappa, C. D., Jimenez, J. L., Lee-Taylor, J., Hayes, P. L., McKeen, S. A., Cui, Y. Y., Kim,

S.-W., Gentner, D. R., Isaacman-VanWertz, G., Goldstein, A. H., Harley, R. A., Frost, G. J., Roberts, J. M., Ryerson, T. B. and Trainer, M. (2018), 'Volatile chemical products emerging as largest petrochemical source of urban organic emissions', *Science* **359**(6377), 760–764.

McDonald, J. C. (1985), 'Health implications of environmental exposure to asbestos.', *Environmental Health Perspectives* **62**, 319–328.

MCM (2023). Accessed: 2024-04.
URL: *http://mcm.york.ac.uk/*

Medina-Ramón, M., Zock, J. P., Kogevinas, M., Sunyer, J., Torralba, Y., Borrell, A., Burgos, F. and Antó, J. M. (2005), 'Asthma, chronic bronchitis, and exposure to irritant agents in occupational domestic cleaning: A nested case-control study', *Occupational and Environmental Medicine* **62**(9), 598–606.

Meininghaus, R., Salthammer, T. and Knöppel, H. (1999), 'Interaction of volatile organic compounds with indoor materials—a small-scale screening method', *Atmospheric Environment* **33**(15), 2395–2401.

Milhem, S. A., Verriele, M., Nicolas, M. and Thevenet, F. (2020), 'Does the ubiquitous use of essential oil-based products promote indoor air quality? a critical literature review', *Environmental Science and Pollution Research* **27**, 14365–14411.

Mintel (2021), 'How COVID-19 has shifted cleaning priorities'. Accessed: 2024-04.
URL: *https://www.mintel.com/insights/household/how-covid-19-has-shifted-cleaning-priorities/*

Mintel (2023), 'Household cleaners – europe'. Accessed: 2024-04.
URL: *https://www.mintel.com*

Missia, D., Kopanidis, T., Bartzis, J., Ventura Silvia, G., De Oliveira Fernandes, E., Carrer, P., Wolkoff, P., Stranger, M. and Goelen, E. (2012), WP4 literature review on, product composition, emitted compounds and emission rates and health end points from consumer products, Technical report.

Moran, R. E., Bennett, D. H., Tancredi, D. J., Wu, X. M., Ritz, B. and Hertz-Picciotto, I. (2012), 'Frequency and longitudinal trends of household care product use', *Atmospheric Environment* **55**, 417–424.

Moreno-Rangel, A. (2020), 'Passivhaus', *Encyclopedia* **1**, 20–29.

Nazaroff, W. W. (2013), 'Exploring the consequences of climate change for indoor air quality', *Environmental Research Letters* **8**(1).

Nazaroff, W. W. (2021), 'Residential air-change rates: A critical review', *Indoor Air* **31**(2), 282–313.

Nazaroff, W. W. and Weschler, C. J. (2004), 'Cleaning products and air fresheners: Exposure to primary and secondary air pollutants', *Atmospheric Environment* **38**(18), 2841–2865.

Nazaroff, W. W. and Weschler, C. J. (2022), 'Indoor ozone: Concentrations and influencing factors', *Indoor Air* **32**(1), e12942.

Nematollahi, N., Kolev, S. D. and Steinemann, A. (2019), 'Volatile chemical emissions from 134 common consumer products', *Air Quality, Atmosphere and Health* **12**(11), 1259–1265.

Nicolas, M., Ramalho, O. and Maupetit, F. (2007), 'Reactions between ozone and building products: Impact on primary and secondary emissions', *Atmospheric Environment* **41**, 3129–3138.

Nielsen, G. D. and Wolkoff, P. (2010), 'Cancer effects of formaldehyde: a proposal for an indoor air guideline value', *Archives of Toxicology* **84**(6), 423–446.

Norbäck, D. (2009), 'An update on sick building syndrome', *Current Opinion in Allergy and Clinical Immunology* **9**(1).

Nørgaard, A. W., Kudal, J. D., Kofoed-Sørensen, V., Koponen, I. K. and Wolkoff, P. (2014), 'Ozone-initiated voc and particle emissions from a cleaning agent and an

air freshener: Risk assessment of acute airway effects', *Environment International* **68**, 209–218.

Omnicom Media Group (2017), 'A Look at the Marketing Evolution of Household Cleaners'. Accessed: 2024-04.
URL: *https://www.annalect.com/a-look-at-the-marketing-evolution-of-household-cleaners/*

Orimoogunje, O. O. I., Ayanlade, A., Akinkuolie, T. A. and Odiong, A. U. (2010), 'Perception on Effect of Gas Flaring on the Environment', *Research Journal of Environmental and Earth Sciences* **2**(4), 188–193.

Pei, G., Xuan, Y., Morrison, G. and Rim, D. (2022), 'Understanding ozone transport and deposition within indoor surface boundary layers', *Environmental Science and Technology* **56**, 7820–7829.

Phillips, M. and Greenberg, J. (1992), 'Ion-Trap Detection of Volatile Organic Compounds in Alveolar Breath', *Clinical Chemistry* **38**(1), 60–65.

Public Health England (2019), Indoor Air Quality Guidelines for selected Volatile Organic Compounds (VOCs) in the UK, Technical report, Public Health England.

Reed, C. J. (2010), The Characterisation and Development of a Passivated Inlet to Selected Ion Flow Tube Mass Spectrometry (SIFT-MS), PhD thesis, University of Canterbury.

Rosales, C. M. F., Jiang, J., Lahib, A., Bottorff, B. P., Reidy, E. K., Kumar, V., Tasoglou, A., Huber, H., Dusanter, S., Tomas, A., Boor, B. E. and Stevens, P. S. (2022), 'Chemistry and human exposure implications of secondary organic aerosol production from indoor terpene ozonolysis', *Science Advances* **8**(8), eabj9156.

Rossignol, S., Rio, C., Ustache, A., Fable, S., Nicolle, J., Même, A., D'Anna, B., Nicolas, M., Leoz, E. and Chiappini, L. (2013), 'The use of a housecleaning product in an indoor environment leading to oxygenated polar compounds and SOA

formation: Gas and particulate phase chemical characterization', *Atmospheric Environment* **75**, 196–205.

Ruiz-Jimenez, J., Heiskanen, I., Tanskanen, V., Hartonen, K. and Riekkola, M.-L. (2022), 'Analysis of indoor air emissions: From building materials to biogenic and anthropogenic activities', *Journal of Chromatography Open* **2**, 100041.

Salthammer, T., Mentese, S. and Marutzky, R. (2010), 'Formaldehyde in the Indoor Environment', *Chemical Reviews* **110**(4), 2536–2572.

Sarwar, G., Olson, D. A., Corsi, R. L. and Weschler, C. J. (2004), 'Indoor Fine Particles: The Role of Terpene Emissions from Consumer Products', *Journal of the Air & Waste Management Association* **54**(3), 367–377.

Saunders, S. M., Jenkin, M. E., Derwent, R. G. and Pilling, M. J. (2003), 'Protocol for the development of the Master Chemical Mechanism, MCM v3 (Part A): Tropospheric degradation of non-aromatic volatile organic compounds', *Atmospheric Chemistry and Physics* **3**(1), 161–180.

Shaw, D. and Carslaw, N. (2021), 'INCHEM-Py: An open source Python box model for indoor air chemistry', *Journal of Open Source Software* **6**(63), 3224.

Shaw, D. R., Carter, T. J., Davies, H. L., Harding-Smith, E., Crocker, E. C., Beel, G., Wang, Z. and Carslaw, N. (2023), 'INCHEM-Py v1.2: A community box model for indoor air chemistry', *EGUsphere* **2023**, 1–32.

Shrestha, P. M., Humphrey, J. L., Carlton, E. J., Adgate, J. L., Barton, K. E., Root, E. D. and Miller, S. L. (2019), 'Impact of outdoor air pollution on indoor air quality in low-income homes during wildfire seasons', *International Journal of Environmental Research and Public Health* **16**(19).

Singer, B. C., Destaillats, H., Hodgson, A. T. and Nazaroff, W. W. (2006), 'Cleaning products and air fresheners: Emissions and resulting concentrations of glycol ethers and terpenoids', *Indoor Air* **16**(3), 179–191.

Singer, B. C., Hodgson, A. T., Hotchi, T., Ming, K. Y., Sextro, R. G., Wood, E. E. and Brown, N. J. (2007), 'Sorption of organic gases in residential rooms', *Atmospheric Environment* **41**, 3251–3265.

Smith, D. and Adams, N. G. (1987), 'The Selected Ion Flow Tube (SIFT): Studies of Ion-Neutral Reactions', *Advances in Atomic and Molecular Physics* **24**, 1–49.

Smith, D. and Španěl, P. (2005), 'Selected ion flow tube mass spectrometry (SIFT-MS) for on-line trace gas analysis', *Mass Spectrometry Reviews* **24**(5), 661–700.

Smith, D., Spanel, P., Thompson, J. M., Rajan, B., Cocker, J. and Rolfe, P. (1998), 'The selected ion flow tube method for workplace analyses of trace gases in air and breath: Its scope, validation, and applications', *Applied Occupational and Environmental Hygiene* **13**(12), 817–823.

Spanel, P. and Smith, D. (1996), 'Selected ion flow tube: a technique for quantitative trace gas analysis of air and breath', *Medical & Biological Engineering & Computing* **34**, 409–419.

Springs, M., Wells, J. R. and Morrison, G. C. (2011), 'Reaction rates of ozone and terpenes adsorbed to model indoor surfaces', *Indoor Air* **21**(4), 319–327.

Steinemann, A. (2015), 'Volatile emissions from common consumer products', *Air Quality, Atmosphere and Health* **8**(3), 273–281.

Steinemann, A. C. (2009), 'Fragranced consumer products and undisclosed ingredients', *Environmental Impact Assessment Review* **29**(1), 32–38.

Steinemann, A., Nematollahi, N., Rismanchi, B., Goodman, N. and Kolev, S. D. (2021), 'Pandemic products and volatile chemical emissions', *Air Quality, Atmosphere and Health* **14**(1), 47–53.

Stönner, C., Edtbauer, A. and Williams, J. (2018), 'Real-world volatile organic compound emission rates from seated adults and children for use in indoor air studies', *Indoor Air* **28**(1), 164–172.

Syft Technologies Training Materials (2014), Quantitation: SIFT-MS Calibration Principles, Technical report, Syft Technologies.

Tang, X., Misztal, P. K., Nazaroff, W. W. and Goldstein, A. H. (2016), 'Volatile Organic Compound Emissions from Humans Indoors', *Environmental Science & Technology* **50**(23), 12686–12694.

Teixeira, B., Marques, A., Ramos, C., Neng, N. R., Nogueira, J. M., Saraiva, J. A. and Nunes, M. L. (2013), 'Chemical composition and antibacterial and antioxidant properties of commercial essential oils', *Industrial Crops and Products* **43**(1), 587–595.

Temkin, A. M., Geller, S. L., Swanson, S. A., Leiba, N. S., Naidenko, O. V. and Andrews, D. Q. (2023), 'Volatile organic compounds emitted by conventional and "green" cleaning products in the U.S. market', *Chemosphere* **341**, 139570.

Terry, A. C., Carslaw, N., Ashmore, M., Dimitroulopoulou, S. and Carslaw, D. C. (2014), 'Occupant exposure to indoor air pollutants in modern European offices: An integrated modelling approach', *Atmospheric Environmen* **82**, 9–16.

UK Legislation (1987), 'The Control of Asbestos at Work Regulations'.
URL: *https://www.legislation.gov.uk/uksi/1987/2115/made*

UK Legislation (2006), 'Health Act'. Accessed: 2024-04.
URL: *https://www.legislation.gov.uk/ukpga/2006/28/contents*

Vardoulakis, S., Giagloglou, E., Steinle, S., Davis, A., Sleeuwenhoek, A., Galea, K. S., Dixon, K. and Crawford, J. O. (2020), 'Indoor exposure to selected air pollutants in the home environment: A systematic review', *International Journal of Environmental Research and Public Health* **17**, 1–24.

Vyskocil, A., Viau, C. and Lamy, S. (1998), 'Peroxyacetyl nitrate: review of toxicity', *Human & Experimental Toxicology* **17**, 212–220.

Wagner, R. L., Farren, N. J., Davison, J., Young, S., Hopkins, J. R., Lewis, A. C., Carslaw, D. C. and Shaw, M. D. (2021), 'Application of a mobile laboratory using a

selected-ion flow-tube mass spectrometer (SIFT-MS) for characterisation of volatile organic compounds and atmospheric trace gases', *Atmospheric Measurement Techniques* **14**(9), 6083–6100.

Wainman, T., Weschler, C. J., Lioy, P. J. and Zhang, J. (2001), 'Effects of Surface Type and Relative Humidity on the Production and Concentration of Nitrous Acid in a Model Indoor Environment', *Environmental Science & Technology* **35**(11), 2200–2206.

Wang, C., Collins, D. B., Arata, C., Goldstein, A. H., Mattila, J. M., Farmer, D. K., Ampollini, L., Decarlo, P. F., Novoselac, A., Vance, M. E., Nazaroff, W. W. and Abbatt, J. P. D. (2020), 'Surface reservoirs dominate dynamic gas-surface partitioning of many indoor air constituents', *Science Advances* **6**, 8973.

Wang, C. M., Barratt, B., Carslaw, N., Doutsi, A., Dunmore, R. E., Ward, M. W. and Lewis, A. C. (2017), 'Unexpectedly high concentrations of monoterpenes in a study of UK homes', *Environmental Science: Processes & Impacts* **19**(4), 528–537.

Wang, H. and Morrison, G. C. (2006), 'Ozone-initiated secondary emission rates of aldehydes from indoor surfaces in four homes', *Environmental Science & Technology* **40**, 5263–5268.

Wang, H., Xiong, J. and Wei, W. (2022), 'Measurement methods and impact factors for the key parameters of VOC/SVOC emissions from materials in indoor and vehicular environments: A review', *Environment International* **168**, 107451.

Wang, N., Ernle, L., Bekö, G., Wargocki, P. and Williams, J. (2022), 'Emission Rates of Volatile Organic Compounds from Humans', *Environmental Science and Technology* **56**(8), 4838–4848.

Wang, Z., Shaw, D., Kahan, T., Schoemaecker, C. and Carslaw, N. (2022), 'A modeling study of the impact of photolysis on indoor air quality', *Indoor Air* **32**(6).

Waring, M. S. and Siegel, J. A. (2013), 'Indoor secondary organic aerosol formation

initiated from reactions between ozone and surface-sorbed d -limonene', *Environmental Science and Technology* **47**(12), 6341–6348.

Weegels, M. F. and Veen, M. P. V. (2001), 'Variation of consumer contact with household products : A preliminary investigation', *Risk Analysis* **21**, 499–512.

Weschler, C. J. (2000), 'Ozone in indoor environments: Concentration and chemistry', *Indoor Air* **10**(4), 269–288.

Weschler, C. J. (2009), 'Changes in indoor pollutants since the 1950s', *Atmospheric Environment* **43**(1), 153–169.

Weschler, C. J. and Carslaw, N. (2018), 'Indoor chemistry', *Environmental Science and Technology* **52**(5), 2419–2428.

Weschler, C. J., Shields, H. C. and Naik, D. V. (1989), 'Indoor Ozone Exposures', *JAPCA* **39**(12), 1562–1568.

Weschler, C. J., Wisthaler, A., Cowlin, S., Tamás, G., Strøm-Tejsen, P., Hodgson, A. T., Destaillats, H., Herrington, J., Zhang, J. and Nazaroff, W. W. (2007), 'Ozone-initiated chemistry in an occupied simulated aircraft cabin', *Environmental Science and Technology* **41**(17), 6177–6184.

Wolkoff, P., Clausen, P. A., Larsen, K., Hammer, M., Larsen, S. T. and Nielsen, G. D. (2008), 'Acute airway effects of ozone-initiated d-limonene chemistry: Importance of gaseous products', *Toxicology Letters* **181**(3), 171–176.

Wolkoff, P., Clausen, P. A., Wilkins, C. K. and Nielsen, G. D. (2000), 'Formation of Strong Airway Irritants in Terpene/Ozone Mixtures', *Indoor Air* **10**(2), 82–91.

Wolkoff, P., Schneider, T., Kildesø, J., Degerth, R., Jaroszewski, M. and Schunk, H. (1998), 'Risk in cleaning: chemical and physical exposure', *The Science of the Total Environment* **215**, 135156.

Won, D., Corsi, R. L. and Rynes, M. (2001), 'Sorptive interactions between vocs and indoor materials', *Indoor Air* **11**, 246–256.

Wong, J. P. S., Carslaw, N., Zhao, R., Zhou, S. and Abbatt, J. P. D. (2017), 'Observations and impacts of bleach washing on indoor chlorine chemistry', *Indoor Air* **27**(6), 1082–1090.

World Health Organisation (2021), 'WHO global air quality guidelines. Particulate matter (PM2.5 and PM10), ozone, nitrogen dioxide, sulfur dioxide and carbon monoxide.'.

World Health Organization (1983), *Indoor air pollutants: exposure and health effects*, World Health Organization, Denmark.

World Health Organization (2010), *WHO guidelines for indoor air quality: selected pollutants*, World Health Organization, Geneva.

World Health Organization (2022), 'Household air pollution'. Accessed: 2024-04. **URL:** *https://www.who.int/news-room/fact-sheets/detail/household-air-pollution-and-health*

Xue, L. K., Saunders, S. M., Wang, T., Gao, R., Wang, X. F., Zhang, Q. Z. and Wang, W. X. (2015), 'Development of a chlorine chemistry module for the Master Chemical Mechanism', *Geoscientific Model Development* **8**(10), 3151–3162.

Yeoman, A. M., Shaw, M., Carslaw, N., Murrells, T., Passant, N. and Lewis, A. C. (2020), 'Simplified speciation and atmospheric volatile organic compound emission rates from non-aerosol personal care products', *Indoor Air* **30**(3), 459–472.

Youssefi, S. and Waring, M. S. (2014), 'Transient secondary organic aerosol formation from limonene ozonolysis in indoor environments: Impacts of air exchange rates and initial concentration ratios', *Environmental Science and Technology* **48**(14), 7899–7908.

Zhang, D.-C., Liu, J.-J., Jia, L.-Z., Wang, P. and Han, X. (2019), 'Speciation of vocs in the cooking fumes from five edible oils and their corresponding health risk assessments', *Atmospheric Environment* **211**, 6–17.

Zhang, G., Mu, Y., Zhou, L., Zhang, C., Zhang, Y., Liu, J., Fang, S. and Yao, B. (2015), 'Summertime distributions of peroxyacetyl nitrate (PAN) and peroxypropionyl nitrate (PPN) in Beijing: Understanding the sources and major sink of PAN', *Atmospheric Environment* **103**, 289–296.